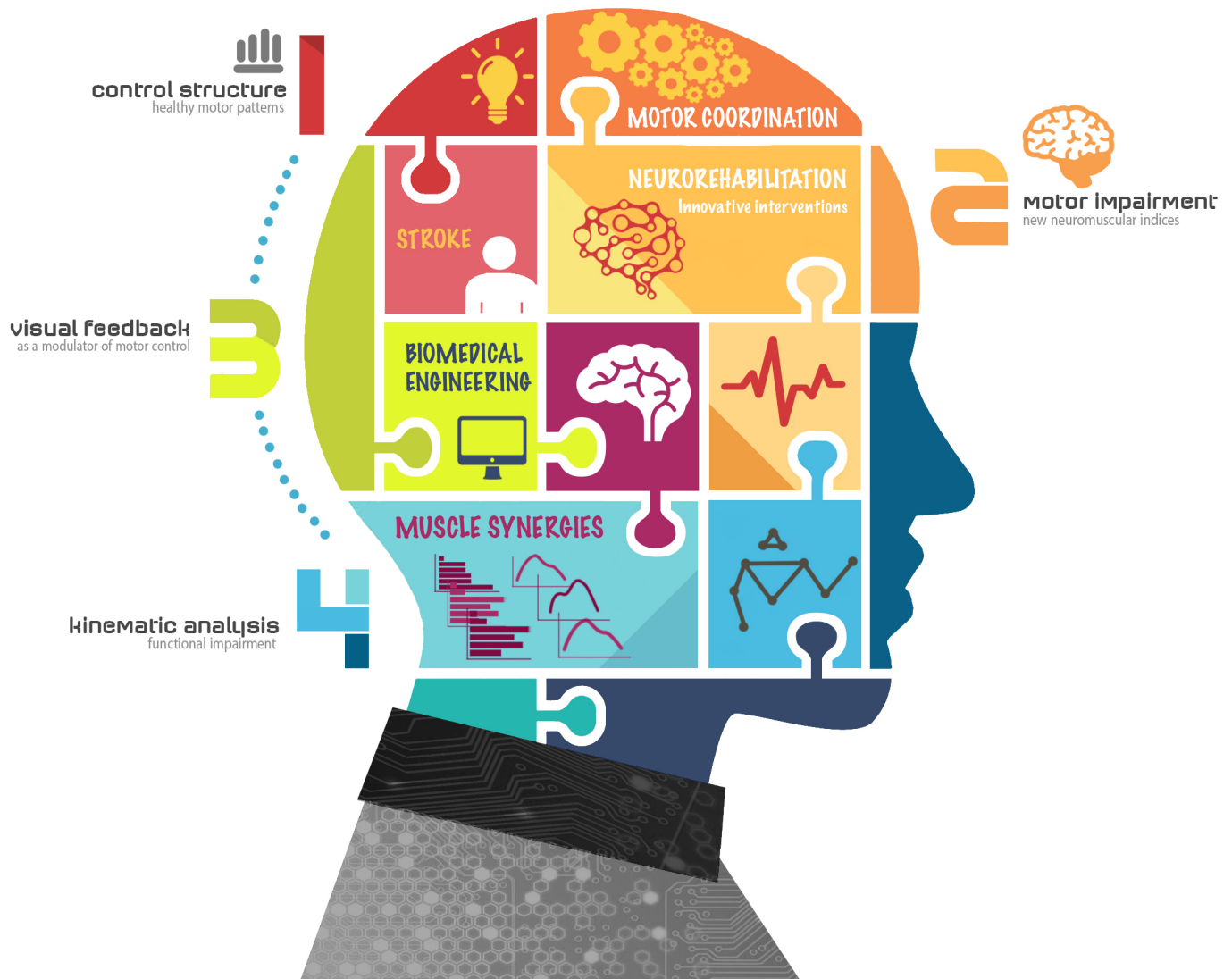


# **Analysis of the interlimb similarity of motor patterns for improving stroke assessment and neurorehabilitation**

**Oiane Urra**



**Directed by**  
Alícia Casals & Raimon Jané





UNIVERSITAT POLITÈCNICA  
DE CATALUNYA  
BARCELONATECH

## *Analysis of the interlimb similarity of motor patterns for improving stroke assessment and neurorehabilitation*

Oiane Urrea Vicario

**ADVERTIMENT** La consulta d'aquesta tesi queda condicionada a l'acceptació de les següents condicions d'ús: La difusió d'aquesta tesi per mitjà del repositori institucional UPCommons (<http://upcommons.upc.edu/tesis>) i el repositori cooperatiu TDX (<http://www.tdx.cat/>) ha estat autoritzada pels titulars dels drets de propietat intel·lectual **únicament per a usos privats** emmarcats en activitats d'investigació i docència. No s'autoritza la seva reproducció amb finalitats de lucre ni la seva difusió i posada a disposició des d'un lloc aliè al servei UPCommons o TDX. No s'autoritza la presentació del seu contingut en una finestra o marc aliè a UPCommons (*framing*). Aquesta reserva de drets afecta tant al resum de presentació de la tesi com als seus continguts. En la utilització o cita de parts de la tesi és obligat indicar el nom de la persona autora.

**ADVERTENCIA** La consulta de esta tesis queda condicionada a la aceptación de las siguientes condiciones de uso: La difusión de esta tesis por medio del repositorio institucional UPCommons (<http://upcommons.upc.edu/tesis>) y el repositorio cooperativo TDR (<http://www.tdx.cat/?locale-attribute=es>) ha sido autorizada por los titulares de los derechos de propiedad intelectual **únicamente para usos privados enmarcados** en actividades de investigación y docencia. No se autoriza su reproducción con finalidades de lucro ni su difusión y puesta a disposición desde un sitio ajeno al servicio UPCommons. No se autoriza la presentación de su contenido en una ventana o marco ajeno a UPCommons (*framing*). Esta reserva de derechos afecta tanto al resumen de presentación de la tesis como a sus contenidos. En la utilización o cita de partes de la tesis es obligado indicar el nombre de la persona autora.

**WARNING** On having consulted this thesis you're accepting the following use conditions: Spreading this thesis by the institutional repository UPCommons (<http://upcommons.upc.edu/tesis>) and the cooperative repository TDX (<http://www.tdx.cat/?locale-attribute=en>) has been authorized by the titular of the intellectual property rights **only for private uses** placed in investigation and teaching activities. Reproduction with lucrative aims is not authorized neither its spreading nor availability from a site foreign to the UPCommons service. Introducing its content in a window or frame foreign to the UPCommons service is not authorized (*framing*). These rights affect to the presentation summary of the thesis as well as to its contents. In the using or citation of parts of the thesis it's obliged to indicate the name of the author.



# **Analysis of the interlimb similarity of motor patterns for improving stroke assessment and neurorehabilitation**

Doctoral thesis

**Oiane Urria Vicario**

Doctoral program in Biomedical Engineering  
Department of Automatic Control  
Universitat Politècnica de Catalunya

Biomedical Signal Processing and Interpretation & Robotics  
groups | **Institute for Bioengineering of Catalonia**

Directed by: Dr. Raimon Jané & Dr. Alícia Casals

Barcelona, July 2016







# INDEX

<b>INDEX</b>	<b>I</b>
<b>ABSTRACT</b>	<b>XI</b>
<b>ACKNOWLEDGEMENTS</b>	<b>XIII</b>
<b>PREFACE</b>	<b>XXI</b>
I. OBJECTIVES	XXI
<i>Main Objective</i>	<i>xxii</i>
<i>Specific Objectives</i>	<i>xxiii</i>
II. ORGANIZATION OF THE MANUSCRIPT	XXV
<b>ABBREVIATIONS</b>	<b>XXIX</b>
<b>PART I. INTRODUCTION</b>	<b>1</b>
1    STROKE	3
1.1 <i>Types and causes</i>	3
1.2 <i>Stroke Statistics</i>	4
1.3 <i>Symptoms during a stroke</i>	5
1.4 <i>Treatment</i>	6
1.5 <i>Prognosis and post-stroke consequences</i>	7
1.5.1    Motor consequences post-stroke	9



## INDEX

---

2	MOTOR IMPAIRMENT SCALES	11
2.1	<i>Classification and types</i>	11
2.1.1	Clinical Scales	11
2.1.2	Outcome Scales	13
2.2	<i>Limitations</i>	15
3	POST-STROKE REHABILITATION	17
3.1	<i>Rehabilitation Areas</i>	18
3.2	<i>The 7 stages of motor recovery</i>	19
3.3	<i>Upper Limb Motor Rehabilitation Strategies</i>	20
3.3.1	Physical rehabilitation	20
3.3.2	Technology-assisted rehabilitation	22
3.3.3	Considerations during motor rehabilitation	25
4	MOTOR COORDINATION	27
4.1	<i>Uncontrolled Manifold Hypothesis (UCM)</i>	28
4.2	<i>Muscle Synergies and the Control Structure</i>	29
4.2.1	Stroke and Muscle Synergies	30
4.2.2	Synergy analysis as a rehabilitation tool	31
4.3	<i>Stroke and neurorehabilitation</i>	33
5	KINEMATICS OF HUMAN MOTION	35
5.1	<i>The Clinical Reference System</i>	36
5.2	<i>Motion of Human Body Segments</i>	38
5.3	<i>Angular Kinematics</i>	39
5.4	<i>Kinematic Chains</i>	40
5.5	<i>Stroke and Kinematics</i>	42
5.5.1	Kinematic indices used in literature	44
5.5.2	Kinematic traits of patients with stroke	45
	<b>PART II. METHODS</b>	<b>49</b>
6	SUBJECT DATABASES	51
6.1	<i>Description of the Databases</i>	51
6.1.1	The database of neurologically intact subjects	51
6.1.2	The database of patients with stroke	52



6.2	<i>Tests Handed Out to Assess Subjects</i>	54
6.2.1	Laterality Index   Edinburgh Handedness Inventory	54
6.2.2	Fugl-Meyer Assessment scale (FM)	55
6.2.3	Functional Independence Measure (FIM)	57
6.3	<i>Ethical Considerations</i>	59
7	EXPERIMENTAL PROTOCOL	61
7.1	<i>General Protocol</i>	61
7.2	<i>Protocol modifications for patients</i>	63
8	EMG DATA	65
8.1	<i>Electrode Placement</i>	68
8.2	<i>EMG Acquisition</i>	68
8.2.1	EMGs of neurologically intact subjects	68
8.2.2	EMGs of patients with stroke	68
8.2.3	Database compatibility	69
8.3	<i>EMG Preprocessing</i>	69
8.4	<i>Synergy Extraction</i>	70
8.4.1	Within-subject synergy matching across limbs	72
8.4.2	Interlimb similarity (ILS) measures	73
9	KINEMATIC DATA	75
9.1	<i>Biomechanical model</i>	76
9.2	<i>Kinematic data acquisition And Processing</i>	77
<b>PART III. STUDIES</b>		<b>81</b>
<b>STUDY 1   INTERLIMB SIMILARITY IN HEALTHY SUBJECTS</b>		<b>85</b>
10	SPECIFIC PROCEDURES (I)	89
10.1	<i>Characterization of EMG Signals</i>	89
10.1.1	Exponential decay model of muscle fiber recruitment	89
10.1.2	Median Frequency	90
10.2	<i>Synergy matching across subjects</i>	91
10.3	<i>Cross-reconstruction</i>	91
10.4	<i>Activity maps</i>	92



## INDEX

---

10.5	<i>Statistical Analyses</i>	93
11	RESULTS (I)	95
11.1	<i>Characterization of EMG Data</i>	95
11.2	<i>Evolution of EMG amplitude across repetitions</i>	98
11.3	<i>Evaluation of muscle fatigue across repetitions</i>	101
11.4	<i>Interlimb similarity of the control structure</i>	102
11.5	<i>Interlimb similarity vs inter-subject similarity</i>	106
11.6	<i>Cross-reconstruction of the control structure</i>	108
11.7	<i>Healthy activity maps</i>	111
12	DISCUSSION (I)	114
12.1	<i>EMG recruitment patterns go beyond handedness</i>	114
12.2	<i>The clinical value of the control structure</i>	115
12.3	<i>Activation coefficients as a key rehabilitation target</i>	117
12.4	<i>Cross-reconstruction quality is Independent of handedness</i>	118
12.5	<i>Exploiting activity maps in rehabilitation</i>	118
13	CONCLUSIONS (I)	120
	<b>STUDY 2   THE EFFECT OF VF IN THE MOTOR CONTROL</b>	<b>123</b>
14	SPECIFIC PROCEDURES (II)	127
14.1	<i>Experimental setup</i>	127
14.2	<i>Kinetic parameters</i>	128
14.3	<i>Within-Subject synergy matching across conditions</i>	129
14.4	<i>Interlimb Difference (ILD) measures</i>	139
14.5	<i>Temporal effect of VF on ILS</i>	140
14.6	<i>Temporal effect of VF on laterality</i>	142
14.7	<i>ILS improvement measures</i>	143
14.8	<i>Intermanual transfer (IMT) measures</i>	143
14.9	<i>Stage by stage synergy extraction</i>	144
14.10	<i>Statistical analyses</i>	146
14.10.1	<i>Interaction effects on VF-driven ILS changes</i>	146



14.10.2	Temporal effect of VF on ILS	146
14.10.3	Interaction effects on IMT measures	147
15	RESULTS AND DISCUSSION (II)	148
15.1	<i>Self - evaluation about the use of VF</i>	148
15.2	<i>The effect of VF on movement Performance</i>	150
15.2.1	The effect of VF on movement duration	150
15.2.2	The effect of VF on the variability of movement duration	154
15.3	<i>The effect of VF on the ILS</i>	159
15.3.1	Control structures in absence and presence of VF	159
15.3.2	Mean ILS: subject by subject	172
15.3.3	Mean ILS: movement by movement	175
15.3.4	ILS: muscle synergies vs activation coefficients	181
15.4	<i>Temporal effects of VF on ILS</i>	184
15.4.1	The effect of VF on the control structure	184
15.4.2	Quantifying the effect of VF on the activation coefficients	195
15.6	<i>Intermanual Transfer (IMT) in the activation coefficients</i>	200
15.6.1	Frequency of occurrence of IMT	200
15.6.2	VF-driven effects: ILS improvement and IMT magnitude	203
15.7	<i>Can subjects learn how to modulate ILS?</i>	205
16	CONCLUSIONS (II)	209
16.1	<i>Major Findings</i>	209
16.2	<i>Final remarks</i>	211
	<b>STUDY 3   INTERLIMB SIMILARITY IN STROKE PATIENTS</b>	<b>215</b>
17	SPECIFIC PROCEDURES (III)	218
17.1	<i>Experimental setup</i>	218
17.2	<i>Defining the reference framework</i>	218
17.3	<i>Quality of kinematic Recordings</i>	219
17.4	<i>Determining movement onset and offset</i>	220
17.4.1	Segmentation from position	220
17.4.2	Segmentation from velocity	222
17.5	<i>Association analysis between ILS and clinical measures</i>	224



## INDEX

---

17.5.1	Linear regression	225
17.5.2	Polynomial regression	226
17.5.3	Pearson's correlation	226
17.6	<i>Cross-reconstruction</i>	227
17.7	<i>Statistical analyses</i>	229
17.7.1	Interaction effects on ILS	229
17.7.2	ILS: Healthy subjects vs Patients with Stroke	230
17.7.3	ILS: no VF vs VF	231
17.7.4	ILS: Right-stroke vs left-stroke patients	231
18	RESULTS AND DISCUSSION (III)	233
18.1	<i>Quality of the Kinematic Recordings</i>	233
18.2	<i>Self - Evaluation of Patients</i>	236
18.3	<i>Characterizing the control structure of stroke patients</i>	239
18.3.1	Composition of the control structure and VAF	239
18.3.2	Synergy matching across conditions	241
18.3.3	Graphical representation of the control structures	248
18.4	<i>ILS in patients with stroke</i>	262
18.4.1	Mean ILS: subject by subject	262
18.4.2	Which factors affect the ILS of the control structure?	265
18.4.3	Mean ILS: movement by movement	268
18.5	<i>Mean ILS: Stroke Patients vs Healthy Subjects</i>	274
18.5.1	Inter-group ILS breakdown: movement by movement	276
18.6	<i>ILS as a marker of motor impairment</i>	280
18.6.1	Association between Fugl-Meyer and Motor-FIM scores	280
18.6.2	Association between ILS and Fugl-Meyer score	282
18.6.3	Association between ILS and Motor-FIM score	289
18.7	<i>Does the dominance of the paretic arm affect ILS?</i>	293
18.8	<i>Does the effectiveness of VF depend on the damaged hemisphere?</i>	296
18.9	<i>Cross-reconstruction of the control structure</i>	300
19	CONCLUSIONS (III)	305
19.1	<i>Major Findings</i>	305
19.2	<i>Final Remarks</i>	309



<b>STUDY 4   KINEMATIC ANALYSIS IN STROKE PATIENTS</b>	<b>313</b>
20 SPECIFIC PROCEDURES (IV)	316
20.1 <i>Kinematic Data Analysis</i>	316
20.1.1 Definition of planar motion	316
20.1.2 Definition of movement geometry	318
20.1.3 Interlimb similarity measures of angular kinematics	323
20.1.4 Kinematic Indices	326
20.2 <i>Logistic regression</i>	328
20.3 <i>Quantification of VF-driven motor improvement</i>	330
20.4 <i>Statistical Analyses</i>	331
21 RESULTS AND DISCUSSION (IV)	332
21.1 <i>Planar trajectories</i>	332
21.2 <i>Evolution of Angular Kinematics</i>	334
21.2.1 Main angle evolution	334
21.2.2 Compensatory angle evolution	339
21.3 <i>Angular evolution, Velocity and Acceleration</i>	343
21.3.1 Qualitative interlimb comparisons	343
21.3.2 Quantitative interlimb comparisons	349
21.4 <i>Comparison of kinematic Indices</i>	352
21.4.1 Paretic vs non paretic arm	352
21.4.2 Linear regressions: Fugl-Meyer score vs Kinematic indices	355
21.5 <i>Kinematic indices as predictors: logistic regression</i>	359
21.6 <i>The effect of VF in angular kinematics</i>	359
21.6.1 ILS <sub>K</sub> measures across conditions (nVF and VF)	360
21.6.2 VF-driven improvement of ILS <sub>K</sub>	363
22 CONCLUSIONS (IV)	368
22.1 <i>Major Findings</i>	368
22.2 <i>Final Remarks</i>	372
<b>PART IV. CONCLUDING REMARKS</b>	<b>377</b>
FUTURE WORK	384
<b>PART V. BIBLIOGRAPHY</b>	<b>387</b>



## INDEX

---

<b>PART VI. DERIVED PUBLICATIONS</b>	<b>409</b>
<b>PART VII. APPENDICES</b>	<b>415</b>
A.    EDINBURGH HANDEDNESS INVENTORY	417
B.    FUGL – MEYER SCALE	418
C.    FUNCTIONAL INDEPENDENCE MEASURE	419
D.    UPPER-LIMB JOINTS AND MUSCLE FUNCTION	420
E.    CUSTOM GUI FOR UPPER-LIMB MOTOR ANALYSIS	421











# ABSTRACT

*Stroke is the leading cause of adult disability, with upper limb hemiparesis being one of the most common consequences. Regaining voluntary arm movement is one of the major goals of rehabilitation. However, even with intensive rehabilitation, approximately 30% of patients remain permanently disabled and only 5 to 20% of them recover full independence. Hence, there is an increasing interest in incorporating the latest advances in neuroscience, medicine and engineering to improve the efficacy of conventional therapies.*

*In the last years, a variety of promising targets have been identified to improve rehabilitation. However, there is no consensus on which measure should be applied as a gold standard to study functional recovery. This fact dramatically hinders the development of new interventions since it turns difficult to compare different clinical trials and draw consistent conclusions about therapeutic efficiency. In addition, available scales are subjective, qualitative and often lead to incongruent outcomes. Indeed, there is increasing suspicion that the lack of optimal assessment measures hampers the detection of benefits of new therapies. Moreover, existing scales totally ignore the neuromuscular state of the patient masking the ongoing recovery processes. In consequence, making appropriate clinical decisions in such environment is almost impossible.*



## ABSTRACT

---

*In light of all these facts, the need for new objective biomarkers to develop effective therapies is undeniable. To give response to these demands we have organized this thesis into two main branches. On the one hand, we have developed an innovative physiological scale that reveals the neuromuscular state of the patient and is able to discriminate between motor impairment levels. The innovation here resides in the concept of interlimb similarity (ILS). Based on the latest findings about the modular organization of the motor system and taking into account that stroke provokes unilateral motor damage, we propose comparing the control structure of the unaffected arm with the control structure of the paretic arm to quantify motor impairment.*

*We have defined the control structure as the set of muscle synergies and activation coefficients needed to complete a task. The advantage of this approach is not only its capacity to provide neuromuscular information about the patient, but also that the ILS is personalized to each patient and can purposely guide rehabilitation based on the patient's own physiological patterns. This supposes a huge advance taking into account the heterogeneity of stroke pathogenesis.*

*On other hand, we have characterized the therapeutic potential of Visual Feedback (VF) as a tool to purposely induce neuroplastic changes. We have chosen VF among the various interventions proven to improve motor performance, because VF is a cheap strategy that can be implemented in almost any rehabilitation center. We demonstrate that VF is able to modulate the human control structure. In healthy subjects, it seems that VF makes accessible the refined dominant motor programs for the nondominant hemisphere giving rise to an increased interlimb similarity of the control structure. Interestingly, in stroke patients VF is able to manipulate the ILS of upper-limb kinematics in favor of finer motor control but a single training session seems not to be enough to fix those changes in the neuromuscular system of a damaged brain.*

*Overall, these findings offer a new promising framework to develop and assess an effective intervention to guide the restoration of the original neuromuscular patterns and avoid unwanted maladaptive neuroplasticity. In conclusion, this thesis seeks moving forward in the understanding of human motor recovery processes and their relationship with neuroplasticity. In this sense, it provides important advances in the design of a new biomarker of motor impairment and tests the power of VF to modulate the neuromuscular control of patients with stroke.*



# ACKNOWLEDGEMENTS

*Izozmendiaren koro erronkaria bailitzan, hiru dira tesi honen azalak erakusten dituen izenak. Kobentzionalismo akademiko hertsia menderatzerik balego oster, ugari beharko liratezke izan, hainbeste izan baitzarete lan honen itzalpean isilik baina tinko eusten egon zaretenok. Horregatik, azala ez bada ere, errekonozimendu oso osoa zuentzat da, zuei eskainia eskuartean duzuen nire bizitza zatia.*

*Zuei, aita eta ama, nigan sinistu eta naizena izaten lortzeagatik. Zuek piztu didazue inguruarekiko jakinmin bizia eta garatu erantzunak bilatzeko grin etenezina. Zuek izan zarete sostengu eta sustatzaile; gida eta txinparta; eta nahiz eta oraindik lana ez zaizuen falta doktoretza-programa honen izenburu zehatza gogoratzeko, zuek zarete dudarik gabe abentura irrikagarri honen erantzule nagusiak.*

*Zuri ere, Nekane, nire lanean erakutsi duzun konfidantza itsuagatik, beti niretzako izan dituzun adore hitz eta keinuengatik. Azken finean, lehenengo egunetik nire ondoan izateagatik inork sekula itzali ezingo dizun begi – disdira horrekin instant*



## ACKNOWLEDGEMENTS

---

*ilunenak argitzen. Sinistu ala ez, egunez egun erakutsi didazun harrotasun hura bihurtu zait edozein zailtasun menderatzeko gai izan den indar eta kemen.*

*A ti Javi, por estar siempre ahí, incondicionalmente ahí donde te he necesitado, cuidando de ese rincón de comprensión y calma que tan vital se convierte cuando se niega a escampar. Tuya es también parte fundamental de esas líneas invisibles que no han quedado escritas en estas páginas pero que forman parte de su contenido y esencia. Gracias por haber entendido las bondades y los caprichos de la investigación, por tu aliento incansable y tu apoyo sin restricciones. Has sido el mejor compañero de viaje que jamás hubiera podido imaginar.*

*No puc oblidar-me tampoc de la meva família catalana que tan bé m'ha cuidat quan la meva casa era lluny. Per de comptat gràcies, mil gràcies per fer-me sentir com a casa i ser-ne part de tot això.*

*Nire lagun eta kide guztiei, a tots els meus amics i companys, que han cedit generosament el temps que els hi corresponia en pro d'aquest repte, de vegades acaparador, de vegades solitari. Ezin denak zaituztet aipatu, tipi geratuko bailiratezke zuentzat ditudan hitz eta desio onak, però sabeu qui sou i sabeu per què sou qui sou.*

*A Carlos, que ha estado pacientemente a mi lado en todas y cada una de las sesiones experimentales, aportando su inestimable perspectiva clínica, compartiendo la alegrías propias de este trabajo pero también la frustración de la confabulación tecnológica (No me odies por arrastrarte al mundo de las ecuaciones diferenciales de la biomecánica y los códigos interminables de Matlab). Y por supuesto, a todos y cada uno de los pacientes que voluntariamente han accedido a someterse a los procedimientos experimentales, sin pedir nada a cambio y ofreciendo su mejor sonrisa y su conversación más personal. Gracias, gracias, gracias. Sin vosotros nada de esto hubiera sido posible. Ojalá la ciencia pueda compensar vuestra magnanimidad. ¡Sois enormes!*

*A Eloy y Josep Maria, mil gracias por permitirme compartir con vosotros la visión menos clínica y probablemente más abstracta de este mal que a tantos y tantas ha*



*robado su sonrisa. Gracias por creer en este proyecto y tender un puente a la ingeniería. Gracias, por abrirme la puerta de vuestra casa. No tengo palabras para expresar lo que ha significado contar con el potencial y el know-how del Institut Guttmann. ¡Simplemente una experiencia indescriptible que me llevo como científica, pero sobre todo como persona!*

*A todos mis compañeros de grupo, que en algún momento u otro me han acompañado en este largo camino. ¡Equipo! ¿Qué hubiera hecho sin vosotros todos estos años? Los primeros que ya volaron, Ainara, Cristian, Puy, y todos los compañeros de la UPC, gracias por mostrarme el corazón del grupo y hacerme sentir parte de esta gran familia. Los que fueron fugaces pero no por eso fútiles, Mireia, Joan, Sara y Yolanda, gracias por vuestro entusiasmo y vuestra frescura ¡Espero que esta vida os vaya preciosa! Y por supuesto, los que aún siguen, Manu (juntos zarpamos y juntos desembarcamos), Leo (mil gracias por sus buenos consejos, doctor), Luis (¿quién nos iba a decir que de pronto, esto era todo?), Javier, Dolores, Miguel Ángel, Roberto Bea, Jordi, Abel y todos los que seguro me dejo, habéis sido testigos y cómplices en primera persona de este viaje que llega a puerto. Gracias por acompañarme.*

*I per acabar o potser començar des del principi, els meus agraïments més sincers als artificis d'aquest projecte: els meus directors de tesi Àlicia i Raimon. Sé que no ha estat fàcil dirigir una tesi en una àrea tan diferent de la que estàveu acostumats. Els interminables debats sobre enfocaments, termes o estils que naixiem de la contraposició de dos mons aparentment tan propers m'han fet adonar dels mil colors que pinten la ciència; però també m'han fet créixer com a investigadora i desenvolupar aptituds que la uniformitat no m'hagués deixat veure. Per això agraeixo especialment que acceptéssiu aquest repte sens dubte doblement complicat. Admiro la vostra valentia per sortir fora de la vostra zona de confort i explorar noves perspectives. Ara entenc perquè esteu on sou. Per mi ha estat tot un orgull poder evolucionar de la mà de dos cervells de la vostra talla.*

*Finalment, gràcies a la Fundació LaCaixa per seguir apostant pel coneixement, per empoderar a les persones amb somnis i creure en una societat sàvia, però sobretot*



#### ACKNOWLEDGEMENTS

---

*crítica i exigent. Gràcies per posar els mitjans perquè preguntes que mai haguessin estat respostes esdevinguin camins prometedors cap al progrés.*

*Així doncs, per tots vosaltres és aquest petit reconeixement, para todos vosotros mi eterno agradecimiento por haber contribuido de una u otra manera a que este gran reto se haya hecho realidad. Zuentzat, bihotzez, esker mila.*







## ACKNOWLEDGEMENTS

---



“**IMPOSSIBLE** IS JUST A BIG WORD THROWN AROUND BY SMALL MEN  
WHO FIND IT EASIER TO LIVE IN THE WORLD THEY'VE BEEN GIVEN  
THAN TO EXPLORE THE POWER THEY HAVE TO CHANGE IT.  
IMPOSSIBLE IS NOT A DECLARATION. IT'S A DARE.  
IMPOSSIBLE IS NOT A FACT. IT'S AN OPINION.  
**IMPOSSIBLE IS POTENTIAL.**  
IMPOSSIBLE IS TEMPORARY.  
IMPOSSIBLE IS **NOTHING.**”

MUHAMMAD ALI



## ACKNOWLEDGEMENTS

---



# PREFACE

## I. OBJECTIVES

This present work is motivated by the relative inefficiency of stroke rehabilitation strategies that make the life of millions of stroke survivors from all over the world awfully complicated. An insightful revision of the state of the art has driven us to identify two major handicaps that hinder the design of effective therapeutic interventions.

On the one hand, there is a concerning lack of standardized objective assessment measures that often lead to inconsistent conclusions from patient to patient and from study to study. It has to be highlighted that stroke patients form an extremely heterogeneous population, posing an added difficulty to the already complex task of



measuring motor impairment and recovery. Besides, existing measures do not provide neuromuscular information about the patient, hampering the understanding of physiological processes underlying motor recovery.

On the other hand, most of the rehabilitative interventions are motivated by empirical (and often qualitative, even subjective) observation of recovery. In other words, these practices are not evidence-based. In general, studies to evaluate effectiveness or to identify which mechanisms are activated by the intervention are never performed or performed after their development and insertion in the clinical practice. As a result, it is very difficult to select the therapy that best fits to the specific needs of each patient and to reliably predict the expected prognosis.

Therefore, the present thesis has been structured into two clearly defined branches to give response to these two major problems.

## MAIN OBJECTIVE

This thesis aims to improve the outcome of upper-limb stroke rehabilitation by:

- Providing a new physiological scale based on the neuromuscular state of the patient to objectively measure motor impairment and the rehabilitation efficiency. Such scale should avoid the negative effect of high inter-subject variability
- Identifying new therapeutic strategies able to modulate the neuromuscular state of patients and boost neurorehabilitation



## SPECIFIC OBJECTIVES

In order to adequately orient the research and facilitate the accomplishment of the aforementioned main objectives, we have identified 4 key areas of study: (1) understanding stroke, (2) understanding motor coordination, (3) setting a physiological scale of motor impairment and (4) identifying key rehabilitation strategies. Within each key area, we have defined a series of specific objectives to be targeted by the present work:

### ► *Understanding Stroke*

- To get familiar with socio-clinical aspects of stroke including
  - Post-stroke consequences, with a special focus on upper-limb motor impairments
  - Traditional and emerging rehabilitation strategies
- To identify the main drawbacks and needs of current rehabilitation protocols

### ► *Understanding Motor Coordination*

- To investigate the intact movement coordination system from a neuromuscular point of view: EMG and muscle synergies
- To check the existence of “healthy movement” patterns that generalize across subjects or across the limbs of the same subject
- To investigate the stroke affected limb’s coordination system from a neuromuscular point of view: EMG and muscle synergies
- To identify the neuromuscular differences that explain impaired motor function
- To select key physiological features to be targeted by a new rehabilitation protocol



► *Setting a Physiological Scale of Motor Impairment*

- To find markers of impaired coordination that are objective and quantitative and reflect the neuromuscular state of the subject
- To validate those markers with clinical scales such as Fugl-Meyer Assessment Scale or Functional Independence Measurement (see subsection 2.1.2 Tests handed out to assess subjects within PART II. METHODS for further information about these scales)

► *Identifying Key Rehabilitation Strategies*

- To define the features of healthy movement coordination to be targeted by rehabilitation
  - Kinematic and kinetic parameters
  - Physiological parameters
- To study the characteristics of existing rehabilitation strategies to identify potential candidates that (1) are able to induce neuroplastic changes while (2) staying cheap and easily implantable
  - Visual Feedback (VF)
  - Neuromuscular Biofeedback
  - Non invasive brain stimulation
  - Robotic Therapy
  - Virtual Reality Gaming
- To test the efficacy of the selected rehabilitation strategy (VF) on regaining motor function, by studying how it affects the neuromuscular system and by verifying whether it can help reestablishing the aforementioned 'healthy pattern'



## II. ORGANIZATION OF THE MANUSCRIPT

This thesis is organized into 7 major parts identified by Roman numerals. These are divided into a variable number of chapters indicated in Arabic numerals (X), which in turn, are divided into several sections (X.X) and subsections (X.X.X.).

### **PART I. INTRODUCTION**

*We introduce the pathogenesis of stroke and its clinical management paying special attention to upper-limb motor impairment. We also review current advances in the field of neurorehabilitation, motor coordination and kinematics of human motion to set the basis of the main research lines presented here and help the reader understand the experiments developed hereafter. Each of these subsections specifically addresses how these advances are related to stroke.*

### **PART II. METHODS**

*This part describes the methods employed in the thesis that are common to all four studies in part III. In broad outline, we explain in detail the experimental protocol, the acquisition process of electromyographic and kinematic data, and how these data are processed and interpreted to get the control structure and quantify the interlimb similarity.*

*Note that methods that are specific to a given study of part III are summarized in a dedicated subsection termed “Specific procedures” within each study.*



### **PART III. STUDIES**

*This part depicts the main scientific milestones contributed by the present work. The section is divided into four studies that address a specific question within the investigation:*

#### **Study 1. Interlimb similarity in healthy subjects**

*Do we share the control strategy in our two arms?*

#### **Study 2. The effect of Visual Feedback in the motor control**

*Has VF the ability to modulate the control strategy of our motor system?*

#### **Study 3. Interlimb similarity in patients with stroke**

*How is the ILS altered in patients with stroke? Can VF manipulate altered ILS?*

#### **Study 4. Kinematic analysis of movements of patients with stroke**

*Is the alteration of the control structure reflected in movement kinematics?*

*Each of these four studies is a self-contained piece of research and is organized into three main subsections: (1) Specific procedures, (2) Results and discussion and (3) Specific Conclusions. As stated previously, (1) Specific procedures describes methods that are only used in the enclosing study. Note that general methods common to all studies are described in the Methods section. Following the same logic, (2) Results and discussion reports the most remarkable findings of each study, and discusses them with regard to existing theories and related investigations. Finally, (3) Specific conclusions are separately exposed and recapitulate the main findings obtained in each study.*

### **PART IV. CONCLUDING REMARKS**

*This part summarizes the major findings contributed by the present thesis. It is the result of an intensive synthesis work that interrelates the results exposed in the four studies of results and highlights the most important contributions to the existing knowledge.*



**PART V. BIBLIOGRAPHY**

*This part lists the scientific references used to review the state of the art, build the working hypotheses and discuss the results found.*

**PART VI. DERIVED PUBLICATIONS**

*This section lists the main scientific contributions produced by this thesis.*

**PART VII. APPENDICES**

*Appendices contain complementary information that may be useful to extend the understanding of the concepts presented here.*



## PREFACE

---



# ABBREVIATIONS

---

## A

---

A	area between the curves
AC	acromion
ADL	activities of daily living

---

## B

---

BB	biceps <i>brachii</i>
BRD	brachioradialis

---

## C

---

CC	cross-correlation coefficient
CNS	central nervous system

---

## D

---

D	dominant arm
DA	deltoid anterior
Deg	degree
DM	deltoid medial
DOF	degree of freedom

---

## E

---

EExt	elbow extension
EFlex	elbow flexion
EMG	electromyography



## ABBREVIATIONS

### F

FIM	functional independence measure
FM	Fugl-Meyer assessment scale
FM-UE	FM for the Upper Extremity

### I

ILD	interlimb differences
ILS	interlimb similarity
ILS <sub>k</sub>	kinematic ILS
IMT	intermanual transfer
IS	infraspinalis

### H

H <sub>i</sub>	<i>i-th</i> activation coefficient
HD	Hausdorff distance

### L

L	left (arm, hemisphere)
LI	laterality Index

### N

ND	nondominant arm
NMF	nonnegative matrix factorization
nVF	no visual feedback

### P

P <sub>i</sub>	<i>i-th</i> patient
PM	pectoralis major

### R

R	right (arm, hemisphere)
ROM	range of motion

### S

S <sub>i</sub>	<i>i-th</i> subject
SAbd	shoulder abduction
SAdd	shoulder adduction
SD	standard deviation
SERot	shoulder external rotation
SIRot	shoulder internal rotation
SP	scalar product

### T

TBL	triceps <i>brachii</i> long head
TS	trapezius superior

### V

VAf	variance accounted for
VF	visual feedback

### W

W <sub>i</sub>	<i>i-th</i> muscle synergy
----------------	----------------------------





## **PART I**

# **Introduction**







# 1 STROKE

A stroke is a cerebrovascular disease that occurs when the supply of blood to the brain is either interrupted or reduced. If such interruption lasts more than a few seconds, the brain does not get enough oxygen or nutrients, which causes brain cells to die within minutes<sup>1</sup>. A stroke can cause lasting brain damage, long-term disability or even death.

## 1.1 TYPES AND CAUSES

Stroke can be classified into 3 main different types depending on its cause:

1. **Ischemic stroke** is the more common kind of stroke (~85%<sup>2</sup>) and occurs when a brain blood vessel is blocked by a blood clot. If the clot is formed *in situ* in an artery that is already narrow, the stroke is called **thrombotic stroke**. In contrast, if the clot is formed in a different place of the body and travels up to the brain, then the stroke is called **embolic stroke**.
2. **Hemorrhagic strokes** occur when a blood vessel becomes weak and bursts open causing a blood leakage into the brain. This kind of stroke is more likely in patients having defects in the blood vessels such as aneurysm or arteriovenous malformation (AVM)<sup>3</sup>. In Spain, 15% of the strokes are hemorrhagic strokes<sup>2</sup>.



3. **Transient Ischemic Attacks** (TIA) occur when the blood supply to the brain is briefly interrupted. These are also known as mini-strokes. The patients experience stroke-like symptoms but they disappear within a day and do not cause permanent damage.

## 1.2 STROKE STATISTICS

### 1 | Overview

- Stroke is the 2<sup>nd</sup> leading cause of death in Europe <sup>4</sup> and 4<sup>th</sup> leading cause of death in the US (after heart disease, cancer and chronic lower respiratory diseases) <sup>5</sup>
- In Spain, stroke is the 1<sup>st</sup> cause of death in women and 2<sup>nd</sup> in men <sup>6</sup>
- In Spain, one person has a stroke every 6 minutes (120,000 people/year) and as a consequence, one person dies every 18 minutes <sup>6</sup>
- 20-30% of the strokes are fatal <sup>2,7</sup>
- 60% of these deaths occur in females
- 75% of strokes occur in people aged over 55-65 years <sup>6,8</sup>, and the risk increases proportionally with age.
- In about a third of strokes in younger adults (<65 years), a cause cannot be identified <sup>9</sup>

### 2 | Morbidity

- Stroke is a leading cause of adult disability
- More than half of all stroke survivors are left dependent for everyday activities <sup>10</sup>
  - 42% will be independent
  - 22% have mild disability
  - 14% have moderate disability
  - 10% have severe disability
  - 12% have very severe disability <sup>11</sup>
- Stroke causes a greater range of disabilities than any other condition <sup>12</sup>



### 3 | Financial Impact of Stroke

- Stroke is one of the most serious socio-sanitary problems <sup>6</sup>
- In some developed countries the direct costs of stroke represent between the 2% and 4% of the total sanitary expenses <sup>6</sup>
- Each stroke costs approximately 4,000€ during the first three months post-stroke, excluding sick leaves <sup>6</sup>
- Stroke costs the EU over 38 billion euros a year <sup>7</sup>
- In Spain, stroke costs over 6,000 million euros a year. That is approximately the 5% of the total sanitary expenses <sup>2</sup>
- In the UK, the costs of stroke are estimated to range between £3,7 billion and £8 billion including direct health care costs, productivity losses due to mortality and morbidity and informal care costs <sup>7, 13</sup>.

## 1.3 SYMPTOMS DURING A STROKE

The symptoms caused by a stroke may be very diverse and depend on how severe the stroke is and the part of the brain that has been damaged. In some cases, a patient may not notice that a stroke has occurred. In other cases, symptoms may burst intermittently for the first day or two. In general, most of the symptoms develop suddenly and without warning. These may include:

- Severe headache if stroke is caused by bleeding
- Change in alertness including sleepiness, unconsciousness and come
- Confusion or loss of memory
- Personality, mood or emotional changes



- Changes in taste and touch including the ability to feel pain pressure or different temperatures
- Problems with eyesight, including decreased vision, double vision or total loss of vision
- Clumsiness, dizziness or abnormal feeling of movement
- Loss of balance and coordination
- Muscle weakness in the face, arm or leg, usually on one side of the body
- Numbness or tingling on one side of the body
- Trouble walking
- Difficulty swallowing
- Difficulty writing, reading, speaking or understanding speech

## 1.4 TREATMENT

Stroke constitutes a medical emergency, so it should be treated urgently as soon as any of its symptoms are detected. Treatment will depend on the cause of the stroke. Thus, medical examination is needed to confirm the stroke and elucidate the causes behind it. If the stroke is caused by a blood clot, a clot-busting drug may be given to dissolve the clot. To be effective, this treatment must be started within 3 to 4.5 hours after the first symptoms have appeared. Other treatments include:

- Blood thinners
- Medicine to control symptoms such as high pressure
- Special procedures or surgery to relieve symptoms or prevent more strokes
- Nutrients and fluids
  - Feeding tube in the stomach



## 1.5 PROGNOSIS AND POST-STROKE CONSEQUENCES

The outlook of stroke depends on several factors:

- The type of stroke (*ischemic strokes have a higher survival rate*)
- The amount of brain tissue that has been damaged
- The brain part that has been damaged (*the affected brain zone determines the impaired body functions*)
- The elapsed time from the stroke onset and the treatment (*prompt treatment can reduce the damage to the brain and the risk to have another stroke*)
- The elapsed time from the stroke onset and rehabilitation (*early rehabilitation has been proven to improve the prognosis*)

Stroke is a fatal condition: approximately 1 out of 5 people die as a consequence of a stroke. Of those who survive to stroke, 58% will be affected by a mild to very severe disability<sup>5</sup>. The post-stroke consequences are very diverse both in nature and severity. Stroke can produce cognitive impairment, swallowing problems or emotional alterations. A detailed list of post-stroke consequences and the associated prevalence is listed in **Table 1**.

In any case, one of the most common consequences post-stroke is motor impairment. Most exactly, upper-limb motor impairment. It is estimated that after stroke, 80% of patients experience acute hemiparesis, whose recovery will strongly depend on the initial motor damage. According to a prospective study developed on 421 stroke patients, 79% of patients with mild upper-limb motor impairment recovered full functionality, whereas only 18% of patients with severe hemiparesis were able to do it<sup>14</sup>.



Furthermore, it has to be taken into account that stroke is a recurrent condition. Having a stroke increases the risk for another (secondary) stroke. Although the risk for a second stroke decreases after the first 3 months following the first stroke <sup>6</sup>, at least 25% of the subjects that suffered a stroke will have a secondary stroke within their lifespan <sup>15</sup>. Fortunately, approximately 80% of secondary stroke may be prevented by acquiring healthy habits and medical interventions. This is critical because recurrent strokes have higher death and disability rates given that the brain is already injured by the original stroke <sup>15</sup>.

<i>DIFFICULTY</i>	<i>PEOPLE AFFECTED (%)</i>
<b><i>General movement</i></b>	80%
<b><i>Arm movement</i></b>	70%
<b><i>Arm hemiparesis</i></b>	40%
<b><i>Walking</i></b>	20%
<b><i>Spasticity</i></b>	19-38%
<b><i>Altered sensation</i></b>	80%
<b><i>Swallowing</i></b>	40%
<b><i>Aphasia</i></b>	33%
<b><i>Visual problems</i></b>	66%
<b><i>Depression</i></b>	29%
<b><i>Emotionalisms in the first 6 months</i></b>	20%
<b><i>Ongoing emotionalism</i></b>	10%
<b><i>Dementia 6 months post-stroke</i></b>	20%
<b><i>Central post-stroke pain</i></b>	5-20%
<b><i>Incontinence one year post-stroke</i></b>	15%

Table 1 Specific consequences post-stroke. Source: <sup>5</sup>



### 1.5.1 *Motor consequences post-stroke*

As previously mentioned, stroke most frequently affects human motion (**Table 1**) producing different ranges of hemiparesis. This means that the movement deficits are limited to the limb contralateral to the side of stroke. Although this thesis focus on the upper limb hemiparesis because it is the most common consequence post-stroke, the motor effects caused by stroke are indistinctly found in the upper and lower limbs and can be summarized in this list:

- **Weakness**: stroke causes weakness in specific muscles
- **Abnormal muscle tone**: during the first stages of stroke, patients present muscle flaccidity that is substituted by increased spasticity in the subsequent recovery phases (see section 3.2 **The 7 stages of motor recovery**).
- **Abnormal postural adjustments**: stroke patients develop compensatory movements to overcome the motor limitation imposed by the disease
- **Pathological synergies**: stroke produces the coupling of muscle-activation
- **Lack of mobility between structures**: stroke reduces the mobility of the shoulder girdle and the pelvic girdle. It seems that during the initial recovery phases, stroke patients fixate selected body segments to diminish motor complexity by reducing the number of motor element that the CNS must control to accomplish a given task.
- **Lost of interjoint coordination**: stroke alters the capacity to coordinate multiple joints during complex tasks such as reaching, giving rise to abnormal movement patterns.
- **Abnormal timing**: stroke alters the timing of components forming a task, producing abnormal movement patterns.



The conjunction of all these effects produces important alteration in the motor capacity of patients with stroke that limits their autonomy and capacity to perform ADLs <sup>14</sup>.



## 2 MOTOR IMPAIRMENT SCALES

Stroke scales aim to summarize the deficits of stroke survivors. These scales document and communicate baseline deficits, track changes over time, and provide prognostic information <sup>16</sup>. Properly evaluating post-stroke patients is a key part of the quality of their care as highlighted by the international guidelines for the management of stroke patients <sup>17</sup>.

In the clinical practice, multiple scales are used to measure different aspects of stroke. Some of them are specific to stroke and many others are extensible to other neurological impairments that share some of their features with stroke. This section briefly introduces some of the most widely used scales in the field of stroke.

### 2.1 CLASSIFICATION AND TYPES

Depending on the scope of the scale, the motor impairment scales are classified into two types: Clinical Scales and Outcome Scales.

#### 2.1.1 *Clinical Scales*

Clinical scales are used to classify stroke and assess baseline stroke severity. These are some of the most widely used scales.



- The National Institutes of Health Stroke Scale (NIHSS)
- The Canadian Stroke Scale (CSS)
- The Scandinavian Stroke Scale (SSS)
- Oxfordshire Classification
- Mathew Scale [Out of use]
- Orgogozo Scale [Out of use]
- Hemispheric Stroke scale [Out of use]

#### 2.1.1.1 *The National Institutes of Health Stroke Scale (NIHSS)*

The NIHSS is a 15-item clinical deficit scale conceived in 1989 to evaluate ability. The NIHSS assesses levels of consciousness, gaze, vision, facial palsy, arm and leg strength, limb ataxia, sensory loss, neglect, dysarthria, and aphasia. Inter-rater agreement ( $K = 0.69$ ) and intra-rater ( $K = 0.77$ ) agreement are very good specially when the rater is a neurologist<sup>18</sup>.

#### 2.1.1.2 *The Canadian Stroke Scale (CSS)*

The CSS is a 4-item scale that assesses motor function differently depending on the cognitive state of the patient. The CSS focuses on consciousness, language and motor function. In addition, it strongly predicts mortality at 1 month and 1 year. The CSS is a validated scale that has been used in clinical trials. The scale correlates well with the NIHSS but it underestimates functional impairments<sup>19</sup>.

#### 2.1.1.3 *The Scandinavian Stroke Scale (SSS)*

The SSS is a 3-item acute scale that assesses speech, facial palsy and gait. It has been used in several clinical trials to either select patients or rate outcome severity<sup>19</sup>. The system has not been tested for validity, reliability or interrater and intrarater reproducibility.

#### 2.1.1.4 *The Oxfordshire Classification*

The Oxfordshire classification is a simple symptom observation test that classifies stroke into 4 categories (Total Anterior Circulation Syndrome, Partial Anterior Circulation Syndrome, Lacunar Circulation Syndrome or Posterior Circulation



Syndrome) according to the type and severity of the neurological impairments apparent in the initial examination<sup>19</sup>.

### 2.1.2 *Outcome Scales*

Outcome scales are used to assess disability following stroke and monitor changes over time. These are some of the most widely used scales.

- The Modified Rankin Scale (mRS)
- The Barthel Index (BI)
- The Glasgow Outcome Scale (GOS)
- Fugl-Meyer Assessment of Motor Recovery after Stroke (FMA)

#### 2.1.2.1 *The modified Rankin Scale (mRS)*

The Rankin Scale is 6-point scale (from 0 to 5) developed in 1957 and later modified to assess the extent of the disability after stroke. The mRS has moderate to excellent interrater reliability and it is considered more powerful than the Barthel Index (BI) as a primary endpoint in clinical trials of stroke therapy<sup>19</sup>.

#### 2.1.2.2 *The Barthel Index (BI)*

The BI is a 10-item test that measures the patient's degree of independence on performing activities of daily living (ADL) such as feeding, chair/bed transfer, grooming, toileting, bathing, walking, stair climbing, dressing, bowel and bladder control. The BI is the most common measure of ADL competence in clinical practice. The BI has been validated by many groups<sup>19</sup>.



#### 2.1.2.3 *The Glasgow Outcome Scale (GOS)*

Initially conceived to rate neurological injury, the GOS is a single-item scale often used in stroke studies. Similar to the mRS, the GOS classifies disability into 5 categories. It has an interrater reliability of 67% but it substantially duplicates the information provided by the mRS<sup>19</sup>.

#### 2.1.2.4 *The Fugl-Meyer Assessment Scale (FM)*

The FM is a 226-item scale designed to evaluate recovery in post-stroke hemiplegic patients across 5 different domains: motor function, sensory function, balance, joint range motion and joint pain. Due to its extension, about 30 minutes are needed to administer the test. A sample of the evaluation sheet can be found in<sup>20</sup> and in Appendix B. The FM has an excellent internal consistency and inter-rater/intra-rater reliability<sup>21</sup>. As a consequence, it is one of the most widely used quantitative measures of motor impairment<sup>22</sup>. In research, the FM is considered a gold-standard to assess motor impairment post-stroke: it is extensively used to validate new scales<sup>23,24</sup>, to assess novel therapeutic approaches<sup>25</sup> and even included in models to predict the outcome of rehabilitation<sup>26,27</sup>. More information can be found in section Fugl-Meyer Assessment scale (FM)).



## 2.2 LIMITATIONS

Due to the incomplete understanding of the processes underlying motor impairment and recovery, measuring the extent of motor deficits and rehabilitation is not a trivial task. Current clinical scales rely on the concept that stroke patients progress through a sequence of well-defined recovery phases (see section **3.2 The 7 stages of motor recovery**). Therapists base their assessment on their visual appreciation of the functional outcome of patients. Obviously this kind of methods are dramatically subjected to the therapist's appreciation, and in consequence, suffer from high inter-rater variability.

In addition, scales based on visual observation completely ignore the neuromuscular state of the patients. Similar symptoms (e.g. lack of mobility) may be produced by totally different causes (e.g. muscle weakness, unrepaired neural damage, spasticity...) that may even occur simultaneously giving rise to extremely complex clinical outcomes. As a result, within this black box it is very complicated to devise the physiological mechanisms underlying motor recovery during rehabilitation.

The application of motor impairment scales generally concludes with a score, either numerical or categorical. The problem here is that this score is not clinically informative<sup>17</sup>. That is, there is not a clear correspondence between the score and what this score means in terms of motor recovery, functional autonomy or disability. Therefore, the interpretation of each scale is limited to numerical increases or decreases that are difficult to identify with ongoing physiological processes. Naturally, the chance to make informed decisions in clinical management is dramatically hindered.



Currently there are tens of available scales that assess a different aspect of the motor function with no well-defined gold-standard nor consensus on the use of one specific scale <sup>28</sup>. However, there is little correspondence between them. Naturally, applying all the available scales to each patient in order to get a complete motor evaluation is virtually impossible in terms of time and resources. Several attempts have been made to define standardized cut-offs to consistently stratify the outcome of the scales according to the level of recovery <sup>29,30,31</sup>. However, the high variability found between scales proves the extreme complexity of the motor recovery process.

Precisely, the tremendous heterogeneity found in stroke poses additional problems to this issue. Just to mention a few: motor recovery is a dynamic process that progresses with time, the initial state of the patients affects the final outcome, and the rate of change may during recovery vary between different levels of ICIDH (International Classification of Impairments, Disabilities and Handicaps)<sup>29</sup>. The ICIDH is the model of illness accepted by the World Health Organization to categorize the consequences caused by a given disease. Such is the natural complexity of the context that there is increasing suspicion that the lack of optimal assessment measures may have made the evaluation of benefits of new therapies less likely <sup>32-34</sup>.

Taken everything together, the need to develop new quantitative scales is a critical obstacle that needs a workaround to advance in the field of motor recovery and rehabilitation. Similarly, the establishment of a gold standard is essential: the interpretation of results would be simplified, new therapeutic interventions could be validated, reliable comparisons between studies would be facilitated and meta-analysis would be much easier (and powerful).



# 3 POST-STROKE REHABILITATION

Although after stroke, our brain has certain degree of spontaneous recovery, most stroke survivors undergo a wide range of disabilities (see **Table 1**) that require rehabilitation. Essentially, the goal of treatment after stroke is to recover as much function as possible and prevent future strokes.

Within 24 to 48 hours after the stroke, rehabilitation is performed right in the hospital and involves promoting independent movement because many individuals are paralyzed or seriously weakened. While patients recover basic skills during the 6 months after stroke, they attend rehabilitation to relearn progressively more complex and demanding tasks, such as bathing, dressing, and using a toilet. Beginning to reacquire the ability to carry out basic activities of daily living represents the first stage in a stroke survivor's return to independence.

Problems moving, thinking and talking often improve in the weeks to months after stroke. For some stroke survivors, though, rehabilitation will be an ongoing process to maintain and refine skills and could involve working with specialists for months or years after the stroke.



## 3.1 REHABILITATION AREAS

There are many and very diverse available rehabilitation approaches to overcome the limitations imposed by stroke. Depending on the target rehabilitation-objective, we can differentiate 5 main rehabilitation areas.

### *3.1.1.1 Language, speech and memory problems*

Patients may have trouble communicating, thinking clearly or with memory after stroke. Speech and language therapists can help learning ways to communicate and improve the memory.

### *3.1.1.2 Muscle and nerve problems*

Stroke may affect only one side or part of one side of the body, causing paralysis or muscle weakness. Physical and occupational therapists can help strengthen the muscles and relearning how to do daily activities.

### *3.1.1.3 Bladder and bowel problems*

Stroke can affect the muscles and nerves that control the bladder and bowels. Medicines and a bladder or bowel specialist are designated to treat these problems.

### *3.1.1.4 Swallowing and eating problems*

Patients may have trouble swallowing after stroke. Speech therapists are indicated to palliate these issues.

### *3.1.1.5 Emotional issues and support*

Stroke survivors may experience quick mood changes and changes in their behavior and judgment. This may make them feel scared, anxious and depressed. Joining patient support groups and visiting professional counselors is strongly recommended.



## 3.2 THE 7 STAGES OF MOTOR RECOVERY

Upon observation of thousands of patients, the Swedish physical therapist Signe Brunnstrom divided the motor recovery post-stroke process from hemiplegia into 6 stages (7, if we include the last recovery stage) <sup>35</sup>.

1. **S1 | Flaccidity:** the patient has no voluntary movements in the affected areas
2. **S2 | Spasticity:** the patient regains small amount of *involuntary* motor function. These first movements are small, spastic and abnormal.
3. **S3 | Increased spasticity:** spasticity reaches its peak and the first minimal voluntary movements emerge. However, these are still small and abnormal, and strongly subjected to pathological synergies.
4. **S4 | Decreased spasticity:** spasticity begins to decline and the patients starts to regain considerable amount of motor function still subject to strong pathological synergies. Nevertheless, movements begin to approach more normal and controlled patterns.
5. **S5 | Coordination:** patients start to be able to deal with pathological synergies, giving rise to more coordinated and complex voluntary movements. During this stage, both spasticity and abnormal movements continue to decline.
6. **S6 | No spasticity:** muscle spasticity disappears completely. The patient regains the ability to control joints individually and coordinates complex reaching movements.
7. **S7 | Recovery:** the patient regains full motor function in the affected areas.



It is interesting to acknowledge that this model of sequential recovery has influenced the development of multiple motor assessment scales that are currently applied in the clinical environment. Among them, probably the Fugl-Meyer (FM-UE) scale of the upper extremity is the best known method<sup>36</sup>.

### 3.3 UPPER LIMB MOTOR REHABILITATION STRATEGIES

About 85% of patients admitted to a hospital for stroke present problems with their arms and hands<sup>37</sup>. Furthermore, stroke-related physical impairments such as muscle weakness, pain, and spasticity can lead to a reduction in the ability to use the stroke-affected arm and hand in daily activities.

There are many rehabilitation protocols designed for regaining function and improving everyday skills. However, the motor rehabilitation protocols for patients with stroke are specifically tailored considering the specific characteristics of the impairments caused by stroke, such as hemiplegia, neurological damage or the advanced age of patients. The list below summarizes the major approaches to stroke rehabilitation:

#### 3.3.1 *Physical rehabilitation*

**Task Specific Rehabilitation.** Task specific rehabilitation is aimed at improving motor skills in performing selected movements and functional tasks. The arm is trained in a functional context to re-learn how to open a bottle, drink a glass of water, or stand up from bed. That way, the individual concentrates on the task, rather than on the specific movement components of the task<sup>38</sup>. Current research suggests that this type of training promotes more functional improvement than traditional rehabilitation<sup>39,40</sup>.

**Task-oriented rehabilitation.** Task oriented rehabilitation focuses on retraining functional tasks by taking into account the interaction of the muskuloeskeletal, perceptual, cognitive and neural systems and the environment. The Bobath concept is an example of this approach. It is applied in the patient assessment and treatment of



different neurological impairments such as stroke<sup>41</sup> or cerebral palsy<sup>37</sup>. The goal is to promote motor learning for efficient motor control in various environments, thereby improving participation and function. This is done through specific patient handling skills to guide patients through initiation and completion of intended tasks<sup>38</sup>.

At its earliest conception, the Bobath concept was focused on regaining normal movements through re-education. Since then, it has evolved to incorporate present-day knowledge on biomechanics, neural and muscle plasticity motor learning and motor control<sup>42,43</sup>. However, despite widespread acceptance of the Bobath concept in stroke rehabilitation, literature has not found it to be superior compared to other treatment approaches<sup>44,45</sup>.

*Range-of-motion therapy* uses stretching exercises and other treatments to help lessen muscle tension and spasticity and regain range of motion. Sometimes medication can help as well.

*Neurofacilitation*. Neurofacilitation strategies aim at retraining motor control by inhibiting abnormal actions (e.g. Constraint Induced Therapy) or promoting movement (e.g. Bilateral Training).

*Constraint-Induced Movement Therapy (CIMT)*. CIMT involves restricting use of the unaffected limb for several hours a day by putting a mitt on it and performing tasks over and over with the affected arm in order to promote its use and improve its function. The EXCITE trial, conducted at 7 academic institutions between 2001 and 2003, showed that this technique promoted use of the affected arm in people with mild to moderate stroke impairment. Improvement lasted at least two years<sup>46</sup>. Other



research is showing that CIMT can actually cause the brain to reorganize and produce significant functional improvement <sup>47</sup>.

*Bilateral training.* Bilateral training involves the execution of identical activities with both arms simultaneously. The existing tendency towards in-phase (i.e., symmetrical movements) and anti-phase (i.e., alternating movements) coordination in healthy subjects suggests a coupling between the upper limbs <sup>48</sup>. Bilateral training exploits the assumption that this coupling facilitates the functional recovery of the impaired arm <sup>49</sup> by activating the intact hemisphere to facilitate the activation of the damaged hemisphere though enhances interhemispheric inhibition <sup>50</sup>. Whether this therapy is superior to other training approaches is a controversial issue: some studies find no significant benefit on using this therapy <sup>51–53</sup> while others describe strong evidence in favor of it <sup>54,55</sup>. For instance, a study using the BATRAC system revealed that although functional improvements achieved by either conventional or bimanual therapy were comparable, the later promoted greater adaptation in brain activation <sup>56</sup>. These differences may arise from the heterogeneity of training protocols and devices used in the therapy.

### 3.3.2 *Technology-assisted rehabilitation*

*Functional Electrical Stimulation (FES)* involves using electrical stimuli to stimulate nerve activity causing their innervated muscles to contract. This way, movement is produced by acting on the natural actuators of the body <sup>57</sup>. FES is usually used to strengthen weak or spastic muscles and prevent muscle atrophy <sup>58</sup>. It also may help with muscle re-education, for instance, by opening a contracted hand. In combination with conventional rehabilitation, FES has been shown to improve rehabilitation outcome <sup>59</sup>.

*Robotic technology* uses robotic devices to assist impaired limbs to perform more repetitive, consistent and measurable motions <sup>57</sup>. Several reviews suggest that robotic therapy improves motor impairment and strength but do not improve the ability to perform ADLs <sup>60,61</sup>. In contrast, some authors conclude that robotic therapy



alone does not produce any beneficial effect on regaining strength and function but combined robotic/physical therapy seems to be more effective than any of them alone<sup>62</sup>. In addition, the progressive shortage of therapists and the increasing number of people needing rehabilitation may benefit from the advanced capacities of robotic devices to assist ADLs and perform highly repetitive tasks as stand-alone or barely supervised systems<sup>57</sup>.

*Virtual reality (VR) and gaming.* This approach provides a realistic, simulated and interactive 3D environment where the patient can perform functional tasks. VR strategies are highly engaging, which is essential to optimize motor learning<sup>39</sup> and can be easily tailored to the individual needs of the patient. Studies have shown that virtual tasks transfer to comparable real world activities and promote higher cardiovascular activity levels during rehabilitation, improving cortical plasticity<sup>63</sup>. Also, gaming is likely to activate the mirror neuron system, shown to have a positive impact on stroke rehabilitation<sup>64</sup>, as the gamer sees an avatar concurrently performing the virtual activity on the screen. Different studies evidence that interactive gaming improves arm function and ADL function. However, it is unclear whether it can help increasing grip strength or gait<sup>65</sup>. Thus, it is essential to identify the key characteristics of this new approach to improve rehabilitation protocols<sup>65</sup>.

*Noninvasive brain stimulation.* Techniques such as Transcranial Magnetic Stimulation (TMS) or Transcranial Direct Current Stimulation (tDCS) of the lesional, contralesional, or bilateral hemispheres of the brain can alter cortical excitability to induce brain plasticity<sup>66</sup>. The primary motor cortex (M1) is the major target of this kind of therapy. Indeed, many studies describe the improvement of at least one motor function after stimulating of the ipsilesional M1<sup>67</sup>. This approach has also been successfully applied in the treatment of aphasia after stroke<sup>68</sup>.



*Biofeedback.* In general terms, the aim of biofeedback is to teach the individual how to modulate his/her physiological activity to promote health and performance. Biofeedback techniques let the individual be aware about the biological functions he/she usually is unconscious of (e.g. heart activity, brain activity or stomach pH). In the field of stroke, biofeedback is centered on monitoring brain and muscle activity. This might help creating greater awareness of muscle contractions and facilitating muscle relaxation and muscle coordination. However, recent studies have described no significant improvement in functional recovery<sup>69,70</sup>.

*Visual feedback.* Visual feedback (VF) consists on providing an external visual cue where the individual can observe his/her own image while performing a given exercise. This method is based on the idea that motor learning occurs due to the iterative corrections of motor errors during movement execution<sup>71</sup>.

But how are motor errors detected? It is believed that the cerebellum possesses an internal efferent copy of our motor system that allows predicting the consequences of the motor commands before they happen, and of course, before the information from the sensory feedback is available<sup>72, 73</sup>. As a result, our brain combines the information from sensory feedback (within which the VF lays) and the information from the predictions of our efferent copy to detect and correct the motor errors on-line.

The role of VF in all this complex process is enormous. We use VF to locate targets, orient our body and detect obstacles. Indeed, the movement of the upper limb can be modeled as a superposition of smooth submovements and it has been suggested that these submovements correspond to visual corrections<sup>74</sup>. This model is consistent with many experiments<sup>75-77</sup>. Indeed, it has been proven that VF boosts the process of motor learning<sup>78</sup>.

Mirror VF is one of the recommended strategies to enforce stroke rehabilitation<sup>79</sup>, as it is simple, inexpensive and can be easily implantable in almost any medical center. What is most appealing is that VF has shown promising results in the rehabilitation of stroke and related syndromes<sup>80,81, 82</sup>. VF allows tracking the position



and velocity of the body during movement execution. This is one of the basis of motor control since our brain uses position and motion feedback to control and correct our movements online<sup>83, 71, 84</sup>. In addition, VF is likely to active neural zones similar to those activated during motor imagery<sup>85</sup>.

Another interesting feature of VF is its ability to induce neural plasticity to improve motor performance<sup>86, 87</sup>. Neurological studies reveal increased ipsilateral M1 activation<sup>86</sup> and reciprocal inter-hemispheric inhibition<sup>85</sup> due to VF. In this sense, it has been demonstrated that the effect of VF affects both ipsilateral and contralateral neural zones, so it has been suggested that VF can help modulating the motor control of the paretic hand<sup>88</sup>.

Although a number of authors have investigated the neurological effects of VF<sup>86,88</sup>, the exact mechanism underlying the beneficial effects of VF remains unclear. This limits the optimal use of VF in clinical practice. Furthermore, the impact of VF in the control structure has not been addressed yet, which is undoubtedly essential to understand the motor learning process and help improving the rehabilitation of neural conditions.

### 3.3.3 *Considerations during motor rehabilitation*

Recovering the use of the arm does bring special challenges. On the one hand, many patients stop using their affected limb and rely on the other limb to perform their ADLs. This is known as the learned non-use syndrome. Not using the impaired arm can lead to a further loss in strength, range of motion, and fine motor skills, which in turn can result in contractures, pain and severe bone loss (osteoporosis)<sup>89</sup>. In addition, early muscle activation is critical for good recovery, so patients should be devoting as much



time as possible to rehabilitation. On the other hand, during rehabilitation patients develop compensatory strategies that are not always beneficial, i.e., they find the way to perform a movement or accomplish a task differently than they usually did before impairment (**Table 2**).

As a result, it is important to define the specific purpose of a protocol, as the goals of clinicians may not always meet those of patients, whose priority is to achieve as much independence as possible. For example, some training protocols may be designed for regaining a function (compensation), while others may aim to relearn how to execute a specific task (recovery). In general terms, patients will aim to regain the function regardless how this is achieved. However, the choice of one strategy over the other might determine which aspect of neuroplasticity is enhanced and limit the efficacy of other forms of plasticity<sup>67</sup>. Thus, based on the severity of the impairment, differentiating between recovery and compensation is essential to determine whether rehabilitation will lead to maladaptive strategies or not<sup>90</sup>.

	RECOVERY	COMPENSATION
Neural	Restoring function in neural tissue that was initially lost because of injury or disease	The residual neural tissue takes over a function lost because of injury or disease
Behavioral: body function (impairment)	Restoring the ability to perform movement in the same manner as it was performed before injury or disease	Performing movement in a manner different from how it was performed before injury or disease
Behavioral: activity (disability)	Restoring the ability to perform a task in exactly the same manner as it was performed before injury or disease	Performing a task in a manner different from how it was

**Table 2 Behavioral and neural recovery according to the World Health Organization International Classification of Function Model.** Source: <sup>42</sup>.



# 4 MOTOR COORDINATION

Motor coordination is the combination of body movements created with kinematic and kinetic parameters to produce intended actions. This involves the integration of sensory and proprioceptive information with the neural processes in the brain and the spinal cord, which plan, control and execute motor commands.

Understanding motor coordination is a problem that has not been solved yet due to the variety of intrinsic neuromechanical properties of the human body that complicate the task:

1. *Motor abundance*: due to the redundancy of the human body, our motor system is able to perform a given task using multiple functionally equivalent solutions<sup>91</sup>.
2. *Motor variability / within-subject variability*: human motor system is inherently unable to produce two identical motor outputs in a row. Indeed, the amount of motor variability depends on its effect on motor effectiveness<sup>92</sup>.
3. *Individuality / inter-subject variability*: every subject exhibits a different motor strategy to perform a task, which depends on evolutionary, developmental and learning processes.



4. *Motor structure*: motor patterns are structured and this structure depends on biomechanical task relevance<sup>93</sup>.
5. *Multifunctionality*: each muscle can contribute to multiple actions and multiple muscles can be combined to produce a variety of tasks.

The human body is composed of 148 movable bones connected by 29, 33 and 85 joints of three, two and one degrees of freedom (DOF) respectively. This makes a total mobility for the human skeletal system of 244 DOFs, with a maneuverability of 238 DOFs<sup>94</sup>. In other words, to position the end effector in space, our brain must specify not 6 but 244 variables, of which 238 are redundant and may be presumably used to optimize the movement.

The large number of elements in the musculoskeletal system turns the production of movement into a problem with many degrees of freedom. That is, a given motor task can be generated by multiple solutions involving different ways of arranging turning, extending and combining the various muscles, joints, and limbs.

Two main hypotheses have been proposed to explain how the nervous system determines a particular solution from the set of possible solutions that can accomplish a motor task equally well: muscle synergies and the uncontrolled manifold hypothesis.

#### 4.1 UNCONTROLLED MANIFOLD HYPOTHESIS (UCM)

Based on the principle of abundance, a more recent hypothesis suggests that instead of reducing the degrees of freedom, the central nervous system uses all of them to ensure flexible and stable motor performance. In other words, the apparently redundant degrees of freedom are thought to be essential for many aspects of the motor control, such as dealing with secondary tasks or unexpected perturbations<sup>95</sup>.

The UCM Hypothesis provides means to quantify synergies<sup>96</sup>. According to this theory, a synergy constitutes a set of elemental variables (degrees of freedom) that stabilize an important performance variable (potentially important variables produced



by the system as a whole). Given a reaching task, the joint angles and positions would represent the elemental variables, while the endpoint coordinates would represent the performance variable. The UCM Hypothesis assumes that the brain acts in the space of elemental variables and selects in the sub-space of manifolds the set of angular values corresponding to the desired endpoint position. Variability is classified then into bad variability, affecting the performance variable and significantly altering the motor outcome and good variability, affecting the elemental variables while keeping the task unchanged.

## 4.2 MUSCLE SYNERGIES AND THE CONTROL STRUCTURE

The first approach to solve the motor redundancy problem was formulated by Nicolai Bernstein, who stated that the central motor system deals with motor redundancy by eliminating redundant degrees of freedom<sup>91</sup>. Bernstein defended the existence of a modular neural strategy that simplifies the generation of motor behavior by reducing the dimensionality of the control problem. According to this theory, a muscle synergy is defined as a pattern of co-activation of muscles recruited by a single neural command signal<sup>97</sup>. Thus, the activation coefficient represents the neural signal that recruits each synergy.

Overall, muscle synergies are combined at different proportions to form a continuum of muscle activation patterns that produce movements. The traditional mathematical methods (Principal Component Analysis, Nonnegative Matrix Factorization, Independent Component Analysis, Correlation Analysis ...) typically applied to characterize muscle synergies are based on the idea that muscle synergies are linearly combined to produce movements. However, due to the nonlinearity of the



neural system it is likely, that muscle synergies only represent local linear mechanisms, that globally produce nonlinear complex behaviors<sup>98</sup>.

Motor modules often reflect optimal coordination patterns that minimize energetic demands given biomechanical constraints<sup>99–101</sup>. Because motor structure depends on task relevance, similar module structures will be found during similar tasks. Indeed, intensive studies on neuromuscular modularity suggest that muscle synergies are task dependent, i.e., synergy organization provides explicit control of task-related variables<sup>99,100</sup>. In the same way, a synergy can activate multiple muscles and a muscle can be part of different synergies. Within this framework, we define the *control structure*, as the set of synergies and activation coefficients needed to perform a task.

The literature produced in the last years contains multiple references supporting this theory and suggesting that normal motor control may be explained by a reduced number of synergies<sup>102–107</sup>. Experimental evidence reveals the existence of such a kind of modular organization in diverse motor systems: grasping in primates<sup>108</sup>, jumping and swimming in frogs<sup>109</sup>, postural control in cats<sup>97,106</sup> or control of posture<sup>110,111</sup>, upper-limb<sup>112,113</sup> and lower limb in humans<sup>114</sup>. Indeed, postural muscle synergies generalize across perturbation types and posture<sup>115,116</sup>.

#### 4.2.1 *Stroke and Muscle Synergies*

Motor impairment, and specifically upper-limb impairment, is one of the disabilities most frequently found among stroke survivors (**Table 1**). During rehabilitation, the recovery of upper-limb function following hemiparetic stroke is characterized by the emergence of abnormal, stereotypical movement patterns that impact the outcome of ADLs<sup>35</sup>. Many studies have attributed such abnormal patterns to the coupling of several joints, giving place to the definition of specific altered synergies that seem to generalize across stroke patients<sup>117–119</sup>. Although little work has been done within the field of muscle synergies to understand how stroke affects motor control in upper limbs, some studies have already demonstrated that stroke typically alters the recruitment patterns of normal synergies while leaving the synergy internal



structure or composition almost intact both in voluntary<sup>120</sup> and reflexive<sup>121</sup> movements. This has been shown to be true in mildly impaired subjects, however, posterior studies have reported evidence of synergy structure merging and fractionation in most impaired subjects<sup>122,123</sup>. More specifically, it seems that the degree of synergy merging is proportional to the severity of the impairment<sup>122</sup>. A similar phenomenon of motor-module fusion has also been reported in the lower limb of stroke patients<sup>124</sup>. Conversely, synergy fractionation appeared only in long-term stroke patients, so this seems to be associated to the time elapsed from the initial injury<sup>122</sup>. Authors hypothesized that synergy fractionation may constitute an adaptive mechanism to compensate motor impairment produced by stroke.

#### 4.2.2 Synergy analysis as a rehabilitation tool

Given the variability of stroke scales, which results from the disparate nature and extent of initial impairment, the success of clinical trials for testing new stroke therapies depends on large sample sizes (600-850 patients to achieve the typical 80% statistical power<sup>125,126,127</sup>). Extensive training of raters and standardization of scales reduce this variability but carries its own costs. Thus, clinical research in stroke would be aided by a reliable, repeatable, and fast scale to assess baseline impairment and its change during recovery. Such measurements would also yield objective to describe motor behavior after a stroke and the effect of different treatments on recovery.

In<sup>125</sup>, authors propose a quantitative set of kinetic and kinematic robotic markers with a high correlation with standard clinical scales such as FMA or mRS (see **Chapter 2. Motor Impairment Scales**). However, movement kinematics does not always correlate with the neuromuscular state of the subject. **Table 3** summarizes the neurological processes that are thought to prompt recovery from stroke. *Cheung et al.*



found that despite important differences in motor performance between the two arms, the synergies of healthy and affected arms were strikingly similar to each other<sup>120</sup>. The same phenomenon applied to subjects with different lesion sizes and locations. Thus, it is likely that kinetic and kinematic markers miss important information about the nature of the recovery that could be essential to avoid maladaptive plasticity, one of the main drawbacks of stroke rehabilitation<sup>90</sup>.

STAGE	NEUROLOGICAL MECHANISMS
<b>Spontaneous Recovery (First days)</b>	<ul style="list-style-type: none"> <li>• Resolution of edema and necrotic tissue</li> <li>• Reperfusion of ischemic penumbra</li> </ul>
<b>Early Recovery</b>	<ul style="list-style-type: none"> <li>• Recruitment of functionally homologous pathways</li> <li>• Disinhibition of redundant neuronal connections</li> <li>• Resolution of diaschisis</li> <li>• Formation of new neural networks to take over function of the damaged areas</li> </ul>
<b>Late recovery</b>	<ul style="list-style-type: none"> <li>• Vicariation (perilesional cortex regain control over the function of the damaged area through somatotopic reorganization)</li> <li>• Secondary cortical reorganization (a distal area with similar function regain control over function of the damaged region)</li> </ul> <p><i>* The activation of either one or the other strategy depends on the extent of the neural lesion</i></p>

**Table 3** Stroke recovery phases and related neurological mechanisms. Source: <sup>128</sup>.

Synergy analysis may constitute a simple and non-invasive tool that provides physiological and objective information on how therapies affect the dynamics of motor recovery. Similarly, it may provide a foundation for the development of individualized therapeutic strategies<sup>129</sup>. Abnormal coupling of joints is a sign of persistent neurological deficit in patients with stroke, resulting in disrupted kinematics and reduced range of motion of voluntary movements<sup>130</sup>. Recent studies provide evidence that targeted motor training can modify abnormal isometric torque patterns<sup>131</sup> and kinematic synergies<sup>130</sup>. Therefore, it may be possible to develop training protocols that directly target abnormal synergy structure or recruitment patterns. Nevertheless, other assistive approaches, such as functional electrical stimulation or cortically driven prosthetic devices, have been proposed to restore muscle synergy structure and recruitment patterns<sup>123</sup>.



### 4.3 STROKE AND NEUROREHABILITATION

The disabilities caused by stroke are a direct consequence of neural damage (see section 1.5 **Prognosis and post-stroke consequences**). It has been reported that the brain has capacity for spontaneous recovery early after stroke. Rehabilitation-driven motor recovery is fast during the first month, but it slows down during the next months until it reaches a plateau after 6 months<sup>132</sup>. It has been hypothesized that this interruption reflects the plasticity limitations of the adult brain. However, there are very few studies addressing how the brain responds to stroke and subsequent therapy.

Some authors have correlated the spontaneous and rehabilitation-driven motor recovery with specific neural changes. Turton *et al.* discovered reduced excitability in the ipsilesional motor cortex that normalized together with the recovery of the impaired arm function during spontaneous recovery<sup>133</sup>. Further, in patients with subcortical stroke Traversa *et al.* reported that the size of the motor map increased with the functional improvement of patients<sup>134</sup>. Some neuroimaging studies indicate that excessive activity in the bilateral sensorimotor network is associated to compensatory strategies developed to improve motor control<sup>135,136</sup> and that normalization of hyper-activation is generally linked to improved motor outcome after rehabilitation. However, there is increasing evidence that chances for better motor recovery rely on the integrity of the ipsilesional sensorimotor cortex and its corticospinal tract<sup>137,138</sup>.

Regarding rehabilitation-induced neural changes, Carrey *et al.* associated a shift in the laterality of the sensorimotor cortex activation from contralesional to ipsilesional with functional grasping improvement<sup>139</sup>. Similarly, Lierpert *et al.* reported an increase in the size of the ipsilesional representation of the affected limb motor cortex in



response to function improvement <sup>140</sup>. Further, there is some evidence that the effectiveness of therapy depends on the neural characteristics of the lesion. For instance, constraint-induced movement therapy has been shown to improve the upper-limb function in chronic patients with sensory disorder or neglect <sup>141</sup>, bilateral training in mildly impaired stroke patients <sup>142</sup> and unilateral training in severely impaired patients <sup>143</sup>. However, at the moment rehabilitation protocols do not assess the neural damage of a patient prior to inclusion and rehabilitation specialists are limited to clinical examination and experience to determine which is the best therapy for each patient.

Taking everything together, it is unquestionable that analyzing the neural response to therapy is essential to understand the motor recovery process and improve the design of successful therapies.



# 5 KINEMATICS OF HUMAN MOTION

The human body can be viewed as a system of rigid links connected by joints. A body is called *rigid* or *solid*, when the distance between any two points within the body remains constant regardless the motion of the body. Similarly, a rigid body preserves the angle between two lines in the body.

Naturally, human body parts are not rigid structures, but in order to study human-body motion, they conveniently behave according to rigid body kinematics. That is, human movement can be studied as a relative position change of the body segments.

In general, the relative motion of one body segment with respect to the adjacent segment implies a combination of translation and rotation. However, when we study gross movements such as walking or gymnastic exercises, the translation can be disregarded due to its small magnitude and the movement can be considered as purely rotational<sup>144</sup>. To do so, we must assume a series of simplifications:

1. The axes of rotation coincide with the joint reference system
2. The axes of rotation coincide with the anatomic axes
3. The joint rotates about multiple axis, which intersect at one point



## 5.1 THE CLINICAL REFERENCE SYSTEM

In order to define joint configuration, a reference system is needed. There are many methods that describe alternative reference systems based in either technical or somatic references, each of them exhibiting their own advantages and limitations. However, the most commonly used system in the clinical practice, and in consequence in related research, is the clinical reference system<sup>145</sup>.

The anatomic posture is defined then the human is standing upright on a horizontal surface with arms hanging straight down at the sides of the body, palms turner forward and head erect (Figure 1). It has to be noted, though, that the clinical system is only valid to describe joint configurations when the body is in the anatomic posture. In contrast, when the joint rotation starts from a nonneutral position or implies complex movements, the clinical system is not suitable.

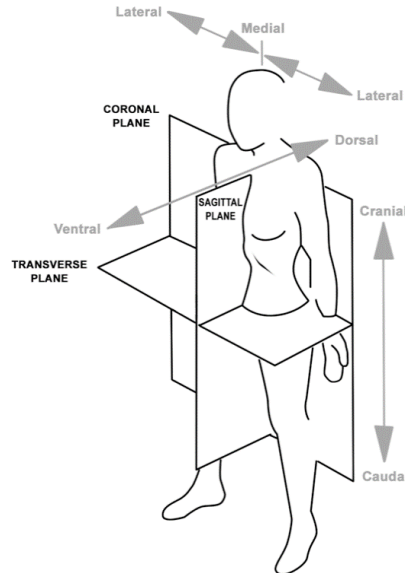


Figure 1 Anatomical posture, cardinal planes and axes of the human body.



From the anatomical posture, we can define the cardinal planes of the human body:

- **SAGITTAL PLANE:** any plane dividing the body into left and right sections. If the plane divides the body into two symmetrical halves, the plane is called the *cardinal* or *principal sagittal* plane. This plane is positioned in an anteroposterior direction.
- **TRANSVERSE PLANE:** any horizontal plane passing through the body when this is in an upright posture. When the plane passes through the body's center of mass, the plane is called the *cardinal* or *principal transverse* plane.
- **CORONAL or FRONTAL PLANE:** any plane going side to side and perpendicular to both sagittal and transverse planes. When the plane passes through the body's center of mass, the plane is called the *cardinal* or *principal frontal* plane. The frontal plane divides the body into anterior and posterior sections.


From the intersection at the right shoulder joint of the cardinal planes, we can define the axes of the human body.

- **ANTERIOPOSTERIOR AXIS:** is defined from the intersection of the sagittal and transverse planes.
- **LONGITUDINAL AXIS:** is defined from the intersection of the sagittal and frontal planes.
- **LATEROMEDIAL / FRONTAL AXIS:** is defined from the intersection of the frontal and transverse planes.



## 5.2 MOTION OF HUMAN BODY SEGMENTS

Human body segments are usually defined as body sections linked by joints. For instance, the head, the trunk, the upper arm, the forearm, the hand, the shank, and thigh, the foot are most studied examples of body segments. The segments move with regard to the adjacent body segment about the linking joint. The main motions of body segments are defined from the cardinal planes:

- **FLEXION-EXTENSION**: occurs when the body segment moves on a sagittal plan
  - **Flexion**: refers to a movement that **decreases** the angle between two body segments
  - **Extension**: refers to a movement that **increases** the angle between two body segments
- **ABDUCTION-ADDUCTION**: occurs when the body-segment moves away from or toward the cardinal sagittal plane
- **INTERNAL-EXTERNAL ROTATION**: occurs when the body segment rotates about the longitudinal axis of the segment. Depending of the joint, this may be also called **SUPINATION-PRONATION**.  
 When this motion occurs, the twist is usually assigned to one of the two joints, proximal or distal. For instance, during shoulder external rotation, the movement can be assigned to either the elbow or the shoulder.
- **CIRCUMDUCTION**: occurs when flexion-extension and abduction-adduction combine, resulting in a circular motion.



### 5.3 ANGULAR KINEMATICS

In biomechanical analysis, the body angles are defined between two body segments, and the vertex of the angle is their common joint. Depending on the reference used to express the angles, these can be absolute or relative angles (**Figure 2**).

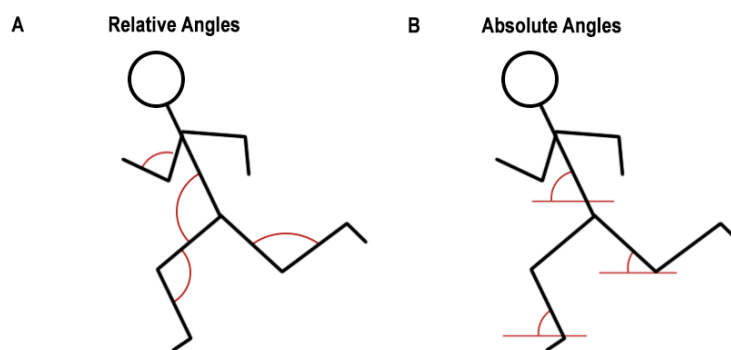


Figure 2 Relative and absolute angles

- **RELATIVE, INCLUDED or JOINT ANGLES:** define the angle between the longitudinal axis of the two adjacent segments (**Figure 2A**).  
✎ Straight fully extended position is generally defined as 0 degrees
- **ABSOLUTE or SEGMENT ANGLES:** define the angle of a segment with respect to a right-horizontal line originating from the proximal end of the segment (**Figure 2B**).



## 5.4 KINEMATIC CHAINS

As stated previously, the human body can be viewed as a system of body segments connected by links (joints). In mechanics, a linkage of rigid bodies is referred to as a kinematic chain. The simplest kinematic chain is composed of two segments connected by a single joint. That is called a *kinematic pair*. Note that virtually any anatomical joint can be studied as a kinematic pair: the trunk and upper-limb linked by the shoulder, the upper-limb and fore-arm linked by the elbow, the upper-limb and hand linked by the wrist, the trunk and thigh linked by the hip ...

Kinematic chains can be either *serial* or *branched*. Serial chains are composed of segments that are part of no more than two kinematic pairs, while branched chains contain at least one segment shared by two or more kinematic pairs. For instance, in the human body, the leg and arm are *serial kinematic chains*, and the trunk is a *branched kinematic chain* when its articulations are ignored.

### *Mobility of the kinematic chains*

The *degrees of freedom* (DOF) determine the mobility of the kinematic chains. A rigid body suspended in the space has 6 DOFs, as it can translate along 3 directions and rotate about 3 axes. In consequence, a system of  $N$  rigid bodies has  $6N$  DOFs. However, this number decreases if some of the segments are not independent, as it happens when segments are connected by joints, or when motion is restricted by constraints. In this case, the system possesses  $6N - m$  DOF, where  $m$  is the number of equations that define the constraints. In any case, the total number of DOF in a kinematic chain is called the *mobility* of the chain.

When studying the human body kinematics, we say that any joint can have as much 6 DOF. However, as we stated at the beginning of this section, for the ease of simplicity the translational motion is disregarded as it is very small compared to the rotational motion. This assumption reduces the maximum DOF of the human joints to



3. Now, given that human joints are constrained by inherent anatomic constraints, they can be classified according to the number of rotational DOFs as:

- **Hinge or revolute joints:** joints with 1 rotational DOF  
*Ex. Finger joints (inter-phalangeal)*
- **Ellipsoidal, saddle-shaped and flat- joints:** joints with 2 rotational DOFs  
*Ex. Sternoclavicular joint*
- **Ball-and-socket or spherical joints:** joints with 3 rotational DOFs  
*Ex. Shoulder (glenohumeral), hip ...*

#### **Calculating the DOFs of the kinematic chains**

Taken everything together, we can estimate the number of DOFs of a kinematic chain using *Gruebler's formula*.

$$F = 6 (N - k) + \sum_{i=1}^k f_i \quad (1)$$

Where  $N$  is the number of segments,  $k$  is the number of joints and  $f_i$  is the number of DOF of the  $i$ th joint. For planar movements, the equation is modified as:

$$F = 3 (N - k) + \sum_{i=1}^k f_i \quad (2)$$

Note that for open kinematic chains (i.e. one end of the chain is free to move), the number of segments equals the number of joints. Thus, for either planar or tridimensional movements, the number of DOFs is:



$$F = \sum_{i=1}^k f_i \quad (3)$$

## 5.5 STROKE AND KINEMATICS

Quantitative measures of human motion are essential to understand the consequences of neural conditions inducing motor impairment such as stroke, and assess the outcome of rehabilitation to determine its efficacy. In other words, measuring human motion is essential to support the decision making process in the clinical practice.

However, although important advances have been made in the description of the human movement both in physiological<sup>146–148</sup> and pathological conditions<sup>149–152</sup>, the clinical practice is still limited to the administration of clinical scales based on pure observation (see subsection **2.1.1 Clinical Scales** for an extended description). The first kinematic approaches measuring rudimentary spatiotemporal characteristics such as execution times or reaching distances<sup>75,153</sup> are far from the impressive range of possibilities that current available technologies offer. This makes even more compelling the need to develop new objective measures to improve the obsolete and subjective scale applied by clinicians. Specially, because the use of clinical and functional scales is not enough to effectively assess motor impairment<sup>22,154</sup>.

According to the review available in<sup>155</sup>, the studies of kinematics found in the literature can be classified into 3 categories depending on their purpose:

1. *Discriminative studies*: kinematic metrics are evaluated to find significant differences between healthy subjects and patients with neurological injury<sup>156</sup>.
2. *Evaluative studies*: kinematic metrics are tested to verify whether they can be used as a reliable measure of motor impairment. To this end, the studies assess the validity (correlation with clinical scales)<sup>156,157</sup>, reproducibility



(consistency between repeated measures)<sup>157</sup> and sensitivity to the functional change<sup>150</sup> of the kinematic metrics.

3. *Predictive studies*: kinematic measures are tested to verify whether they can serve to predict the outcomes in clinical scales using regression<sup>158</sup>.

The study of upper-limb motion is generally more complex than the study of the gait due to its non-repetitive nature. At present, most of the studies addressing the upper-limb kinematic behavior of stroke patients focus on functional movements (reaching, grasping, drawing circles or squares...) or Activities of Daily Living (ADL)<sup>155</sup>. However, the kinematic study of ADLs and reaching movements is complex as it involves the simultaneous coordination of multiple joints. As a result, linking the functional outcome and the neuromuscular state of the patient is not straightforward. For this reason, in this thesis we have selected a set of single-DOF (or single-joint) movements used by the clinical gold standard to assess the motor impairment caused by stroke (Fugl-Meyer scale). Another interesting point of using single-DOF movements is that they avoid motor equivalence produced by the redundancy of the multiple DOFs of the human body that may mislead the correct interpretation of results



### 5.5.1 Kinematic indices used in literature

The literature offers a wide range of metrics to assess motor performance from a kinematic perspective and characterize motor impairment. The most widely employed metrics can be classified into eight categories according to the movement feature characterized (**Table 4**).

A – FUNCTIONAL RANGE OF MOTION
<p>A1 – <i>Joint range of motion (ROM)</i>: maximum displacement achieved by the joint</p> <p>A2 – <i>Reaching range of motion*</i>: it is related to the hand displacement during a reaching task and quantifies the maximum displacement achieved by the end effector (normally expressed in Cartesian coordinates)</p>
B – SPEED
<p>B1 – <i>Movement time</i>: time required to complete a task. It is an indirect measure of movement speed.</p> <p>B2 – <i>Mean velocity</i>: the average velocity of the end-effector along the entire movement.</p> <p>B3 – <i>Peak velocity</i>: maximum velocity attained by the end-effector. This metric is more often used than the mean velocity<sup>155</sup>.</p>
C – MOVEMENT EFFICACY
<p>C1 – <i>Active movement index</i>: percentage of the task that the subject performs voluntarily (actively). Usually robotic devices are need to compute this metric.</p> <p>C2 – <i>Index of Curvature/Direct efficiency*</i>: ratio between the real end-effector path and the length of the desired trajectory. The closer to one the index (physiological behavior), the straighter is the trajectory toward the target.</p> <p>C3 – <i>Index of performance*</i>: a function of movement time, deviation from the target and size of the target. It is a measure of movement quality.</p>
D – MOVEMENT ACCURACY
<p>D1 – <i>Tracking error*</i>: mean distance from the Euclidean distance between points of the real and desired hand trajectories.</p> <p>D2 – <i>Target error*</i>: end-effector error around the target placement.</p>
E – MOVEMENT SMOOTHNESS
<p>E1 – <i>Ratio between mean and maximum velocity</i>: in healthy subjects this ratio should be close to 1.</p> <p>E2 – <i>Number of velocity peaks / movement units</i>: normal reaching movements display only one peak.</p> <p>E3 – <i>Mean arrest period ratio*</i>: ratio between the movement time in which hand stops and the total movement time.</p> <p>E4 – <i>Number of zero-crossings in acceleration profile</i>: number of base line crossings by the acceleration</p> <p>E5 – <i>Jerk</i>: rate of change of the acceleration profile (third time derivative of position)</p> <p>E6 – <i>Spectral arc-length</i>: derived from the amplitude and Fourier magnitude spectrum from the velocity profile</p>
F – MOVEMENT COORDINATION



F1 – <i>Inter-joint correlation*</i> : Pearson Correlation Index between the displacement of two adjacent joints [Only applicable to movements involving the coordination of several joints]
G – MOVEMENT CONTROL STRATEGY
G1 - <i>Time to velocity peak*</i> : time elapsed from movement onset to the instant when maximal velocity is achieved. The velocity profiles of normal reaching movements are symmetrical and characterized by a single peak. A peak displaced to the left is related to large deceleration periods, and displaced to the right, to disrupted movements <sup>159</sup> .
H – TORQUE PRODUCTION
H1 – <i>Elbow maximum angular velocity</i> : first time derivative of elbow angle.

**Table 4** Kinematic metrics available in the literature to describe motor impairment. Indices marked with an \* are specific of reaching movements.

5.5.2 *Kinematic traits of patients with stroke*

Although the healthy and impaired human movement are well characterized, the need to develop a reliable quantitative metric to assess motor impairment has not been met yet. Undoubtedly, the kinematic indices may play a role in this issue. This section summarizes the major findings about the kinematic characteristics of the upper-limb of patients with stroke.

The motor behavior of patients with stroke is characterized by strongly stereotyped patterns that dramatically hinder their ability to efficiently perform in their daily lives. These patterns are usually provoked by involuntary coactivations of upper-limb muscles <sup>160,161</sup>. Fundamentally, patients are unable to uncouple shoulder abduction and elbow flexion (pathological flexion synergy), and shoulder adduction and elbow extension (pathological flexion extension) <sup>162</sup>. Thus, their natural ability to control their joints independently is suppressed.

As a result, studies focusing on upper-limb kinematics have found important differences when comparing populations of patients with stroke and healthy subjects. During drinking, stroke patients exhibited significantly longer movement times, lower



velocity peaks, oscillatory velocity patterns (in contrast to the typical bell-shaped healthy pattern) and more numerous movements units<sup>149</sup>. These characteristics are general for many complex tasks. Indeed, goal-directed tasks in patients with stroke are characterized by slowness, spatial and temporal segmentation and smaller amplitude<sup>163–165</sup>.

Generally, it is assumed that a preplanned goal-directed movement is efficient when peak velocity is achieved around the 40% to 50% of the reaching time<sup>166</sup>. It has been suggested that the ability to plan movements is preserved in stroke<sup>164,167,168</sup>. However, stroke patients exhibit premature peaks due to longer deceleration phases, which have been attributed to affected feedback and feedforward control<sup>169</sup>. In addition, during pointing and reaching the interjoint coordination is disrupted<sup>165,170</sup>.

Also, patients with stroke develop significant compensatory strategies to overcome the limitations imposed by their motor impairment<sup>171,172</sup>. For instance, during drinking patients present significantly higher shoulder abduction to overcome reduced ability to extend the elbow<sup>149</sup>. Similarly, patients exhibit significantly larger trunk protraction during the reaching phase to overcome the same inability<sup>149</sup>. Interestingly, the level of intensity of these strategies constituted a significant feature to discriminate between motor impairment level. Indeed, compensatory trunk movements seem to have a strong correlation with motor impairment level<sup>173</sup>.

Motor alterations due to stroke are non static and tend to evolve along with motor recovery. For this reason, it is very important to specify at which stage of recovery correspond each identified motor state. Brunnstrom and Bobath published detailed descriptions of the evolution of the stereotypic patterns of patients with stroke<sup>35,174</sup> (see section **3.2 The 7 stages of motor recovery**). As a matter of fact, several studies have reported a number of kinematic features that can significantly discriminate motor impairment levels (e.g. mild, moderate, severe motor impairment) supporting the idea of a sequential recovery process<sup>149</sup>. Indeed, longitudinal studies have demonstrated that kinematic features can evaluate motor control changes during recovery in response to multiple rehabilitation types such as strength training<sup>169</sup>, task



specific training <sup>175</sup>, constraint induced movement therapy <sup>176</sup>, robotic training <sup>177</sup> and bilateral motor retraining <sup>55</sup>. Therefore it is very likely that kinematic analysis may constitute a good candidate to develop new objective measures of motor impairment due to stroke.










## PART II

# Methods

 The methods described in this section are common to all the chapters in the thesis. Specific methods that only apply to a given section are described within the corresponding section.







# 6 SUBJECT DATABASES

This section describes the demographic and clinical details of the subjects recruited to build the databases that were used for the studies.

## 6.1 DESCRIPTION OF THE DATABASES

This present thesis was developed using 2 human databases that were specifically designed and subsequently built to fulfill its objectives. The first database (database H) was built with neurologically intact subjects (**Table 5**) and the second database (database P) was built with patients that had suffered a stroke (**Table 6**). Regarding the thesis organization, database H served as substrate for studies 1 and 2 and database P for studies 3 and 4. These studies are described in detail in **PART III. STUDIES**.

### 6.1.1 *The database of neurologically intact subjects*

This database was composed of 6 neurologically intact subjects (age 25-36). All subjects were right-handed males with no known neurological impairment. Prior to the experiment, subjects were asked to answer a series of questions included in the Edinburgh Handedness Inventory (see description of the test in subsection **6.2.1 Laterality Index | Edinburgh Handedness Inventory**) to assess their handedness. The output of the test is a measure of handedness known as the Laterality Index (**Table 5**).



SUBJECT ID	AGE	LATERALITY INDEX	GENDER
S1	31	90.0	Male
S2	29	100.0	Male
S3	32	85.0	Male
S4	30	100.0	Male
S5	36	80.0	Male
S6	24	100.0	Male
TOTAL	30.3 ± 3.9	92.5 ± 8.8	6/6 Male

**Table 5 Description of database H: neurologically intact subjects.** Laterality Index was assessed using the Edinburgh Handedness Inventory (see description of the test below). The last row indicates mean ± SD. In the case of gender, the last row indicates de ratio of males.

### 6.1.2 *The database of patients with stroke*

Patients were recruited by specialized clinical staff from the Guttmann Institute. All patients were over 18 and had suffered the stroke at most, 6 months prior to the experiment. Patients with cognitive impairment, severe visual impairments, severe neuropsychological impairments such as aphasia, attention deficit disorder, or that may have trouble to understand the instructions given by the researcher were excluded from the study. Similarly, patients with bilateral stroke, no ability to move their upper limb at all, or showing strong signs of spasticity or ataxia were discarded.

PATIENT ID	AGE	LATERALITY INDEX	GENDER
P1	62	100.0	Male
P2	44	100.0	Male
P3	44	100.0	Female
P4	30	100.0	Female
P5	51	90.0	Male
P6	56	90.0	Male
TOTAL	47.8 ± 11.2	96.7 ± 5.2	4/6 Male

**Table 6 Description of database P: patients with stroke.** Laterality Index was assessed using the Edinburgh Handedness Inventory. The last row indicates mean ± SD. In the case of gender, the last row indicates de ratio of males.

**Table 6** provides general statistical information about the database of patients. As with healthy subjects, the natural handedness of patients was assessed through the



Edinburgh Handedness Inventory. In this case, patients were asked to answer the items considering their hand preferences prior to stroke.

**Table 7** contains the clinical details of the patients composing database P. To assess the sensorimotor function of the upper-limb, patients were evaluated with the Fugl-Meyer assessment scale for the upper-extremity (FM-UE). This scale quantifies the level of upper-limb impairment with an index ranging from 0 to 66 points. In addition to that, patients were further evaluated with the Functional Independence Measure (FIM). Both, the FM-UE and the FIM were administered by certified specialists in the Guttmann Institute. More information about these scales can be found in Chapter [2. Motor Impairment Scales](#).

ID	Elapsed time	Paretic arm	Recurrent stroke	FM-UE	FIM-cat	Stroke type / Location	Injury location
P1	4 m	R	No	59	4	Ischemic / Cortical	Frontal/Parietal (L)
P2	4 m	L	Yes*	47	5	Hemorrhagic / Subcortical	Basal ganglia (R)
P3	4.25 m	L	No	58	5	Hemorrhagic / Cortical	Parietal/Temporal/Frontal (R) and Frontal (L)
P4	1.5 m	R	No	59	5	Ischemic / Cortical	Frontal / Parietal / Temporal (L)
P5	4 m	L	No	40	4	Hemorrhagic / Subcortical	Basal Ganglia (R)
P6	2.25 m	R	No	58	5	Ischemic/NA	Unspecified

**Table 7 Clinical description of database P.** Elapsed time since stroke (m = months). Paretic arm: R = Right arm, L = Left Arm. FM-UE: Fugl-Meyer Upper-Extremity score. The Fugl-Meyer score refers to the upper-limb motor evaluation and it is scored in a basis of 66 points. FIM-cat: Independence category determined by the Functional Independence Measure: 0 = Non functional, 1 = Dependent – Level 1, 2 = Dependent – Level 2, 3 = Dependent – Supervision, 4 = Independent on flat surface, 5: Independent. \*P2 was totally recovered from his previous stroke. Injury location was determined via Computerized Axial Tomography scan.



Following general consensus (i.e. <sup>178, 36</sup>), the motor impairment of patients displaying a FM-UE within the range of [0 - 20] was classified as severe; [21 - 50] as moderate; and [51-66] as mild.

## 6.2 TESTS HANDED OUT TO ASSESS SUBJECTS

This section details the tests used to characterize diverse aspects of the subjects composing the databases used in this work.

### 6.2.1 Laterality Index | Edinburgh Handedness Inventory



The Edinburgh Handedness Inventory<sup>179</sup> is a measurement scale used to assess the hand dominance of a person. The test is composed of 10+2 items that evaluate the person's preference to use his either right or left arm during everyday activities. A copy of the Edinburgh Handedness Inventory can be found in the Appendix A. Edinburgh Handedness Inventory.

Left Hander's LI distribution		Right Hander's LI distribution	
LI	Decile	LI	Decile
-100	10 <sup>th</sup> Left	100	10 <sup>th</sup> Right
-100 ≤ LI < -92	9 <sup>th</sup> Left	95 ≤ LI < 100	9 <sup>th</sup> Right
-92 ≤ LI < -90	8 <sup>th</sup> Left	92 ≤ LI < 95	8 <sup>th</sup> Right
-90 ≤ LI < -87	7 <sup>th</sup> Left	88 ≤ LI < 92	7 <sup>th</sup> Right
-87 ≤ LI < -83	6 <sup>th</sup> Left	84 ≤ LI < 88	6 <sup>th</sup> Right
-83 ≤ LI < -76	5 <sup>th</sup> Left	80 ≤ LI < 84	5 <sup>th</sup> Right
-76 ≤ LI < -66	4 <sup>th</sup> Left	74 ≤ LI < 80	4 <sup>th</sup> Right
-66 ≤ LI < -54	3 <sup>rd</sup> Left	68 ≤ LI < 74	3 <sup>rd</sup> Right
-54 ≤ LI < -42	2 <sup>nd</sup> Left	60 ≤ LI < 68	2 <sup>nd</sup> Right
-42 ≤ LI < -28	1 <sup>st</sup> Left	48 ≤ LI < 60	1 <sup>st</sup> Right
-28 ≤ LI < 48 Middle			

**Table 8 Distribution of the Laterality Index (LI) in the population.** A subject with a LI ranging from 28 to 48 is considered ambidextrous.

The outcome of the test is a laterality index (LI) that ranges from -100 to 100. **Table 8** displays the distribution of the LI in the population. Negative LIs attribute left



handedness while positive LIs attribute right handedness to the person being evaluated.

Due to the motor impairment produced by stroke, actual motor abilities of stroke patients do not reflect their real handedness. Thus, the test was applied asking patents to report their hand use referred to their preferences before having suffered the stroke.

---

### 6.2.2 Fugl-Meyer Assessment scale (FM)



The Fugl-Meyer test (FM) or the Fugl-Meyer assessment scale was especially designed to quantify motor impairment after stroke based on motor performance. Its use is recommended for clinical trials of stroke rehabilitation as it is one of the most comprehensive measures of motor impairment<sup>22</sup>. A copy of the FM questionnaire can be found in the Appendix B. Fugl – Meyer Scale.

The full scale is a 226-point Likert-type scale distributed into 5 domains: motor function, sensory function, balance, passive joint range of motion, and joint pain. Each domain contains a different number of items, each scored on a 3-point ordinal scale:

- *0 = cannot perform*
- *1 = performs partially*
- *2 = performs fully*

Because the total number of possible points that a subject can achieve in each domain varies, the relative importance of each domain within the overall FM score differs from domain to domain. **Table 9** displays the maximal points that can be scored in each domain, and the percentage of the the final FM score that each domain contributes.



DOMAIN	MOTOR FUNCTION	SENSORY FUNCTION	BALANCE	PASSIVE JOINT MOTION	JOINT PAIN
<b>TOTAL POINTS</b>	100	24	14	44	44
<b>RELATIVE WEIGHT</b>	44.2%	10.6%	6.2%	19.5%	19.5%

Table 9 Point distribution of the Fugl-Meyer scale into its 5 composing domains.

The score of the motor function domain ranges from 0 (hemiplegia) to 100 (normal motor performance) and it is divided into 66 points for the upper-extremity and 34 points for the lower-extremity. Due to the characteristics of the study, we only focused on the upper-limb motor domain (**Table 10**). Thus, the scores presented in this work are calculated in a 66-points basis. This score is commonly known as the FM-UE (Fugl Meyer – Upper Extremity) score.

UPPER-EXTREMITY	LOWER-EXTREMITY
<i>Shoulder retraction</i> <i>Shoulder abduction</i> <i>Shoulder elevation</i> <i>Shoulder abduction to 90°</i> <i>Shoulder adduction/internal rotation</i> <i>Shoulder external rotation</i> <i>Shoulder flexion 0–90°</i> <i>Shoulder flexion 90–180°</i> <i>Elbow flexion</i> <i>Elbow extension</i> <i>Forearm supination</i> <i>Forearm pronation</i> <i>Forearm supination/pronation (elbow at 0°)</i> <i>Forearm supination/pronation (elbow at 90°, shoulder at 0°)</i> <i>Hand to lumbar spine</i> <i>Wrist flexion/extension (elbow at 0°)</i> <i>Wrist flexion/extension (elbow at 90°)</i> <i>Wrist extension against resistance (elbow at 0°)</i> <i>Wrist extension against resistance (elbow at 90°)</i> <i>Wrist circumduction</i> <i>Finger flexion</i> <i>Finger extension</i> <i>Extension of MCP joints, flexion of PIPs/DIPs</i> <i>Thumb adduction</i> <i>Thumb opposition</i> <i>Grasp cylinder</i> <i>Grasp tennis ball</i> <i>Finger-nose speed</i> <i>Finger-nose tremor</i> <i>Finger-nose dysmetria</i>	<i>Hip flexion</i> <i>Hip extension (supine)</i> <i>Hip adduction (supine)</i> <i>Knee flexion (supine)</i> <i>Knee flexion (sitting)</i> <i>Knee flexion (standing)</i> <i>Knee extension (supine)</i> <i>Ankle dorsiflexion (supine)</i> <i>Ankle dorsiflexion (sitting)</i> <i>Ankle dorsiflexion (standing)</i> <i>Ankle plantar flexion (supine)</i> <i>Heel-shin speed</i> <i>Heel-shin tremor</i> <i>Heel-shin dysmetria</i> <i>Knee reflex</i> <i>Hamstring reflex</i> <i>Ankle reflex</i>



<i>Finger flexion reflex</i> <i>Biceps reflex</i> <i>Triceps reflex</i>	
<b>TOTAL = 66 POINTS</b>	<b>TOTAL = 34 POINTS</b>

Table 10 Items of the Fugl-Meyer motor function domain classified regarding whether they evaluate the upper- or lower- limb extremity function.

### 6.2.3 Functional Independence Measure (FIM)



The Functional Independence Measure (FIM) is a functional scale adapted to the International Classification of Impairment, Disabilities and Handicaps system. It was originally developed to overcome the sensitivity and comprehensiveness limitations of the Barthel Index. Unlike the Fugl-Meyer scale, the FIM is not stroke-specific and it is widely used to assess patients with traumatic brain injury, multiple sclerosis, spinal cord injury or even elderly subjects undergoing rehabilitation.

The FIM assesses 6 areas of function (Self-care, Sphincter control, Mobility, Locomotion, Communication and Social cognition). These areas fall into 2 domains: motor (13 items) and cognitive domain (5 items), and are referred to as the Motor-FIM and the Cognitive-FIM. The Motor-FIM is based on the items of the Barthel Scale. A copy of the FIM assessment questionnaire can be found in the Appendix C. Functional Independence Measure.

Each item is scored on a 7-point ordinal Likert scale depending on how much assistance is required by the individual to carry out activities of daily living. The percentages displayed below indicate the effort percent performed by the subject to complete the task.



**Complete Dependence**

- 1 = Total Assistance (Subject < 25%)
- 2 = Maximal Assistance (Subject > 25%)

**Modified Dependence**

- 3 = dependence – Level 1: moderate assistance (Subject > 50%)
- 4 = dependence – Level 2: moderate assistance (Subject > 75%)
- 5 = dependence – Supervision (Subject =100%)

**Independent**

- 6 = Modified Independence (Device)
- 7 = Complete Independence (Timely, safely)

The FIM classifies patients into 6 categories depending on the outcome:

- 0 = non functional
- 1 = dependent – Level 1
- 2 = dependent – Level 2
- 3 = dependent – Supervision
- 4 = independent on flat surface
- 5 = independent

The FIM was administered by certified specialists to patients with stroke in the Guttmann Institute. Healthy subjects were not evaluated with the FIM.



### 6.3 ETHICAL CONSIDERATIONS

The experiments with **database H** were carried out in the lab of the Biomedical Signal Processing and Interpretation group located at the Institute of Bioengineering of Catalonia (Barcelona). The Institutional Review Board of the Institute approved all the procedures used. Written informed consent was required for participation in the study.

The experiments with **database P** were carried out in the Movement Analysis lab of the Guttmann Institute (Barcelona) under the strict supervision of specialized clinical staff. The Guttmann's Institute Ethics Committee approved all the procedures used. Written informed consent was required for participation in the study.







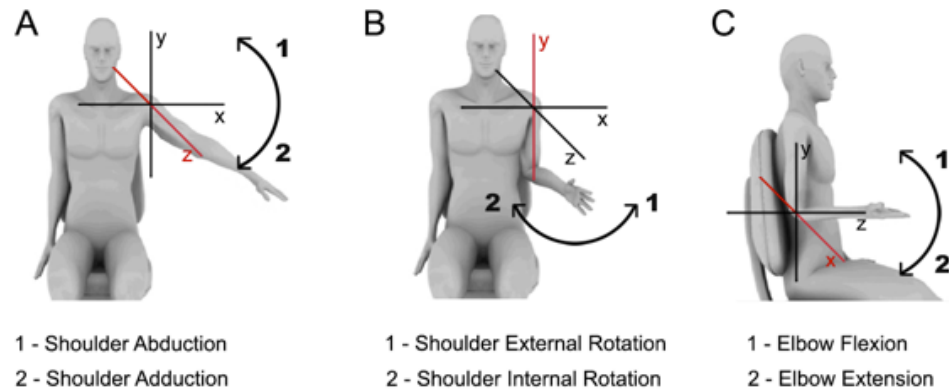
# 7 EXPERIMENTAL PROTOCOL

## 7.1 GENERAL PROTOCOL

The movements analyzed in this study correspond to the main movement patterns affected by stroke. The key-point of this selection is that all movements are included in the items of the Fugl-Meyer Assessment scale, which is a gold standard to evaluate motor recovery after stroke (**Figure 3**): shoulder abduction (SAbd), shoulder external rotation (SERot), and elbow flexion (EFlex); and their respective opposites, shoulder adduction (SAdd), shoulder internal rotation (SIRot), and elbow extension (EExt). Each movement was studied in its dynamic form, i.e., the amplitude of the active joint changed with time, and not in the isometric form.

To evaluate shoulder abduction, subjects were asked to laterally raise their arm 90° away from the midline of the body starting at the anatomical position (arm extended along the body) with the palm of the hand facing inwards. To evaluate shoulder external rotation, subjects were asked to bend their elbow 90° with the palm of the hand facing their stomachs and to rotate their elbow externally as much as they could and as long as the elbow did not detach from the body. To evaluate elbow extension, the elbow was bended from anatomical position (0°) to 90° with the palm of the hand facing upwards.





**Figure 3 Experimental protocol.** Movement patterns analyzed in the study correspond to the main movement patterns affected by stroke: A1, shoulder abduction; B1, shoulder external rotation; C1, elbow flexion; A2, shoulder adduction; B2, shoulder internal rotation; C2, elbow extension. Red axis indicates the axis around which rotation occurs.

The respective antagonist movements, i.e., shoulder adduction, shoulder internal rotation and elbow extension, consisted of bringing back the upper-arm to the initial position following the same trajectory but in the opposite direction. For instance, during shoulder adduction, subjects were asked to lower the arm toward the body starting with the arm describing  $90^\circ$  with the body midline and so on. Note that these movements require the active engagement of just one degree of freedom of a single joint. Thus, they constitute an atomic kinematic unit, the combinations of which can produce multiple complex movement patterns such as eating or reaching an object

Subjects performed 30 repetitions of each movement with both arms separately. The upper-limb was not attached to any particular fixture. For each trial, movement onset was indicated by a combination of visual and auditory stimuli that cued every 2.15 seconds. This period was enough for a healthy subject to complete a repetition comfortably while avoiding too long waiting periods between repetitions. One minute was allowed between each set of 30 repetitions to rest and switch movement. In order to avoid learning effects, the arm and movement order was randomly chosen for each subject.



## 7.2 PROTOCOL MODIFICATIONS FOR PATIENTS

The experimental protocol applied to patients was exactly the same as the procedure described above except in some details:

**Repetition number:** in order to avoid excessive tiredness that could bias the experiment results, patients were asked to perform sets of 20 repetitions (instead of 30) in each trial.

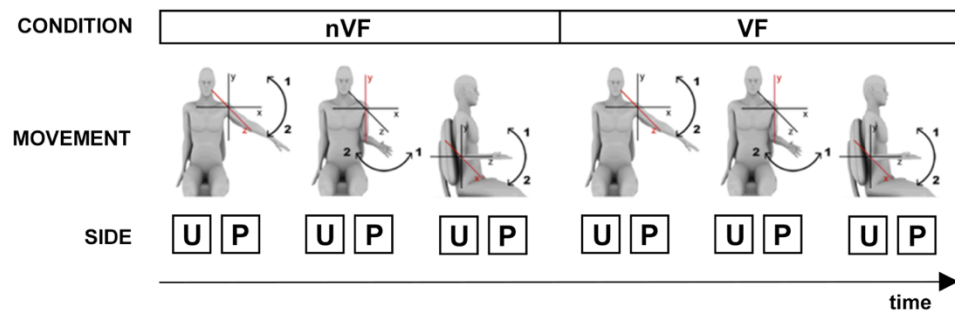
**Repetition frequency:** for some patients 2.15 seconds was not enough to complete a movement. Thus, the movement repetition frequency was individually adapted according to the possibilities of each patient. **Table 11** shows the frequency used for each patient during the experimental session.

Patient	P1	P2	P3	P4	P5	P6
Velocity	1X	0.72X	1X	1X	1X	1X

**Table 11** Movement repetition frequency allowed during the experimental protocol for each patient. 1X equates to the frequency used by neurologically intact subjects (1 repetition/2.15s)



**Timing of the experimental protocol:** a standardized sequence was applied to every patient to complete the experiment. The first slot of movements was completed in absence of VF and then, in presence of VF. VF feedback was provided placing a full-body mirror in front of patients so that they could track the trajectory of their upper-limbs (Specific Procedures (II), **Figure 19**). Within each slot, the ordering of the movements was the following: shoulder abduction/adduction – shoulder internal / external rotation – elbow flexion / extension. Each patient performed every movement first with the unaffected arm, and then with the paretic arm (**Figure 4**).



**Figure 4** Timing of the experimental protocol for patients with stroke. U, unaffected arm; P, paretic arm.



## 8 EMG DATA

The workflow needed to convert raw EMG signals into muscle synergies is formed by a concatenation of steps schematized in **Figure 5**. Each of these steps is explained in detail in the subsections enclosed within the present section.



Figure 5 Flow chart of the EMG data acquisition and processing to extract muscle synergies.

Note that in view the high amount of EMG signals we foresaw that we were going to process and analyze along the thesis, we decided to invest some effort on building a robust custom designed GUI to automate the process and facilitate the monitoring and assessment of the analysis. The GUI offers a wide range of analytic and visualization capabilities that can be discovered in depth in Appendix E. Custom GUI For Upper-Limb Motor Analysis. However, in the next few lines we offer a representative overview of some of the most useful capabilities that the GUI presents.



#### CUSTOM DESIGNED GUI FOR EMG ANALYSIS

In order to automate the process and facilitate the replicability of the study, we have built a customized GUI that bundles the package of functions developed during this thesis to process the acquired EMG recordings, extract the control structure and analyze key features. **Figure 6** shows some of the processing phases that can be monitored through the GUI. Further information can be found in Appendix E. Custom GUI For Upper-Limb Motor Analysis.



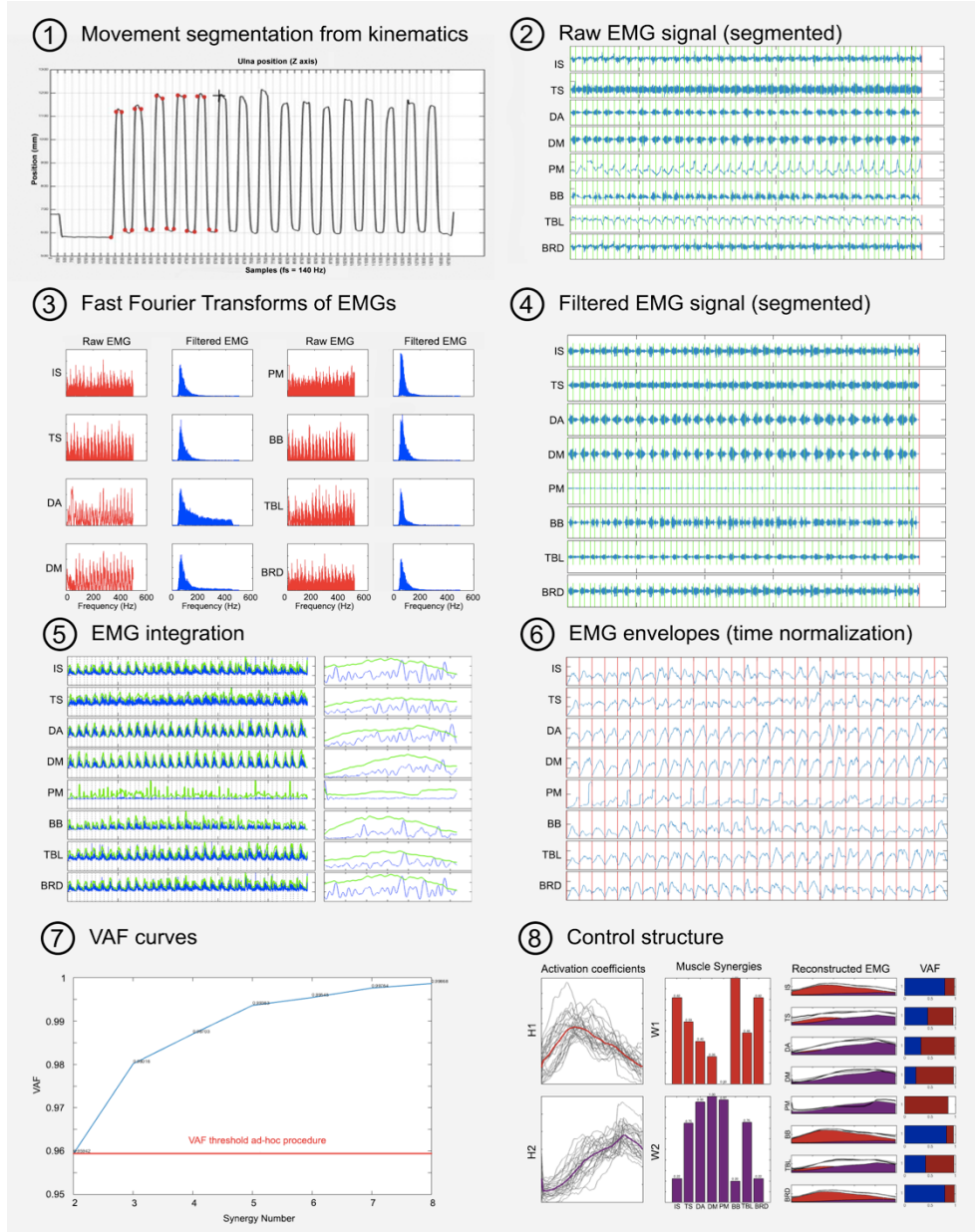


Figure 6 Examples of the visualization capabilities offered by the custom designed GUI to monitor EMG processing and synergy extraction.



## 8.1 ELECTRODE PLACEMENT

Surface EMG signals were recorded from 8 elbow and shoulder muscles from each arm in accordance with published guidelines<sup>180</sup>. We selected the muscles that were most relevant in the execution of the movements under analysis: infraspinatus (IS), trapezius superior (TS), deltoid anterior (DA), deltoid medial (DM), pectoralis major (PM), biceps brachii (BB), triceps brachii long head (TBL) and brachioradialis (BRD). The reference electrode was placed on the ipsilateral wrist. Following the aforementioned guidelines, after the electrodes were placed and fixed, we performed the physiological tests designated for each muscle to ensure the correct placement of the electrodes and reduce the level of crosstalk.

## 8.2 EMG ACQUISITION

### 8.2.1 *EMGs of neurologically intact subjects*

Signals were acquired with the EMG100C system (Biopac Systems, Inc.) at a sampling rate of 1000 Hz and a gain of 500 using a pair of disposable Ag/AgCl disc electrodes on each muscle (10 mm in diameter, 1.5 cm inter-electrode distance; EL501 foam electrode, Biopac Systems, Inc.). A notch filter was used to remove 50-Hz interference. During the recordings, we on-line marked the movement onset and offsets at the instants where subjects initiated and terminated each movement repetition. Thus, after recording EMG signals were segmented using these marks to exclude resting periods from the analysis.

### 8.2.2 *EMGs of patients with stroke*

Signals were acquired with the PocketEMG system (HP - BTS Bioengineering Inc.) at a sampling rate of 1000 Hz and a gain of 500 using a pair of disposable Ag/AgCl electrodes on each muscle (24 mm in diameter, 1.5 cm inter-electrode distance; H92SG foam-hydrogel electrode, Covidien<sup>TM</sup> - Kendall<sup>TM</sup>). In order to exclude resting periods from the analysis, EMG signals were segmented using the position data obtained from



kinematics recordings to identify movement onset and offset (see section 17.4 **Determining movement onset and offset** in Study 3).

### 8.2.3 *Database compatibility*

In order to ensure the comparability between the two databases, since each was acquired with a different equipment that may have affected the result of the acquisition, we carried out an extra experimental session with both systems. That is, we asked a subject to repeat the experimental session twice, one using the BIOPAC System and the second one using the PocketEMG system. Next, we extracted the corresponding control structure using the muscle synergy extraction method explained below (see equations ( 4 ), ( 5 ) and ( 6 )) and we tested whether the control structures extracted from the two EMG datasets were comparable. We confirmed that the number of synergies extracted, the muscle weights and the activation coefficients were comparable using the two procedures (we allowed a 10% of tolerance in the similarity). Therefore, we concluded that the equipment did not introduce significant interferences on the data acquisition process and that the two databases were comparable.

## 8.3 EMG PREPROCESSING

Signals were low-pass ( $f = 450\text{Hz}$ ) and notch filtered ( $f = 50\text{ Hz}$ ) to remove high-frequency noise and 50-Hz interference respectively. Then, EMG segments corresponding to movement repetitions were concatenated and high-pass filtered using a zero-phase Butterworth ( $n=6$ ) filter with a cutoff frequency of 50 Hz to remove any low-frequency motion artifact and demeaned. EMG features were extracted from these signals.



In order to extract the control structure (see Section 8.4 Synergy Extraction), additional preprocessing steps were required. Namely, linear envelopes of EMGs were calculated and integrated over 350 ms intervals, the EMG of each muscle was normalized to the maxima of the 30 repetitions and the length of each repetition was normalized in time to 100 equally spaced points interpolating each repetition in one dimension.

## 8.4 SYNERGY EXTRACTION

Muscle synergies and their corresponding activation coefficients were extracted from the EMGs averaged for each movement and subject across the 30 repetitions. Muscle synergies are modeled as:

$$\mathbf{D}(t) = \sum_{i=1}^N \mathbf{W}_i \cdot H_i(t) + \epsilon \quad (4)$$

where,  $\mathbf{D}(t)$  is the vector of EMG signals at time  $t = 1, 2 \dots L$ ,  $N$  is the number of muscle synergies,  $\mathbf{W}_i$  is the time-invariant muscle vector representing the  $i$ th muscle synergy,  $H_i(t)$  is the nonnegative time-varying activation coefficient for the  $i$ th synergy and  $\epsilon$  is any residual activity. In our case, there are  $m = 8$   $\mathbf{D}(t)$  vectors of length  $L = 100$  corresponding to the recorded muscles for each movement and arm.

For easier handling of the model, equation (4) may be written in matrix notation:

$$\hat{\mathbf{D}}(\mathbf{t}) = \mathbf{V} = \mathbf{W}\mathbf{H} \quad (5)$$

Where,  $\hat{\mathbf{D}}(\mathbf{t})$  is the approximation of  $\mathbf{D}(\mathbf{t})$  from the extracted muscle synergies and activation coefficients,  $\mathbf{V}$  is the reconstructed matrix of 8 EMGs,  $\mathbf{W}$  is the matrix concatenating the  $N$  muscle synergies in columns ( $\mathbf{W} \in R^{m \times N}$ ), and  $\mathbf{H}$  is the matrix concatenating the corresponding  $N$  activation coefficients in rows ( $\mathbf{H} \in R^{N \times L}$ ). Synergies were extracted from the EMG of each subject's arm using nonnegative matrix



factorization (NMF) <sup>125</sup>. The usual approach to find  $\mathbf{W}$  and  $\mathbf{H}$  is by minimizing the differences between  $\mathbf{V}$  and  $\mathbf{WH}$  using multiplicative update rules as described in <sup>181</sup>:

$$\min_{\mathbf{W}, \mathbf{H}} f(\mathbf{W}, \mathbf{H}) \equiv \frac{1}{2} \sum_{i=1}^N \sum_{j=1}^m V_{ij} - (\mathbf{WH})_{ij})^2 \quad (6)$$

subject to  $W_{ia} \geq 0, H_{bj} \geq 0, \forall i, a, b, j$

This approach alternatively fixes one matrix and improves the other, but it is claimed to lack convergence properties <sup>182</sup>. To solve this problem, we have implemented a two-phase extraction procedure combining the multiplicative update rules and the optimization method called “Alternating Nonnegative Least Squares using Projected Gradients”. This method optimizes both matrices simultaneously and it has shown to overcome the limitations of the multiplicative update rules <sup>182</sup>. Brief, because the multiplicative update rules show a fast initial convergence, we apply this method in the first phase to obtain the  $\mathbf{W}$  and  $\mathbf{H}$  matrices that will initialize the second phase. That is, we use these matrices as  $\mathbf{W}_{\text{init}}$  and  $\mathbf{H}_{\text{init}}$  to start the algorithm, which is explained in detail in <sup>182</sup>. The outputs of this second phase are the synergies and activation coefficients used in the subsequent study.

The NMF requires  $N$  to be set prior to any computation. Thus, to set the adequate  $N$ , we successively increased the number of synergies extracted, from one to the number of muscles recorded, and selected the minimum number of synergies required for an EMG reconstruction *Variance Accounted For* (VAF) of 90%. At all, we run 576 (6 subjects x 2 sides x 6 movements x 8 muscles) separate synergy extractions. We did not pool the datasets corresponding to different movements because one of the aims of this study was to characterize the task-specific muscle activity needed to



perform a given movement in absence of neurological damage, to apply it into the corresponding rehabilitation exercises. That is the reason why, each extraction was run on a matrix of size  $8 \times 3000$  (8 muscles, 30 repetitions of 100 time-samples) corresponding to the concatenated EMG data of each movement and each subject's arm. For similar reasons, we run synergy extractions separately over different subjects because we wanted to verify whether different subjects have different control structures and to which extent are these control structures different from each other.

As we explain in detail in PART III. STUDIES, after synergy extraction the dataset consisted of 144 pairs of muscle synergies [ $8 \times 1$ ] and activation coefficients matrices [ $1 \times 100$  time-samples] corresponding to 6 subjects  $\times$  2 arms  $\times$  6 movements  $\times$  2 components of the control structure. Note that in order to make results physiologically more comprehensible, we worked on the average activation coefficient of the 30 repetitions.

#### 8.4.1 *Within-subject synergy matching across limbs*

Because the ordering of the control structure components resulting from NMF is random, the activation coefficient sorted in first place (H1) in the left arm of a subject may correspond with the activation coefficient sorted in the second place (H2) in the right arm of that subject. Thus, before computing the ILS, it is essential to adequately match the activation coefficients across arms and across conditions (grouping H1s with H1s and H2s with H2s) so that the activation coefficients labeled  $H_i$  in the right and left arms of the same subject (both without and with VF) correspond to the same physiological manifestation.

We considered that the physiologically matching muscle synergies and activation coefficients from the left and right arm were the pair of elements resulting in a higher Interlimb Similarity measure (see subsection 8.4.2 below for a detailed description of Interlimb Similarity measures and section 14.3 **Within-Subject synergy matching across conditions** for further details on the matching procedure).



#### 8.4.2 Interlimb similarity (ILS) measures

Interlimb similarity (ILS) was defined as the similarity between the control structure of right (R) and left (L) arms. Due to the obvious differences in the origin of muscle synergies and activation coefficients, most adequate measures were used to quantify the ILS in each case. The ILS between **muscle synergies** was calculated using scalar products and the ILS between activation coefficients was calculated using the cross-correlation coefficients.

##### A | ILS of muscle synergies

To calculate scalar products, we first normalized the muscle synergy vectors ( $\mathbf{W}_i$ ) to one by dividing them by their norm. Unit vector can be identified by the circumflex:

$$\widehat{W}_i = \frac{W_i}{\|W_i\|} \quad (7)$$

Scalar products were then calculated as:

$$ILS_{Wi} = \widehat{W}_{i,R} \cdot \widehat{W}_{i,L} \quad (8)$$

where  $\widehat{W}_{i,s}$  is the normalized  $i$ th synergy extracted from the  $s$  side,  $s \in \{R, L\}$ .



### B | ILS of activation coefficients

ILS between the  $i$ th activation coefficients was quantified as the **maximum cross-correlation coefficient** given the delay  $\tau$ :

$$ILS_{Hi} = \max_{\tau} \frac{\sum_{n=0}^{N-1} H_{i,L}[n] \cdot H_{i,R}[n + \tau]}{\sqrt{\sum_{n=0}^{N-1} H_{i,L}^2[n] \cdot H_{i,R}^2[n + \tau]}} \quad (9)$$

where  $N$  is the total number of samples in the activation coefficient, and  $n$  the  $i$ th sample.

To complement this perspective, we defined an alternative index based on the dissimilarity concept. That is, we first quantified the dissimilarity between activation coefficients by averaged point by point differences and then, calculated the ILS by subtraction. This index is referred along the thesis as  $1 - \text{ILD}$ .

$$ILS_{Hi} = 1 - \text{ILD} = 1 - \frac{\sum_{n=1}^N |H_R[n] - H_L[n]|}{N} \quad (10)$$

where  $N$  is the total number of samples in the activation coefficient, and  $n$  the  $i$ th sample.



## 9 KINEMATIC DATA

👉 *Kinematic data was only acquired in the database of patients with stroke.*

Kinematic data recording was done using the system SMART-D (BTS Bioengineering). The BTS SMART-D System is an opto-electronic system composed of 6 infrared cameras that detect the tridimensional position of reflecting markers (passive markers) attached to the moving limb. Furthermore, the system is endowed with two synchronized video cameras (**Figure 7**). The use of opto-electronic systems based on either passive or active markers is considered the gold standard technology for human movement analysis<sup>155</sup>.

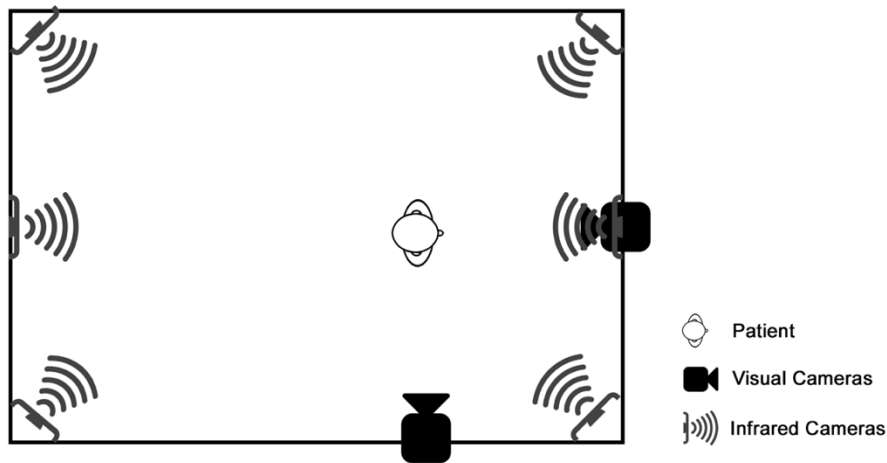


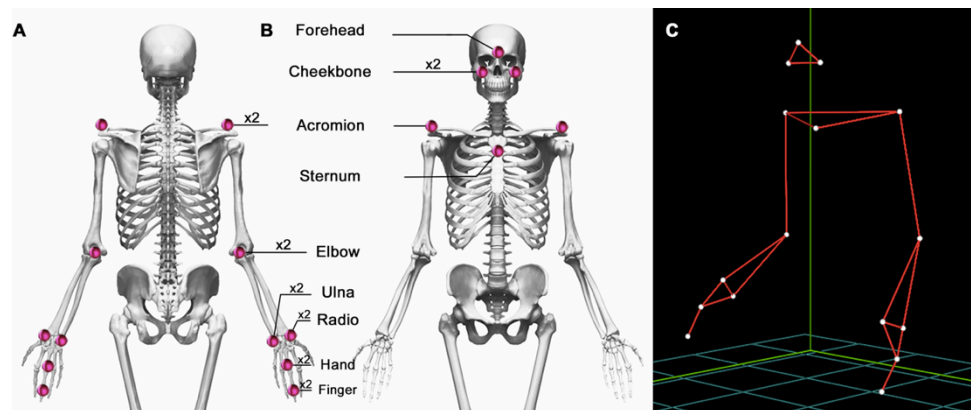
Figure 7 Configuration of the cameras in the Movement Analysis lab of the Guttman Institute



Infrared cameras were arranged around the lab and located approximately 2m above ground level. In contrast, visual cameras were located in front of the patient and orthogonal to his right side at approximately 1m above ground level.

## 9.1 BIOMECHANICAL MODEL

The biomedical model used in this work is an adaptation of the model employed in the Guttmann Institute for the upper-limb<sup>183</sup>, which is in turn a modification of the model by Rab and colleagues<sup>184</sup>. The final model adapted for this thesis gets rid of the markers located in the pelvis, sacrum and posterior neck in the original model, and of the markers located in the object to grasp (**Figure 8**).



**Figure 8 Anatomical location of the markers to record kinematics data.** A – Front view, B – Back view, C – Biomechanical model of the markers after 3D reconstruction. At all 16 markers were placed in each patient. Bilateral markers. i.e., markers that are placed symmetrically in both sides of the body are indicated by x2.

As a result of these modifications, the final model ended up being composed of 16 markers, 20 segments and 5 macro-segments. These 5 macro-segments are described under these lines:

1. **HEAD:** Triangular macro-segment built up from the forehead and cheekbone markers. This macro-segment allows tracking the rotation of the head and neck to discard neuromuscular artifacts due to the observation of the moving limb. Its reference segment is the torso.



2. **TORSO:** Triangular macro-segment built up from the acromion and sternum markers. Its reference segments are any of the coordinate axis within the ground-reference system placed on the lab floor.
3. **UPPER-ARM:** Linear macro-segment built up from the acromion to the elbow. Its reference segment is the torso.
4. **FOREARM:** Linear macro-segment built up from the elbow to a virtual marker located between the ulna and the radio. Its reference segment is the upper-arm.
5. **HAND:** Triangular macro-segment built up from the markers located in the ulna, the radio and the hand. Its reference segment is the forearm.

## 9.2 KINEMATIC DATA ACQUISITION AND PROCESSING

In order to complete the kinematic data acquisition process, we followed a sequence of steps. Regardless the motion capture system used, the opto-electronic systems require very similar protocols. The flow chart of the steps that we applied is schematized in **Figure 9**.



Figure 9 Flow chart of the kinematic recording and processing process.

Infrared systems are characterized by high precision and sampling rates. According to the technical sheet, the position error of the SMART-D system is less than 0.2 mm.



### 1 | Marker placement

A qualified specialist from the Guttmann Institute was responsible of this phase. Patients were endowed with a set of reflecting markers fixed with double-sided adhesive tape. When necessary, hairy zones were shaved to enhance marker adhesion.

At all, 16 markers were attached to the skin of the patients distributed unilaterally along the longitudinal axis of their upper-body or bilaterally along the two sides (**Figure 8**). Bilateral markers, that is, the markers with a symmetric correspondence in both sides are indicated by the inscription 'x2'. The anatomical correspondence of each marker is listed in **Table 12**.

MARKER	ANATOMICAL PLACEMENT
FOREHEAD	Nasion
CHEEKBONE	Malar bone (bilateral)
STERNUM	Jugular low-neck
ACROMION	Acromion (bilateral)
ELBOW	Olecranon (bilateral)
ULNA	Radial styloid (bilateral)
RADIO	Ulnar styloid (bilateral)
HAND	Third metacarpal head (bilateral)
FINGER	Third distal phalanx (bilateral)

**Table 12 Anatomical correspondence of kinematics markers.** Bilateral means that markers for that position were placed symmetrically in both sides of the body.

Because the placement of these markers will determine the spatial position and trajectory of the markers, it is essential to complete this phase accurately.

### 2 | Calibration

Prior to every experimental session (1 patient = 1 session), the system was calibrated to ensure accurate measurement and subsequent 3D reconstruction. During calibration, known references were presented to the acquisition system.



### *3 / Acquisition*

While patients were performing the movements, the acquisition system simultaneously recorded the 3D coordinates of each marker at a sampling rate of 140 Hz and the video images.

### *4 / Tracking*

Tracking is the first step after data acquisition. During tracking, the system identifies the position of the reflecting marker in each time-point, as long as at least 3 cameras out of the 6 cameras composing the registering system have registered the marker. Due to occlusions, the system may miss certain positions and certain time-points (see section **18.1. Quality of the Kinematics Recordings** in Study 3).

### *5 / 3D Reconstruction*

During this stage, the set of 3D points identified in the tracking stage was assigned to the corresponding anatomical labels according to the biomechanical model. As the labels were assigned, the program automatically joined the markers drawing the body segments. The resulting reconstructed conjunct of segments for each frame is shown in **Figure 8C**.

This process was repeated for every time frame to complete the 3D trajectory of the markers. In other words, after this stage, each marker was provided with a series of time-depending 3D positions that define the spatial trajectory described by that marker during movement execution.









## **PART III**

# **Studies**







The present part “Studies” is organized into 4 studies, each of them addressing a very specific question about the thesis:

**Study 1 | ILS in healthy subjects**

*Do we share the control strategy in our two arms?*

**Study2 | The effect of Visual Feedback in the motor control**

*Has VF the ability to modulate the control strategy of our motor system?*

**Study 3 | ILS in patients with stroke**

*How is the ILS altered in patients with stroke? Can VF manipulate altered ILS?*

**Study 4 | Kinematic analysis of movements of patients with stroke**

*Is the alteration of the control structure reflected in movement kinematics?*

Each of these studies is a self-contained piece of research and is organized into 3 main sections: (1) Specific procedures, (2) Results and discussion and (3) Conclusions. Specific procedures describe methods that are only used in a given study. Note that general methods common to all studies are described in the Methods part. Following the same logic, specific conclusions of each study are separately exposed.







1

2




4

3

## Study 1

# Interlimb similarity in healthy subjects

Do we share the control structure between limbs?

 This study corresponds to the paper entitled “Interlimb Differences of Human Upper-Limb Motor Control during Natural Motor Behaviors” [currently under review]. This is the reason why the structure is slightly different and Results and Discussion are separately presented unlike in the rest of the studies.







# Abstract

*Handedness provides functional advantages to the dominant limb, but the origin of such difference remains largely elusive. Here, we hypothesize that handedness does not affect the modular structure of motor control, this being highly conserved across limbs within a subject. Confirming such hypothesis is of great clinical interest to improve the rehabilitation of neural conditions inducing hemiplegia.*

*In order to enhance the value of the study, we have analyzed the 6 main movement patterns affected by stroke. We have characterized the motor strategy of these movements by studying the electromyography (EMG) of 8 upper-limb muscles in each side. We have calculated relevant spectral and temporal EMG features, and extracted the control structure (i.e. the set of muscle synergies and activation coefficients) needed to perform each of these tasks. Subsequently, we have conducted an inter-limb comparison with all these elements.*

*Our results revealed that muscle recruitment patterns inferred from EMG features, differ from right and left arm differently in each subject. In contrast, the control structure exhibits a substantial within-subject inter-limb similarity, significantly higher than the corresponding inter-subject similarity. Indeed, we demonstrate that the muscle activity of a limb can be reconstructed with an accuracy of over 90% using the control structure of the opposite limb.*

*EMG features are extremely variable and inconsistent with any handedness principle. In contrast, the control structure is highly conserved across limbs and may serve as a powerful tool to guide rehabilitation. Thus, this study provides a complete framework to inspire novel and effective motor interventions.*







# 10 SPECIFIC PROCEDURES (I)

## 10.1 CHARACTERIZATION OF EMG SIGNALS

### 10.1.1 *Exponential decay model of muscle fiber recruitment*

To produce voluntary movements, motor units are sequentially recruited generating submaximal contractions<sup>185</sup>. This process can be indirectly tracked by inspecting the amplitude of the EMG signal, as it reflects the number and size of muscle fibers recruited by the muscle under analysis<sup>185–187</sup>. Thus, to investigate whether there are differences in the recruitment patterns of right and left arms, we analyzed the changes undergone by the EMG amplitude across repetitions.

We calculated the peak amplitude of each muscle in every repetition and we plotted the evolution of EMG peaks across repetitions. Because the peak sequence showed a similar trend in every muscle, we averaged EMG peak curves across the eight muscles. Subsequently, we fit the averaged curves to the decreasing form of the exponential decay model, which is defined by:

$$Y = Y_0 + (C - Y_0) \cdot (1 - e^{-kx}) \quad (11)$$



where  $Y$  represents the amplitude of the EMG peak (mV),  $Y_0$  represents the amplitude of the EMG peak in the first repetition (mV),  $C$  represents the amplitude of the EMG peak after stabilization (mV),  $K$  represents the rate constant (repetitions<sup>-1</sup>) and  $x$  represents the repetition number.

This model is usually employed to describe first order kinetics, i.e., processes governed by a rate of change that depends on the size of the population producing such change<sup>188</sup>. In the case of muscles, we can assume that the amount of muscle fibers present in the upper-limb is finite. In consequence, during muscle contraction the amount of fibers that are available for recruitment decreases gradually, as does the capacity to increase the EMG amplitude<sup>189</sup>. The goodness of fit of the model was assessed using the  $R^2$  value and the sum of squares, defined as the absolute sum of squares of the distances from the data-points to the fitted curve.

### 10.1.2 Median Frequency

Voluntary muscle activity is characterized by relatively low force levels (10-15% of maximal force) and low motoneurone firing rates (10-20 Hz)<sup>190</sup>. Shifts in the median frequency (MDF) are indicative of muscle fatigue<sup>191</sup>. MDF is defined as the frequency at which the EMG power spectrum (PSD) is divided into two regions with equal power. This can be mathematically stated as:

$$\int_0^{MDF} P(f)df = \int_{MDF}^{f_{upper}} P(f)df = \frac{1}{2} \int_0^{f_{upper}} P(f)df \quad (12)$$

where  $P(f)$  denotes the PSD of the EMG signal,  $f_{upper}$  denotes the upper frequency of the EMG spectrum and  $f$  is frequency (Hz). Thus, in order to evaluate whether successive movement repetitions induced muscle fatigue, we studied the evolution of the MDF along repetitions. To this end, we estimated the PSD of each repetition from the periodogram applying rectangular time windows. Then, the area between the PSD and its frequencies was calculated and MDF was set as the frequency corresponding to half of this area.



## 10.2 SYNERGY MATCHING ACROSS SUBJECTS

For inter-subject comparisons, we classified the synergies obtained from all subjects into two classes using 2-node hierarchical cluster trees based on the Minkowski distance. In both cases, activation coefficients were matched according to the matching of their corresponding synergies. We calculated the similarity between the control structures of all possible pairs of subjects. The right and left inter-subject similarities provided for each dynamic component result from averaging all these pair-comparisons.

## 10.3 CROSS-RECONSTRUCTION

The scalar product and the cross-correlation coefficient quantify the degree of structural similarity between synergies and activation coefficients respectively, but may not necessarily reflect functional similarity, that is, the extent to which similar muscle synergies or activation coefficients represent similar muscle activities. From a physiological perspective, the functional similarity is what is important when it comes to interpret the similarity between the control structures as similar motor behaviors. Therefore, in order to quantify the functional interlimb similarity between muscle synergies and activation coefficients, we reconstructed the muscle activity of a limb from the control structure of the opposite limb and we compared it with the original EMG signal. Cross-reconstruction was performed by multiplying one of the terms of the control structure (either  $H$  or  $\mathbf{W}$ ), by the corresponding term of the opposite limb. We use the term ‘crossed-synergies’ to refer to the cross-reconstruction performed from the synergy vectors ( $\mathbf{W}$ ) of the opposite limb, and ‘crossed-activations’ to refer to the cross-reconstruction performed from the activation coefficients ( $H$ ) of the opposite limb. This process was repeated for every movement and subject. To quantify the



quality of the cross-reconstruction, we calculated the  $VAF_{cr}$ , i.e., the VAF of the cross-reconstructed muscle signals with respect to the original EMG signals. However, note that the  $\epsilon$  term of the model (Equation ( 4 )) implies the existence of an inherent loss of reconstruction accuracy that biases the  $VAF_{cr}$ . Thus, we also report a corrected VAF ( $VAF_{cr}^*$ ), calculated with reference to  $VAF_{ref}$ . The latter estimates the reconstruction accuracy of the EMG signal with respect to the original reconstruction (V term of Equation ( 5 )).

$$VAF_{cr}^* = \frac{VAF_{cr}}{VAF_{ref}} \quad ( 13 )$$

## 10.4 ACTIVITY MAPS

The activity maps represent the muscle activity needed to perform a given movement in absence of neurological impairment. Given that the control structure is movement specific, these maps could serve to guide the rehabilitation of the paretic arm. Thus, they have been purposely structured rehabilitation-oriented. Muscles are arranged in the y-axis by the position of their electrodes along the longitudinal axis of the body (from proximal to distal). In consequence, the vertical arrangement of muscles coincides with the position of the muscle belly, the part of the muscle where most contractile fibers reside. This is relevant to rehabilitation as both the degree of impairment<sup>192</sup> and the effectiveness of rehabilitation<sup>193,194</sup> depend on the muscle's distance to the trunk. Time is plotted on the x-axis, with time needed to perform a repetition of each movement normalized to 100 points. Time normalization is essential to overcome the natural variability of the human motor coordination, which even in the most standardized movement repetitions induces important within-subject trial-to-trial variability both in terms of duration and kinematic characteristics of the movements<sup>195</sup>. Having these maps normalized in time, not only allows applying them regardless the duration of each repetition, but also comparing them between subjects and limbs.



To estimate the muscle activity corresponding to each movement, we solved inversely equation ( 4 ) for each limb. In other words, the muscle activity displayed by the activity maps corresponds to the  $V$  matrices obtained by multiplying the  $W$  and  $H$  matrices of each subject's limb and movement (Equation ( 5)). The  $V$  matrices retain the relevant control features of the original EMG signal while getting rid of the  $\varepsilon$  term (Equation ( 4 )), which corresponds in large part to signal noise. Also,  $V$  matrices substantially reduce the amount of inherent variability of the motor system, as they are estimated from the average muscle activity used to produce a given movement over 30 repetitions. We normalized the activity values obtained to the range of  $[0,1]$  and we generated a surface plot for each movement. The lines seen in the maps connect points with the same muscle activity. The intensity of this activity is expressed by a color gradient, with reddish colors meaning higher activity and bluish colors lower activity (Figure 19).

## 10.5 STATISTICAL ANALYSES

Wilcoxon signed rank tests were used to assess differences between right and left inter-subject similarities. For each movement, we compared  $N_{\text{Inter-subject}} = 30$  interlimb similarity measures corresponding to the 15 pairs of possible comparisons between subjects that were concatenated for either  $W1$  and  $W2$ , or  $H1$  and  $H2$  of right and left arms. Wilcoxon rank sum test was used to assess differences between interlimb and right or left inter-subject similarities. In this case, for each movement we compared  $N_{\text{Inter-subject}} = 30$  inter-subject similarity measures against  $N_{\text{Interlimb}} = 12$  interlimb similarity measures corresponding to the concatenation of each subject's interlimb similarity measures of either  $W1$  and  $W2$ , or  $H1$  and  $H2$ . These comparisons were done separately for synergies (scalar products) and activation coefficients (cross-correlation coefficients). Finally, Friedman tests were used to assess differences in the similarity



measures of more than two groups. Friedman test is a non-parametric test used for one-way repeated measures analysis of variance by ranks. As such, we used it to assess differences in similarity measures across different movements ( $N_{\text{Interlimb}} = 12$  or  $N_{\text{Inter-subject}} = 30$ ,  $C = 6$  groups of movements), as well as to assess differences in the cross-reconstruction VAF across different movements ( $N_{\text{VAF}} = 6$  subjects  $\times$  2 sides;  $C = 6$  groups of movements) and muscles ( $N_{\text{VAF}} = 6$  subjects  $\times$  2 sides  $\times$  6 movements;  $C = 8$  groups of muscles).



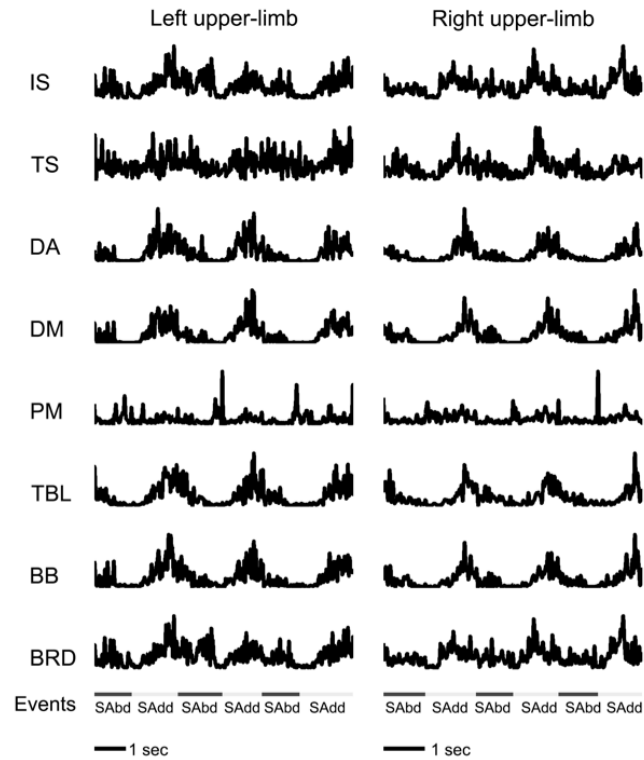
# 11 RESULTS (I)

## 11.1 CHARACTERIZATION OF EMG DATA

**Figure 10** shows representative examples of EMG signals all collected from subject 2 (S2) during shoulder abduction and shoulder adduction alternating movements. Shown are 6 consecutive movement repetitions performed with the left arm (**Figure 10A**) and right arm (**Figure 10B**). Visual inspection of EMG data suggests that muscle activity of both limbs bear substantial resemblance when performing the same movement. It can also be observed that upper-limb muscles co-activate by groups following a pattern that replicates across different trials.

Upon visual inspection, it can be observed that upper-limb muscles are prone to co-activate in groups following a pattern that replicates across trials. Notably, the activation onset of each muscle varies in time from muscle to muscle giving rise to a marked muscular activation sequence. For instance, shoulder abduction is initiated by a simultaneous coactivation of infraspinatus (IS), trapezius superior (TS) and the deltoid heads (DA and DM), the last two decreasing in the second half of the movement execution period. The activity decrease of the deltoid heads coincides with the activity onset of the pectoralis major (PM). In contrast, shoulder adduction is clearly initiated by TS and PM and subsequently mediated by the progressive activation of IS and a bit later, the deltoid heads. This kind of coordinated behavior is observed in all the movements under analysis.



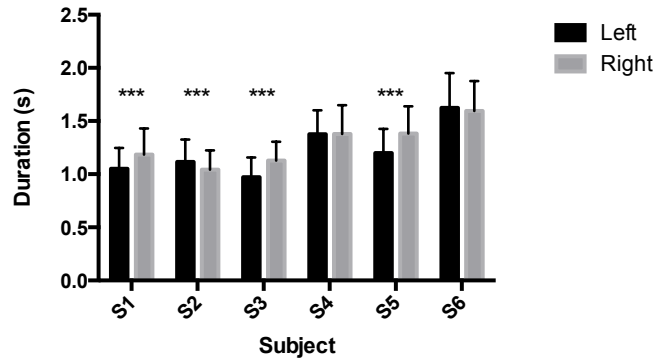


**Figure 10** Example of EMG data of a representative subject. Shown are EMG data collected from 8 upper-limb muscles (indicated in the y-axis) during shoulder abduction and adduction repetitions of subject S2. EMG data are high-pass filtered (cutoff of 50 Hz), demeaned, rectified and subsequently low-pass filtered (cutoff of 20 Hz). A, EMGs of 6 consecutive movement repetitions from the left upper-limb. B, EMGs of 6 consecutive movement repetitions from the right upper-limb. Bottom lines indicate the duration of EMG segments corresponding to alternated shoulder abduction (SAbd) and shoulder adduction (SAdd) repetitions.

Movement durations ranged between 0.9 and 1.6 seconds from subject to subject and movement to movement. We investigated whether subjects tend to perform longer movements with either their right or left arm. For each movement and subject, we compared the average duration of the 30 repetitions of both arms and we found that in effect, most subjects tend to perform longer movements with either one or the other arm (**Figure 11**). Interestingly, although all subjects were right-handed, subjects #1, #3 and #5 performed significantly slower movements with their right arms (S1: 1.05s – 1.18s; Paired t-test;  $p < 10^{-7}$ ;  $t_{\text{ratio}} = 5.75$ ;  $n = 180$  | S3: 0.97s – 1.13s; Paired



t-test;  $p < 10^{-14}$ ;  $t_{\text{ratio}} = 8.21$ ;  $n = 180$  | S5: 1.20s – 1.38s; Paired t-test;  $p < 10^{-11}$ ;  $t_{\text{ratio}} = 7.13$ ;  $n = 180$ ), whereas subject #2 performed significantly slower movements with his left arm (1.12s – 1.04s; Paired t-test;  $p < 10^{-3}$ ;  $t_{\text{ratio}} = 3.51$ ;  $n = 180$ ). We found no significant differences for subjects #4 and #6. Note that the variable  $t_{\text{ratio}}$  refers to the mean of the differences between each set of right-left pairs divided by the standard error of the differences.



**Figure 11 Interlimb comparison of movement duration across subjects.** Bars represent the mean movement duration of each subject averaged across the 30 repetitions of each movement. Error bars are SD. Black bars correspond to left arm movements and grey bars correspond to right arm movements. Significant interlimb differences were identified through the paired t-test (\*\*\*) =  $p < 0.001$ ).



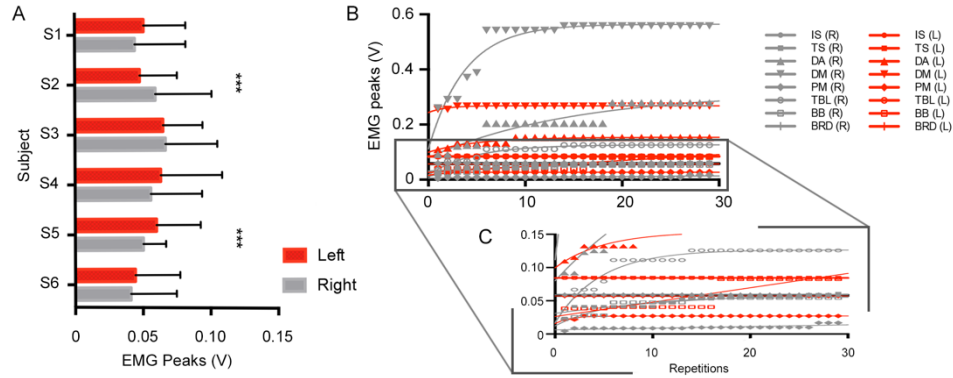
## 11.2 EVOLUTION OF EMG AMPLITUDE ACROSS REPETITIONS

**Figure 12A** shows the amplitude of EMG peaks averaged for each subject across movement repetitions. When comparing the left and right arm average peak values, we found that some subjects (S1, S4, S5 and S6) exhibited higher EMG peaks in their left arms while subjects S2 and S3 exhibited higher EMG peaks in their right arms. These inter-limb differences were found to be statistically significant in subjects S2 and S5 (S2:  $0.048 \text{ V} - 0.059 \text{ V}$ ; Paired t-test;  $p < 10^{-2}$ ;  $t_{\text{ratio}} = 3.08$ ;  $n = 180$  | S5:  $0.06 \text{ V} - 0.05 \text{ V}$ ; Paired t-test;  $p < 10^{-3}$ ;  $t_{\text{ratio}} = 3.57$ ;  $n = 180$ ). Interestingly, subjects exhibiting higher EMG peak values in their right arms coincide with those exhibiting faster movements in their right arms and vice versa.

A representative example of the evolution of the EMG peaks of all muscles can be seen in **Figure 12B** and **Figure 12C** (the dataset corresponds to the shoulder abduction of subject S2). The trend described follows an exponential decay model in all 8 muscles. The curve fit is very accurate ( $R^2_{\text{Left muscles}} = \{1, 0.90, 0.84, 0.76, 1, 0.87, 0.59, 0.91\}$  and  $R^2_{\text{Right muscles}} = \{0.75, 0.34, 1, 1, 0.88, 0.92, 0.94, 1\}$ ). In the case of right TS, the  $R^2$  value is 0.34 but given that the SS was quite small ( $SS = 0.00048$ ) we can still conclude that the curve describes reasonably well the shape of the data. This excellent curve fit found in this example generalizes to all subjects and movements, indicating that the muscle fiber recruitment strategy might be similar in this kind of movements.

The models show that subjects reach a higher and earlier plateau always in one of their arms compared to the opposite arm. In the case displayed, we can observe that the peaks of the right infraspinatus (IS) reach a larger plateau than the left IS, the peaks of the right deltoid anterior (DA) reach a larger plateau than the left DA and so on. Interestingly, this asymmetry is expressed in the same manner in all movements performed by S2. That is, the curve described by the EMG peaks of S2 are always faster and taller in the right side. Nonetheless, again the favored side is subject-specific (varies from subject to subject).





**Figure 12 Inter-limb differences in the evolution of EMG peak amplitude.** (a) Inter-limb comparisons of right and left mean EMG peak amplitudes. Bars indicate the mean EMG peak amplitude of each subject averaged across all repetitions, movements and muscles. Error bars are SD. Significant inter-limb differences were identified through the paired t-test (\*\*\*) =  $p < 0.001$ . (b) Evolution of EMG peak amplitude for each muscle across movement repetitions. Data are from a representative subject (S2) and movement (SAbd). Red data-points indicate left arm muscles and grey data-points indicate right arm muscles. Each line fits the exponential decay model for the corresponding muscle. (c) Enlargement of panel b view in the range of 0 – 0.15 V.

The parameters of the fitted models are contained in **Table 13**. These results come in agreement with the gradual rise in amplitude reported during repetitive voluntary contractions<sup>196,197</sup>. This amplitude rise reflects a fiber recruitment pattern according to which, during the first repetitions only a small fraction of all available fibers is recruited and as the exercise progresses, new fresh fibers are recruited until a maximum is reached. Interestingly, the kinetic and magnitude characteristics of the exponential decay curves (i.e. the recruitment pattern) differ from subject to subject, and from limb to limb. In conclusion, these results reveal significant interlimb differences in the muscle recruitment patterns that go beyond handedness. Note that although all subjects were right handed, interlimb differences were not found always in the same side. Instead, some subjects exhibited faster and taller exponential decay



curves in their right arm, while others in their left arm. These findings suggest that interlimb differences are highly subject-specific, at least in this regard.

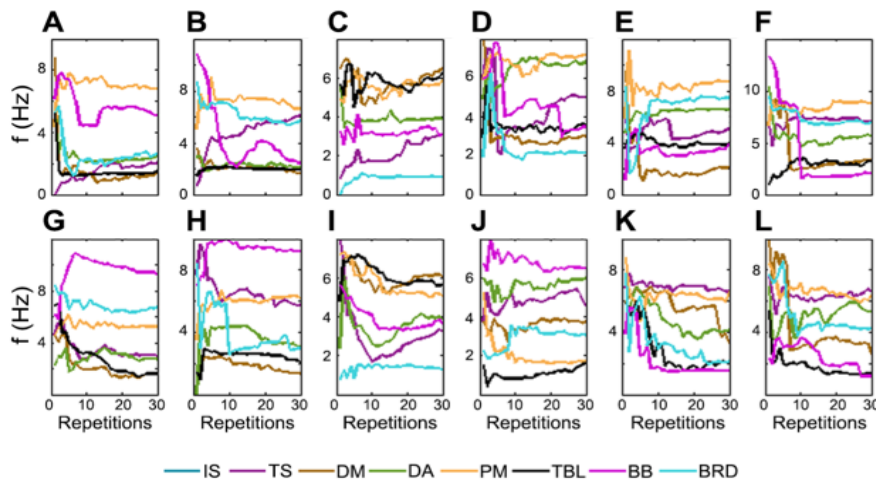
Subject	Movement	$Y_0$	C	k
S2	SAbd (L)	0.089	0.107	0.050
	SAbd (R)	0.048	0.150	0.185
	SAdd (L)	0.040	0.074	0.324
	SAdd (R)	-0.073	0.095	1.266
	SERot (L)	0.025	0.041	0.067
	SERot (R)	0.024	0.038	0.160
	SIRot (L)	0.011	0.038	0.101
	SIRot (R)	0.020	2.538	0.000
	EFlex (L)	0.006	0.030	0.294
	EFlex (R)	0.009	0.040	0.151
	EExt (L)	0.012	0.029	0.185
	EExt (R)	0.020	0.039	0.076
S5	SAbd (L)	0.046	0.121	0.242
	SAbd (R)	0.053	0.090	0.078
	SAdd (L)	0.024	0.080	0.401
	SAdd (R)	0,024	0.071	0.079
	SERot (L)	0.065	0.079	0.128
	SERot (R)	0.029	0.058	0.796
	SIRot (L)	0.011	0.051	0.395
	SIRot (R)	0.029	0.052	0.092
	EFlex (L)	0.022	0.035	0.057
	EFlex (R)	0.014	0.055	0.073
	EExt (L)	0.011	0.030	0.041
	EExt (R)	0.012	0.043	0.074

**Table 13 Parameters of the exponential decay model of representative subjects S2 and S5.**  $Y_0$  represents the amplitude of the EMG peak in the first repetition (mV), C represent the amplitude of the EMG peak after stabilization (mV) and K represents the rate constant (repetitions<sup>-1</sup>). See Equation ( 11 ) in Specific Procedures for further details. L – left arm, R – right arm.



### 11.3 EVALUATION OF MUSCLE FATIGUE ACROSS REPETITIONS

Increases in EMG amplitude are also considered indicative of muscle fatigue<sup>198</sup>. Therefore, in order to discard that the observed amplitude rise was due to muscle fatigue, we studied the evolution of the MDF across repetitions. In particular, we searched for shifts in the EMG spectrum towards lower frequencies that are indirect indicatives of muscle fatigue<sup>191</sup>. The curves displaying the evolution of the MDF during the execution of the 6 movements under analysis by a representative subject (S5) are shown in **Figure 13**.



**Figure 13** Evolution of MDF values across repetitions of a representative subject (S5). **A**, Left shoulder abduction. **B**, Left shoulder adduction. **C**, Left Shoulder external rotation. **D**, Left Shoulder internal rotation. **E**, Left elbow flexion. **F**, Left elbow extension. **G**, Right shoulder abduction. **H**, Right shoulder adduction. **I**, Right Shoulder external rotation. **J**, Right Shoulder internal rotation. **K**, Right elbow flexion. **L**, Right elbow extension.

The shape of MDF curves does not reflect any evident sign of fatigue. Instead, we detected an abrupt decrease of the MDF in few muscles in almost all movements,



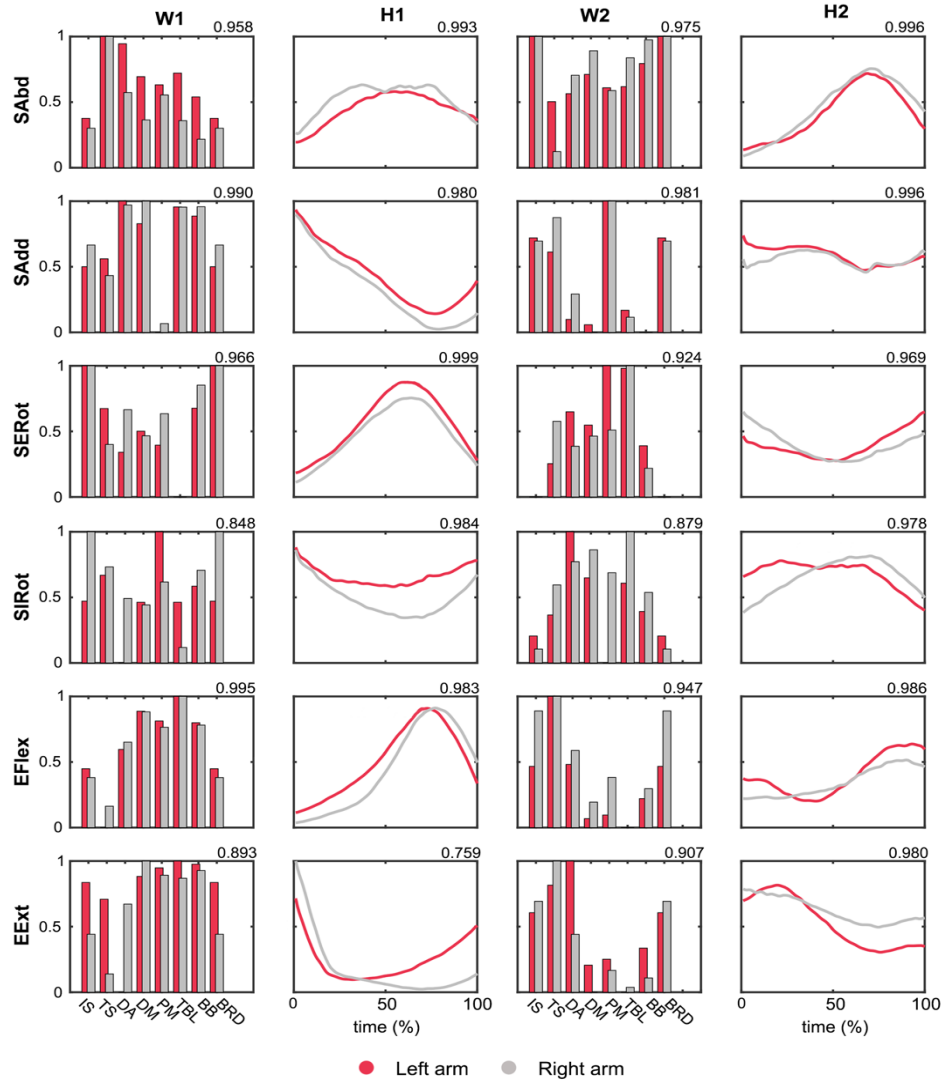
this happened within the first 10 repetitions and not by the end of the exercise, as it would be expected if such shift was caused by fatigue. Moreover, these movements were executed without weight by young men aged between 25 and 35, so, as expected, such early decrease in the MDF cannot be attributed to fatigue. Most of these premature MDF drops, such as TS in **Figure 13A** or DA in **Figure 13I** were preceded by an abrupt increase in the MDF. In fact, such MDF rise coincides with the time period in which the exponential growth of EMG peak amplitude is detected.

## 11.4 INTERLIMB SIMILARITY OF THE CONTROL STRUCTURE

In the second part of the study, we examined the control structure of the main movement patterns affected by stroke in absence of neurological damage. We found that the control structure of these movements can generally be explained by two synergies. Although in few cases (9/72) 3-synergy models were needed to reach the VAF threshold of 90% the mean VAF value of these exceptions was roughly 0.90 ( $0.8936 \pm 0.0047$ ). Hence, we decided to use the 2-synergy models to simplify comparisons.

**Figure 14** shows the control structure of a representative subject during the 6 movements under analysis. Bar plots represent the two muscle synergies, while curves represent the corresponding activation coefficients. As we can see, there is a large correspondence between left and right arm control structures for each movement, both in terms of synergies and activation coefficients. Within-synergy muscle weights are very similar between the right and left arms. Likewise, the activation coefficients of right and left arm draw highly resembling shapes, suggesting the existence of common activation patterns and timing in both limbs. Indeed, the inter-limb similarity measures indicated in the top right corner of each plot confirm that the control structure of a subject is highly conserved between the right and left arm. Of course, this scenario was pretty alike in all subjects.





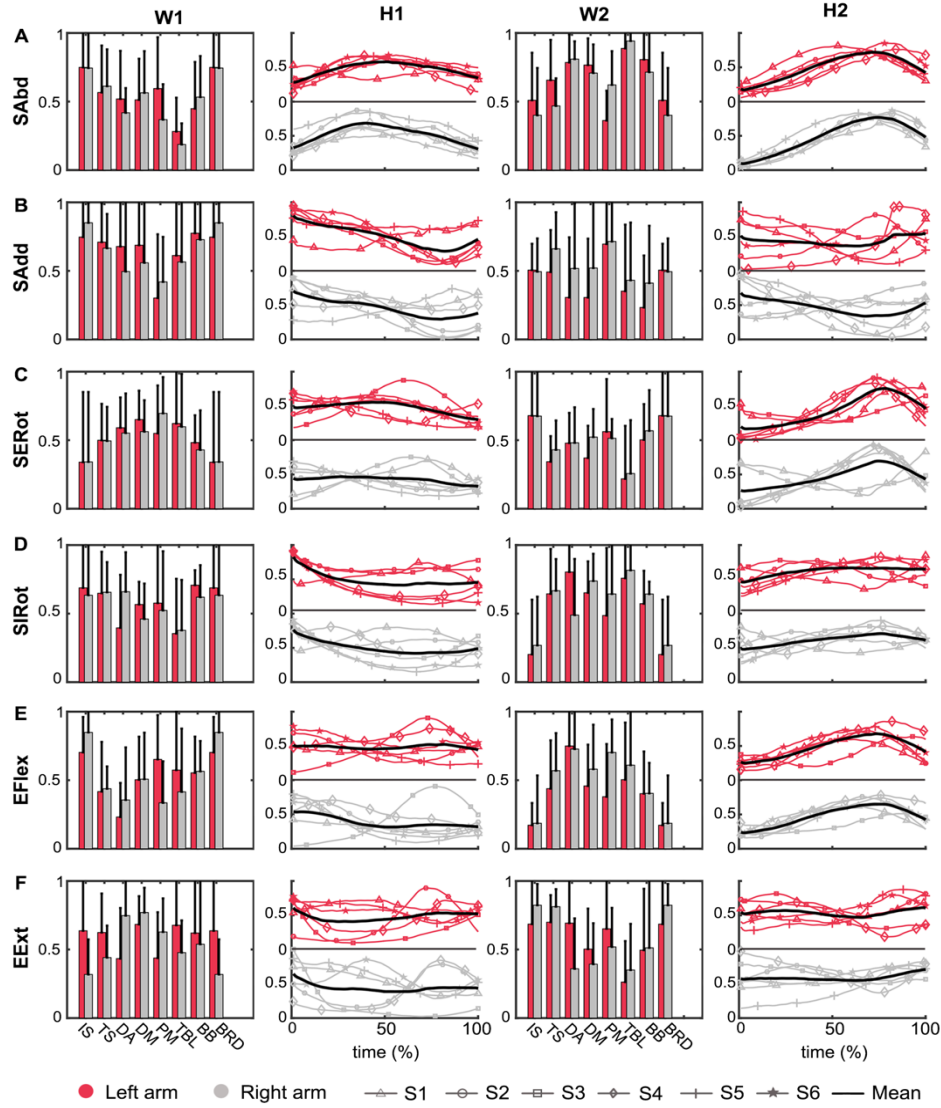
**Figure 14 Control structure of the movements under analysis of a representative subject.** A, Shoulder abduction (SAbd). B, Shoulder adduction (SAdd). C, Shoulder internal rotation (SIRot). D, Shoulder external rotation (SERot). E, Elbow flexion (EFlex). F, Elbow extension (EExt). W1 and W2 are synergy 1 and synergy 2 composed of infraspinatus (IS), trapezius superior (TS), anterior deltoid (DA), medial deltoid (DM), pectoralis major (PM), triceps brachii long head (TBL), biceps brachii (BB), brachioradialis (BRD). H1 and H2 are the corresponding activation coefficients of W1 and W2. Red bars and curves form left arm control structure and grey bars and curves form right arm control structure. The numbers in the right top corner of each plot are the inter-limb similarity measures: scalar product for muscle synergies and cross-correlation coefficient for activation coefficients.



**Figure 15** extends this perspective to the entire population and shows the control structure of the studied population averaged for each movement: bars represent the muscle synergies of each movement averaged across the population, while thick black curves represent the corresponding mean activation coefficients. In general, the average control structure is consistent between limbs and well differentiated from movement to movement suggesting that synergies and activation coefficients are movement specific. However, the error bars denote that there is a high inter-subject variability in the muscle synergies of all movements.

Consistently, although the activation coefficients of a subject tend to converge to a common curve shared in the population, the individual activation coefficients of several subjects show important deviations from the average curve. For instance, the average activation coefficient of synergy 1 (H1) in shoulder internal rotation (**Figure 15D**) is a concave curve, but the activation coefficients of S1 and S2 depict convex shapes. Interestingly, these two subjects preserve such convex shape in their two limbs. Similar individual exceptions can be found in the H1 curve of S3 and S4 during elbow flexion (**Figure 15E**) or in the H2 curve of S3 during shoulder external rotation (**Figure 15C**). In all these cases, the individual activation coefficients deviate from the mean curve, but are found to be very similar in the two arms of each subject. These findings indicate that 1) a common control structure cannot be generalizable to all subjects and 2) subjects presenting a control structure that deviates from the average control structure, preserve such particular control structure in their two limbs.





**Figure 15 Mean control structures of the movements under analysis.** A, Shoulder abduction (SAbd). B, Shoulder abduction (SAdd). C, Shoulder internal rotation (SIRot). D, Shoulder external rotation (SERot). E, Elbow flexion (EFlex). F, Elbow extension (EExt). Six graphs are plotted for the control structure of each component, those on the left and right of each column showing the control structure of the left and right arms respectively. W1 and W2 are mean synergy 1 and synergy 2. Bars are the mean of all subjects  $\pm$  SD. H1 and H2 are the corresponding activation coefficients of W1 and W2, each line-style representing a subject. Red bars and curves form left arm control structures and grey bars and curves form right arm control structures. The thick dark line represents the mean activation coefficient.

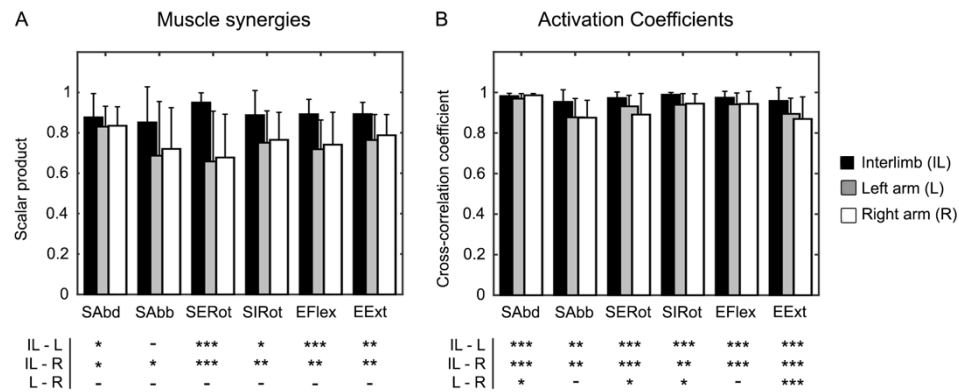


## 11.5 INTERLIMB SIMILARITY VS INTER-SUBJECT SIMILARITY

**Figure 16** compares the average interlimb similarity measures with the left and right inter-subject similarity measures. In the case of *muscle synergies* (**Figure 16A**), interlimb similarity ranged between  $0.8517 \pm 0.1761$  and  $0.9499 \pm 0.0482$ , while inter-subject similarity ranged between  $0.6585 \pm 0.2488$  and  $0.8352 \pm 0.0939$ . Statistically, interlimb similarity was significantly higher than left inter-subject similarity in all cases (Wilcoxon rank-sum test;  $p =$  see **Figure 16A**;  $N = 30$  vs  $12$  for each movement) except in shoulder adduction (SAdd). Interlimb similarity was also significantly higher than right inter-subject similarity in all cases (Wilcoxon rank-sum test;  $p =$  see **Figure 16A**;  $N = 30$  vs  $12$  for each movement). Finally, we found no significant differences between the left and right inter-subject similarities (Wilcoxon signed-rank test;  $p =$  see **Figure 16A**;  $N = 30$  for each movement).

In the case of *activation coefficients* (**Figure 16B**), inter-limb similarity ranged in average between  $0.9536 \pm 0.0598$  and  $0.9889 \pm 0.0109$ , while inter-subject similarity ranged between  $0.8693 \pm 0.1088$  and  $0.9861 \pm 0.0085$ . In this case, inter-limb similarity was also significantly higher than right or left inter-subject similarities in every movement (Wilcoxon rank-sum test;  $p =$  see **Figure 16B**;  $N = 30$  vs  $12$  for each movement). Unlike muscle synergies, we found significant differences in the inter-subject similarity of right and left activation coefficients (Wilcoxon signed-rank test;  $p =$  see **Figure 16B**;  $N = 30$  for each movement). Friedman tests revealed that similarity varies from movement to movement ( $p < 0.05$ ), suggesting that the degree of conservation of the control structure depends on movement characteristics. In effect, movements involving rotatory degrees of freedom around the longitudinal axis, i.e., shoulder internal and external rotation, showed more variability than the rest of movements.





**Figure 16 Similarity measures of the control structure.** Similarity is measured in terms of scalar products for synergies (A) and cross-correlation coefficients for activation coefficients (B). Black bars indicate interlimb similarity; grey bars indicate inter-subject similarity in the left arm; and white bars indicate inter-subject similarity in the right arm. Movements are shoulder abduction (SAbd), shoulder external rotation (SERot), elbow extension (EExt), shoulder abduction (SAdd), shoulder internal rotation (SIRot) and elbow flexion (EFlex). Similarity measures are averaged across the two synergies. Bars are mean of all subjects  $\pm$  SD. p-value of left vs right arm comparisons (L-R, Wilcoxon signed rank test); left arm vs inter-limb comparisons (L-IL, Wilcoxon rank sum test); and right arm vs inter-limb comparisons (R-IL, Wilcoxon rank sum test) are indicated below each panel with \*  $p<0.05$ ; \*\*  $p<0.01$ ; \*\*\*  $p<0.001$ .

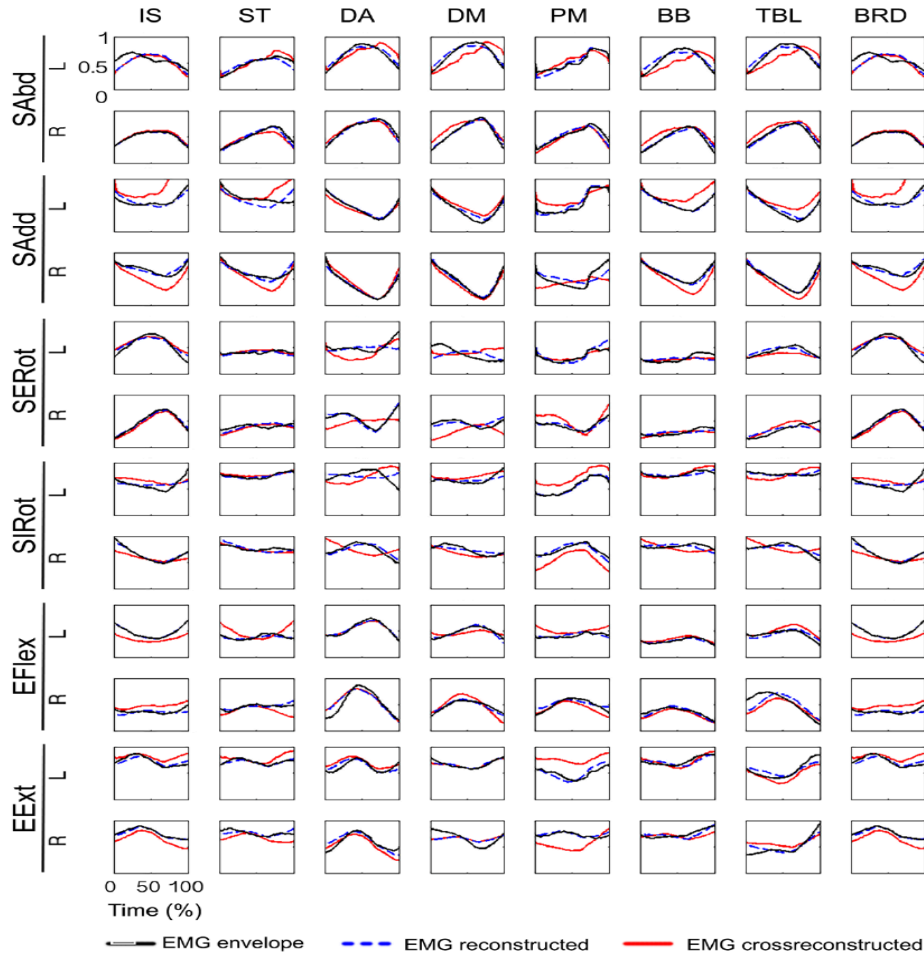


## 11.6 CROSS-RECONSTRUCTION OF THE CONTROL STRUCTURE

To functionally prove within-subject limb interchangeability of the control structure, we cross-reconstructed the muscle activity of one limb with the synergies or the activation coefficient of the opposite limb. **Figure 17** shows the original muscle activity, the reconstruction from the original control structure, and the cross-reconstruction from the control structure of the opposite limb of a representative subject. Because the reconstruction quality was similar for all subjects, we only show the results for one individual. One can easily appreciate that the 3 curves shown in the graphs are very similar to each other. Thus, these graphs demonstrate that the activity of every muscle can be accurately reconstructed using the control structure of the opposite limb, supporting our hypothesis that the control structure of the unaffected arm could serve as a reference to rehabilitate the paretic arm in neurological conditions causing hemiplegia, such as stroke<sup>199</sup>.

The cross-reconstruction accuracy exceeds a VAF of 0.95 in most cases and is never below 0.90 (**Figure 18**). We found no significant differences in the reconstruction accuracy between right and left arms (Wilcoxon signed rank test;  $p > 0.05$ ;  $N = 36$ ), or across movements (Friedman test;  $p > 0.05$ ;  $N_{\text{Subject} \times \text{movements}} = [6 \times 6]$ ) or muscles (Friedman test;  $p > 0.05$ ;  $N_{\text{Subject} \times \text{movement} \times \text{muscles}} = [36 \times 8]$ ). Similarly, we did not find significant differences in the accuracy when the muscle activity was cross-reconstructed from either the synergy or the activation coefficient of the opposite limb (Wilcoxon signed rank test;  $p > 0.05$ ;  $N_{\text{Subject} \times \text{movement}} = 36$ ).

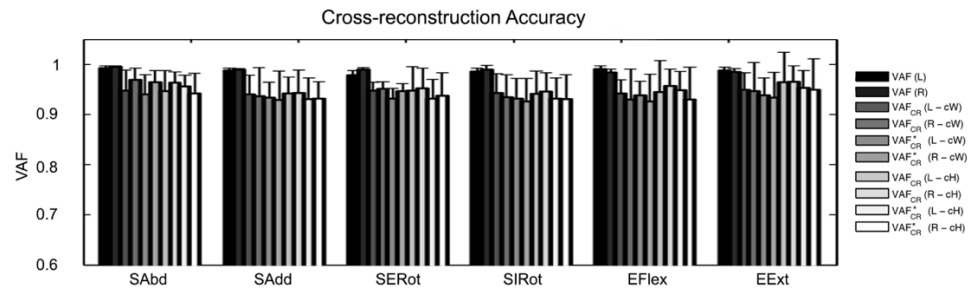




**Figure 17 Cross-reconstruction curves of muscle activity from a representative subject.** Black lines represent EMG envelopes; dotted blue lines represent reconstructed muscle activity from the muscle synergies and red lines represent the cross-reconstructed muscle activity from the activation coefficients of the opposite limb. Each column represents a muscle: brachioradialis (BRD), biceps brachii (BB), triceps brachii long head (TBL), pectoralis major (PM), medial deltoid (DM), anterior deltoid (DA), trapezius superior (TS) and infraspinatus (IS). Movements are arranged in pairs of rows with the first row corresponding to left arm activity (L) and second to the right arm activity (R): shoulder abduction (SAAbd), shoulder abduction (SAAdd), shoulder external rotation (SERot), shoulder internal rotation (SIRot), elbow flexion (EFlex) and elbow extension (EExt). Data are from a representative subject.



On the other hand, the few deviations observed in the cross-reconstruction curves were mainly vertical shifts along the y-axis. This means that these deviations are due to differences in the amplitude of the muscle activity of the opposite limb, and not due to differences in the temporal course of the activations. These observations are supported by the results shown in **Figure 12**, in which we demonstrate that different subjects tend to produce higher EMG amplitudes with specifically their right or left arm.



**Figure 18** Cross-reconstruction accuracy for shoulder abduction (SAbd), shoulder adduction (SAdd), shoulder external rotation (SERot), shoulder internal rotation (SIrot), elbow flexion (EFlex) and elbow extension (EExt). As a reference, the first two columns indicate the reconstruction accuracy achieved using the original synergies. VAF<sub>CR</sub> is the accuracy of the cross-reconstruction based on the activation coefficients (cH) or synergies (cW) with respect to the original muscle activity and VAF\*<sub>CR</sub> is accuracy with respect to the reconstructed muscle activity. Values are mean VAF  $\pm$  SD.



## 11.7 HEALTHY ACTIVITY MAPS

As we found that the control structure of the main movement patterns affected by stroke is movement specific, we provide a set of comprehensive maps that illustrate the muscle activity needed to control such movements when the motor control is not impaired. These maps have been designed to be simple and intuitive, so that they can be easily applied in rehabilitation. Indeed, the activity maps are the dynamic equivalent to the isometric references used in <sup>200</sup> to reduce the effect of the abnormal flexion-extension synergies in patients with stroke.

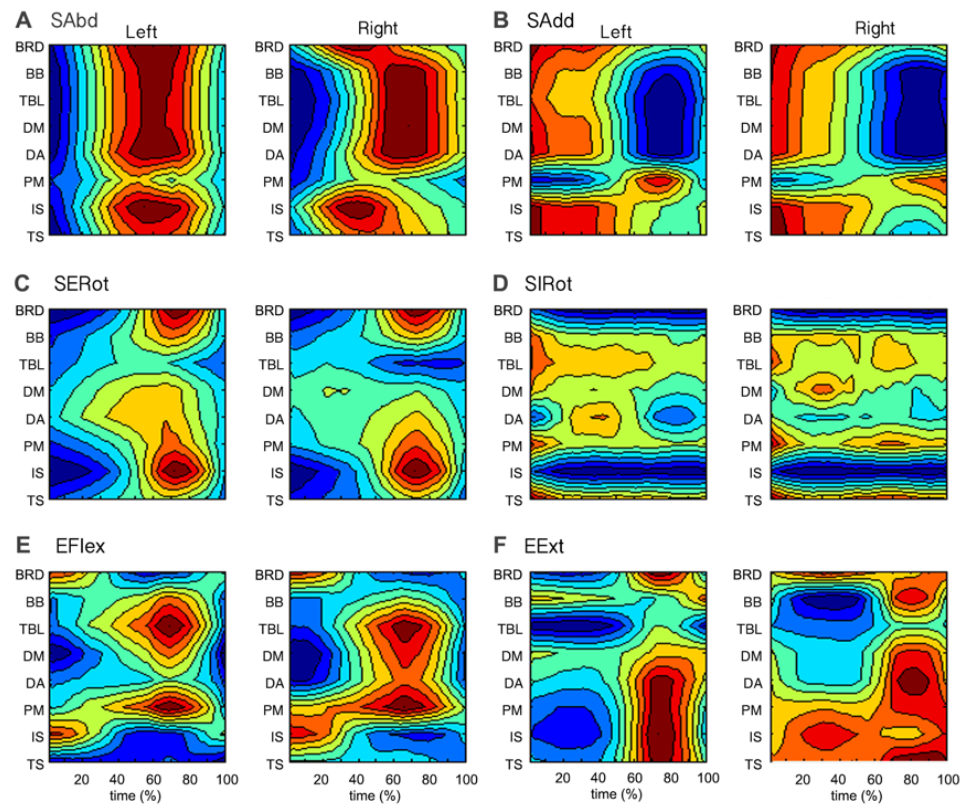
**Figure 19** displays a representative example of right and left arm activity maps of the 6 movements under analysis. Reading the activity maps is extremely straightforward. For instance, according to the activity map depicted in **Figure 19A**, in order to produce shoulder abduction, arm muscles are progressively activated until they reach an activity maximum in the middle of the movement, after which they are progressively relaxed.

In contrast, at the beginning of shoulder adduction (**Figure 19B**), the coactivation of IS, TA, DA, DM, TB, BB and BRD presumably allows developing the force needed to counteract gravitational forces and maintain the full arm extended parallel to the ground. As the movement progresses and the arm is lowered lead by gravity, such coactivation is gradually decreased. By the end of the movement, we detect activity of the pectoralis major (PM), and this is likely to be responsible of decelerating the arm to pose it smoothly along the body.

During shoulder external rotation (**Figure 19C**) maximum muscle activity is detected by the end of the movement (>70% of movement completion), with special involvement of most proximal and distal muscles. This is probably because subjects tended to force



the external rotation beyond their articular amplitude, which made them contract excessively the rotator cuff muscles, such as the IS. In order to keep the forearm attached to the body, such excessive contraction was also detected in the elbow flexors.



**Figure 19 Activity maps of movements in absence of neurological damage.** Each map represents the activity of individual muscles during the execution of the main movement patterns affected by stroke. **A**, Shoulder abduction (SAbd). **B**, Shoulder adduction (SAdd). **C**, Shoulder external rotation (SERot). **D**, Shoulder internal rotation (SIRot). **E**, Elbow flexion (EFlex). **F**, Elbow extension (EExt). Muscles are sorted in the y-axis according to the position of their electrodes along the longitudinal axis of the body, with distal muscles placed at the top and proximal muscles at the bottom: brachioradialis (BRD), biceps brachii (BB), triceps brachii long head (TBL), medial deltoid (DM), anterior deltoid (DA), pectoralis major (PM), infraspinatus (IS) and trapezius superior (TS). The horizontal axis represents the time line of the movement execution, normalized to 100 points. Colors reflect the intensity of the activation with red colors indicating high intensity activations and blue colors low intensity activations. Data are from a representative subject.



In the opposite movement (**Figure 19D**), the internal rotators such as deltoids (DA and DM) and PM play an important role at the beginning of the execution, which decreases with time. Similarly, flexor muscles, such as TBL and BB seem to synchronize and coactivate with the rotators to keep the elbow flexed against gravitational forces.

The elbow flexion (**Figure 19E**) is governed by a progressive activity of the proximal muscles (BB, TBL, DM, DA and PM), which reaches a maximum approximately at the 80% of the movement completion, after which it decreases gradually. The movement is dominated by the main agonist/antagonist activity of biceps (BB) and triceps (TBL), which can be clearly observed as an activity peak in the map.

This is less visible in the elbow extension movement (**Figure 19F**), presumably because subjects tended to drop the forearm in favor of gravity exerting almost no force to perform that movement, except proximal muscles that were activated to keep the arm attached to the trunk during movement execution. Notably, all the activity maps reflect a high correspondence in the control structure of the two limbs. Note that the activity maps support the existing physiological knowledge about upper-limb movements regarding muscle participation, and in addition, provide detailed information about the coactivation and timing patterns of these muscles.



# 12 DISCUSSION (I)

## 12.1 EMG RECRUITMENT PATTERNS GO BEYOND HANDEDNESS

Our primary aim was to investigate the way handedness is reflected in human motor control. In the first part of the study, we characterized EMG signals of right and left upper-limb muscles. Due to the inherent variability of motor control, the electromyographic features vary substantially from subject to subject<sup>201</sup>. For this reason, we performed EMG characterization at individual level.

Although the accurate reconstruction of recruitment pattern requires more sensitive techniques such as intra-muscular EMG, the study of the evolution of the EMG peak amplitude together with the MDF allowed us to infer the way muscle fibers are recruited during repetitive voluntary movements. Our results suggest that during the first repetitions (~10) there is a progressive recruitment of muscle fibers that tend to saturate following an exponential decay model. Such model indicates that during the first repetitions only a small fraction of all available fibers are recruited and as the exercise progresses, new fresh fibers are added until a maximum is reached. Accordingly, a gradual rise in amplitude has been identified during repetitive voluntary contractions<sup>196,197</sup>.

On the other hand, the MDF rise coincides with the time period in which the exponential growth of the EMG peak amplitude occurs, suggesting that during the first repetitions, the gradual recruitment of muscle fibers is associated to a rise in the excitation rate of muscle fibers that also reaches its maximum, presumably until the initial signs of fatigue appear. This behavior has also been observed during intermittent isometric contractions<sup>190,202</sup>.



Interestingly, the aforementioned patterns vary substantially from subject to subject. Indeed, although all subjects were right-handed, we found significant inter-limb differences among subjects. Namely, some subjects tended to perform significantly slower movements with their dominant arm and *vive versa*. We also found differences in the kinetic characteristics of the exponential decay model such as the slope (recruitment rate) and the time to reach the plateau phase. Again, inter-limb differences did not favor always the same side. Instead, some subjects exhibited faster and taller exponential decay curves in their right arm, while others in their left arm. These differences may be attributed to individual biomechanical, physiological and behavioral inter-limb heterogeneity<sup>187</sup> and suggest that muscle recruitment patterns may not be determined by handedness. As a matter of fact, Franz *et al.* discovered that bimanual tasks were not necessarily lead by the dominant arm<sup>203</sup>. In conclusion, it turns obvious that the motor control is heavily tuned at individual level. Hence, mastering control mechanisms for clinical applications may require considering individual parameters subject by subject.

## 12.2 THE CLINICAL VALUE OF THE CONTROL STRUCTURE

In the second part of the study, we analyzed the control structure of the main movement patterns affected by stroke based on the hypothesis that the control structure may overcome the high inter-subject (and inter-limb) variability found in EMG features. The patterns analyzed constitute what is clinically known as abnormal flexion-extension synergies<sup>35</sup>. We have focused on these patterns first, because they constitute one of the main and best known causes of motor impairment in stroke<sup>117</sup>; and second, because training these patterns separately leads to significant functional improvement<sup>131,200</sup>. Note that the fact that these tasks have just one degree of



freedom may explain why two synergies are enough to explain at least 90% of the muscle activity variance.

Demonstrating that healthy subjects share the same control structure in their two limbs is of great clinical value to improve rehabilitation of neurological conditions causing hemiplegia. Our results demonstrate that inter-limb similarity of the control structure is very high. Moreover, it is significantly higher than inter-subject similarity both, for muscle synergies and activation coefficients. The reason for such a large inter-subject variability is that certain subjects seem to develop alternative control strategies that deviate from the common control structure. Synergy flexibility has already been reported in several studies addressing inherent muscle variability<sup>204</sup> and the effect of training<sup>205,206</sup>. In particular, Nazarpour and colleagues demonstrated the dynamic emergence of new synergies modulated by feedforward and feedback mechanisms that vary on a trial-to-trial basis. This may explain partly the observed inter-subject variability, as different subjects may develop different muscle synergies to carry out a task, depending on their previous personal experience with such or even similar tasks<sup>207</sup>. Interestingly these individual new strategies are still very similar between the two limbs of those subjects, and this empowers the potential of the control structure in the clinical practice.

As a matter of fact, we have proven that the muscle activity of a limb can be very accurately reconstructed (> 90%) from the control structure of the opposite limb. This finding has important implications for rehabilitation, since it means that our body stores a copy of essential control data in both arms that can be employed to functionally guide restoration processes, when one of the two copies is damaged or lost as it happens with hemiparesis.

In conclusion, if we extrapolate the findings herein reported to clinical practice, it seems evident that 1) clinical practice should avoid the use of standards when it comes to motor interventions since generalizations might disregard subjects' important motor particularities and hinder rehabilitation and 2) thanks to the high conservation degree exhibited between the control structure of the two limbs, hemiplegia treating



therapies could be properly tailored based on the control structure of the healthy side. In particular, given that stroke seems not to alter the muscle synergies of the unaffected limb<sup>120</sup>, we propose taking the control structure of each subject's unaffected limb as the reference to ensure the best possible similarity to the control structure that they had before the stroke.

### 12.3 ACTIVATION COEFFICIENTS AS A KEY REHABILITATION TARGET

Differences in motor skills between the dominant and nondominant arms have been extensively characterized in various domains including kinematic, kinetic and task performance<sup>203,208, 209</sup>, attributing advantageous features to the dominant arm. Tseng *et al.* studied limb differences in motor performance and reported that the nondominant arm showed higher error, more variable paths and higher joint variance<sup>208</sup>. In the face of such differences, some authors have proposed that the controllers of the two limbs are functionally different<sup>210</sup>. Our results reveal that the inter-subject similarity of the activation coefficients varies significantly from the dominant arm to the nondominant arm (but not in muscle synergies), suggesting that these coefficients may account for the performance differences induced by handedness and experience. This implies that the part of the control structure that is designed to accept some sort of flexibility to manage the inherent variability<sup>93</sup> of movement optimization and fine-tuning processes are activation coefficients. In consequence, one should expect that patients could learn how to modify their activation coefficients with the appropriate therapeutic design. That is to say, the dynamic capability for adaptation and tuning of activation coefficients may be a key aspect to exploit in rehabilitation. Moreover, several studies agree that the deteriorated motor performance of stroke patients arises from altered synergy recruitment patterns but not from the synergy composition (except in the most severe cases)<sup>120,178</sup>. In other words, abnormal activation



coefficients might be the cause of motor impairment. Thus, attempting to restore the original activation coefficients based on the patterns preserved in the healthy side might be the right approach to boost rehabilitation. Interestingly, our results indicate that cross-reconstruction can be performed with accuracy over 90% from either the activation coefficient or the synergies of the opposite limb. This gives experimental evidence that relearning how to activate muscles according to a healthy recruitment pattern may lead to improved motor function. In any case, it seems evident that activation coefficients constitute a promising therapeutic target.

## 12.4 CROSS-RECONSTRUCTION QUALITY IS INDEPENDENT OF HANDEDNESS

Neural conditions such as stroke are as likely to damage the dominant as the nondominant side. Our results show that the cross-reconstruction accuracy did not vary with the limb. Therefore, this kind of rehabilitation could be used regardless of which side is affected. Similarly, the cross-reconstruction accuracy does not vary with the type of movement or muscles, suggesting that all eight muscles can be trained with equal chances of success in the six movements under analysis. These characteristics are a very promising basis for the development of a new rehabilitation strategy in which the control structure of the unaffected arm is used as a reference to train the affected arm.

## 12.5 EXPLOITING ACTIVITY MAPS IN REHABILITATION

Describing healthy movement patterns in a comprehensive manner is essential to improve motor rehabilitation. Experimental evidence indicate that the spatial distribution of EMG amplitude is task specific so that it may be used to control a robotic arm<sup>211</sup>. Although it is true that the EMG maps used in these studies correspond to high-density EMG maps, certain authors verified that just few channels were needed to characterize each task, particularly those localized above the main agonist of the task<sup>212</sup>. Thus, it is reasonable that the activity maps presented here, which comprise the main muscles involved in the movements under analysis, capture most relevant neuromuscular characteristics of those movements while providing low-density spatial



information about muscle disposition. As a matter of fact, in each intended movement, the maps show a distinct and repeatable pattern that generalizes across both limbs.

Functional electrical stimulation (FES), which has been proven to promote functional recovery<sup>213,214</sup>, is a great candidate to exploit the proposed activity maps. FES uses electric currents to stimulate muscle nerves in a precise sequence and amplitude to resemble functional tasks. Before proceeding to clinical trials, the output of FES controller is simulated using diverse forward dynamic models<sup>215–217</sup>. However, tuning these models is not straightforward, as many morphometric and physiological input variables that cannot be always easily obtained are needed<sup>218</sup>. As explained before, our maps are individual representations of the muscle activations used to produce a movement in the absence of neurological impairment. Because these maps represent the particular neuromuscular control of each subject and include time and amplitude information, they have the potential to circumvent the biomechanical models and be straightly used to program the stimulation cues of FES so that patients would get their muscles stimulated following the activation patterns of their non-impaired limb.



# 13 CONCLUSIONS (I)

The present study investigates the inter-limb differences exhibited by the human neuromuscular control, with special focus on the upper-limb movement patterns affected by stroke since rehabilitation may strongly benefit from the conclusions herein extracted. The study confirms that EMG signals are tremendously variable among subjects and inconsistent with any handedness-dominance principle. In contrast, the control structure overcomes this drawback showing a significantly high inter-limb similarity than can be exploited in rehabilitation. Indeed, we demonstrate that the muscle activity of a limb can be reconstructed from the control structure of the opposite limb. Overall, when it comes to clinical applications these results highlight the importance of considering individual motor control strategies to avoid wrong generalizations that may not fit every patient. Therefore, we suggest using the control structure of the unaffected limb as a reference to rehabilitate the paretic limb of stroke patients. Of course, further research is needed to verify whether restoring the original control structure in the affected arm can improve its function. However, these are extremely promising results for rehabilitation. Thus, in view of the clinical potential of the control structure, we are already working in this line with stroke patients .













## Study 2

# The effect of VF in healthy motor control

Has VF the ability to modulate the control strategy  
of our motor system?







# Abstract

*Visual feedback (VF) is applied in a variety of therapies to recover motor skills after stroke. However, the exact mechanisms underlying the beneficial effects of VF remain unclear, limiting its optimal use in clinical practice. In this study, we hypothesize that VF may have the capacity to modulate the neuromuscular organization based on the error correction mechanisms of our motor system. To this end, we have characterized the effects that executing movements in presence of VF induces in the control structure of healthy subjects. We have discovered that VF is able to increase the ILS, specially in subjects that report feeling comfortable with the use of VF. Indeed, it seems that VF is more prone to modulate the nondominant control structure and approach it to the control structure of the dominant arm. In light of such observation, we propose that VF may facilitate the transfer of superior motor programs stored in the dominant hemisphere to optimize the nondominant arm's motor control. In order to test this hypothesis, we have also quantified the intermanual transfer (IMT) of the dominant control structure to the nondominant arm during the execution of a complete set of standard rehabilitation routines. We demonstrate that IMT is the main mechanism by which VF increases interlimb similarity and we show that the magnitude of IMT can be up to 75% in neurologically intact subjects. Thus, this study provides sound physiological evidence to encourage the use of VF in motor rehabilitation.*







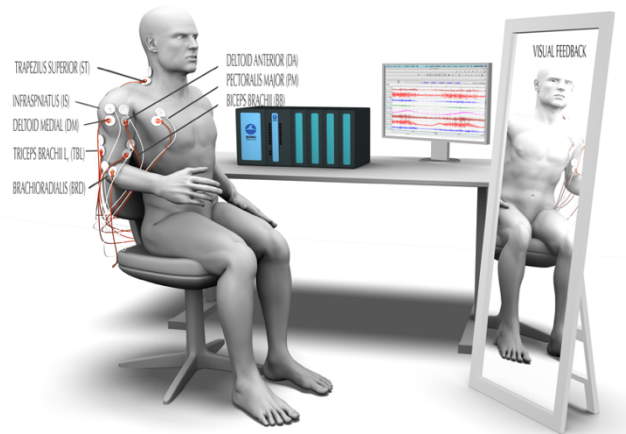
# 14 SPECIFIC PROCEDURES (II)

## 14.1 EXPERIMENTAL SETUP

The experiments described in this study were carried out with healthy subjects from **database H**. During the experimental session subjects had to perform a set of 12 exercises taken from standard upper-limb rehabilitation routines that covered the basic range of motion of elbow and shoulder. Each exercise consisted on a simple movement involving one-degree of freedom in elbow or shoulder. The experimental protocol was the same as the one described in the section **Experimental protocol**, except that each movement was performed twice: in absence and presence of VF.

VF was provided by allowing the subjects to track their movements using a full-body mirror that covered the entire trajectory of their movements (**Figure 19**). The mirror was placed orthogonal to the axis around which the movement was produced to ensure the best possible view of the trajectory. Subjects were asked to perform the repetitions as similar as possible and to use VF to correct the movements if necessary.





**Figure 20 Experimental setup** during the trials performed in presence of VF. A full-body mirror was used to cover the entire trajectory of the movements.

At the end of the experimental session, subjects were asked to fill in a questionnaire to evaluate the overall experience and the sensations they perceived during the experiment. The questionnaire was comprised of 5 questions (**Table 14**) and answers were given

in the form of numeric values ranging from 1 (I do not agree) to 5 (I do agree).

#	Statement
Q1	I had practiced these exercises before
Q2	The mirror made me lose the focus
Q3	I sometimes forgot to look to the mirror
Q4	I tried to do movement repetitions as similar as possible
Q5	I found big differences between the executions of movements done with right or left arm

**Table 14** Items of the questionnaire filled by subjects after finishing the experimental routine.

## 14.2 KINETIC PARAMETERS

We conducted a preliminary study about the effect of VF on movement kinetics, by analyzing the effect of VF on movement speed and on the variability of movement speed across repetitions. In order to assess movement-speed we computed the movement duration (in seconds) of each movement-repetition. Note that movement duration is an indirect measure of movement speed (longer movements indicate slower movements and vice versa).

Movement duration was defined as the time period elapsed from movement onset to movement end. For each repetition, movement onset was visually determined



as the instant in which the upper-limb changed position to start the trajectory. Analogously, movement end was visually determined as the instant in which the upper-limb stopped at the end of the required trajectory.

To estimate the mean duration of each movement we averaged for each subject, arm and condition, the measures of duration calculated for each movement-repetition. The variability of movement duration was assessed by computing the standard deviation (SD) of the aforementioned 30 measures for each subject, arm and condition.

### 14.3 WITHIN-SUBJECT SYNERGY MATCHING ACROSS CONDITIONS

In order to compare the control structure meaningfully, we need to match the synergies and activation coefficients across limbs (right vs left) and VF conditions (nVF vs VF). Because the synergy extraction process does not sort the synergies according to any criterion, synergies labelled as W1 or W2 across different limbs or VF conditions may not correspond to the same motor module. In other words, each time that we conduct a synergy extraction, we get 2 synergies labelled W1 and W2. Thus, for each movement we have 4 sets of 2 synergies:  $\{W1, W2\}_{L,nVF}$ ,  $\{W1, W2\}_{R,nVF}$ ,  $\{W1, W2\}_{L,VF}$ ,  $\{W1, W2\}_{R,VF}$ . However, since synergies are separately extracted for each limb and condition, we cannot guarantee that for example what is labelled as  $W1_{L,VF}$  and  $W1_{R,VF}$  correspond to the same motor module. Note that the same logic applies for activation coefficients H1 and H2.

In consequence, it is essential to match the synergies and activation coefficients across limbs and VF conditions. Such matching process is performed based on similarity criteria between activation coefficients. **Table 15** shows an example of how synergies might be incorrectly sorted after synergy extraction. Note that synergy extraction is done separately for each column (arm x condition). Therefore, this process only



guarantees to have a single W1 and W2 in each column, but not to physiologically match W1s and W2s from different columns correctly.

NO VISUAL FEEDBACK (nVF)			VISUAL FEEDBACK (VF)	
Side	Left limb	Right limb	Left limb	Right limb
Physiological Motor Module <sub>1</sub>	W <sub>1</sub>	W <sub>2</sub> *	W <sub>1</sub>	W <sub>1</sub>
Physiological Motor Module <sub>2</sub>	W <sub>2</sub>	W <sub>1</sub> *	W <sub>2</sub>	W <sub>2</sub>

**Table 15** Example of incorrect synergy matching after a synergy extraction process for a given subject and movement. W1 and W2 are labels given to synergy 1 and 2. Rows indicate physiological motor programs that may be different from the labelling given by the synergy extraction algorithm. Asterisks indicate the control structure incorrectly matched according to the other 3 conditions.

To fulfill this objective, we guided the matching process starting by sorting the activation coefficients, because visually supervising the similarity of activation coefficients is easier than for synergies. Naturally, synergies were subsequently matched according to their corresponding sorted activation coefficients. Overall, the aim of the matching process is to sort the activation coefficient following this distribution:

NO VISUAL FEEDBACK (nVF)			VISUAL FEEDBACK (VF)	
Side	Left limb	Right limb	Left limb	Right limb
Physiological Motor Program <sub>1</sub>	H <sub>1</sub>	H <sub>1</sub>	H <sub>1</sub>	H <sub>1</sub>
Physiological Motor Program <sub>2</sub>	H <sub>2</sub>	H <sub>2</sub>	H <sub>2</sub>	H <sub>2</sub>

**Table 16** Target matching of activation coefficients across limbs and conditions after synergy matching process

Note that the movements under analysis were reliably reconstructed with 2-synergy models. Therefore, for the right (R) and left (L) arms we could define W1R, W2R, W1 L, W2 L and their corresponding scalar products  $S1 = W1R \cdot W1L$ ,  $S2 = W2R \cdot W2L$ ,  $S1x = W1R \cdot W2L$ ,  $S2x = W2R \cdot W1L$  for each condition (nVF and VF). (see subsection 8.4.2 Interlimb similarity (ILS) measures to find the exact formulation of the scalar product used).



#### 14.3.1.1 Synergy Matching / Step 1

In the first step, we performed within-subject interlimb synergy matching applying the following rule for each subject and movement:

```

if S1x > S1 AND S2x > S2

    swap H1 and H2 in the right side

elseif (S1x > S1 AND S2x < S2) OR (S2x > S2 AND S1x < S1)

if S1x + S2x > S1 + S2

```

Matlab Code 1 Pseudocode used to match synergies

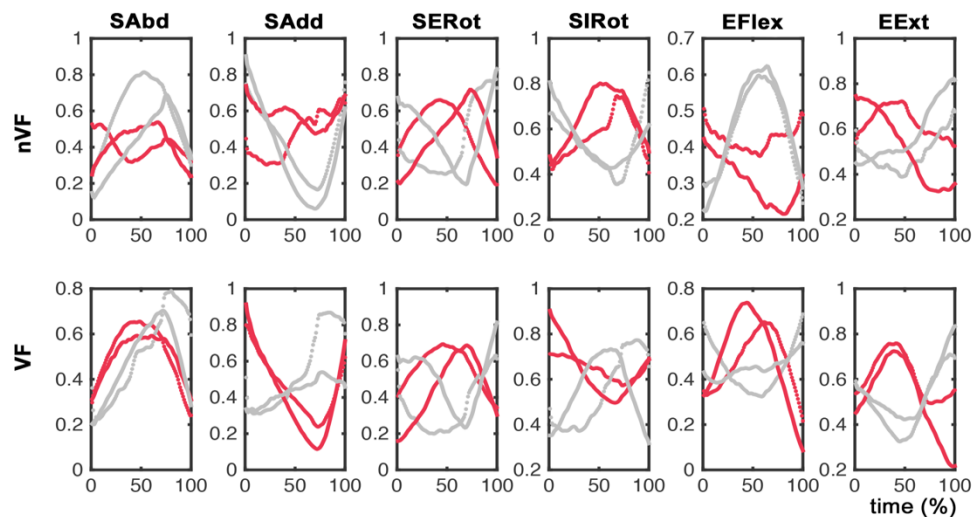
This process guarantees a correct match between H<sub>1R</sub> and H<sub>1L</sub>, and H<sub>2R</sub> and H<sub>2L</sub> within each condition; but does not ensure that activation coefficients are appropriately matched across conditions. That is, returning to the tables used in the previous examples, after this first step, activation coefficients should be correctly matched by [2x2] cell-pairs, but there still might be errors across conditions ([1x4] cell-rows) (Table 17).

NO VISUAL FEEDBACK (nVF)			VISUAL FEEDBACK (VF)	
Limb side	Left limb	Right limb	Left limb	Right limb
Physiological Motor Program <sub>1</sub>	H <sub>1</sub> : { H <sub>1R</sub> - H <sub>1L</sub> } <sub>nVF</sub>		H <sub>2</sub> : { H <sub>2R</sub> - H <sub>2L</sub> } <sub>VF</sub> *	
Physiological Motor Program <sub>2</sub>	H <sub>2</sub> : { H <sub>2R</sub> - H <sub>2L</sub> } <sub>nVF</sub>		H <sub>1</sub> : { H <sub>1R</sub> - H <sub>1L</sub> } <sub>VF</sub> *	

**Table 17** Example of possible incorrect synergy matching cases after the first matching step. W1 = synergy1; W2 = synergy 2. Asterisks indicate the control structure incorrectly matched with regard to the opposite condition.

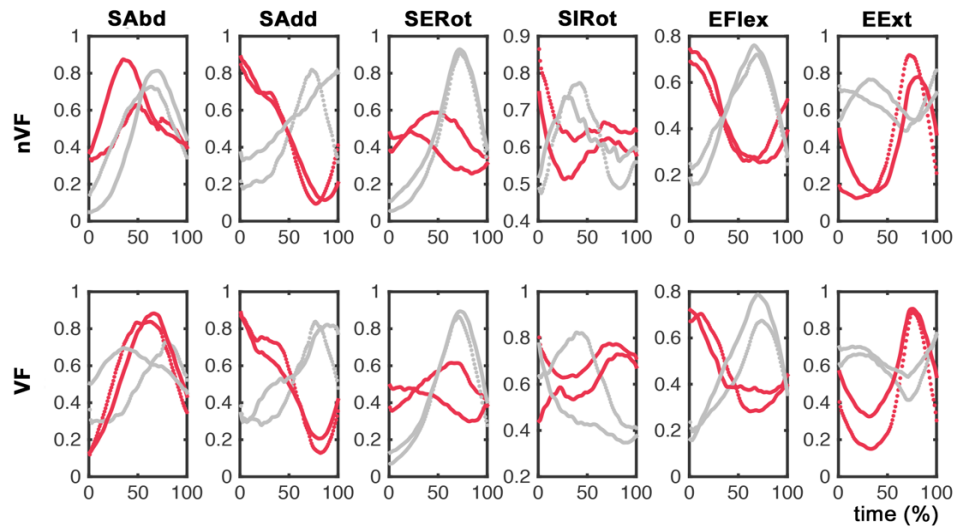


The results of this first step for each subject and movement are shown in the following series of figures. As we can visually observe, the matching process returns  $H_1$  and  $H_2$  activation coefficients properly matched for each condition (nVF and VF). That is, the shapes of right and left  $H_1$  activation coefficients (red curves) are very similar in all cases, as well as right and left  $H_2$  activation coefficients (grey curves). However, one can easily find examples in which  $H_1$  activation coefficients (red lines) obtained in absence of VF correspond to the activation coefficients labelled as  $H_2$  (grey curves) obtained in presence of VF (**Figure 21** - SAbd, SIRot, EFlex; **Figure 24** – EExt, **Figure 25** - SAdd). Thus, it is quite evident that a second matching step is needed to match right and left activation coefficients, across conditions.

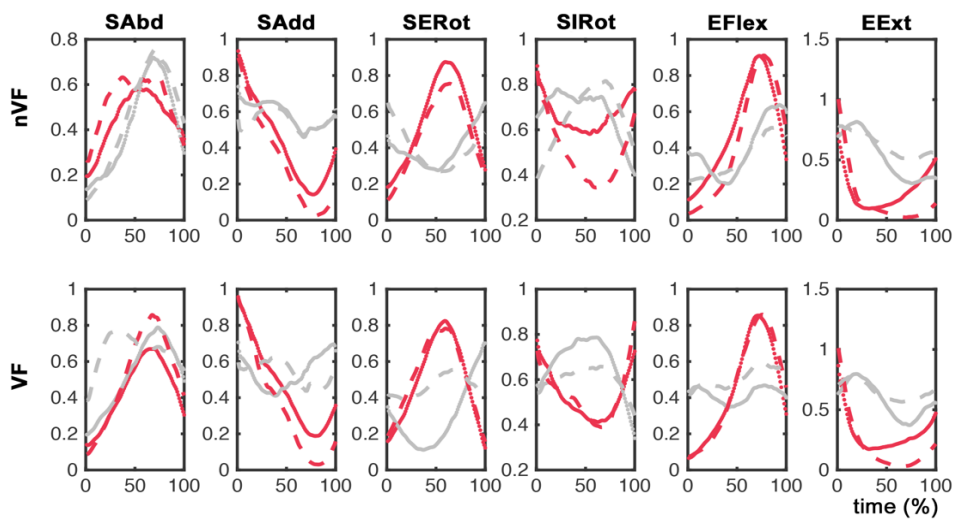


**Figure 21** Activation coefficients of SUBJECT 1 after the first step of synergy matching. Rows 1 and 2 represent activation coefficients of movements performed in absence and presence of VF respectively. Red lines are  $H_1$  and grey lines are  $H_2$ . Dotted lines correspond to left arm and dashed lines to right arm activation coefficients.





**Figure 22** Activation coefficients of **SUBJECT 2** after the first step of synergy matching. See the legend of **Figure 21** for a complete and detailed description of the figure.



**Figure 23** Activation coefficients of **SUBJECT 3** after the first step of synergy matching. See the legend of **Figure 21** for a complete and detailed description of the figure.



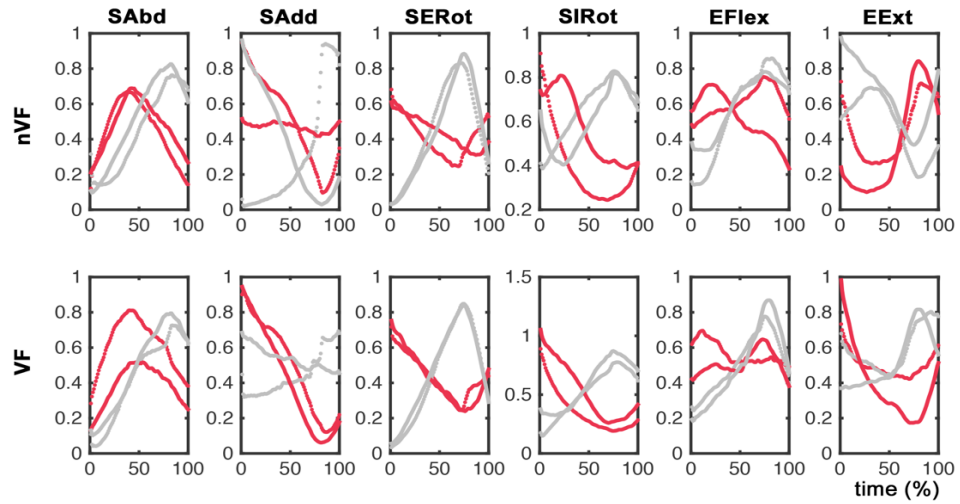


Figure 24 Activation coefficients of SUBJECT 4 after the first step of synergy matching. See the legend of Figure 21 for a complete and detailed description of the figure.

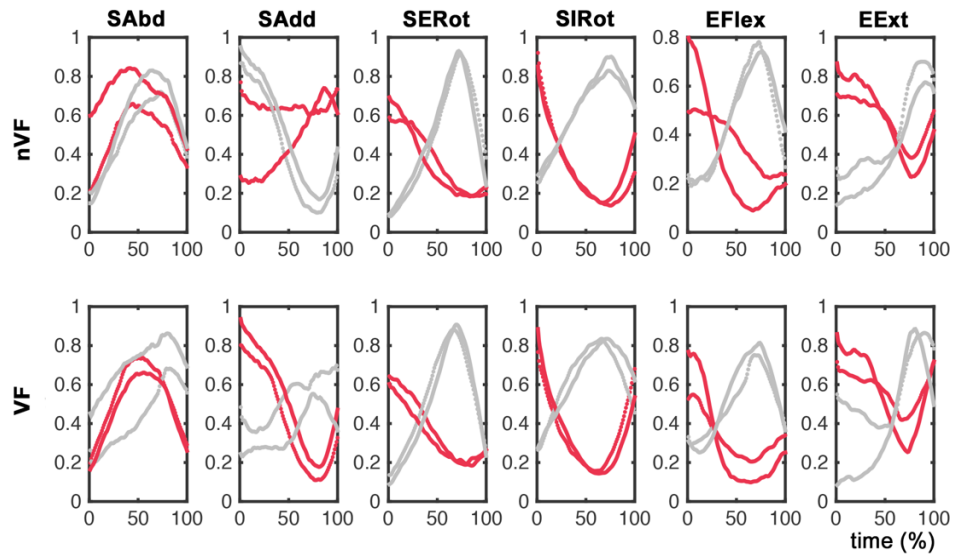


Figure 25 Activation coefficients of SUBJECT 5 after the first step of synergy matching. See the legend of Figure 21 for a complete and detailed description of the figure.



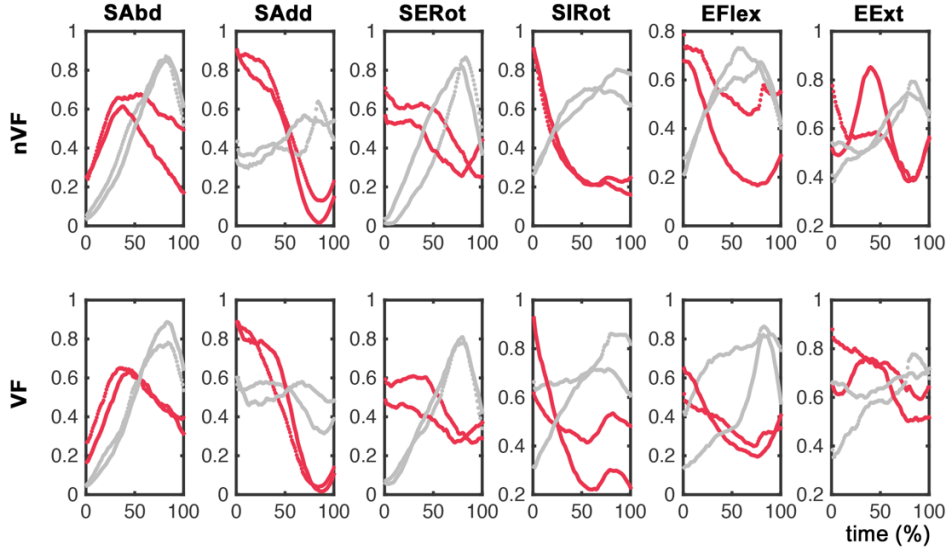


Figure 26 Activation coefficients of SUBJECT 6 after the first step of synergy matching. See the legend of Figure 21 for a complete and detailed description of the figure.

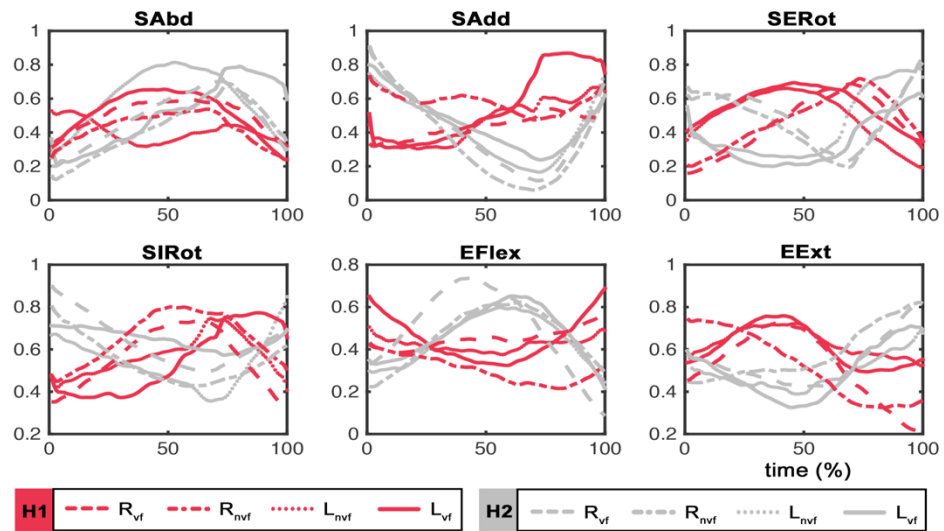
#### 14.3.1.2 Synergy Matching / Step 2

In the second step, we matched synergies across conditions. To do so, we computed the mean activation coefficients for each condition:

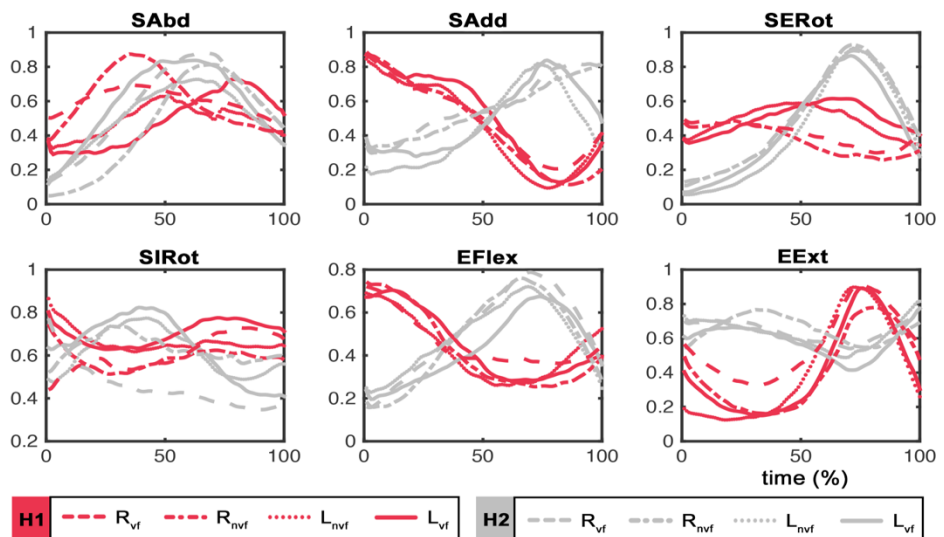
- $\langle H1_{nvf} \rangle = \text{mean}(H1_{R_{nvf}}, H1_{L_{nvf}})$
- $\langle H2_{nvf} \rangle = \text{mean}(H2_{R_{nvf}}, H2_{L_{nvf}})$
- $\langle H1_{vf} \rangle = \text{mean}(H1_{R_{vf}}, H1_{L_{vf}})$
- $\langle H2_{vf} \rangle = \text{mean}(H2_{R_{vf}}, H2_{L_{vf}})$

And we applied the same algorithm used in the first step, but using the aforescribed averaged synergies instead of  $H1_R$ ,  $H2_L$ ,  $H2_R$  and  $H2_L$ . The final result of the matching process after applying this step can be seen in the following figures.





**Figure 27** Activation coefficients of **SUBJECT 1** after the full process of synergy matching. Each plot displays the activation coefficients H1 (red lines) and H2 (grey lines) of each movement. R – Right arm, L – Left arm, nvf – movements performed in absence of visual feedback, vf – movements performed in presence of visual feedback.



**Figure 28** Activation coefficients of **SUBJECT 2** after the full process of synergy matching. See the legend of **Figure 27** for a complete and detailed description of the figure.



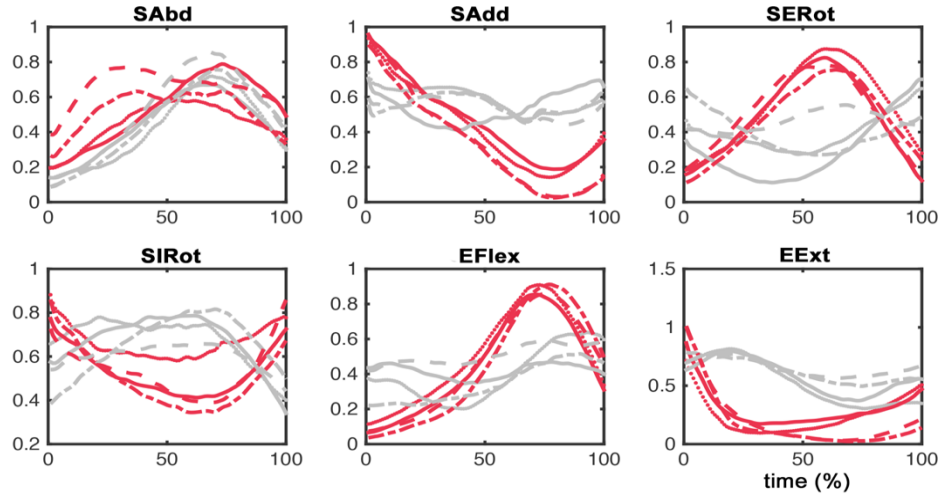


Figure 29 Activation coefficients of SUBJECT 3 after the full process of synergy matching. See the legend of Figure 27 for a complete and detailed description of the figure.

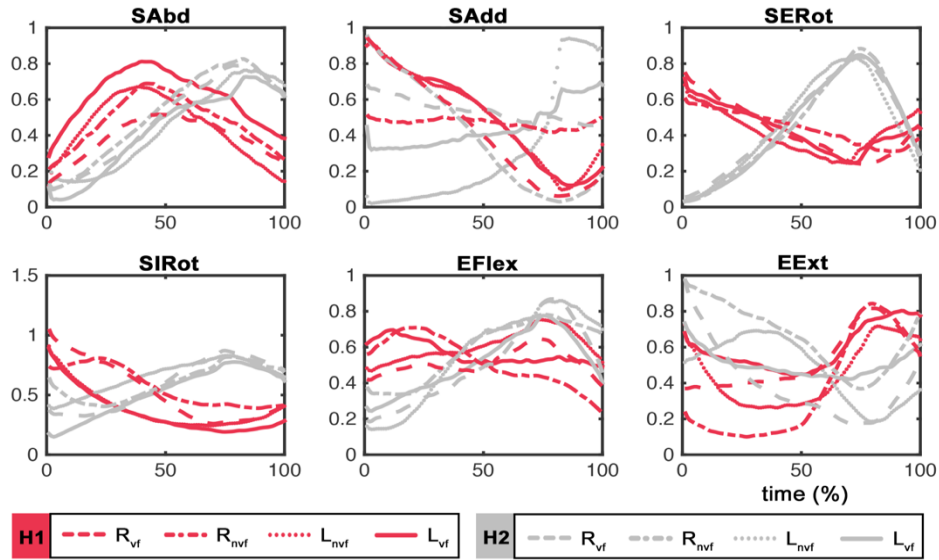


Figure 30 Activation coefficients of SUBJECT 4 after the full process of synergy matching. See the legend of Figure 27 for a complete and detailed description of the figure.



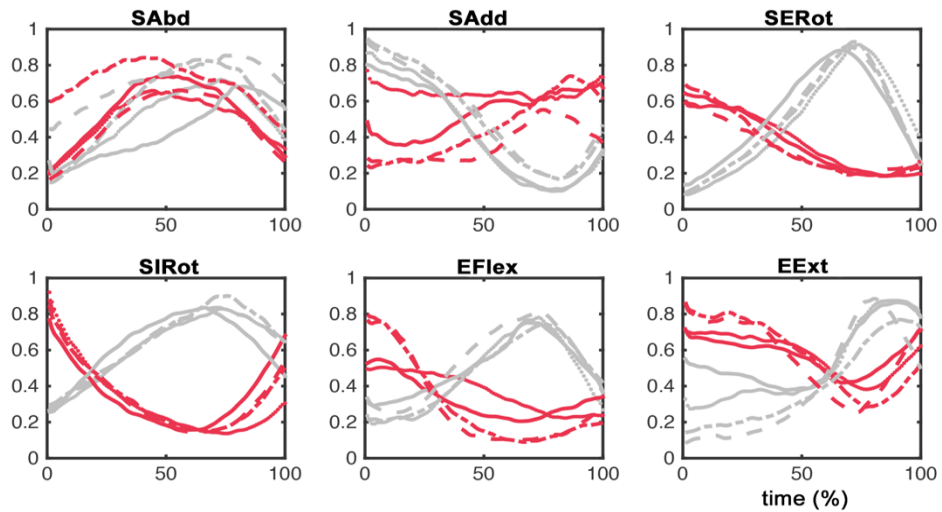


Figure 31 Activation coefficients of SUBJECT 5 after the full process of synergy matching. See the legend of Figure 27 for a complete and detailed description of the figure.

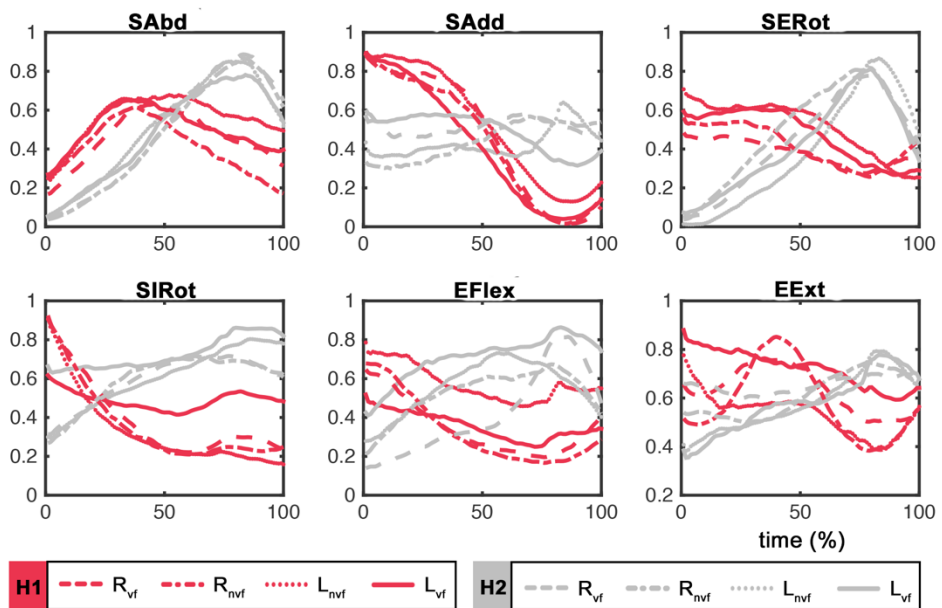


Figure 32 Activation coefficients of SUBJECT 6 after the full process of synergy matching. See the legend of Figure 27 for a complete and detailed description of the figure.



Note that according to this procedure the subindices 1 and 2 of activation synergies (**W1** and **W2**) and activation coefficients (**H1** and **H2**) are just used for identification purposes and do not express any kind of relationship between them. One can easily confirm from the observation of **Figure 27** to **Figure 32**, that after applying the synergy matching process all the activation coefficients tagged H1 and all the activation coefficients tagged H2 represent the same functional element within the neuromuscular control of a given movement for every subject, condition and arm.

#### 14.4 INTERLIMB DIFFERENCE (ILD) MEASURES

In order to understand the effect of VF in the control structure of the upper-limb, we studied the ILS from a different perspective. We defined the interlimb difference (ILD), as a measure to quantify the relative difference between the right and left arm synergies or activation coefficients. Unlike scalar products and cross-correlation coefficients, ILD measures allow us to compare the interlimb differences of muscle synergies and activation coefficients with respect to each other.

For **muscle synergies**, the ILD was formulated as:

$$ILD_W(\%) = \frac{|W_R - W_L|}{N} \cdot 100 \quad (14)$$

where:

- $W$  is the vertical concatenation of the 2 muscle synergy vectors  $W1$  and  $W2$
- The subindices  $R$  and  $L$  indicate right or left arms respectively
  - $N$  is the length of  $W$ . In this case,  $N = 16$ , since there are 8 muscles in each synergy.



For **activation coefficients**, the ILD was formulated as:

$$ILD_H(\%) = \frac{\sum_{n=1}^N |H_R[n] - H_L[n]|}{N} \cdot 100 \quad (15)$$

where:

- H is the horizontal concatenation of the 2 activation coefficients H1 and H2
- The subindices R and L indicate right or left arms respectively
- N is the length of H, i.e., 200, as each activation coefficient is 100 time-points long.

## 14.5 TEMPORAL EFFECT OF VF ON ILS

The visual inspection of the evolution of the ILS throughout the time-course of the movement execution revealed important dynamic changes in the temporal trend of the ILS (see subsection 15.4.1 **The effect of VF on the control structure**). According to the model used to characterize the control structure in this study (Equation (4)), muscle synergies are time invariant constructs while activation coefficients represent time-varying constructs. Therefore, for obvious reasons, this section pays special attention to the time course of the activation coefficients.

We analyzed the effect of VF on ILS ( $ILS_{VF}$ ) with respect to the ILS found in absence of VF ( $ILS_{nVF}$ ). That is, we compared the difference between the right and left activation coefficients found in absence of VF with the difference between the right and left activation coefficients found in presence of VF (Equation (16)). To do so, we defined a tolerance threshold of 10%. In other words, we considered that VF increased ILS above the ILS found in absence of VF if the following inequality was fulfilled:

$$VF\Delta_{ILS} \text{ if } \frac{|H_{i,R} - H_{i,L}|_{nVF}}{|H_{i,R} - H_{i,L}|_{VF}} > 1.10 \quad (16)$$



Alternatively, we considered that VF decreased ILS below the ILS found in absence of VF if the following inequality was fulfilled:

$$VF \nabla_{ILS} \text{ if } \frac{|H_{i,R}-H_{i,L}|_{nVF}}{|H_{i,R}-H_{i,L}|_{VF}} < 0.909 \quad (17)$$

Where:

- $\triangle_{ILS}$  indicates increase in ILS
- $\nabla_{ILS}$  indicates decrease in ILS
- $H_i$  is the *i*th activation coefficient
- R subindex refers to right arm activation coefficient
- L subindex refers to left arm activation coefficient

Because the activation coefficients are 100 time-points long, calculating the time-percent of each trend was extremely straightforward. The aforescribed inequalities were checked for each time-point. Time-points fulfilling the first inequality were considered to belong to the time periods in which VF increased ILD and vice versa.

Next, we examined the length of each trend. We only considered movement-portions that lasted at least 10% of the total movement execution (i.e. movement-portions that were more than 10 data-points long) following the same trend. Taking into account the low frequency associated to human voluntary movements, we assumed that trends shorter than the aforementioned 10% of the execution-time arose from numerical artifacts produced by the computation, so, we discarded them.



## 14.6 TEMPORAL EFFECT OF VF ON LATERALITY

We studied whether VF modifies the control structure by modulating the right or left arm activation coefficient. To do so, we compared the within-limb difference of the activation coefficients found in absence of VF and presence of VF for each limb. As in the previous section, a tolerance threshold of 10% was defined. We considered that the effect of VF acted over the **left arm** activation coefficient to modulate the control structure if the following inequality was fulfilled:

$$VF \rightarrow L \text{ if } \frac{|H_{i,nVF} - H_{i,VF}|_L}{|H_{i,nVF} - H_{i,VF}|_R} > 1.10 \quad (18)$$

Alternatively, we considered that the effect of VF acted over the **right arm** activation coefficient to modulate the control structure if the following inequality was fulfilled:

$$VF \rightarrow R \text{ if } \frac{|H_{i,nVF} - H_{i,VF}|_L}{|H_{i,nVF} - H_{i,VF}|_R} < 0.909 \quad (19)$$

Where:

- $H_i$  is the *i*th activation coefficient
- R subindex refers to right arm activation coefficient
- L subindex refers to left arm activation coefficient

We calculated the time-percent during which VF acted on either right or left activation coefficients by applying the steps explained in the previous section.



## 14.7 ILS IMPROVEMENT MEASURES

ILS between activation coefficients was quantified as the maximum cross-correlation coefficient given the delay  $\tau$ :

$$ILS_x = \max_{\tau} \frac{\sum_{n=0}^{N-1} H_{i,L}[n] \cdot H_{i,R}[n+\tau]}{\sqrt{\sum_{n=0}^{N-1} H_{i,L}^2[n] \cdot H_{i,R}^2[n+\tau]}} \quad x \in \{nVF, VF\} \quad (20)$$

where,

- $H_{i,S}$  is the  $i$ -th activation coefficient from right (S=R) or left (S=L) arm
- $n$  is time-point  $n \in [0, 100]$

The improvement of ILS generated by VF was calculated as the ratio between the ILS found with VF, with respect to the ILS found in absence of VF:

$$ILS_{improvement} (\%) = \frac{ILS_{VF}}{ILS_{nVF}} \cdot 100 - 100 \quad (21)$$

## 14.8 INTERMANUAL TRANSFER (IMT) MEASURES

Projecting one signal (reference pattern) onto another signal (test pattern) is a way to detect the presence of specific patterns as components of much more complex signals. Therefore, the cross-correlation between dominant activation coefficients (D, test pattern) and nondominant activation coefficients (ND, reference pattern) is a measure of “*how much*” of the test pattern is present in the reference pattern, or in



other words, a measure of IMT. However, because cross-correlation is a relative measure, the need exists to reference it to a baseline, in order to provide comparable metrics.

In this section we considered two possible IMT-types. On the one hand, we hypothesized that VF may transfer the original control of the dominant arm (i.e., in absence of VF) to the nondominant arm. We termed this type of IMT,  $IMT_0$ , and was calculated as:

$$IMT_0 = \frac{\max(xcorr(D_{nVF}, ND_{VF}))}{\max(xcorr(D_{nVF}, ND_{nVF}))} \cdot 100 - 100 \quad (22)$$

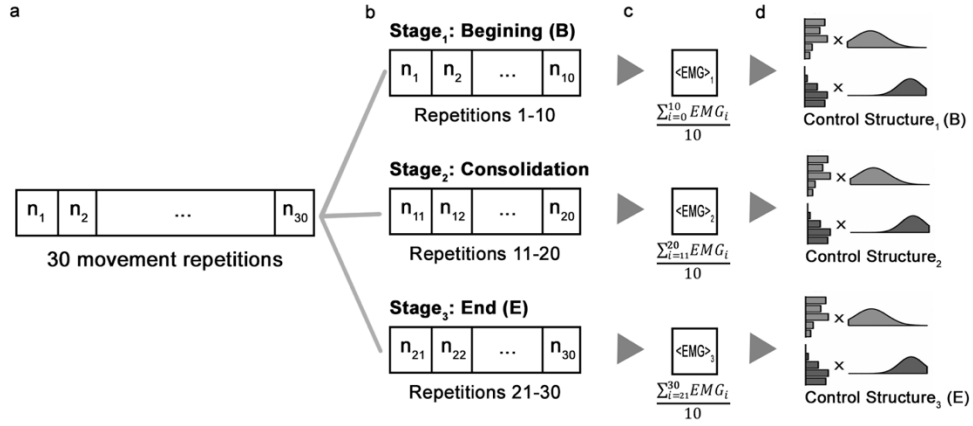
On the other hand, we hypothesized that VF may not only modulate the motor control of the nondominant arm, but also the motor control of the dominant arm. Thus, VF may transfer the VF-modulated dominant control, instead of the original control. This type of IMT was termed  $IMT_{VF}$  and was calculated as:

$$IMT_{VF} = \frac{\max(xcorr(D_{VF}, ND_{VF}))}{\max(xcorr(D_{nVF}, ND_{nVF}))} \cdot 100 - 100 \quad (23)$$

## 14.9 STAGE BY STAGE SYNERGY EXTRACTION

In order to study potential learning-effects, we went back to the EMG signals that we had just before extracting the regular control-structure. These EMG signals were processed following exactly the same steps as the processing-steps described in the section 8. EMG Data (See **PART II. METHODS**) with several modifications. See **Figure 33** for detailed explanation.





**Figure 33 Muscle synergy extraction workflow for the study of learning effects.** The schema illustrates the steps to obtain 3 consecutive average control structures from a single concatenated EMG signal corresponding to the 30 repetitions executed for each movement, by one subject's arm in one condition (nVF or VF). a) Single preprocessed and concatenated EMG signal consisting of 30 repetitions b) Consecutive and concatenated EMG signals consisting of 10 repetitions c) Averaged EMG signals d) Consecutive control structures extracted from the corresponding averaged EMG signals.

Essentially, instead of averaging the 30 repetitions into a single averaged EMG signal, we separated the repetitions into 3 different stages (**Figure 33b**) in the following manner:

- Beginning (B): repetitions 1 to 10
- Consolidation (C): repetitions 11 to 20
- End (E): repetitions 21 to 30

Next, we averaged the 10 repetitions conforming each stage for each subject, movement and arm separately for each condition (**Figure 33c**). As in the regular



method, the resulting averaged EMGs were 8 x 100 matrices corresponding to 8 muscles and 100 time-points.

From that moment on (**Figure 33d**), the synergy extraction and matching process was exactly the same as the one applied in the regular processing workflow (equations ( 4 ) and ( 6 )). The only difference was that instead of having a single control structure for each movement and arm (30 repetitions averaged by movement and arm), this process resulted in 3 control structures (10 repetitions averaged in each stage by movement and arm) (**Figure 33d**). The ILS measures were also calculated following the regular process (equations ( 8 ) and ( 9 )).

## 14.10 STATISTICAL ANALYSES

This section describes the set of statistical analyses applied to analyze the results of the Study 2.

### 14.10.1 *Interaction effects on VF-driven ILS changes*

We applied ANOVA tests to assess whether the ILS similarity changes induced by VF were affected by potential interaction effects from individual subjects and movements. In this regard, we carried out N-Way analysis of variance (using Matlab's built-in *anovan* function). Significant interaction was assumed if  $p < 0.05$ .

### 14.10.2 *Temporal effect of VF on ILS*

Wilcoxon signed-rank tests were used to detect significant interlimb (right vs left) and inter-condition (nVF vs VF) differences in the temporal measures of effect of VF. In particular, we applied to different statistical designs:

- **Test-type 1:** The percent time during which VF acted on the left arm vs the percent time during which VF acted on the right arm
- **Test-type 2:** The percent time during which VF increased ILS vs the percent time during which VF decreased ILS



Wilcoxon signed-rank test were applied to 3 different datasets:

- Dataset 1: time percent of all movements and subjects (1 test)
- Dataset2: time percent of all movements in each subject (6 tests)
- Dataset3: time percent of each movement (6 tests)

To allow these comparisons we concatenated the vectors corresponding to H1 and H2 to evaluate the control structure as a whole. That is, columns 1 and 3 of **Table 27** were concatenated one after the other into one vector. Also, columns 2 and 4; columns 5 and 7; and columns 6 and 8.

#### 14.10.3 *Interaction effects on IMT measures*

We applied two-way ANOVA test to assess the effect of each independent variable (subjects and movements) on the magnitude of ILS improvement and IMT induced by VF. We also use this test to examine possible interactions between the variables. That is, we investigated whether the effect of subjects significantly varied from movement to movement and vice versa.



# 15 RESULTS AND DISCUSSION (II)

This study is aimed at studying the effect of VF on the motor control of the upper-limb in healthy subjects. Along these lines, we provide a detailed report about the changes induced by VF in the control structure and the final functional output. Results are related to the individual preferences of subjects about applying VF.

## 15.1 SELF - EVALUATION ABOUT THE USE OF VF

summarizes the answers given by subjects after finishing the experimental session. For most subjects (5/6) the exercises used in the experiment were not new since they had practiced them before. Regarding VF, most subjects (5/6) affirmed that performing movements while being required to use VF was not disrupting and that they used the VF whenever they were asked to. Also, all subjects (6/6) said that they tried to do movement repetitions as similar as possible between them.

However, interesting exceptions were found that are very likely to affect the way the motor control of those subjects reacts to VF, and as a consequence, the results in this section:

1. **Subject 6** had never practiced the exercises before (Q1), so lower motor performance and higher motor-learning effects are expected on his results. He also recognized that VF made him lose the focus (Q2). Thus, we expect not to see a motor performance improvement in presence due to VF.



2. **Subject 4** recognized that he sometimes failed to make movement repetitions as similar as possible (Q4). In consequence, we expect higher interlimb differences during motor performance.
3. **Subject 2 and subject 5** found substantial performance differences between the right and left arm (Q5). Therefore, as with subject 4, we expect higher interlimb differences during motor performance.

	SUBJECTS					
	S1	S2	S3	S4	S5	S6
Q1	5	5	5	5	5	1
Q2	1	1	1	1	1	3
Q3	1	1	1	3	1	1
Q4	5	4	5	5	5	5
Q5	1	4	2	1	3	1

**Table 18** Answers given by the subject in the auto-evaluation questionnaire delivered after the experiment. Q1 – I had practiced these exercises before. Q2 – The mirror made me lose the focus. Q3 – I sometimes forgot to look to the mirror. Q4 – I tried to do movement repetitions as similar as possible. Q5 – I found big differences between the executions of movements done with the right or left arm. Answers were given as numeric values ranging from 1 (I do not agree) to 5 (I fully agree).

Be that as it may, because these inter-subject differences are directly related to motor control and the way VF can help learning or outperforming motor skills, it is very likely to find diverse inter-subject motor responses along the experiment. Therefore, these inter-subject particularities should be always kept in mind to ensure the adequate interpretation of the results.

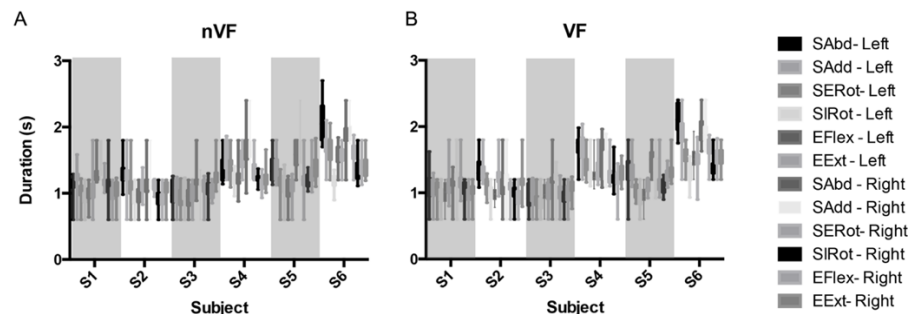


## 15.2 THE EFFECT OF VF ON MOVEMENT PERFORMANCE

This section is aimed at studying the effect of VF in the performance of movements. In particular, we focused on the effect of VF in the movement duration (and indirectly movement speed) and in the variability of movement duration.

### 15.2.1 *The effect of VF on movement duration*

**Figure 34** represents the duration of the movements executed by each subject in absence (**Figure 34A**) and presence of VF (**Figure 34B**) averaged across the 30 repetitions. Overall, movement duration seems to be quite a consistent within-subject characteristic across movements, with SD being around between 18% and 20% of the mean duration in all cases. However, major duration differences can be found from subject to subject.

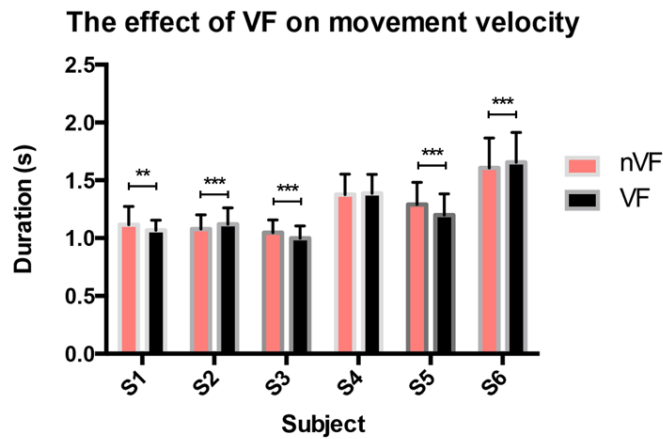


**Figure 34** Mean movement duration for each subject. A - In absence of Visual Feedback, B - In presence of Visual Feedback. Bars are mean duration  $\pm$  SD (s) across 30 repetitions.

For instance, subject 4 and subject 6 describe substantially slower movements (mean movement duration =  $1.38 \pm 0.25$ s and  $1.61 \pm 0.31$ s respectively), compared to the rest of the subjects ( $1.12 \pm 0.23$ s,  $1.07 \pm 0.20$ s,  $1.05 \pm 0.29$ s and  $1.2 \pm 0.26$ s). These patterns were replicated, both in absence and presence of VF (mean movement duration =  $1.06 \pm 0.19$ s;  $1.12 \pm 0.22$ s;  $1.00 \pm 0.19$ s;  $1.38 \pm 0.24$ s;  $1.20 \pm 0.24$ s;  $1.66 \pm 0.31$ s respectively).



Indeed, N-way ANOVA test reveals statistically significant differences of movement duration between subjects ( $p < 0.001$ ,  $F_{5,4261} = 1117.95$ ), movement types ( $p < 0.001$ ,  $F_{5,4261} = 397.44$ ), arm dominance ( $p < 0.001$ ,  $F_{1,4261} = 62.11$ ) and VF ( $p < 0.001$ ,  $F_{1,4261} = 6.57$ ). Similarly, significant interaction effects were found between subject and movement-type ( $p < 0.001$ ,  $F_{25,4261} = 25.57$ ), subject and arm dominance ( $p < 0.001$ ,  $F_{5,4261} = 59.59$ ), subject and VF ( $p < 0.001$ ,  $F_{5,4261} = 17.04$ ), movement-type and side ( $p < 0.01$ ,  $F_{5,4261} = 3.09$ ), movement-type and VF ( $p < 0.05$ ,  $F_{5,4261} = 2.72$ ), and arm dominance and VF ( $p = 0.01$ ,  $F_{1,4261} = 10.91$ ).



**Figure 35** Mean movement duration per subject in absence (red bars) and presence (black bars) of Visual Feedback. Bars are mean  $\pm$  SD. Means are calculated for both arms of each subject across the 30 repetitions of all 6 movements. \*\*  $p < 0.01$ , \*\*\*  $p < 0.001$ .

We found that in most subjects, VF modifies the average execution velocity of movements (**Figure 35**). However, the effect of VF varies from subject to subject. Indeed, VF significantly increases the execution velocity in S1, S3 and S5, while

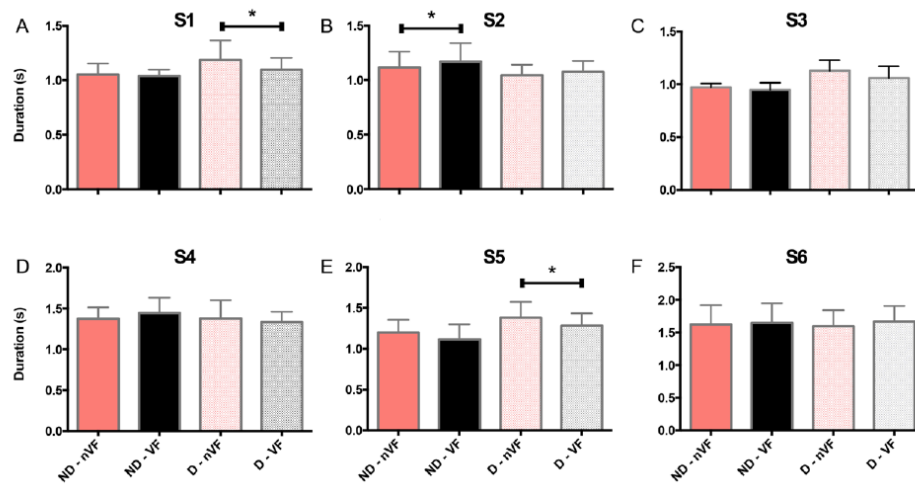


decreasing the execution velocity in S2 and S6. Interestingly, S6 admitted that VF made him lose the focus. This may explain why the movements he performed in presence of VF were slower. In S4, the effect of VF on the execution velocity is negligible. Expressed statistical significance is estimated using Wilcoxon signed-rank test for each subject. For each subject, we compared a pair (nVF vs VF) of 12 element-vector created by concatenating the 6 mean movement durations (averaged across 30 repetitions) of each arm. Note that in general, subjects describing faster movements are more susceptible of increasing the execution velocity in presence of VF.

Next, we separated the movement speed data by arm-dominance and condition (**Figure 36**). In general, a similar impact of VF is reproduced in both arms. That is, if VF increases movement execution velocity with respect to the movement execution found in absence of VF, such increase occurs in both arms. Consistently, if VF decreases movement execution velocity with respect to the movement execution found in absence of VF, the decrease occurs in both arms. Interestingly, whether VF increases or decreases the movement speed will depend on the subject analyzed.

Regarding inter-arm comparisons, we found no significant differences in the movement speed due to arm laterality. In other words, the speed achieved in absence of VF by the right and left arm of a given subject was similar, as so was the speed achieved by the right and left arm in presence of VF. However, the statistical tests determined that VF affected predominantly one or either the other arm in those subjects recognizing interlimb differences in their ability to execute movements. In particular, Wilcoxon signed-rank tests revealed that VF significantly increased movement execution velocity in the dominant arm of S1 and S5 ( $p < 0.05$ ), while significantly decreasing the execution velocity of the nondominant arm of S2 ( $p < 0.05$ ). Precisely, subjects S2 and S5 admitted experiencing important differences between right and left arm during movement execution. This may indicate that the effect of VF is especially relevant when the maximum possible motor performance has not been achieved yet.

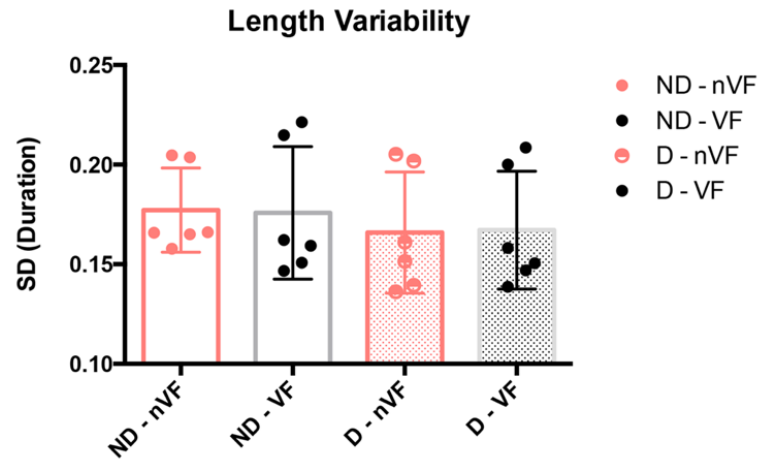




**Figure 36** The effect of VF in movement velocity sorted by arm dominance. Each plot (A-F) contains data from a subject (S1-S6). Bars are mean duration (averaged across 6 movements and 30 repetitions) +/- SD. ND - Nondominant arm, D - Dominant arm, nVF - non visual feedback, VF – visual feedback. \* $p < 0.05$ .



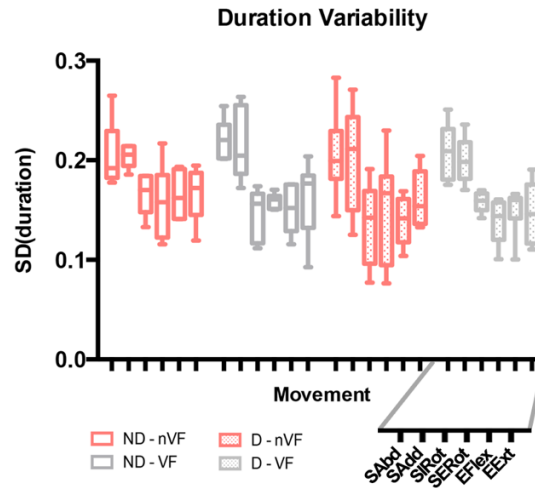
### 15.2.2 The effect of VF on the variability of movement duration



**Figure 37 Movement duration variability by arm-side and condition.** Variability is expressed as SD. Data points are the mean variability of each subject across movements and repetitions. Bars are the mean variability +/- SD of the SD of all subjects.

We investigated whether VF affects the inherent movement variability existing in humans. One way of addressing this issue, is by analyzing the variability in the duration of the execution of each movement repetition, as it does not only reflect a variation in the velocity but also important kinematic adaptations to slower or faster executions. **Figure 37** shows the mean variability of movement execution classified by arm dominance and VF condition. Overall, dominant arm movements ( $SD_D = 0.1659$ ) are less variable than nondominant arm movements ( $SD_{ND} = 0.1772$ ). This fact is also true in presence of VF, where variability of movement duration is  $SD_D = 0.1672$  against  $SD_{ND} = 0.1758$ . Interestingly, VF contributes to slightly reduce such variability in the nondominant arm. It has to be said, though, that these differences did not reach statistical significance (Wilcoxon signed rank test,  $p > 0.05$ ), but this may be due to the high intersubject variability found in the results. It is also plausible that because the subjects under analysis are not affected by any neurological or motor condition, the effect of VF is too humble so as to reach significance.





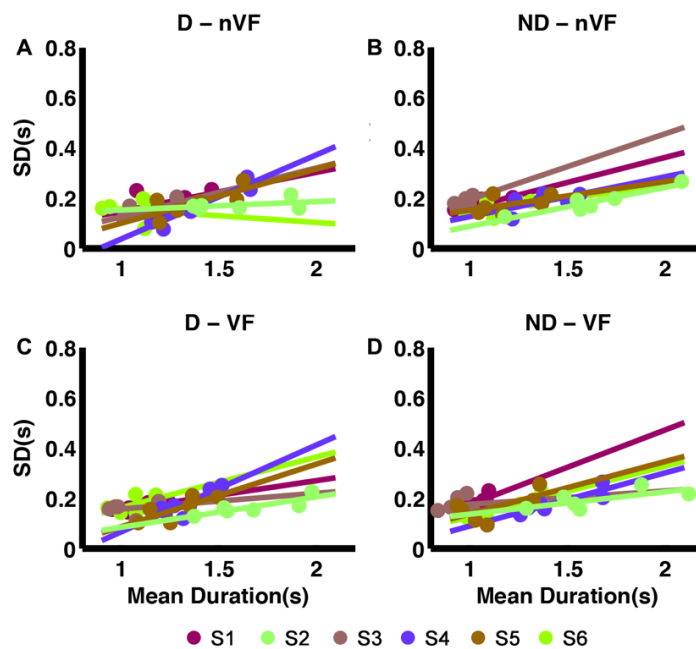
**Figure 38** Variability of movement duration per movement type. Variability shown is calculated by averaging the SD of movement duration across subjects and repetitions. Boxes extend from quartile Q1 to Q3 and whiskers cover 9 to 95 percentiles. The inner horizontal line indicates the median. Data is divided in 4 groups: ND – nondominant arm, D – dominant arm, nVF – non visual feedback, VF – visual feedback. Ticks in the horizontal axis indicate the movements under analysis.

Next, we analyzed the movement variability found in each movement type across subjects and repetitions (**Figure 38**). We found that some movements tend to be more variable than others. In particular, longer movements such as shoulder abduction and adduction are clearly more variable than the rest of the movements. Indeed, the analysis of variance revealed a significant effect of the executed movement-type on the variability of movement duration ( $p < 0.001$ ,  $F_{5,85} = 19.18$ ). No interaction effects were found between subjects, movement or arm dominance.

Following the later observation, we investigated whether movement length and variability was correlated (**Figure 39**). Our results indicate that there is a positive correlation between movement duration and movement variability across repetitions,



and such positive correlation is conserved in all subjects regardless the existence of VF.  $R^2$  values of each linear fit are displayed in the table below (**Table 19**). The coefficient of determination  $R^2$  is the fraction of the y-variable that is explained by the variation of the x-variable. The significance of the model is assessed using the F-statistic. The F statistic is computed under the assumption that the model contains a constant term. That is, models with negative  $R^2$  indicate that these are not appropriate for the data.



**Figure 39** Relationship between movement duration and duration variability for the A – Dominant arm (D) with no visual feedback, B – Nondominant arm (ND) with no visual feedback, C – Dominant arm with visual feedback, D – Nondominant arm with visual feedback. Each color represents a subject, and a data point in each data subset is the mean duration of a movement-type averaged across repetitions. Variability is expressed as SD. Lines represent linear regression of every dataset.



$R^2$  values express the variability explained by the linear regression model, and are calculated as one minus the ratio between the residual sum of squares and the total sum of squares:

$$R^2 = 1 - \frac{SS_{resid}}{SS_{total}} \quad (24)$$

Where  $SS_{resid}$  is the residual sum of squares, and  $SS_{total}$  is the total sum of squares.

R2 - VALUE				
Subject	D - nVF	D - VF	ND - nVF	ND - VF
S1	0.2618	0.5932	0.7150*	0.5070
S2	0.0139	0.3663	0.2371	0.6998*
S3	0.3836	0.0732	0.3932	0.0140
S4	0.8902	0.6976*	0.3545*	0.7610*
S5	0.5557*	0.6041	0.2435	0.4283
S6	0.1759	0.7397*	0.8958*	0.5104

**Table 19 Goodness of fit of the linear regressions** shown in **Figure 39** expressed as  $R^2$ -value. ND – nondominant arm, D – dominant arm, nVF – non visual feedback, VF – visual feedback. \* p-value associated to the F-statistic < 0.05.

Indeed, VF tends to substantially modify the magnitude of correlation between the duration of movement execution and the variability. However, as in the previous cases, the nature of such modification varies from subject to subject. In most nondominant arms (S1, S2, S4, S5), VF increases the slope of the linear regression. That is, in presence of VF, the slower the movement, the greater the speed variability. In S3 and S6, the effect of VF is just the opposite. Regarding arm side, the pattern of modification of the dominant arm matches the pattern of the nondominant arm, except in S1 and S6 for which VF increases the slope in one arm, and decreases it in the other (**Figure 40**).



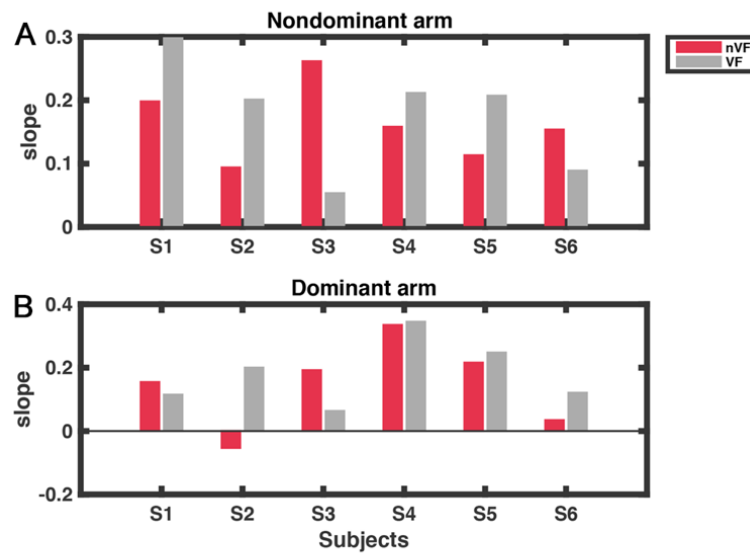


Figure 40 Effect of VF in the magnitude of correlation of movement duration and movement duration-variability in the A – nondominant arm and B – dominant arm. Bars are the slope of the linear regression calculated previously for each subject. nVF – no visual feedback, VF – visual feedback.



## 15.3 THE EFFECT OF VF ON THE ILS

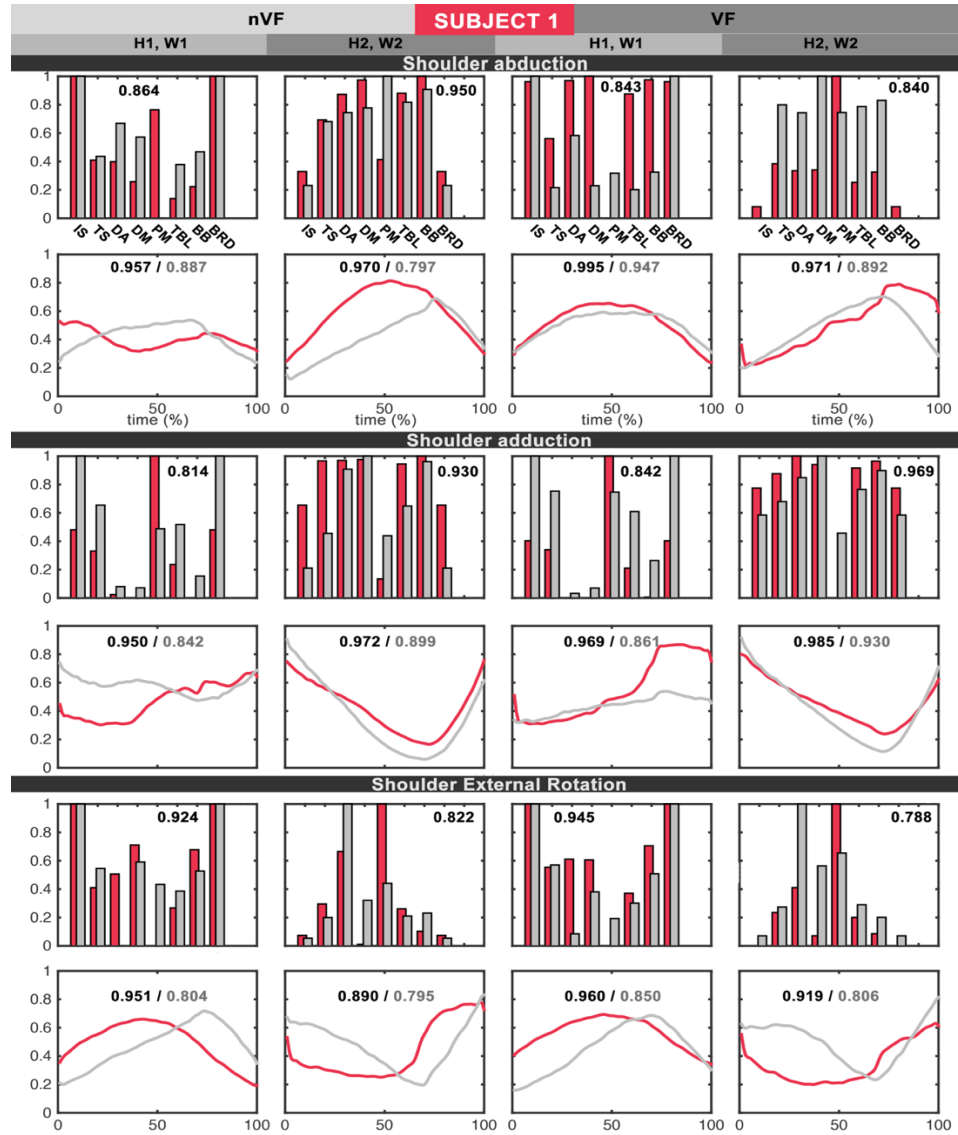
This section is aimed at studying whether VF has the ability to modify the ILS of muscle synergies and activation coefficients. Because we found significant interaction of subjects and movement-types with the effect of VF in the ILS of the control structure, the results described in this section are separately explained for subjects and movement-types.

### 15.3.1 *Control structures in absence and presence of VF*

The following set of figures depicts the control structure of each healthy subject in absence and presence of VF. The effect of VF in each subject is illustrated by a pair of figures, the first one containing the control structures of shoulder abduction, shoulder adduction and shoulder external rotation in absence and presence of VF, and the second one containing the control structures of shoulder external rotation, elbow flexion and elbow extension, also in absence and presence of VF.

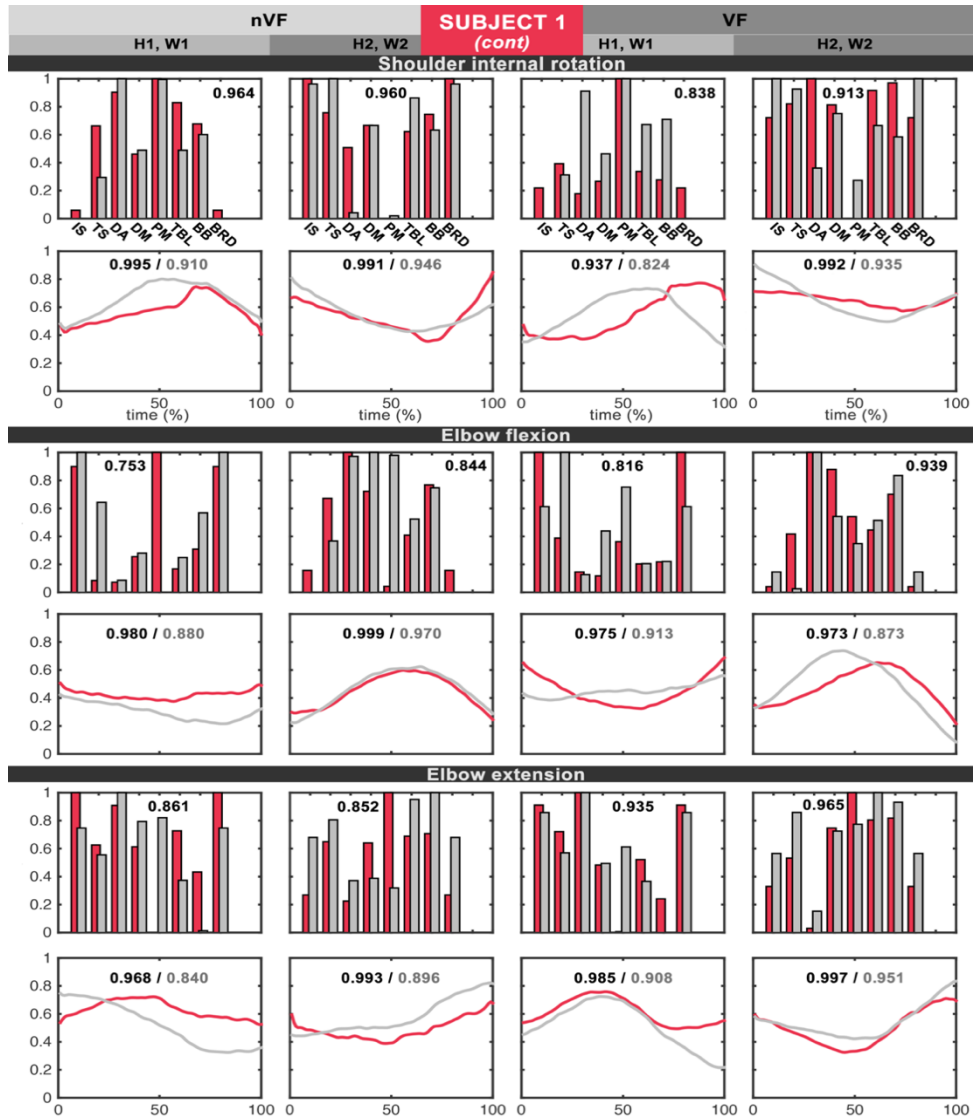
Each plot within the figure is accompanied by a series of numbers that indicate the ILS of muscle synergies and activation coefficients. The ILS of muscles synergies is measured with scalar product, whereas for the ILS of activation coefficients we provide two measures, the first one is the cross-correlation coefficient and the second one is 1 – ILD.





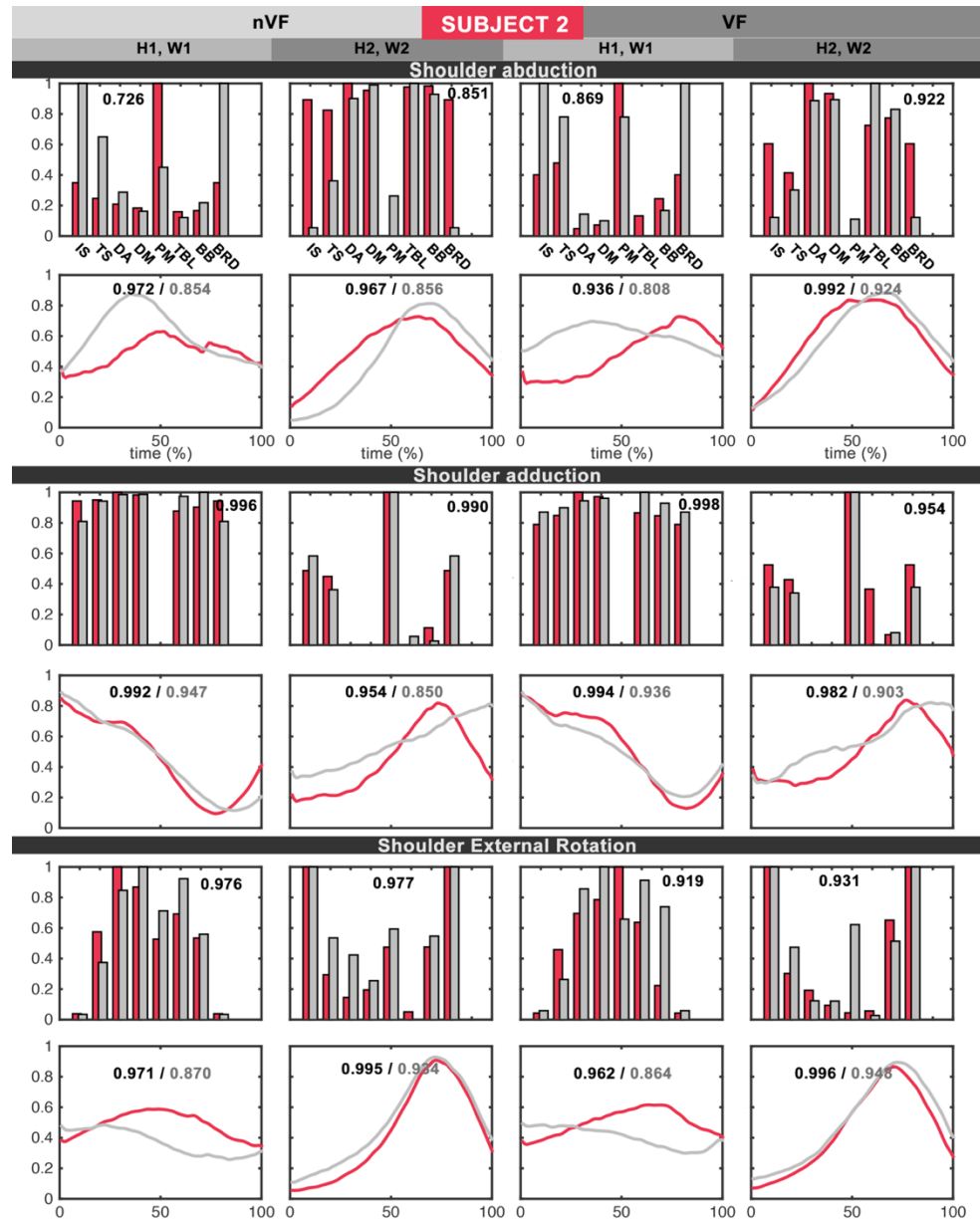
**Figure 41** Graphical representation of the control structure of **SUBJECT 1** and related ILS measures **PART 1/2**: shoulder abduction, shoulder adduction and shoulder external rotation. Bars are muscle synergies and curves are activation coefficients. Red elements belong to the control structure of the nondominant arm and grey elements to the dominant arm. The numbers indicated in each plot are scalar products for muscle synergies and **Cross-correlation coefficient / 1 - ILD** for activation coefficients.





**Figure 42** Graphical representation of the control structure of **SUBJECT 1** and related ILS measures **PART 2/2**: shoulder internal rotation, elbow flexion and elbow extension. Bars are muscle synergies and curves are activation coefficients. Red elements belong to the control structure of the nondominant arm and grey elements to the dominant arm. The numbers indicated in each plot are scalar products for muscle synergies and **Cross-correlation coefficient / 1 - ILD** for activation coefficients.





**Figure 43** Graphical representation of the control structure of SUBJECT 2 and related ILS measures  
**PART 1/2:** See the legend of Figure 41 for a complete and detailed description of the figure.



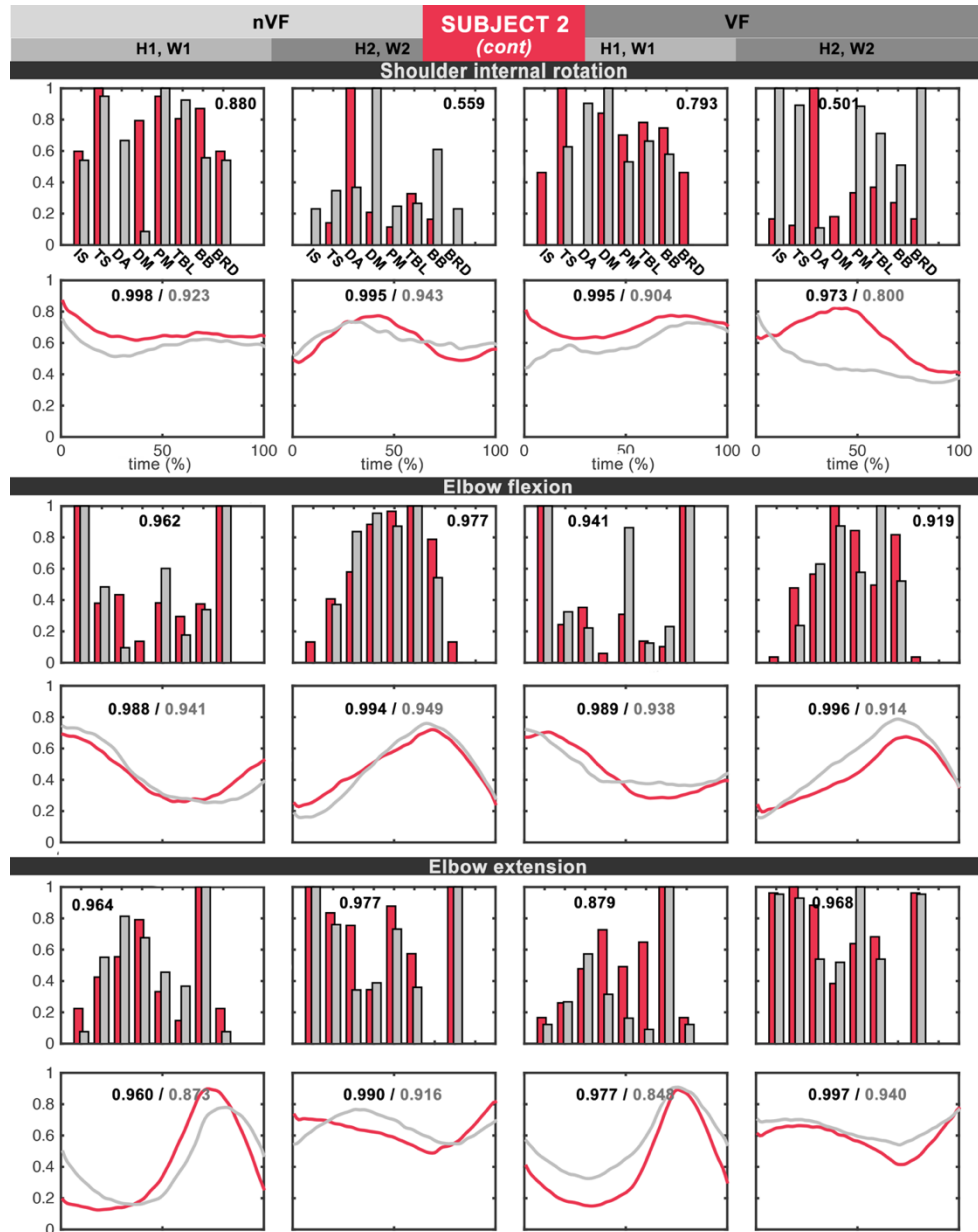
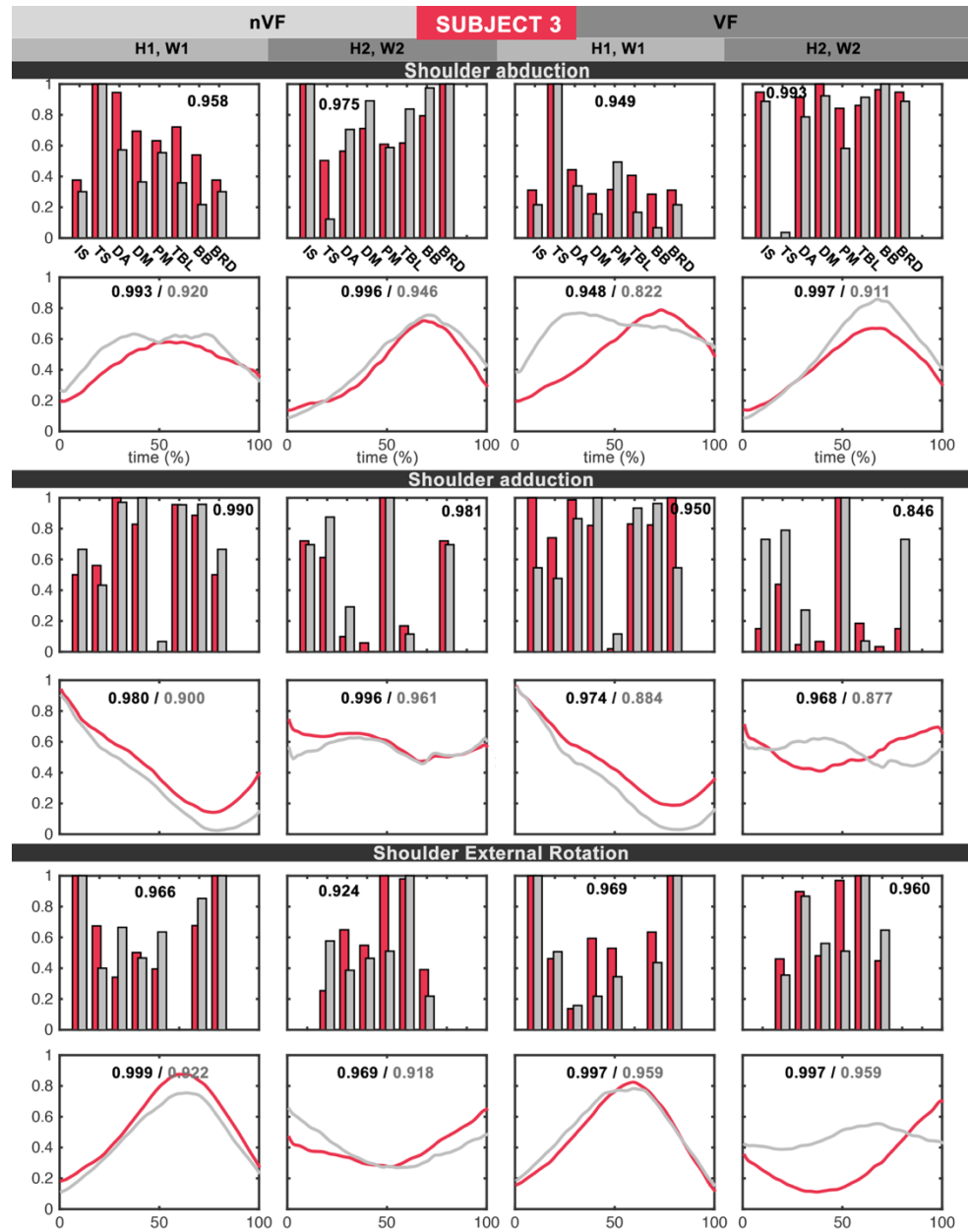


Figure 44 Graphical representation of the control structure of SUBJECT 2 and related ILS measures  
PART 2/2: See the legend of Figure 42 for a complete and detailed description of the figure.





**Figure 45** Graphical representation of the control structure of SUBJECT 3 and related ILS measures  
**PART 1/2:** See the legend of Figure 41 for a complete and detailed description of the figure.



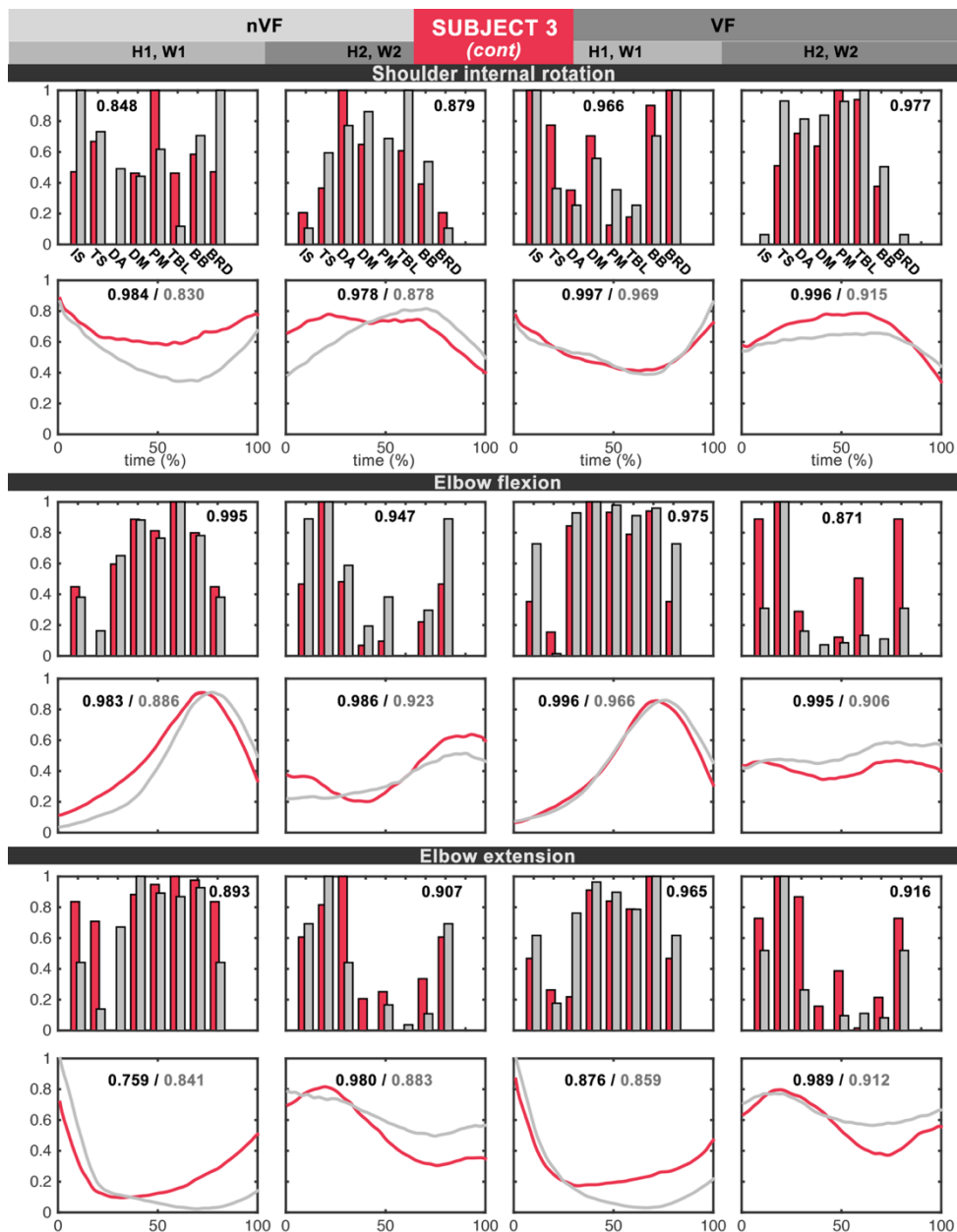
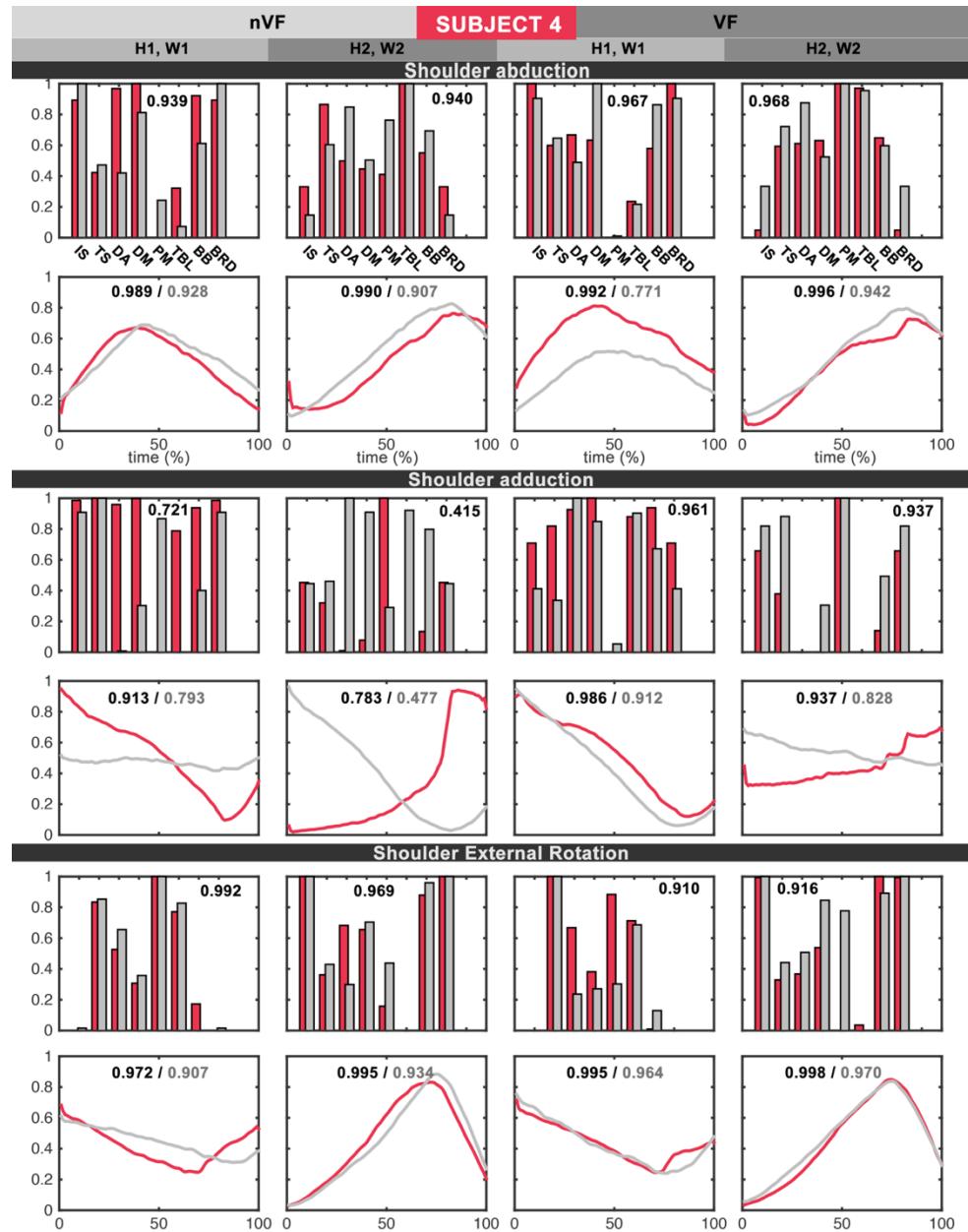


Figure 46 Graphical representation of the control structure of SUBJECT 3 and related ILS measures  
PART 2/2: See the legend of Figure 42 for a complete and detailed description of the figure.





**Figure 47** Graphical representation of the control structure of SUBJECT 4 and related ILS measures  
**PART 1/2:** See the legend of Figure 41 for a complete and detailed description of the figure.



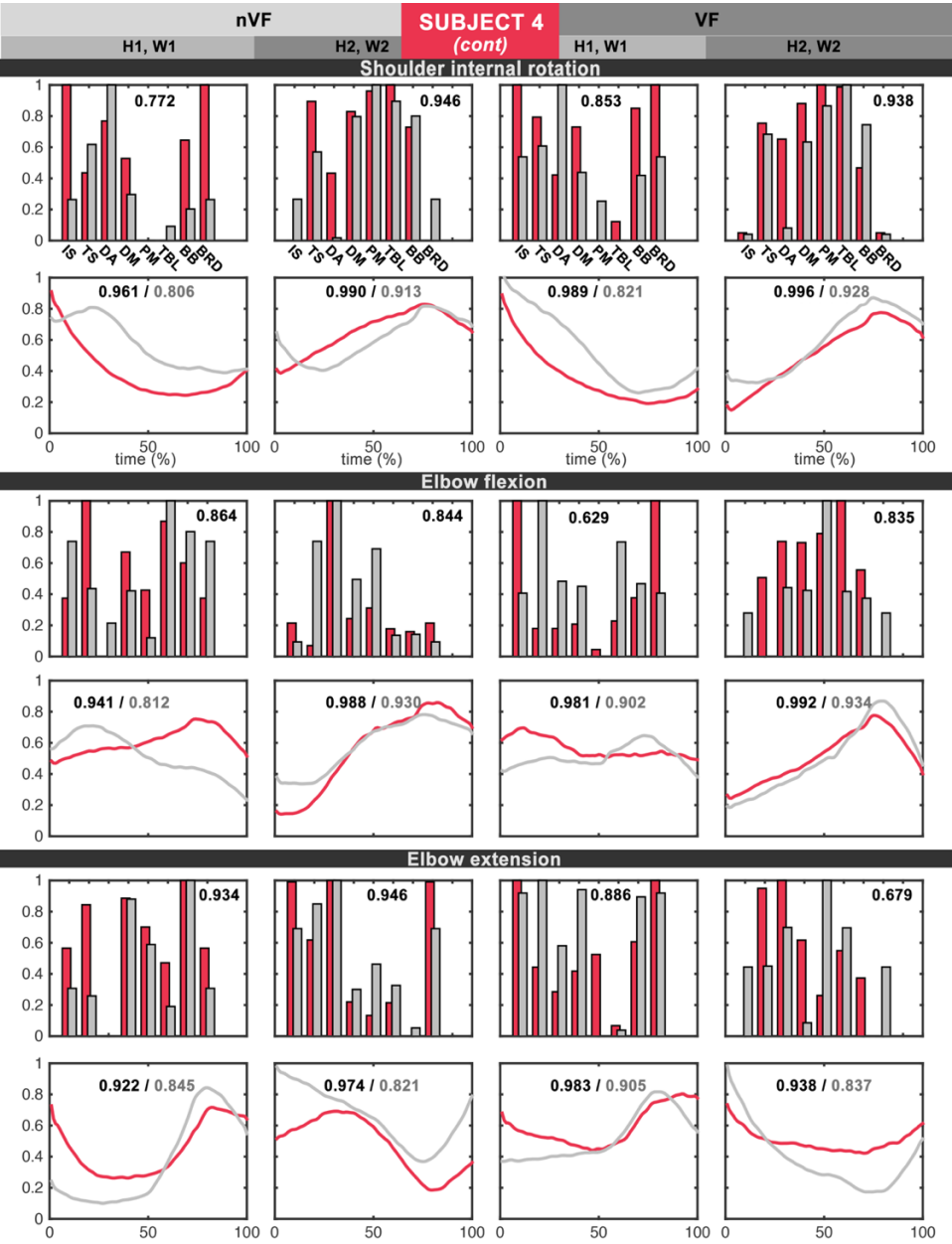
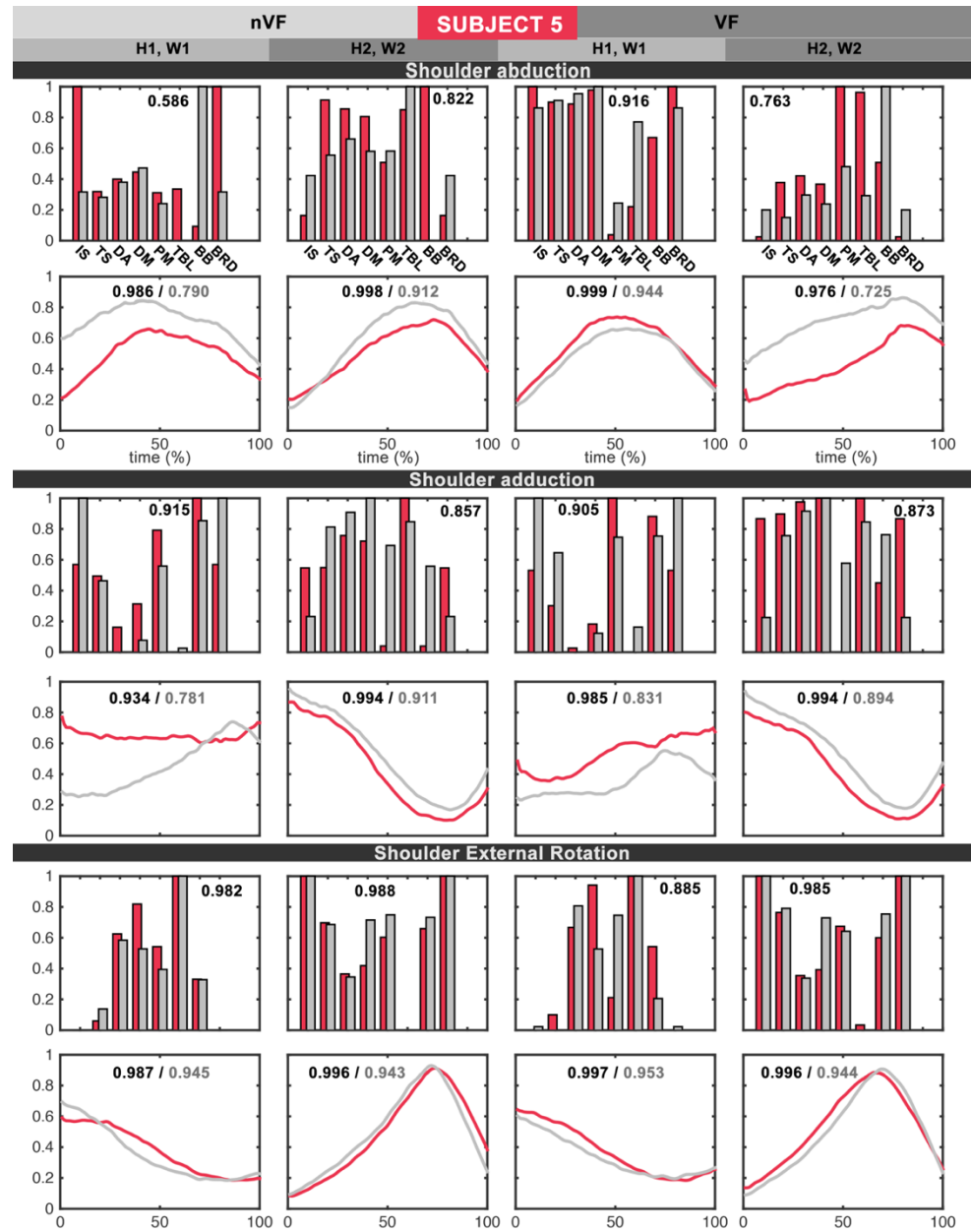


Figure 48 Graphical representation of the control structure of SUBJECT 4 and related ILS measures  
PART 2/2: See the legend of Figure 42 for a complete and detailed description of the figure.





**Figure 49** Graphical representation of the control structure of SUBJECT 5 and related ILS measures  
**PART 1/2:** See the legend of **Figure 41** for a complete and detailed description of the figure.



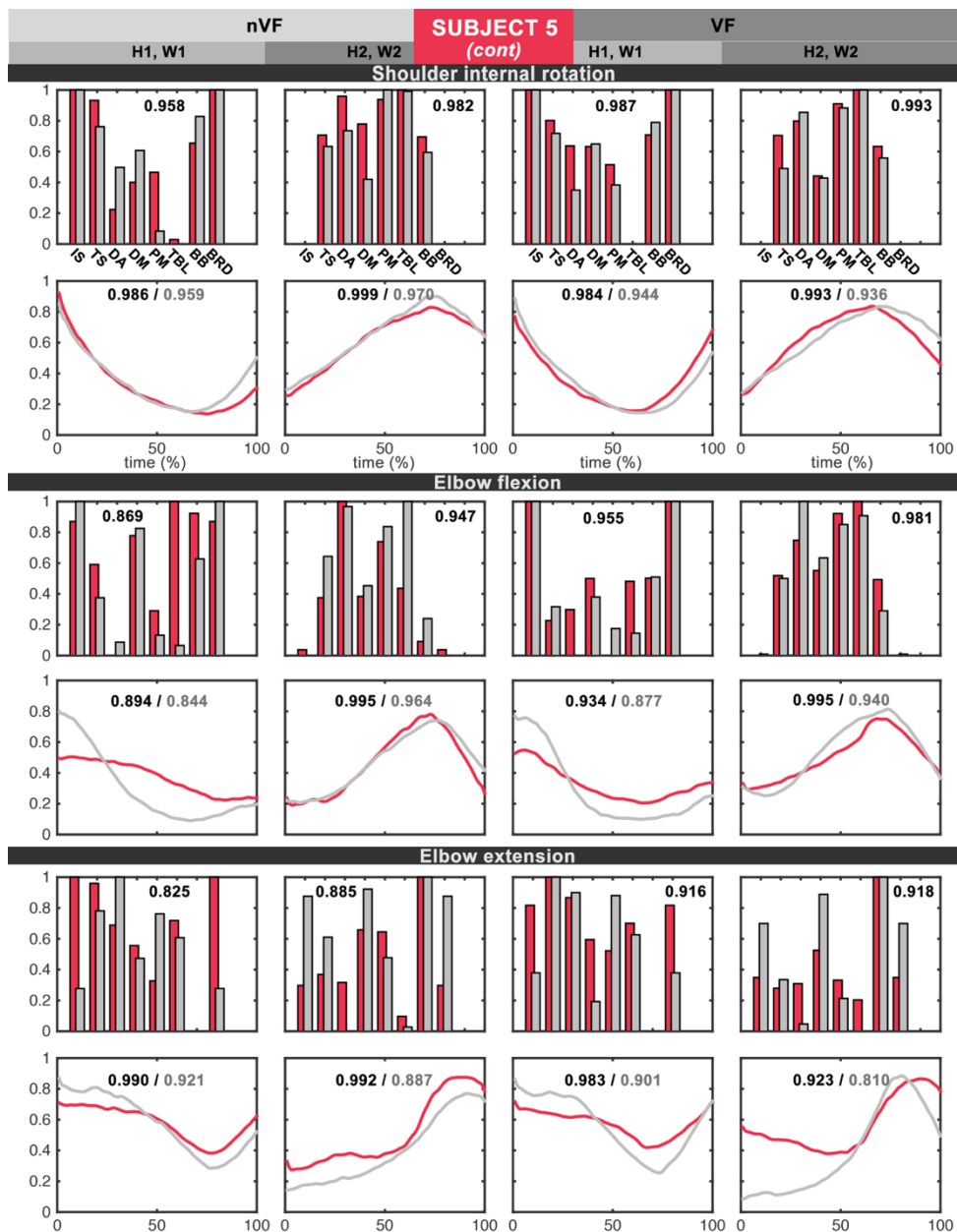


Figure 50 Graphical representation of the control structure of SUBJECT 5 and related ILS measures  
 PART 2/2: See the legend of Figure 42 for a complete and detailed description of the figure.



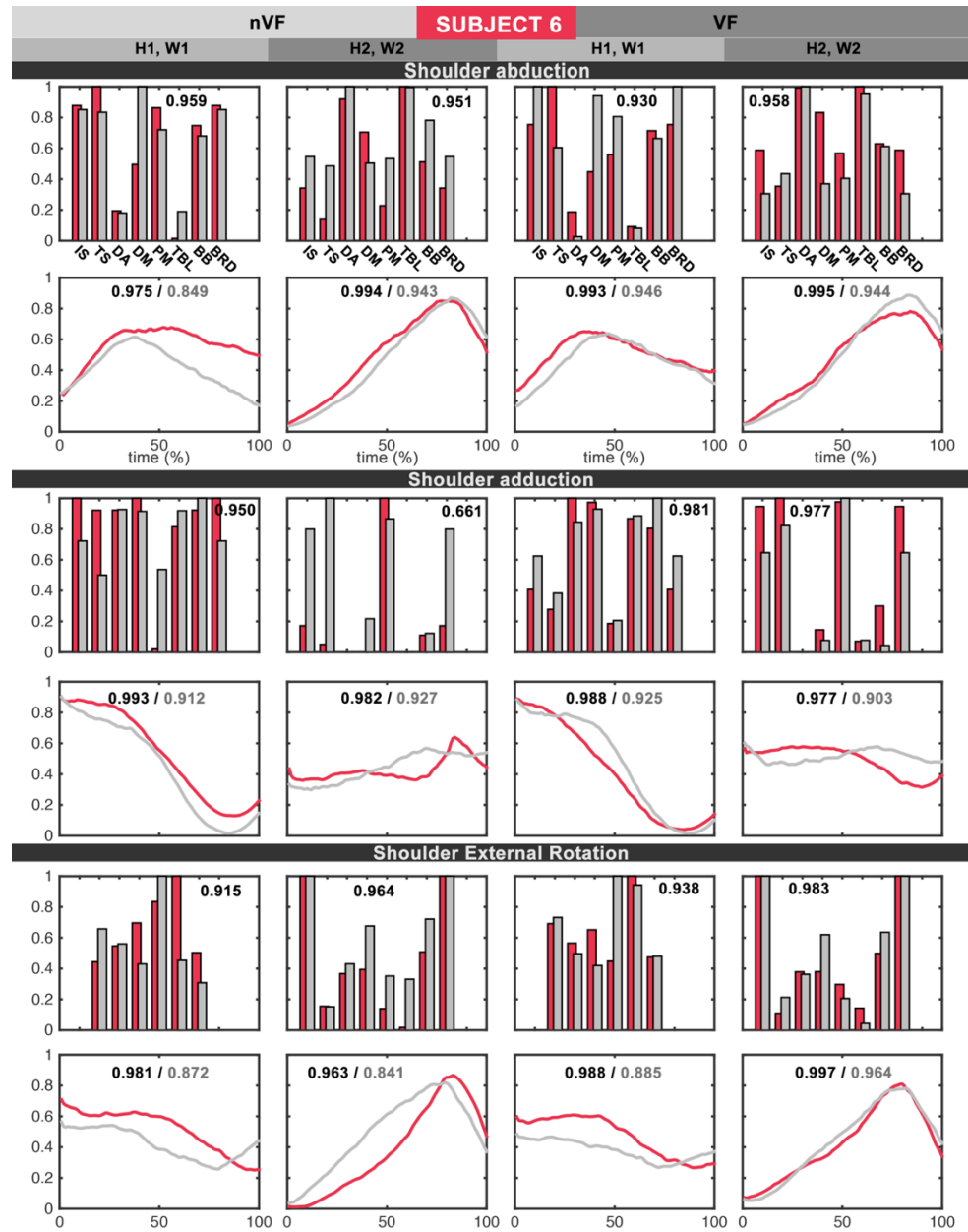


Figure 51 Graphical representation of the control structure of SUBJECT 6 and related ILS measures  
PART 1/2: See the legend of Figure 41 for a complete and detailed description of the figure.



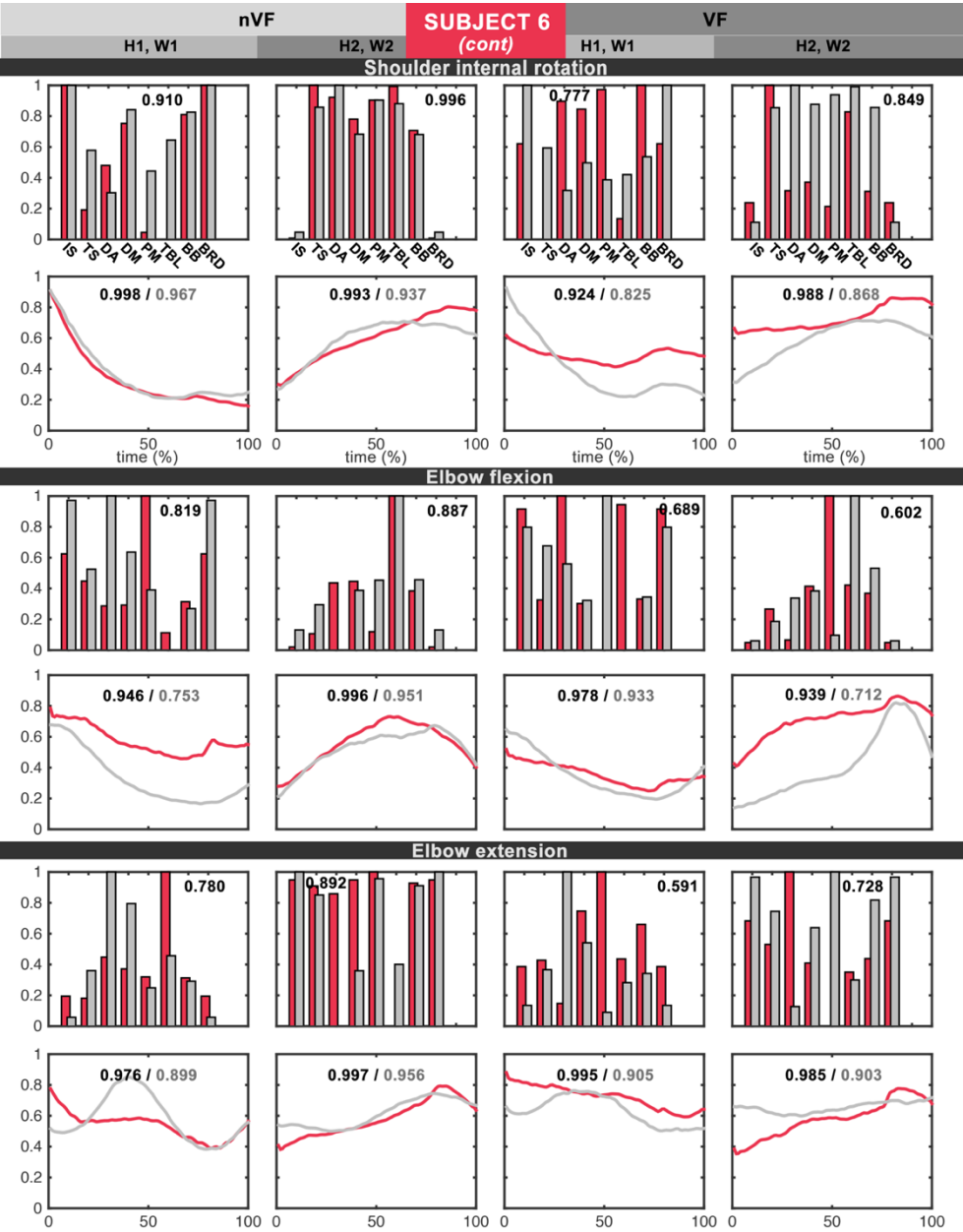
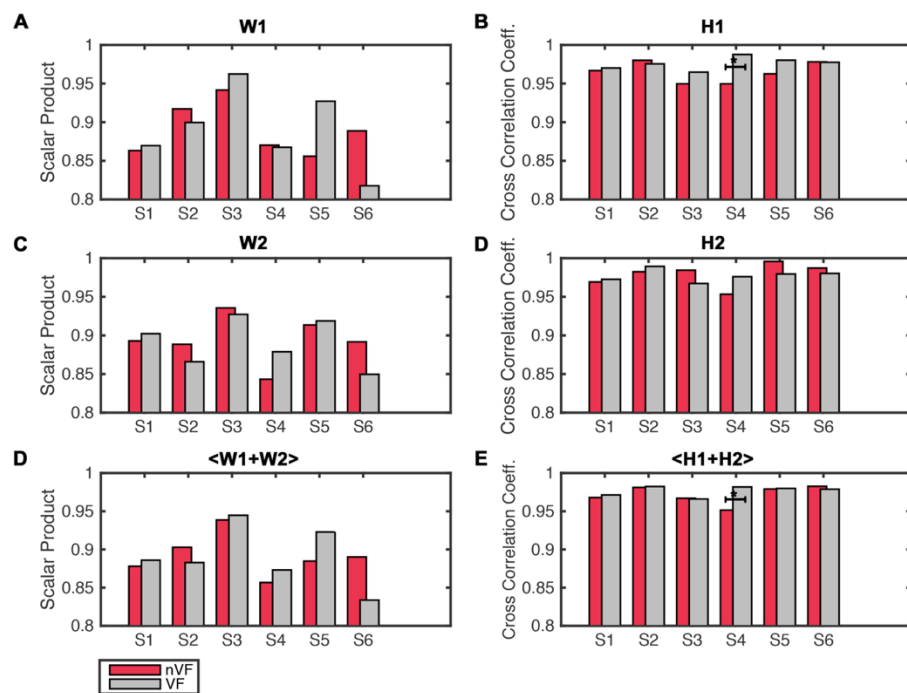


Figure 52 Graphical representation of the control structure of SUBJECT 6 and related ILS measures  
PART 2/2: See the legend of Figure 42 for a complete and detailed description of the figure.



### 15.3.2 Mean ILS: subject by subject

**Figure 53** shows the within-subject ILS of the control structure averaged across movements. Despite substantial inter-subject differences, the overall effect of VF is to increase the ILS of the control structure. **Figure 53E** shows that VF increases the ILS of synergies in 4 out of 6 subjects. A similar effect can be seen in **Figure 53F**, regarding the activation coefficients. Interestingly, subject 6, for whom the ILS decreased in presence of VF was the only subject reporting that VF made him lose the focus on the movements performed.



**Figure 53** Per subject ILS of A – Synergy 1, B – Activation coefficient 1, C – Synergy 2, D – Activation Coefficient 2, E – Average ILS of synergies 1 and 2, F – Average ILS of activation coefficients 1 and 2. Bars are the ILS averaged across the 6 movements for each subject (S1-S6). Red bars represent the ILS found in absence of VF and grey bars represent the ILS found in presence of VF. \*  $p < 0.05$  for Wilcoxon Signed Rank test.

We performed a set of Wilcoxon signed rank test, which compared the ILS found in presence and absence of VF for each subject. The tests revealed that the ILS increase



induced by VF was significant only in subject 4. **Table 20** shows the p-values resulting from all the statistical tests performed in this section.

P-VALUES OF WILCOXON SIGNED RANK TEST						
	S1	S2	S3	S4	S5	S6
W1	0.5625	0.5625	0.8438	1	0.4375	0.2188
W2	0.8438	0.4375	1	0.84375	0.5625	0.8438
<W1,W2>	0.6772	0.2036	0.7910	0.8501	0.2036	0.2334
H1	0.5625	0.6875	0.6875	<b>0.0313</b>	0.1563	0.5625
H2	0.3125	0.2188	1	0.3125	0.0625	0.4375
<H1, H2>	0.3013	0.6772	0.7910	<b>0.0122</b>	0.9097	0.9697

**Table 20** p-values of Wilcoxon rank test comparing ILS in absence and presence of VF for each subject across the 6 movements. Significant results ( $p < 0.05$ ) are highlighted in bold.

During data analysis we observed substantial inter-subject differences but also substantial differences between movement types. Therefore, we carried out N-Way analysis of variance in order to discard possible interactions between factors (subjects, movements) and the effect of VF, which may lead to incorrect conclusions. In particular, we applied N-way ANOVA tests on 6 different datasets:

1. ILS measures of W1s
2. ILS measures of W2s
3. Concatenated ILS measures of W1 and W2 [ $ILS_{W1}$  ;  $ILS_{W2}$ ]
4. ILS measures of H1s
5. ILS measures of H2s
6. Concatenated ILS measures of H1 and H2 [ $ILS_{H1}$  ;  $ILS_{H2}$ ]

Results of the 6 N-way ANOVA tests may be found in **Table 21-Table 23**. These results reveal a significant interaction ( $p < 0.05$ ) between subjects and movement types (subj x mov) in all cases. Note that in the case of W1 (**Table 21**), the effect of subject on ILS is significant while the interaction 'subj x mov' scraps significance ( $p = 0.0522$ ). In



any case, these results bring to light the need to analyze the ILS measures separately for each movement and subject.

N-WAY ANOVA		DATASET: ILS OF W1			DATASET: ILS OF W2			
Factor	Sum of Squares	d.f.	F	Prob > F	Sum of Squares	d.f.	F	Prob > F
Subject	0.0785	5	2.6672	<b>0.0459</b>	0.0456	5	0.8591	0.5219
Movement	0.0677	5	2.2990	0.0754	0.0387	5	0.7293	0.6081
Condition	10 <sup>-05</sup>	1	0.0042	0.9488	10 <sup>-4</sup>	1	0.0246	0.8767
Subj x Mov	0.2854	25	1.9388	0.0522	0.5584	25	2.1043	<b>0.0343</b>
Subj x Cond	0.0327	5	1.1108	0.3798	0.0109	5	0.2057	0.9570
Mov x Cond	0.0317	5	1.0779	0.3964	0.0598	5	1.1276	0.3716
Error	0.1472	25			0.2653	25		
Total	0.6432	71			0.9790	71		

**Table 21** Results of N-WAY ANOVA tests performed on ILS measures of synergies W1 and W2. Significant p-values are highlighted in bold. d.f. degrees of freedom.

N-WAY ANOVA		DATASET: CONCATENATED ILS OF [W1, W2]			DATASET: CONCATENATED ILS OF [H1, H2]			
Factor	Sum of Squares	d.f.	F	Prob > F	Sum of Squares	d.f.	F	Prob > F
Subject	0.1043	5	2.7872	<b>0.0214</b>	0.0064	5	1.2221	0.3046
Movement	0.0755	5	2.0176	0.0828	0.0088	5	1.6658	0.1501
Condition	10 <sup>-5</sup>	1	0.0083	0.9274	10 <sup>-4</sup>	1	0.9054	0.3437
Subj x Mov.	0.6140	25	3.2830	<b>10<sup>-5</sup></b>	0.0528	25	2.0102	<b>0.0083</b>
Subj x Cond	0.0325	5	0.8687	0.5051	0.0048	5	0.9057	0.4807
Mov. x Cond	0.0704	5	1.8831	0.1042	0.0039	5	0.7473	0.5900
Error	0.7257	97			0.1019	97		
Total	1.6224	143			0.1795	143		

**Table 22** Results of N-WAY ANOVA tests performed on the concatenated ILS measures of synergies W1 and W2; and activation coefficients H1 and H2. Significant p-values are highlighted in bold. d.f. degrees of freedom.



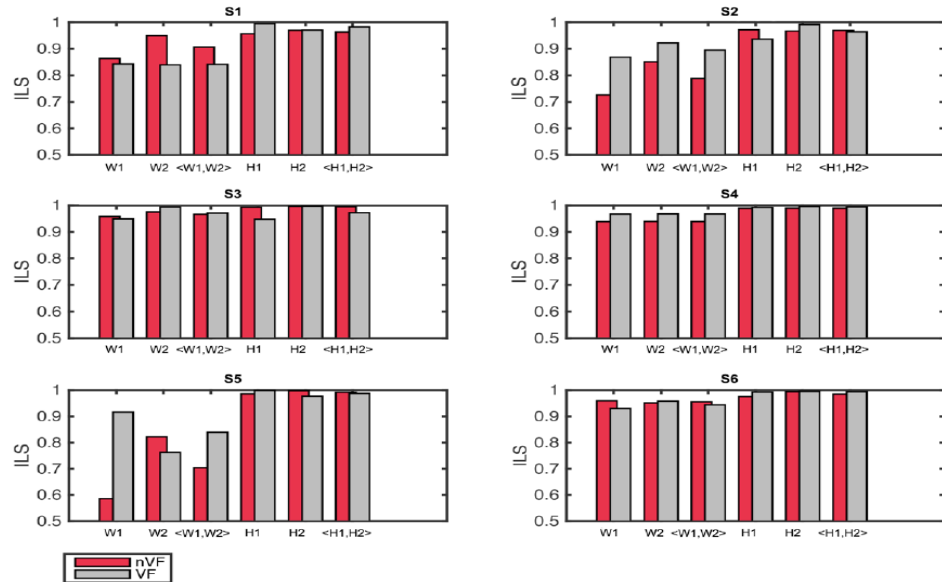
N-WAY ANOVA		DATASET: ILS OF H1			DATASET: ILS OF H2			
Factor	Sum of Squares	d.f.	F	Prob > F	Sum of Squares	d.f.	F	Prob > F
Subject	0.0035	5	1.4454	0.2429	0.0051	5	1.3316	0.2833
Movement	0.0091	5	3.7773	<b>0.0110</b>	0.0099	5	2.5861	0.0511
Condition	0.0024	1	4.8929	<b>0.0363</b>	10-5	1	0.0334	0.8564
Subj x Movem	0.0562	25	4.6471	<b>10<sup>-4</sup></b>	0.0438	25	2.2936	<b>0.0214</b>
Subj x Cond	0.0037	5	1.5236	0.2184	0.0035	5	0.9231	0.4825
Movem x Cond	0.0055	5	2.2577	0.0798	0.0035	5	0.9089	0.4910
Error	0.0121	25			0.0191	25		
Total	0.0925	71			0.0848	71		

**Table 23 Results of N-WAY ANOVA tests performed on ILS measures of activation coefficients H1 and H2.** Significant p-values are highlighted in bold. d.f. degrees of freedom.

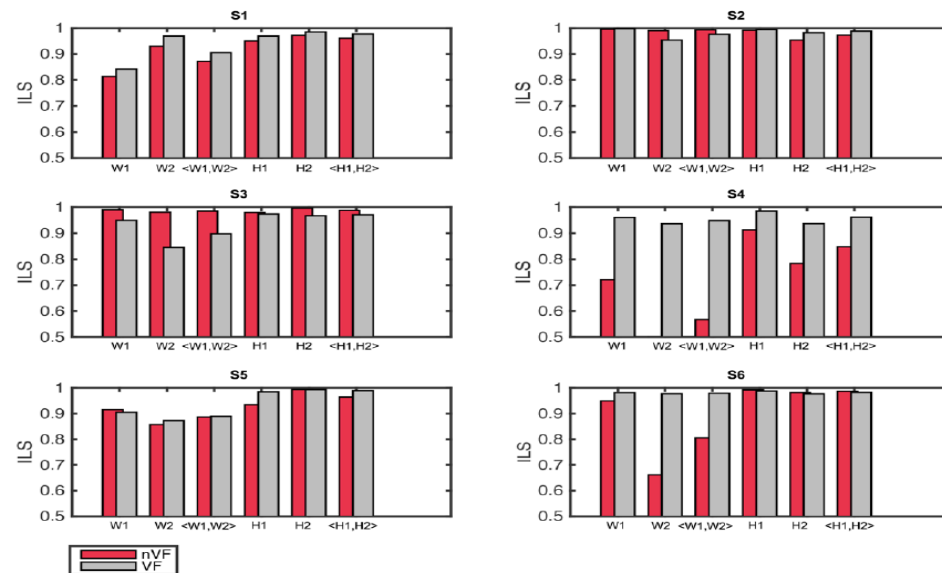
### 15.3.3 Mean ILS: movement by movement

**Figure 54** to **Figure 59** show the ILS similarity measures found during the execution of the 6 movements under analysis. The subplots found in each figure correspond to the ILS of a subject. These bar plots clearly illustrate the interaction effect reported by the N-way ANOVA tests between movements and subjects. That is, the effect of VF on ILS changes depending on subjects and movements. For instance, during shoulder internal rotation (**Figure 57**), VF reduces ILS in subject 1 and 6 (S1, S6), whereas VF increases ILS in subject 3 and 4 (S3, S4). In contrast, VF increases ILS in subject 1 during elbow flexion (**Figure 58**), whereas VF reduces ILS in subject 6.





**Figure 54 Within-subject ILS measures during SHOULDER ABDUCTION.** Bars are ILS measures of shoulder abduction (scalar product for synergies and cross-correlation coefficient for activation coefficients) for each subject (S1-S6). <W1,W2> and <H1,H2> represent the averaged ILS of the two synergies or activation coefficients respectively. Red bars represent movements performed in absence of VF and grey bars represent movements performed in presence of VF.



**Figure 55 Within subject ILS measures during SHOULDER ADDUCTION.** See the legend of Figure 54 for a complete and detailed description of the figure.



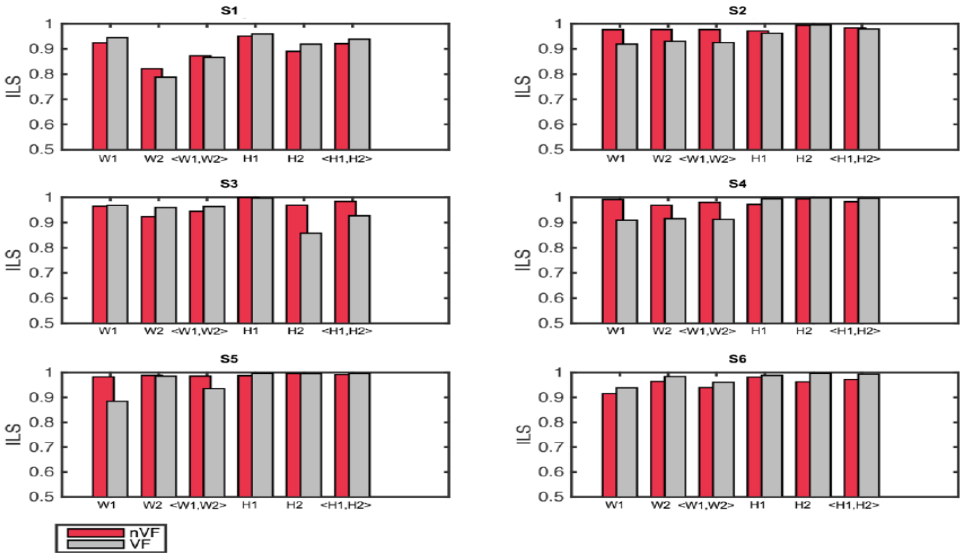


Figure 56 Within subject ILS measures during SHOULDER EXTERNAL ROTATION. See the legend of Figure 54 for a complete and detailed description of the figure.

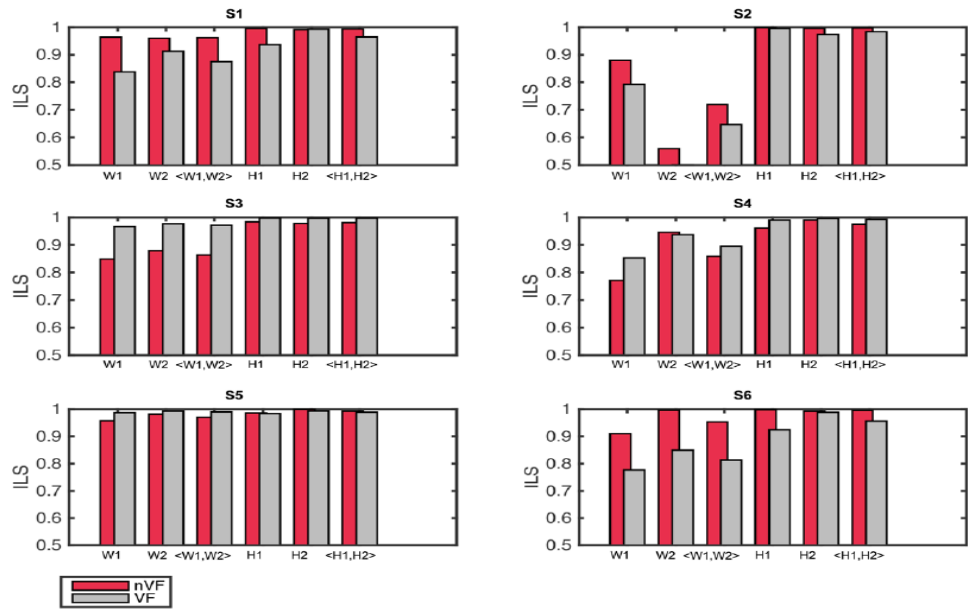


Figure 57 Within subject ILS measures during SHOULDER INTERNAL ROTATION. See the legend of Figure 54 for a complete and detailed description of the figure.



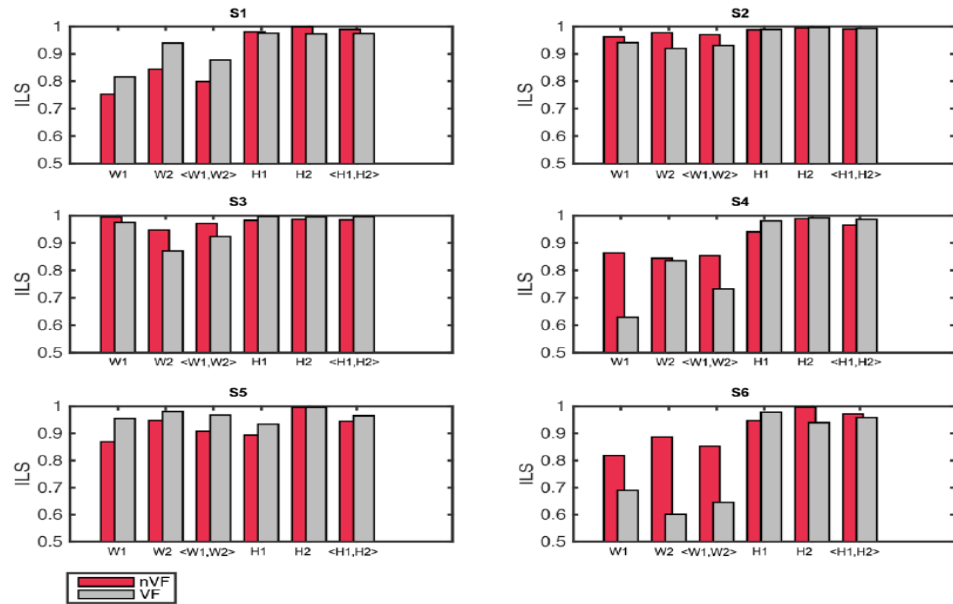


Figure 58 Within subject ILS measures during ELBOW FLEXION. See the legend of Figure 54 for a complete and detailed description of the figure.

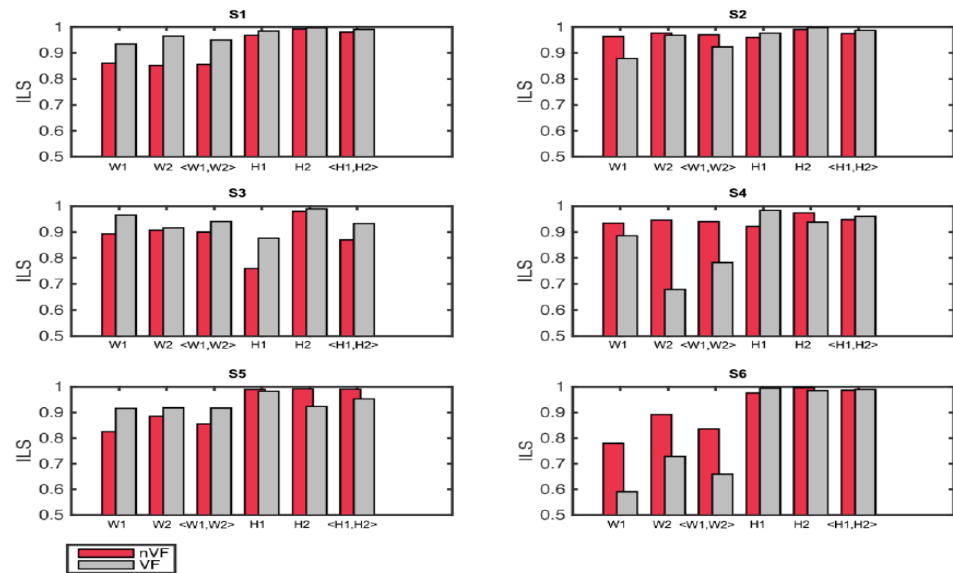
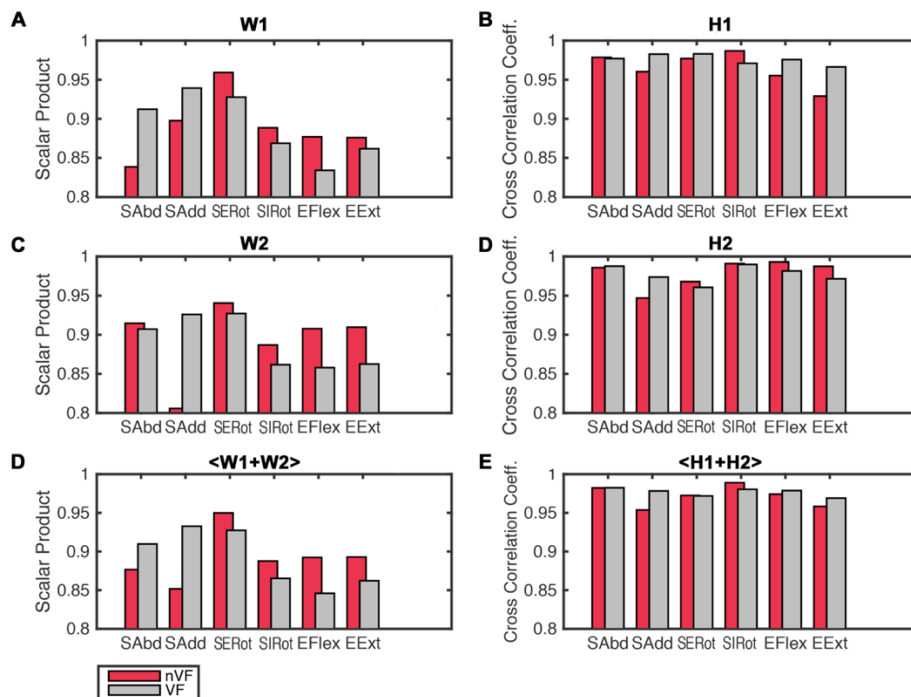


Figure 59 Within subject ILS measures during ELBOW EXTENSION. See the legend of Figure 54 for a complete and detailed description of the figure.



The inter-movement variability manifested by these figures is very likely to be due to differences in the inherent difficulty to execute each movement and to different personal skills to perform each movement. It has to be noted that when the questionnaire about the experiment was carried out, subjects affirmed having different training intensity, intermanual skills and experience with the movements analyzed (Table 18).



**Figure 60** Per movement ILS of A – Synergy 1, B – Activation coefficient 1, C – Synergy 2, D – Activation Coefficient 2, E – Average of ILS of synergies 1 and 2, F – Average of ILS of activation coefficients 1 and 2. Bars are the ILS averaged across the 6 subjects for each movement. Red bars represent the ILS found in absence of VF and grey bars represent the ILS found in presence of VF. \*  $p < 0.05$  for Wilcoxon Signed Rank test.



The ILS measures averaged across subjects can be found in **Figure 60**. Although previous results indicate that VF affects the ILS differently depending on movements and subjects, the effect of VF can be generalizable across movements. On the whole, VF tends to (1) increase ILS during shoulder abduction and adduction, (2) to decrease ILS during shoulder internal and external rotation, specially at synergy level, and (3) to decrease the ILS during elbow flexion and extension at synergy level, while increasing the ILS of activation coefficients.

We performed a set of Wilcoxon signed rank tests to compare the ILS found in presence and absence of VF for each movement. The tests revealed that the differences induced by VF at movement level did not reach significance (**Table 24**). This is probably due to the high inter-subject differences that may interfere with the statistical tests.

P-VALUES OF WILCOXON SIGNED RANK TEST PER MOVEMENT						
	SAbd	SAdd	SERot	SIRot	EFlex	EExt
W1	0.5625	0.5625	0.4375	0.5625	0.5625	1.0000
W2	1.0000	0.4375	0.4375	0.5625	0.5625	0.8438
<W1,W2>	0.5693	0.3013	0.1514	0.4238	0.3804	0.6772
H1	1.0000	0.3125	0.3125	0.5625	0.0938	0.0625
H2	0.3125	0.6875	0.5625	0.8438	1.0000	0.4375
<H1, H2>	0.5186	0.2036	0.2334	0.5693	0.3013	0.4238

Table 24 p-values of Wilcoxon rank test comparing the ILS measures obtained in absence and presence of VF for each movement. Significant results ( $p < 0.05$ ) are highlighted in orange.



#### 15.3.4 ILS: muscle synergies vs activation coefficients

The objective of this section is to study whether the ILS of the control structure differently affects muscle synergies and activation coefficients. Note that comparing the ILS of muscle synergies and activation coefficients in terms of scalar products and cross-correlation coefficients is not possible since they arise from different quantification strategies. Therefore, in order to solve this problem, we defined the interlimb difference (ILD) measure (see **14. Specific Procedures (II)**).

ILD measures evidence that right and left activation coefficients are more similar between each other than muscle synergies (**Table 25**), which may indicate that the muscle synergies are much more sensitive to handedness than activation coefficients. In other words, that muscle synergies account for the largest interlimb differences due to handedness.

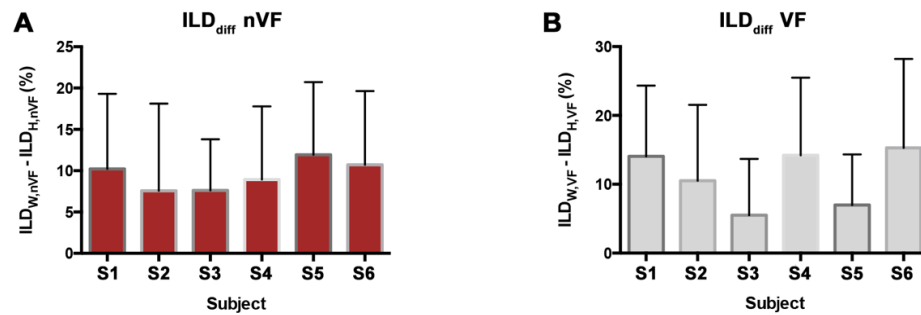
	ILD – nVF (%)		ILD – VF (%)	
	Muscle Synergies	Activation Coefficients	Muscle Synergies	Activation Coefficients
S1	22.990 ± 6.737	12.775 ± 5.744	24.979 ± 8.475	10.915 ± 4.820
S2	17.117 ± 10.506	9.537 ± 4.044	21.125 ± 14.023	10.602 ± 5.157
S3	17.550 ± 8.263	9.925 ± 3.926	15.895 ± 5.497	10.390 ± 5.842
S4	25.992 ± 14.416	16.061 ± 12.626	24.931 ± 10.655	10.724 ± 6.347
S5	21.701 ± 10.389	9.771 ± 6.511	17.834 ± 9.263	10.845 ± 7.052
S6	20.672 ± 7.649	9.949 ± 6.223	25.991 ± 13.275	10.713 ± 6.843

**Table 25** Per subject ILD values of muscle synergies and activation coefficients in absence of VF. Data are mean ± SD.

**Figure 61** graphically illustrates within-subject differences between the ILD of synergies and the ILD of activation coefficients averaged across the 6 movements for each subject. The bar plots confirm that the ILD is lower for activation coefficients than



for synergies in all cases, both in absence of VF (**Figure 61A**) and presence of VF (**Figure 61B**).



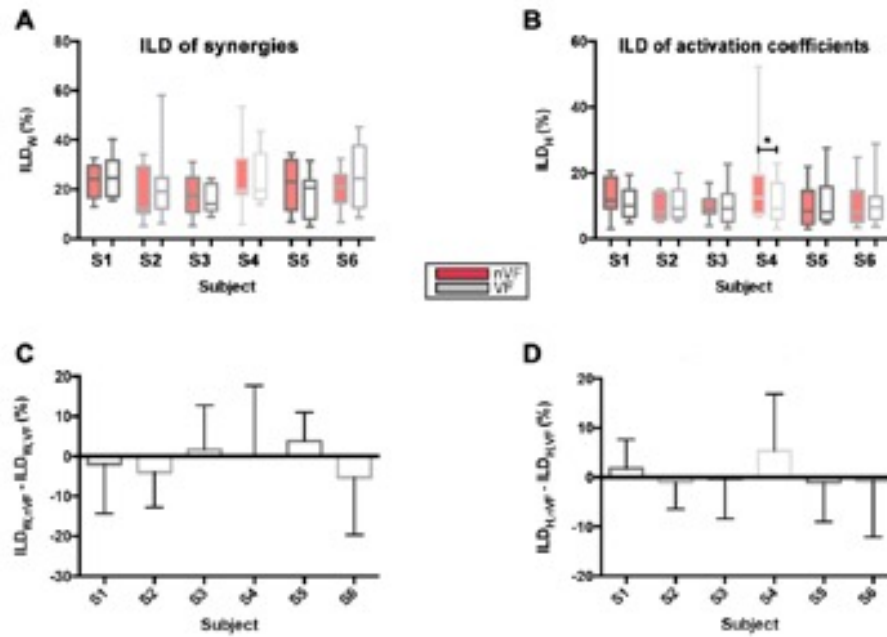
**Figure 61** Within-subject differences of ILD of synergies and activation coefficients A – In absence of VF and B – In presence of VF. ILD differences are calculated as  $ILD_W - ILD_H$  for each condition. Bars are mean  $\pm$  SD of ILD differences of all movements for each subject.

Wilcoxon signed rank tests were performed for each subject comparing the ILD differences between synergies and activation coefficient of each movement in absence and presence of VF (nVF vs VF). The outcome of the test revealed no statistical difference between the two conditions, suggesting that VF affects the magnitude of ILD similarly for synergies and activation coefficients ( $p_{S1} = 0.5186$ ,  $p_{S2} = 0.1514$ ,  $p_{S3} = 0.6221$ ,  $p_{S4} = 0.3013$ ,  $p_{S5} = 0.1099$ ,  $p_{S6} = 0.3013$ ).

**Figure 62** shows the average ILD of the control structure of each subject in presence and absence of VF. As it was already reported in the case of ILS, the effect of VF studied from the point of view of ILD also varies from subject to subject. Wilcoxon signed rank test revealed that differences between the ILD of the control structure in absence and presence of VF were only statistically significant in the case of the activation coefficients of subject S4, for which, VF significantly decreased the ILD. It is remarkable, that Wilcoxon signed rank test also proved statistically significant the increase of ILS found in the activation coefficients of S4 (**Figure 53B, E**). This coincides with the subject presenting the higher ILS change induced by VF (**Figure 62C, D**). The



absence of statistical significance in the rest of the subjects might be explained by the fact that for them the mean ILS change induced by VF is much lower.



**Figure 62** Interlimb differences of A – Synergies and B – Activation coefficients. Each box represents the ILD found across the 6 movements performed by a subject in a given condition. Boxes extend from quartile Q1 to Q3 and whiskers cover the 5<sup>th</sup> to 95<sup>th</sup> percentiles. The inner horizontal line indicates the median. ILD is expressed in percentage. Red boxes correspond to movements performed in absence of VF and grey boxes correspond to movements performed in presence of VF. C - Per subject subtraction of  $ILD_{N VF}$  and  $ILD_{VF}$  of muscle synergies and D – activation coefficients. Bars are the average subtraction of 6 movements  $\pm$  SD.



## 15.4 TEMPORAL EFFECTS OF VF ON ILS

This section is aimed at analyzing whether the impact of VF has a dynamic component on the control structure of the upper-limb. That is, whether the impact of VF changes throughout the time-course of the movement. According to the model used to characterize the control structure in this study, muscle synergies are time invariant constructs while activation coefficients represent time-varying constructs. Therefore, for obvious reasons, this section pays special attention to the time course of the activation coefficients.

### 15.4.1 *The effect of VF on the control structure*

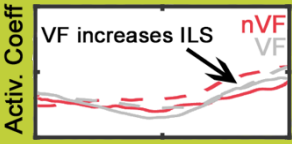

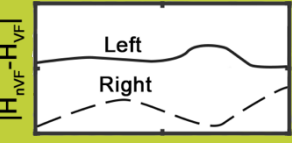
The following series of figures illustrate how VF affects the weights of the muscle synergies and the time-course of the activation coefficients for each subject and movement. Each figure shows the modulation of the control structure of a subject. Graphics should be conveniently interpreted applying the following guidelines:

- **Muscle synergies:** higher bars indicate higher ILD, thus, if VF induces an ILS increase, then grey bars should be shorter than red bars.
- **Activation coefficients:** thin curves are activation coefficients H1 and H2, thus, if VF induces an ILS increase, then the pair of grey curves should be closer than the pair of red curves in each plot. This effect might be easily detected by observing whether the thick grey line (which represents the difference between right and left activation coefficients in presence of VF) is closer to zero than the thick red line (which represents the difference between right and left activation coefficients in absence of VF).

This kind of plots also allow to qualitatively assess whether the approach of the right and left arm activation coefficients is caused either because the left arm activation coefficient shifts towards the right arm activation coefficient or vice versa. To assess this effect, we should compare the height of the black dashed (right arm) and solid (left arm) lines, which represent the difference between one arm's activation coefficients in



presence and absence of VF. One of the interesting aspects of these plots is that the effect of VF on the ILS can be dynamically assessed over the time. A schematic explanation of these plots can be found in **Table 26**.

GRAPHICAL EXAMPLE	OBSERVATION	MEANING
	If grey lines are CLOSER to each other than red lines*	VF increases ILS
	If grey lines are FARTHER to each other than red lines	VF decreases ILS
	When thick grey line passes BELOW thin red line*	VF is increasing ILS
	When thick grey line passes ABOVE thin red line	VF is decreasing ILS
	When dashed black line passes BELOW solid black line*	VF increases ILS affecting right arm activation coefficients
	When solid black line passes ABOVE dashed black line	VF increases ILS affecting left arm activation coefficients

**Table 26** Tips to interpret the meaning of the plots located in the second and third column of Figure 63 to Figure 68. The asterisk (\*) indicates the observation that describes the graphical example given in the first column of the table. The other observation always corresponds to the opposite situation.

#### 15.4.1.1 Representative analysis of subject 1

For the ease of interpretation and comprehension, the analysis of **subject 1** is fully developed. **Subject 1** shows substantial ILD in muscle synergies, specially during long movements (**Figure 63A,B,E,F**): both red and grey bars are overall taller. In contrast, during shorter movements the ILD is less pronounced (**Figure 63 C,D**). Due to the high inter-movement variability it is difficult to identify consistent patterns across movements and subjects, i.e., for some movements such as shoulder abduction (**Figure 63A**), the ILD is higher in presence of VF than in absence of VF: grey bars are taller; while



for other movements, such as elbow extension (**Figure 63F**), the ILD is lower in presence of VF than in absence of VF: grey bars are shorter than red bars.

Regarding activation coefficients, the course of thick lines demonstrates that **subject 1** tends to increase ILS due to VF. In most movements (**Figure 63A, B-H2, C, E-H1, F**), grey thick lines (VF) pass below red thick lines (nVF) indicating that VF reduces the differences between right and left arm activation coefficients. Interestingly, during shoulder external rotation (**Figure 63C**) there is a sort of adaptation process in which, the beneficial effect of VF is appreciated in the second half of the movement. We can visually track this phenomenon by checking whether grey solid and dashed lines get closer to each other than their counterpart red lines. The opposite behavior would indicate that VF decreases ILS.

From this type of plots, we can also investigate whether VF preferentially induces changes over the activation coefficients of right or left arm. To do so, we should examine solid and dashed black lines: the line that passes above indicates the main arm affected by VF. In the case of **subject 1**, VF mainly influences left arm activation coefficients in all movements (**Figure 63A-D**) except in elbow flexion and extension in which black dashed lines pass above solid lines. Again, it is interesting to notice the existence of different time shifts during the effect of VF. For instance, during shoulder internal rotation, the decrease of ILS induced by VF coincides with a deviation of the left H1 activation coefficient from the original  $H1_L$  found with nVF (**Figure 63D**).



#### 15.4.1.2 *General analysis of all subjects*

In general terms, unlike in the case of muscles synergies, the effect of VF in activation coefficients is more consistent across movements. VF tends to bring right and left arm activation coefficients closer. That is, VF tends to decrease ILD (or to increase ILS). This effect is observed in most subjects, for clear references see **Figure 63A**, **Figure 65E**, **Figure 66B** or **Figure 68A**: thick grey lines which represent ILD in presence of VF pass lower than thick red lines representing ILD in absence of VF along the 100 time-points. However, it has to be highlighted the existence of a mixed effect along time. That is, in most cases, VF increases ILS above the ILS found in absence of VF during a certain period of time but not during the full execution of the movement. Indeed, during short time-lapses the ILS of VF drops below the ILS found in absence of VF. See **Figure 63D**, **Figure 64F** or **Figure 65F** for illustrative references.

On the other hand, solid black lines pass substantially higher than dashed black lines along time indicating that VF is taking its effect on left arm motor control. See **Figure 65B**, **Figure 67C** and **D** or **Figure 68D** for clear references. Note that in these cases the curve-approximation observed in presence of VF occurs because the left arm activation coefficient shifts toward the right arm activation coefficient.

The opposite effect can be also observed in some cases (**Figure 64D-H2**, **Figure 68B**): dashed black lines pass above solid black lines indicating that in this cases VF preferentially affects the right arm motor control. However, in this case, VF decreases ILS since thick grey lines which represent ILD in presence of VF pass above thick red lines representing ILD in absence of VF along the 100 time-points. Also, during shoulder adduction of subject 1 (**Figure 63B**) right activation coefficients are more dissimilar than left activation coefficients in absence and presence of VF (i.e. dashed lines pass above solid lines) indicating that VF acts over the right arm activation coefficients to increase

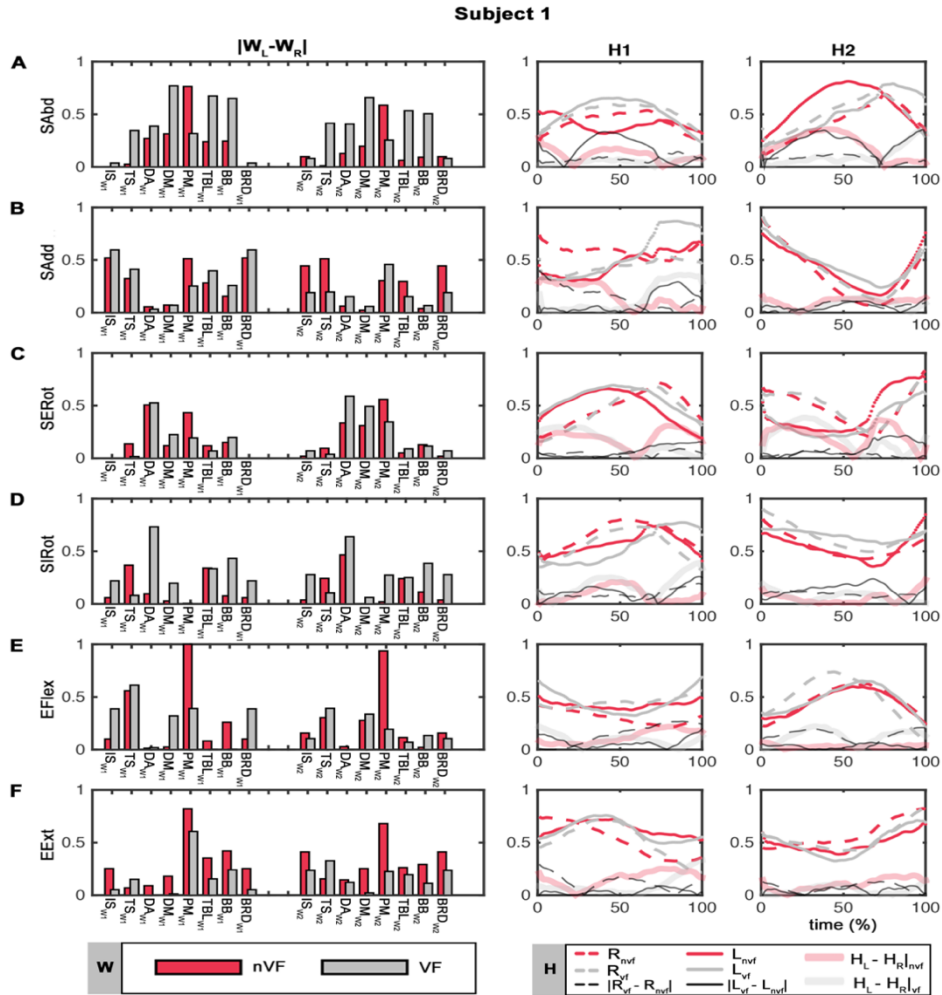


ILS. A similar behavior can be observed during shoulder abduction of subject 5 (**Figure 67A**).

In conclusion, in general the control structure of the left arm is more prone to be modulated by VF than the control structure of the right arm at the level of activation coefficients. Overall, solid black lines (left arm) pass above dashed black lines (right arm) indicating that the differences between the activation coefficients in presence and absence of VF are more accused in the left arm. However, as demonstrated, several exceptions may occur.

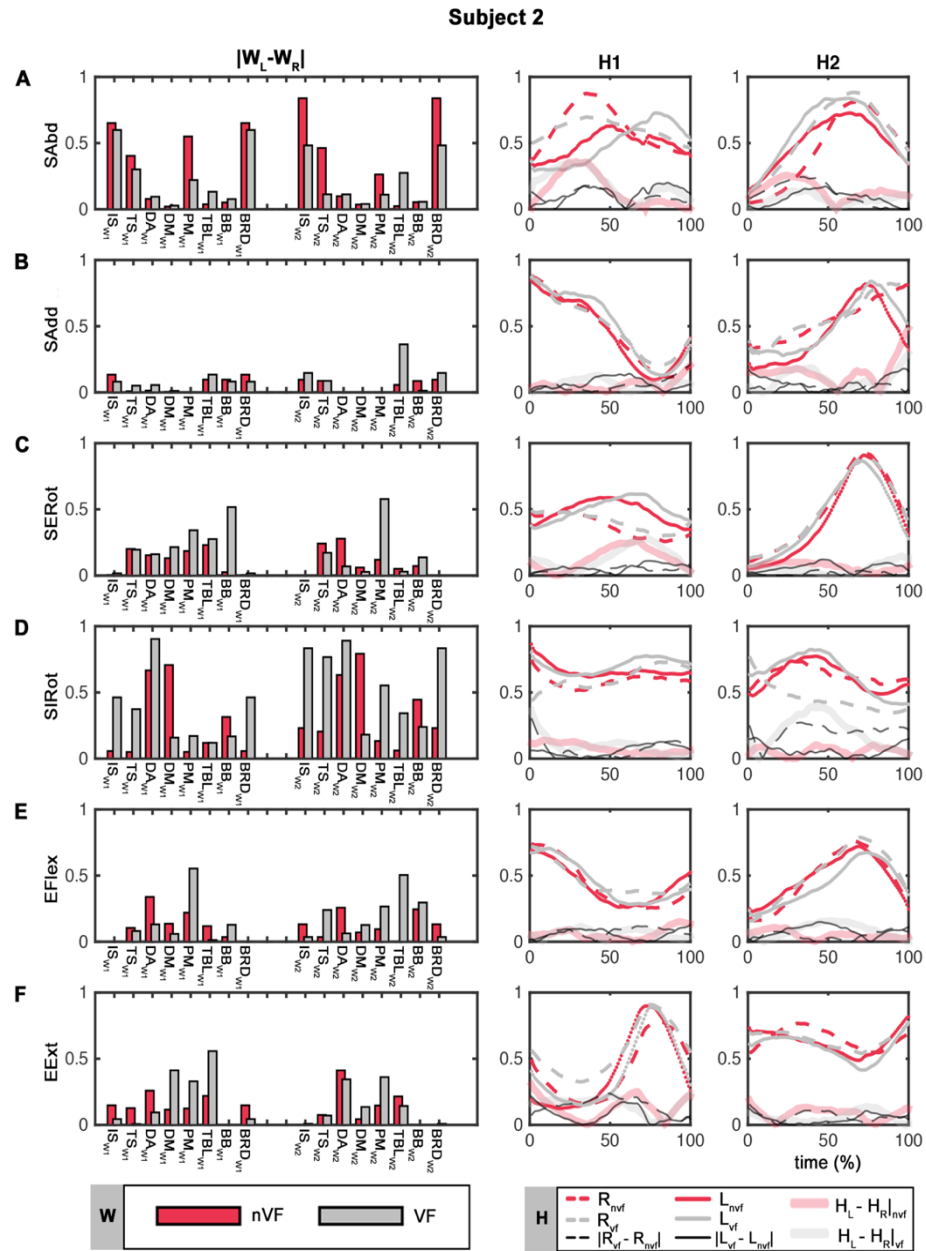
In any case, from these graphics we can conclude that VF modulates the control structure in a dynamic way. Apparently, VF does not generate a new control structure. Instead, VF tends to bring closer the right and left activation coefficients maintaining the basic shape of the activation coefficients found in absence of VF. Thus, we should probably talk about a tuning process driven by VF instead of a modification process. In addition, it seems that the mechanisms by which VF orchestrates the tuning of the control structure is by modulating the activation coefficient of the left arm. That is, the effect of VF is mainly reflected on the non-dominant side. Finally, we must emphasize that in some movements the described effects may be transient and combine at different time portions of the same execution.





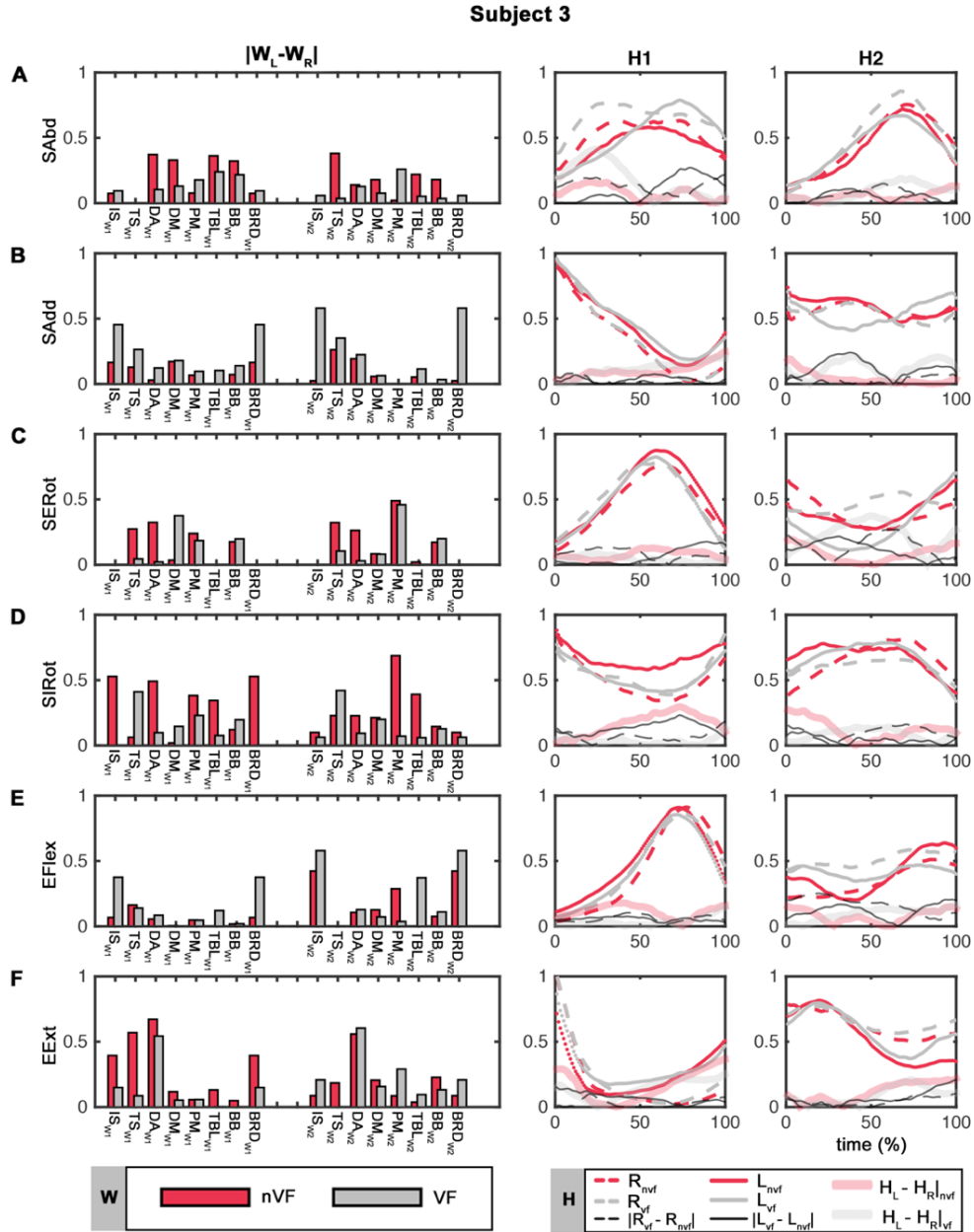
**Figure 63 VF-driven modulation of the control structure of SUBJECT 1** during A - Shoulder Abduction B - Shoulder Adduction C - Shoulder External Rotation D - Shoulder Internal Rotation E - Elbow Flexion F - Elbow Extension. Bar plots indicate the absolute interlimb weight differences calculated as  $|W_L - W_R|$  for each muscle in absence (red bars) and presence (grey bars) of VF. The adjacent curve plots show the time-course of the activation coefficients H1 and H2 respectively. Dashed lines are right activation coefficients, and solid lines are left activation coefficients in absence (red lines) and presence (grey lines) of VF. Thick red and grey lines represent the absolute interlimb difference of activation coefficients calculated as  $|H_L - H_R|$  in absence and presence of VF respectively. Black lines indicate within-limb differences in absence and presence of VF of right arm (dashed lines) and left (solid lines) arm activation coefficients.





**Figure 64** VF-driven modulation of the control structure of **SUBJECT 2**. See the legend of **Figure 63** for a complete and detailed description of the figure.





**Figure 65 VF-driven modulation of the control structure of SUBJECT 3.** See the legend of Figure 63 for a complete and detailed description of the figure



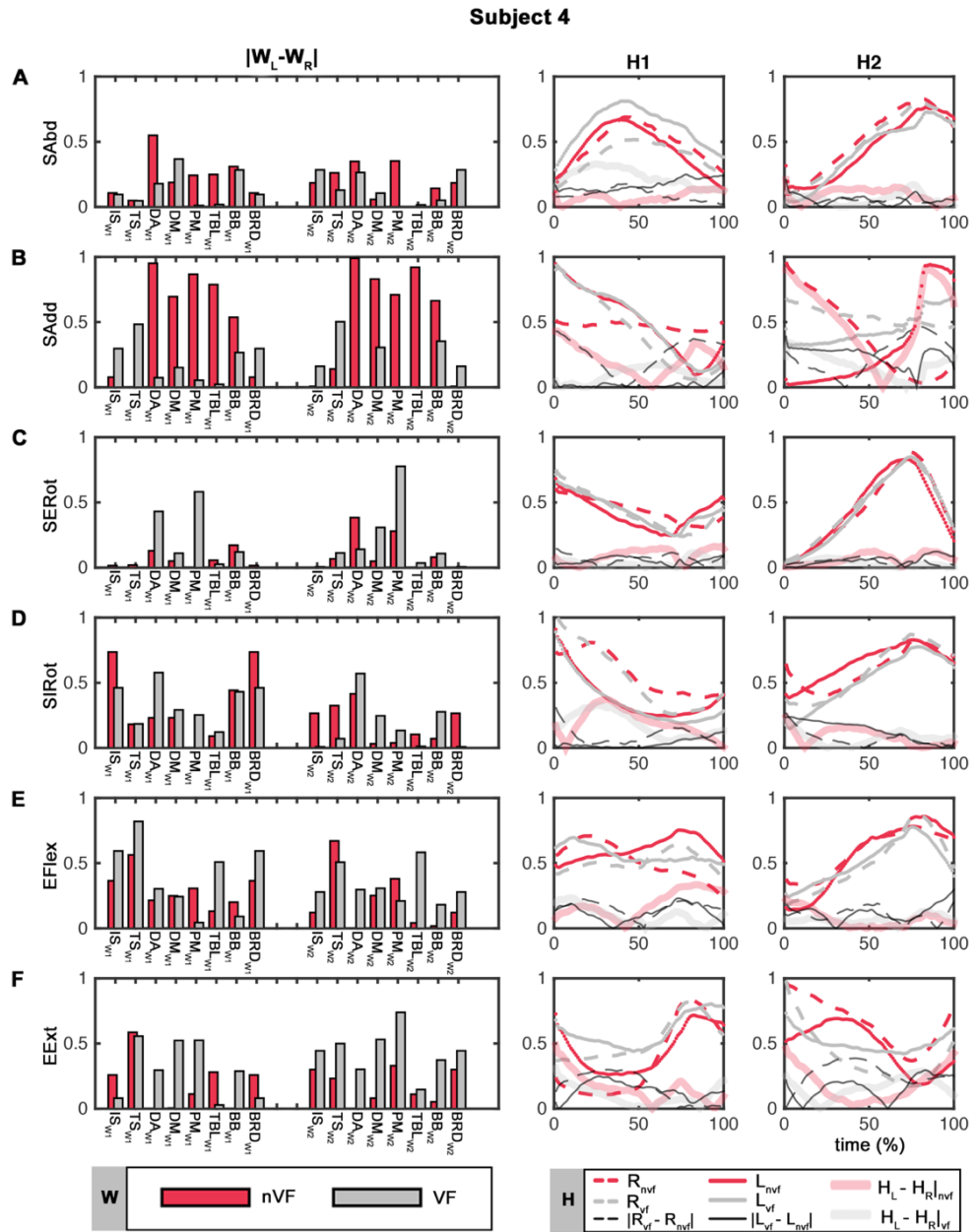


Figure 66 VF-driven modulation of the control structure of SUBJECT 4. See the legend of Figure 63 for a complete and detailed description of the figure.



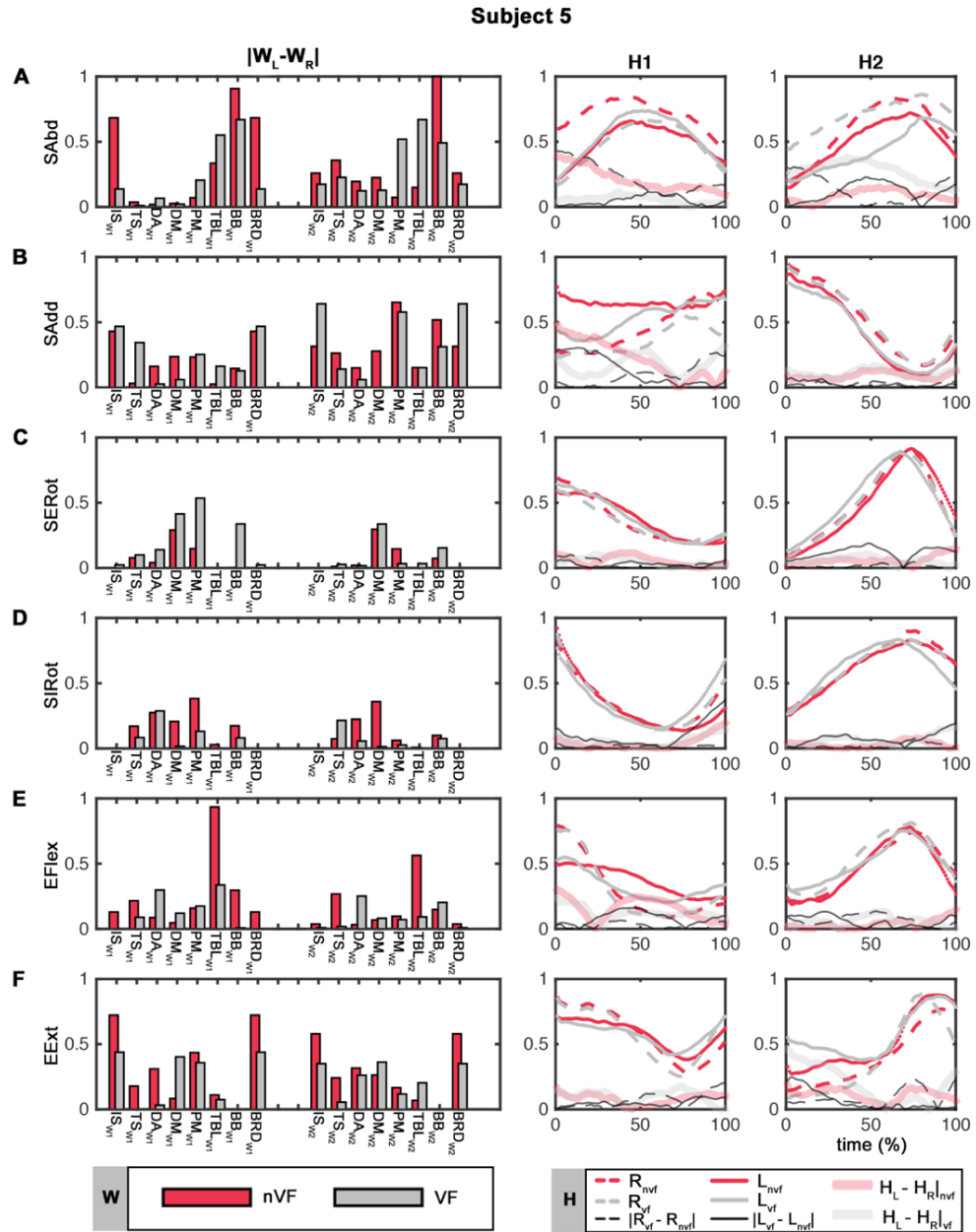


Figure 67 VF-driven modulation of the control structure of SUBJECT 5. See the legend of Figure 63 for a complete and detailed description of the figure.



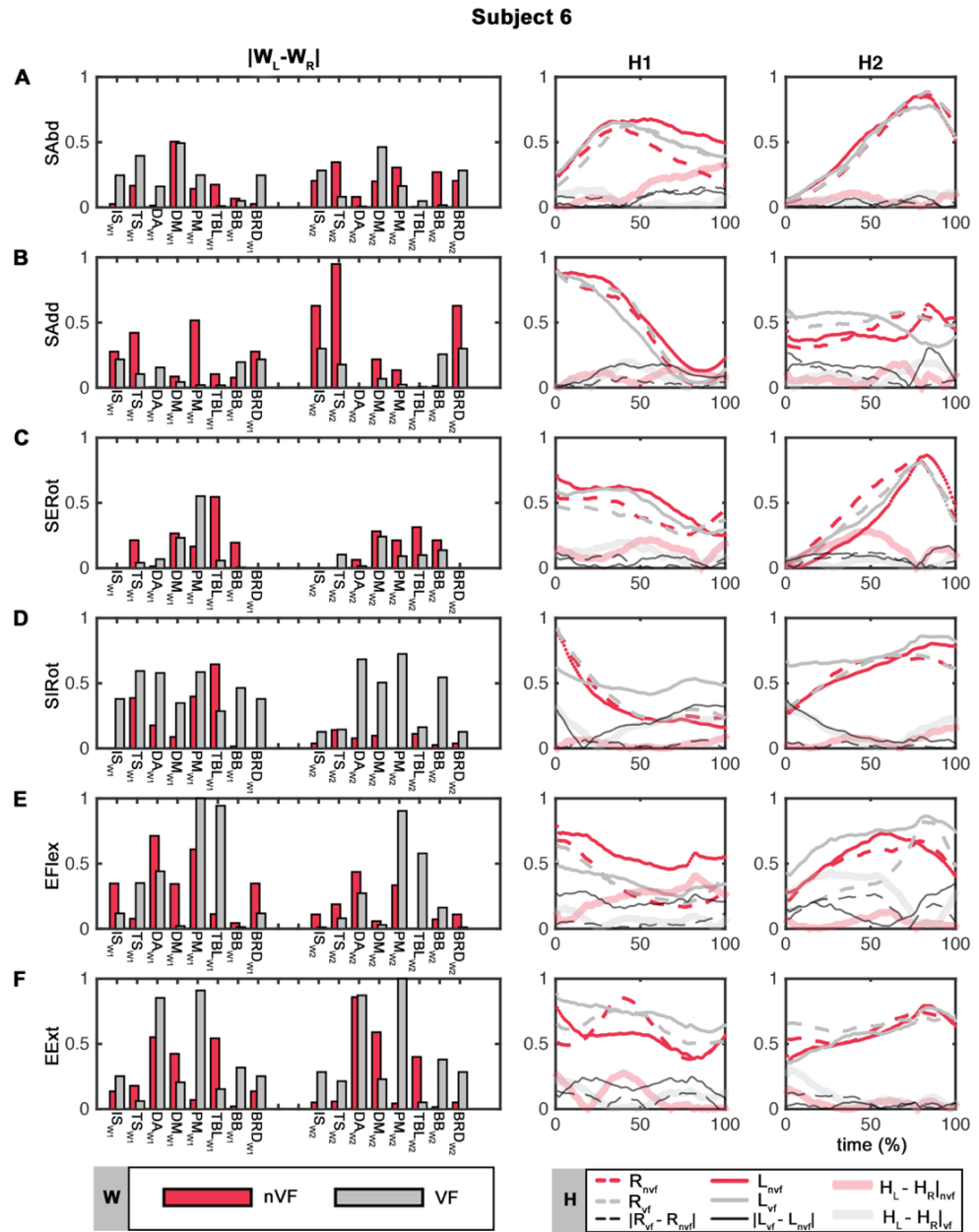


Figure 68 VF-driven modulation of the control structure of SUBJECT 6. See the legend of Figure 63 or a complete and detailed description of the figure.



#### 15.4.2 *Quantifying the effect of VF on the activation coefficients*

**Figure 63** to **Figure 68** reveal the existence of mixed VF-induced patterns along movement execution. That is, during the course of some movements VF alternatively increases and then decreases ILS (with respect to the ILS found in absence of VF) and alternatively affects the control structure of right and then left arm. Thus, we quantified the percent of the movement-execution in which VF increased/decreased ILS or VF affected the activation coefficients of rather right or left arm for each subject and movement.

**Table 27** describes the duration of the effect of VF in each subject and movement expressed as the time-percentage of the full movement execution. As suggested by the visual inspection of figures **Figure 63** to **Figure 68**, this analysis confirms that VF preferentially acts over the left activation coefficient. In average, VF modulates the left H1 activation coefficients during the  $47.06 \pm 29.29\%$  of the movement execution time against the  $39.39 \pm 29.65\%$  of the time modulated in the right activation coefficients. In the case of H2, VF modulates the left H2 activation coefficients during the  $48.44 \pm 26.92\%$  of the movement execution time against the  $35.72 \pm 26.86\%$  of the time modulated in the right activation coefficients. That is, VF acts over the left activation coefficients between the 30% and 35% more frequently than over the right activation coefficients. On the other hand, VF increases ILS during longer time in H1 than in H2. Wilcoxon signed-rank tests revealed no significant differences.



Tolerance 10%		LATERALITY				EFFECT ON ILS			
		L	R	L	R	▲ ILS	▼ ILS	▲ ILS	▼ ILS
S	M	H1	H1	H2	H2	H1	H1	H2	H2
S1	SAbd	66%	24%	91%	0%	66%	15%	71%	27%
	SAdd	32%	64%	40%	47%	53%	47%	73%	17%
	SERot	41%	29%	42%	13%	41%	34%	34%	44%
	SIRot	53%	25%	61%	28%	0%	67%	18%	56%
	EFlex	21%	78%	12%	86%	57%	38%	0%	85%
	EExt	13%	81%	27%	51%	73%	22%	54%	12%
S2	SAbd	53%	0%	39%	51%	0%	54%	94%	0%
	SAdd	56%	24%	71%	11%	33%	52%	67%	0%
	SERot	67%	17%	87%	0%	36%	51%	65%	29%
	SIRot	43%	41%	0%	88%	36%	55%	0%	66%
	EFlex	23%	52%	49%	31%	21%	45%	25%	68%
	EExt	0%	81%	25%	43%	23%	46%	65%	22%
S3	SAbd	36%	55%	37%	33%	0%	68%	22%	47%
	SAdd	57%	21%	94%	0%	20%	50%	18%	81%
	SERot	45%	54%	30%	45%	60%	26%	11%	66%
	SIRot	79%	0%	16%	69%	85%	0%	58%	39%
	EFlex	48%	45%	23%	76%	93%	0%	21%	54%
	EExt	74%	26%	57%	0%	52%	39%	59%	0%
S4	SAbd	74%	16%	63%	27%	0%	80%	51%	27%
	SAdd	0%	98%	51%	47%	68%	27%	89%	0%
	SERot	39%	52%	37%	47%	70%	18%	64%	34%
	SIRot	11%	85%	62%	0%	61%	29%	42%	53%
	EFlex	16%	46%	36%	36%	54%	26%	27%	68%
	EExt	36%	56%	13%	67%	87%	11%	43%	53%
S5	SAbd	0%	81%	43%	54%	100%	0%	0%	100%
	SAdd	42%	56%	41%	40%	41%	55%	0%	69%
	SERot	42%	42%	99%	0%	47%	20%	17%	69%
	SIRot	88%	0%	86%	12%	0%	74%	32%	66%
	EFlex	81%	0%	44%	48%	51%	35%	15%	68%
	EExt	33%	54%	26%	67%	14%	64%	32%	57%
S6	SAbd	0%	79%	50%	27%	62%	37%	53%	24%
	SAdd	92%	0%	87%	0%	60%	28%	24%	63%
	SERot	44%	36%	59%	21%	38%	34%	96%	0%
	SIRot	93%	0%	100%	0%	0%	91%	28%	70%
	EFlex	100%	0%	31%	50%	87%	12%	0%	92%
	EExt	96%	0%	15%	71%	35%	59%	0%	72%
MEAN (t %)		47.06	39.39	48.44	35.72	45.11	39.14	38.00	47.17
STD (time %)		29.29	29.65	26.92	26.86	29.03	22.74	28.44	28.39

Table 27 Percent duration of the effect of VF with respect to the movement execution time. S, subject; M, movement. Columns 1 to 4 express the percent time during which VF acts on either right (R) or left arm (L) of H1 and H2 activation coefficients. Columns 5 to 8 express the percent time during



which VF increases ( $\Delta$ ) or decreases ( $\nabla$ ) the ILS of H1 and H2 activation coefficients. The last two rows indicate the mean time (%) and corresponding SD during which VF exerts the described effect in each column.

Due to the high intersubject and intermovement variability of the effect of the VF demonstrated in the previous sections of this study, we grouped the results shown in **Table 27** by subjects (**Table 28**) and movements (**Table 29**). **Table 28** evidences that VF affects each side differently depending on the subjects, although the affection of the left arm seems to constitute the most generalized trend. In particular, VF preferentially acts on the left control structure of H2 in all subjects and of H1 in subject 2, subject 3, subject 5 and subject 6. The effect of VF on the ILS is less generalizable because different results are found depending the activation coefficients analyzed.

Tolerance 10%		VF acts on				Effect of VF on ILS			
		L	R	L	R	▲ ILS	▼ ILS	▲ ILS	▼ ILS
S	M	H1	H1	H2	H2	H1	H1	H2	H2
S1	All	37.67%	50.17%	45.50%	37.50%	48.33%	37.17%	41.67%	40.17%
S2	All	40.33%	35.83%	45.17%	37.33%	24.83%	50.50%	52.67%	30.83%
S3	All	56.50%	33.50%	42.83%	37.17%	51.67%	30.50%	31.50%	47.83%
S4	All	29.33%	58.83%	43.67%	37.33%	56.67%	31.83%	52.67%	39.17%
S5	All	47.67%	38.83%	56.50%	36.83%	42.17%	41.33%	16.00%	71.50%
S6	All	70.83%	19.17%	57.00%	28.17%	47.00%	43.50%	33.50%	53.50%

**Table 28 Mean duration-percentages of the effects of VF averaged by subjects.** S, subject; M, movement. Columns 1 to 4 express the percent time during which VF acts on either right (R) or left arm (L) of H1 and H2 activation coefficients. Columns 5 to 8 express the percent time during which VF increases ( $\Delta$ ) or decreases ( $\nabla$ ) the ILS of H1 and H2 activation coefficients. The last two rows indicate the mean time (%) and corresponding SD during which VF exerts the described effect in each column.



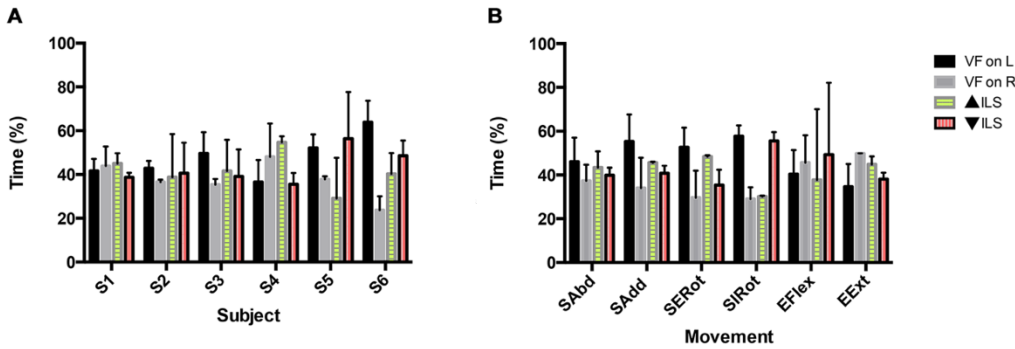
The side preferences of VF actuation also vary from movement to movement (**Table 29**), but in this case, results are more variable from H1 to H2. This variability presumably explains why Wilcoxon signed-rank tests revealed no significant differences.

Tolerance 10%		VF acts on				Effect of VF on ILS			
		L	R	L	R	▲ ILS	▼ ILS	▲ ILS	▼ ILS
M	S	H1	H1	H2	H2	H1	H1	H2	H2
SAbd	A	38.17%	42.50%	53.83%	32.00%	38.00%	42.33%	48.50%	37.50%
SAdd	A	46.50%	43.83%	64.00%	24.17%	45.83%	43.17%	45.17%	38.33%
SERot	A	46.33%	38.33%	59.00%	21.00%	48.67%	30.50%	47.83%	40.33%
SIRot	A	61.17%	25.17%	54.17%	32.83%	30.33%	52.67%	29.67%	58.33%
EFlex	A	48.17%	36.83%	32.50%	54.50%	60.50%	26.00%	14.67%	72.50%
EExt	A	42.00%	49.67%	27.17%	49.83%	47.33%	40.17%	42.17%	36.00%

**Table 29** Mean duration-percentages of the effect of VF averaged by movements. M, movement; S, subject; A, All. Columns 1 to 4 express the percent time during which VF acts on either right (R) or left arm (L) of H1 and H2 activation coefficients. Columns 5 to 8 express the percent time during which VF increases (▲) or decreases (▼) the ILS of H1 and H2 activation coefficients. Last two rows indicate the mean time (%) and corresponding SD during which VF exerts the described effect in each column.

The results of **Table 28** and **Table 29** are visually summarized in **Figure 69**. **Figure 69** gains consistency over the conclusions drawn from the aforementioned results by considering the control structure as a whole instead of analyzing H1 and H2 separately. At subject level, **Figure 69A** just reinforces the observations explained in the previous paragraphs. However, it is interesting to highlight that at movement level, **Figure 69B** reveals that VF tends to behave differently depending on the joint actuated in the movement: it primarily modulates left arm activation coefficients in shoulder movements, while acting over right arm during elbow movements.





**Figure 69** Mean duration-percentages of the effects of VF averaged by **A** – subjects and **B** - movements. Bars are mean time percentage +/- SD (%). Means are calculated by averaging the values corresponding to the two synergies of the 6 movements of each subject (A) and the two synergies of the subjects of each movement (B). Black bars - mean percent time during which VF acts on the left arm (L); Grey bars - mean percent time during which VF acts on the right arm (R); Green bars – mean percent time during which VF increases ( $\triangle$ ); Red bars – mean percent time during which VF decreases ( $\nabla$ ) ILS.



## 15.6 INTERMANUAL TRANSFER (IMT) IN THE ACTIVATION COEFFICIENTS

The results shown in the subsection “15.4.2 Quantifying the effect of VF on the activation coefficients” indicate that VF tends to preferentially act on the control structure of the non-dominant arm by modulating the left activation coefficients. This trend is found in most subjects and it is specially strong in shoulder movements (**Figure 71**). In light of this findings, we hypothesized that VF may transfer the motor strategy of the dominant arm to the non-dominant arm as a mechanism to increase ILS.

Consequently, in this section we have extended this work with the hypothesis that VF may improve motor control by transferring the superior motor programs stored in the dominant hemisphere towards the nondominant hemisphere. Evidences for intermanual transfer (IMT) of skills have extensively been reported in various fields<sup>221,222</sup>, but to the best of our knowledge, the role of VF as a facilitator of IMT has not been addressed yet.

Here we consider two possible scenarios for VF to induce IMT of motor control. On the one hand, VF may transfer to the nondominant arm the original activation patterns found in the dominant arm, that is, the control structure extracted in absence on VF. On the other hand, VF may also modify the control structure of the dominant arm (not only the nondominant arm) and transfer the VF-modulated dominant control instead of the original dominant control. In this section we study these two forms of IMT and we quantify their occurrence during the execution of standard stroke rehabilitation exercises of elbow and shoulder.

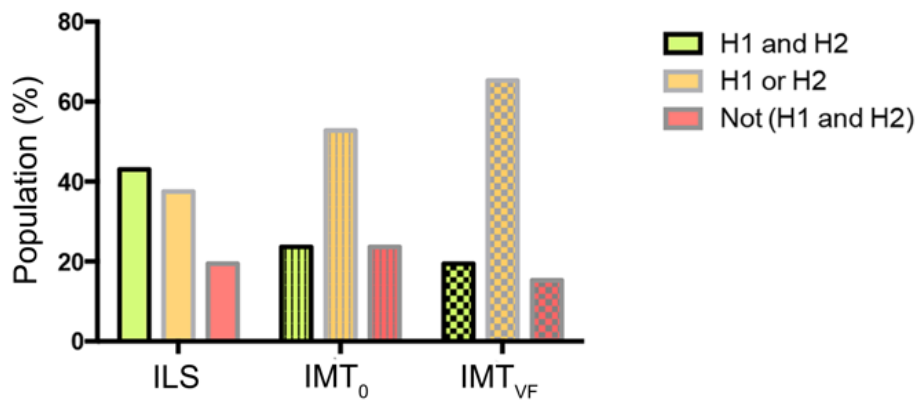
### 15.6.1 *Frequency of occurrence of IMT*

In the first place, we analyzed the frequency at which the two types of IMT considered here occur in the population, and we compared it with the frequency at which VF-induced ILS (**Figure 70**). Frequency was defined as the percentage of subjects



that showed VF-induced ILS or IMT during the movements under analysis. We quantified whether these phenomena occurred:

- Both, in H1 and H2
- Just in H1 or H2
- Neither in H1 nor in H2



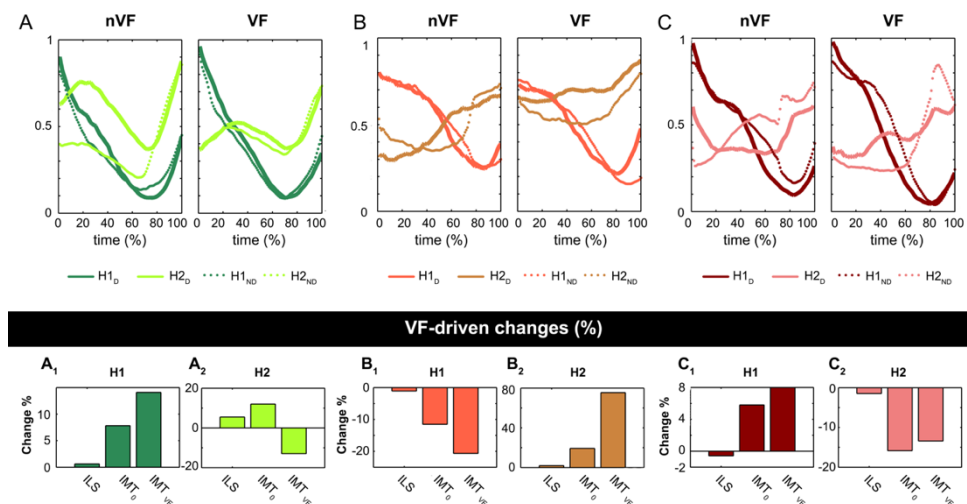
**Figure 70.** Frequency in population of VF-induced modulation types of the activation coefficients. Bars indicate percentage of cases in which VF increased ILS, IMT<sub>0</sub> or IMT<sub>VF</sub>. Green bars indicate an increase in the two activation coefficients, orange bars indicate an increase in only one activation coefficient and red bars indicate a decrease in both activation coefficients

**Figure 70** indicates that VF most frequently increases ILS and induces IMT of the dominant activation pattern across subjects and movements. Regarding ILS, VF increases the ILS of at least one activation coefficient in 81.95% of the cases analyzed. That is the sum of the cases in which VF increased the ILS of both activation coefficients (41.67% of the cases) and at least one activation coefficient (40.28%). Regarding IMT, VF produces IMT<sub>0</sub> and IMT<sub>VF</sub> of at least one of the dominant activation coefficients in 75.00% and 83.33% of the cases respectively. Unlike ILS, IMT phenomena were less



frequently found in both activation coefficients. Instead, IMT normally occurred in either one or other activation coefficient.

A more exhaustive analysis revealed that the scope of this phenomenon. In 41.67% of the cases VF increases the ILS in the two activation coefficients, and in 40.25% of the cases in just one activation coefficient. VF produces  $IMT_0$  (or  $IMT_{VF}$ ) in both synergies in 29.17% (20.83%) of the cases and in only one synergy in 45.83% (62.5%) of the cases. Only in 18.05% of the cases VF does not increase the ILS in any activation coefficient. In the same way, only in 16.67% of the cases VF does not produce IMT in any activation coefficient.



**Figure 71. Types of modulation induced by VF in the activation-coefficients** – representative examples. A – Increase of ILS in both synergies. B - Increase of ILS in only one synergy. C - Decrease of ILS in both synergies. Columns 1 and 2 show the activation coefficients in absence and presence of VF respectively. Solid and dotted lines represent the activation coefficients of the dominant (D) and nondominant (ND) arm respectively.  $X_1$  and  $X_2$  (with  $X \in \{A, B, C\}$ ) indicate the magnitude of increase (%) of ILS,  $IMT_0$  and  $IMT_{VF}$  induced by VF in H1 and H2 respectively.

Given the heterogeneous scenario found from subject to subject and movement to movement, we individually analyzed each case and identified 3 common behaviors that generalized across subjects. **Figure 71** illustrates these 3 behaviors found during the 3 types of VF-modulation: ILS,  $IMT_0$  and  $IMT_{VF}$ . We observed that when VF increased



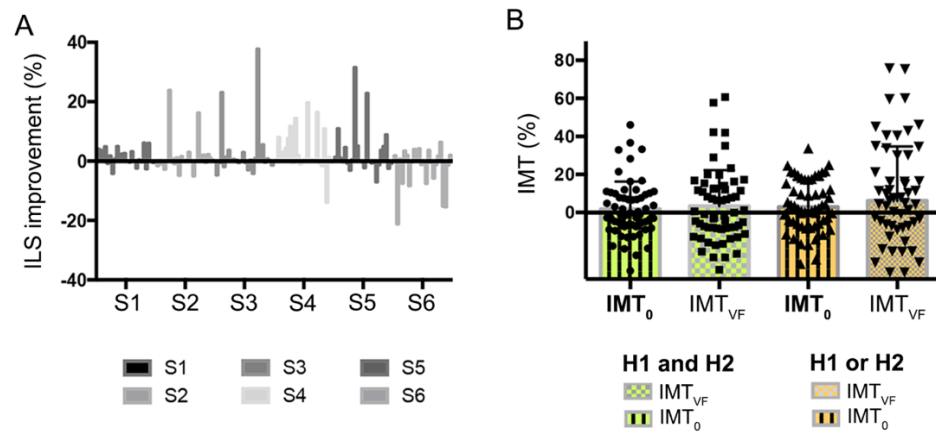
ILS, the shape of the nondominant activation coefficient tended to take the form of the dominant activation coefficient (**Figure 71A** and **B** in **H2**). Certainly, these observations were numerically confirmed by an increase in either the  $IMT_0$  or the  $IMT_{VF}$  (**Figure 71A<sub>1</sub>**); or even in both values (**Figure 71A<sub>2</sub>** and **B<sub>2</sub>**).

Interestingly, VF decreased ILS mainly due to two reasons. First, because the ILS found in absence of VF was so high that there was little scope for improving such similarity and any deviation from the original curve was numerically reflected as a decrease in the ILS (**Figure 71B-H1**: Note that in this case despite the decrease in the ILS, the fundamental shape of the two curves remains very similar). Second, because VF modulated the curve of the nondominant arm producing a totally different shape with respect to the original shape (**Figure 71C – H2**. Note that in this case the curve of the dominant arm remains almost the same).

### 15.6.2 VF-driven effects: ILS improvement and IMT magnitude

**Figure 72A** shows the magnitude of ILS change induced by VF in the activation coefficients of each subject's movements. As we can see, the predominant effect of VF is to increase ILS. In average, VF increases ILS by  $4.64 \pm 7.21\%$ . Note that this increase is quite substantial taking into account that the mean ILS of these subjects in absence of VF ranged between 0.95 and 0.98. Notably, in subjects with movements exhibiting lower baseline ILS, the improvement induced by VF can reach as high as 23.85%. 2-way ANOVA tests showed a significant effect of subjects ( $F_{5,72} = 3.14$ ;  $p < .05$ ) and movement types ( $F_{11,72} = 2.6$  ;  $p < .01$ ) in the magnitude of ILS change. The interaction between subjects and movement types was also significant ( $F_{55,72} = 3.14$ ;  $p < .01$ ).





**Figure 72 Magnitude of VF induced changes** A –ILS changes (%) in individual subjects. Each bar represents the ILS change induced by VF in the activation coefficient of one movement. B –Increase of IMT (%) in the cases in which VF enhances ILS in H1 and H2 (green bars) and in H1 or H2 (orange bars). Bars are mean IMT  $\pm$  SD. Data-points indicate the VF-induced increase of IMT (%) in individual cases (subjects' movements).

**Figure 72B** shows the average IMT induced by VF in subjects for which VF increased the ILS. VF induced  $IMT_0$  in 46.66% of the cases and  $IMT_{VF}$  in 48.3% of the cases for which ILS increased in H1 and H2. Likewise, VF induced  $IMT_0$  in 58.62% of the cases and  $IMT_{VF}$  in 56.89% of the cases for which ILS increased in at least one activation coefficient. Although the average IMT was moderate ( $13.48 \pm 11.68\%$ ;  $18.42 \pm 15.40\%$ ;  $12.10 \pm 8.95\%$ ;  $25.13 \pm 21.41\%$  respectively), it varied substantially from subject to subject and could be up to 75% in certain subjects. However, 2-way ANOVA indicated no significant effects of subjects or movement in the magnitude of IMT ( $p > .05$ ). Our results indicate that ILS increases are not always related to IMT, suggesting the existence of additional VF-induced mechanisms complementary to IMT able to increase ILS.



## 15.7 CAN SUBJECTS LEARN HOW TO MODULATE ILS?

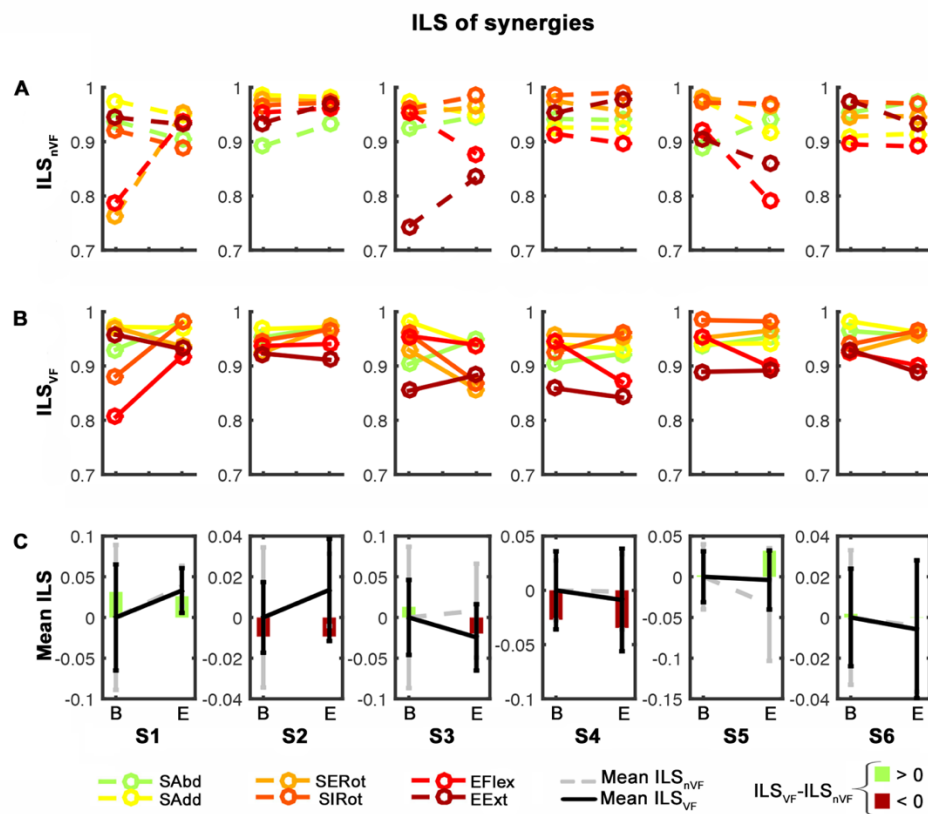
This section aims at studying whether subjects are able to learn how to increase ILS across the 30 repetitions performed during the execution of a movement. To this end, we compared the control structure of each movement at the beginning of the sequence of repetitions and at the end of that sequence.

In order to study the potential learning effects that repeating a given exercise may have on the motor control, for each movement we compared the ILS found at the first 10 repetitions (B stage) with the last 10 repetitions (E stage) of the movement execution. Individual results for the muscle synergies and activation coefficients of each subjects are shown in **Figure 73** and **Figure 74** respectively.

In general, the differences found in the control structure between the 2 stages are minimal in most movements. However, some subjects show substantial differences in the ILS of the 2 stages, indicating that the motor control of the upper limb has the ability to be tuned across repetitions. That is the case of subject 1 during elbow flexion and shoulder internal rotation, or subject 3 during elbow extension. For the rest of the subjects, we believe that given the simplicity of the exercises, they did not feel much motivation to improve the performance, because they already executed the movement quite well even in absence of training. Thus, it is very likely that the changes in the ILS, specially when it drops, are due to the laziness or tedium that increased with repetitions. Another hypothesis is that there is a maximal ILS limit that a subject can achieve, from which improving the ILS may require more sophisticated techniques than simple repetitions (or even a limit that cannot be simply surpassed). Note also that in all cases in which the ILS stayed constant or dropped, the initial ILS (stage E) was very high (above 0.9) leaving little scope for improving it.

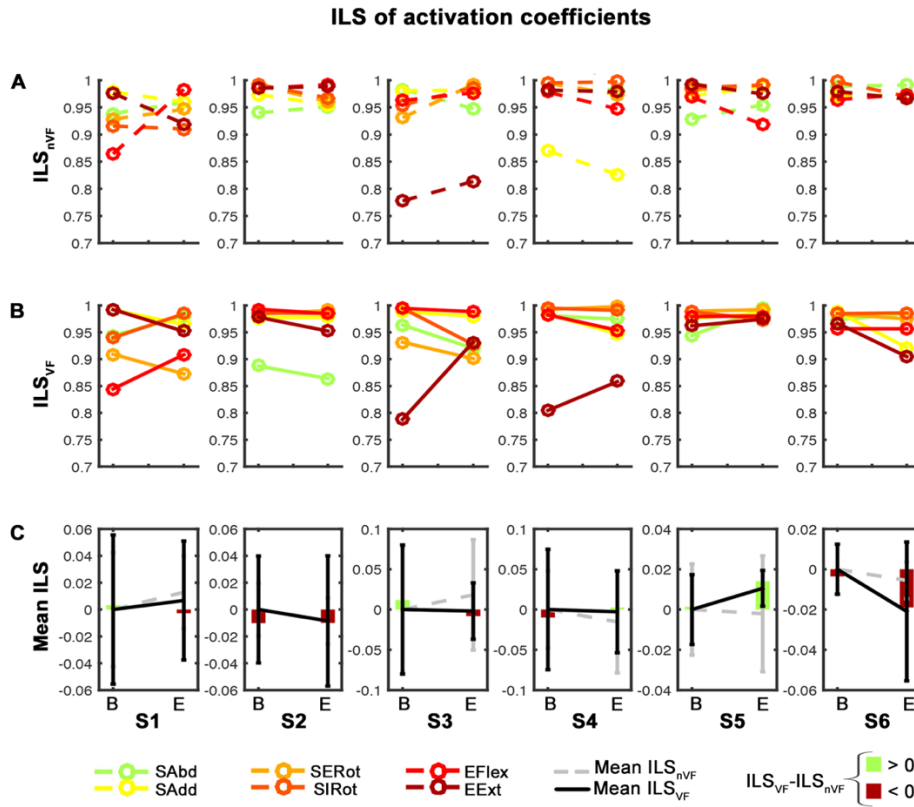


In any case, the interesting point of these results is that subjects really have the capacity to tune their control structure using methods as simple as repeating the execution of a movement. This finding suggests that the tuning of control structure may play an important role in the motor learning process, which is a key aspect in any motor rehabilitation program.



**Figure 73** Inter-repetition learning effect on the ILS of muscle synergies. A – Evolution of the ILS of synergies across repetitions in absence of VF. B – Evolution of the ILS of synergies across repetitions in presence of VF. C – Mean ILS found in presence and absence of VF at the beginning (B) and at the end stage (E). Data-points are mean ILS averaged across the 6 movements for each subject and stage  $\pm$  SD. Bars indicate differences between conditions: bars are green if  $ILS_{VF} > ILS_{nVF}$  and vice versa. The horizontal axis in all graphics represents the stages across repetitions: B – beginning E – end.





**Figure 74 Inter-repetition learning effect on the ILS of activation coefficients.** A – Evolution of the ILS of activation coefficients across repetitions in absence of VF. B – Evolution of the ILS of activation coefficients across repetitions in presence of VF. C – Mean ILS found in presence and absence of VF at the beginning (B) and at the end stage (E). Data-points are mean ILS averaged across the 6 movements for each subject and stage  $\pm$  SD. Bars indicate differences between conditions: bars are green if  $ILS_{VF} > ILS_{nVF}$  and vice versa. The horizontal axis in all graphics represents the stages across repetitions: B – beginning E – end.

The study of these figures also allows us to investigate the potential effect that the use of VF may have on the inter-repetition learning process. Coherent with what we found in previous analyses, the effect of VF varied from subject to subject and movement to movement. In subjects 1 and 5, the use of VF substantially improved the



ILS across repetitions with respect to the improvement found in absence of VF (**Figure 73C** and **Figure 74C**). In subject 2 and 3, although the ILS increased with repetitions, the increase found in absence of VF was more pronounced than in presence of VF. In subject 4, we found no substantial differences between repetitions and in subject 6 the ILS decreased in both conditions across repetitions. Taking everything together, it seems evident that the effect of VF is not homogeneous in all subjects. These results come in accordance with the heterogeneous answers found in the questionnaire filled by subjects after performing the experiment. According to them, not all subjects found equally helpful the use of VF, and in most extreme cases, some of them found the presence of VF disrupting.



# 16 CONCLUSIONS (II)

## 16.1 MAJOR FINDINGS

This section was dedicated to investigate the effect of VF on the control structure of the upper-limb movements. The following lines describe the most remarkable findings within this section. It has to be noted that along the section important inter-subject differences came up regarding the behavior of the motor control and the effect of VF. Precisely, we pay special attention to the individual exceptions found to the general trends described below as we believe that such exceptions are crucial to shed light to the understanding of the motor control.

### MOVEMENT SPEED

- In subjects for whom VF was helpful for improving motor performance, VF tends to significantly speed up movement execution. For those subjects for whom VF was disrupting or who did not concentrate in doing similar repetitions, the effect was the opposite.
- The effect of VF on movement speed does not seem to depend on arm dominance. However, we did find significant interlimb differences in the impact of VF in subjects recognizing interlimb differences in motor performance while executing the experimental protocol.



## INTERLIMB SIMILARITY (ILS)

- The effect of VF on ILS show significant interaction between subjects and movement types, indicating the importance of analyzing the results regarding ILS separately for each movement and subject.
  - At *subject level*, VF tends to increase the ILS of the control structure in all subjects except in the subject for whom VF was disrupting.
  - At *movement-type level*, VF is especially prone (1) to increase ILS during shoulder abduction and adduction, (2) decrease ILS during shoulder rotations and (3) increase ILS during elbow flexion and extension at the level of activation coefficients, while decreasing it at synergy level.
- The ILS of activation coefficients is higher than the ILS of muscles synergies, suggesting that muscle synergies may account for main interlimb differences due to handedness. However, VF similarly affect the magnitude of ILS in muscle synergies and activation coefficients.

## TEMPORAL FEATURES OF VF-DRIVEN MODULATION

- The effect of VF is dynamic on time. That is, the ILS increase induced by VF is not constant during the entire time that a movement lasts. Instead, it is interspersed with brief ILS drops.
- In general, VF tends to bring together the activation coefficients of the right and left arms, instead of generating a new motor control strategy.



## LATERALITY OF VF-DRIVEN MODULATION

- VF acts over the left activation coefficients between the 30 and 35% more frequently than over the right activation coefficients. That is, the control structure of the non-dominant arm is more prone to be modulated by VF at the level of activation coefficients.
- VF tends to primarily modulate left arm activation coefficient during shoulder movements, while preferentially acting over right arm during elbow movements.

## INTERMANUAL TRANSFER

- VF increases the ILS of the motor control mainly by transferring the control strategy of the dominant arm towards the nondominant arm.
- VF induces two-types of complementary IMT. On the one hand, VF transfers the original motor control of the dominant arm. On the other hand, VF shows also the potential to modulate the control structure of the dominant arm, and to transfer this modified strategy to the nondominant arm.

## 16.2 FINAL REMARKS

In conclusion, in this section we demonstrate that VF increases the ILS of the motor control mainly by transferring the control strategy of the dominant arm towards the nondominant arm. In particular, we provide evidence that VF induces two-types of complementary IMT. On the one hand, VF transfers the original motor control of the dominant arm. On the other hand, VF shows also the potential to modulate the control



structure of the dominant arm, and to transfer this modified strategy to the nondominant arm.

Diverse performance advantages have been attributed to the dominant arm over the nondominant arm<sup>223,224</sup>. According to our results, VF most frequently induces IMT of the dominant activation patterns to the nondominant arm denoting an important role of this mechanism during VF at improving motor control. In the domain of stroke, it seems that the concept of dominant and nondominant arm should be reformulated to unaffected and paretic sides respectively as the kinematics of the paretic arm of stroke patients closely resembles the nondominant arm of healthy subjects<sup>225</sup>. Thus, it is very likely that stroke patients may benefit from mirror therapy because VF transfers the intact skills of the unaffected arm to the control structure of the paretic arm.

Some authors report that the extent of IMT might be age-dependent. In particular, they describe a considerably larger IMT in healthy young adults (< 35 years) than in older population (> 60 years)<sup>226,227</sup>. It has to be noted that the average age of our healthy population was  $30.33 \pm 3.93$ , while according to the US Centers for Disease Control and Prevention, about 75% of all strokes occur in people over the age of 65<sup>228</sup>. Thus, although stroke can occur at any age (the average age of our database of patients with stroke was  $47.33 \pm 11.18$ ), in general, one should expect more reduced IMT rates than the ones reported in this study in older patients.

Apparently, VF is not always beneficial in terms of motor control. In about a fifth of the cases VF does neither increase ILS nor induce IMT. Indeed, several cases reveal VF modulating the activation coefficients to a completely novel shape. Accordingly, the ANOVA tests indicate that the magnitude of ILS improvement induced by VF depends on subjects and movement types. We previously reported that the efficiency of VF was related to subjects feeling comfortable with it<sup>229</sup>. Therefore, further research is needed to investigate whether this is a fixed personal constraint, or conversely, whether subjects can learn how to use VF to modulate their control structure.



Although the magnitude of IMT found is moderate, we speculate that this is because subjects presented quite a high ILS (even in absence of VF) so that the scope for improving it was very limited. However, this scenario is very unlikely to be found in rehabilitation. In fact, substantial differences in the control structure of the paretic and healthy arm of stroke patients have been recurrently reported, especially regarding the activation coefficients<sup>120, 122</sup>. Consequently, it is expected that patients with stroke can benefit from a greater extent of VF-induced IMT during rehabilitation. Taken everything together, this study provides sound physiological evidence to encourage the incorporation of VF in the design of new stroke rehabilitation approaches.

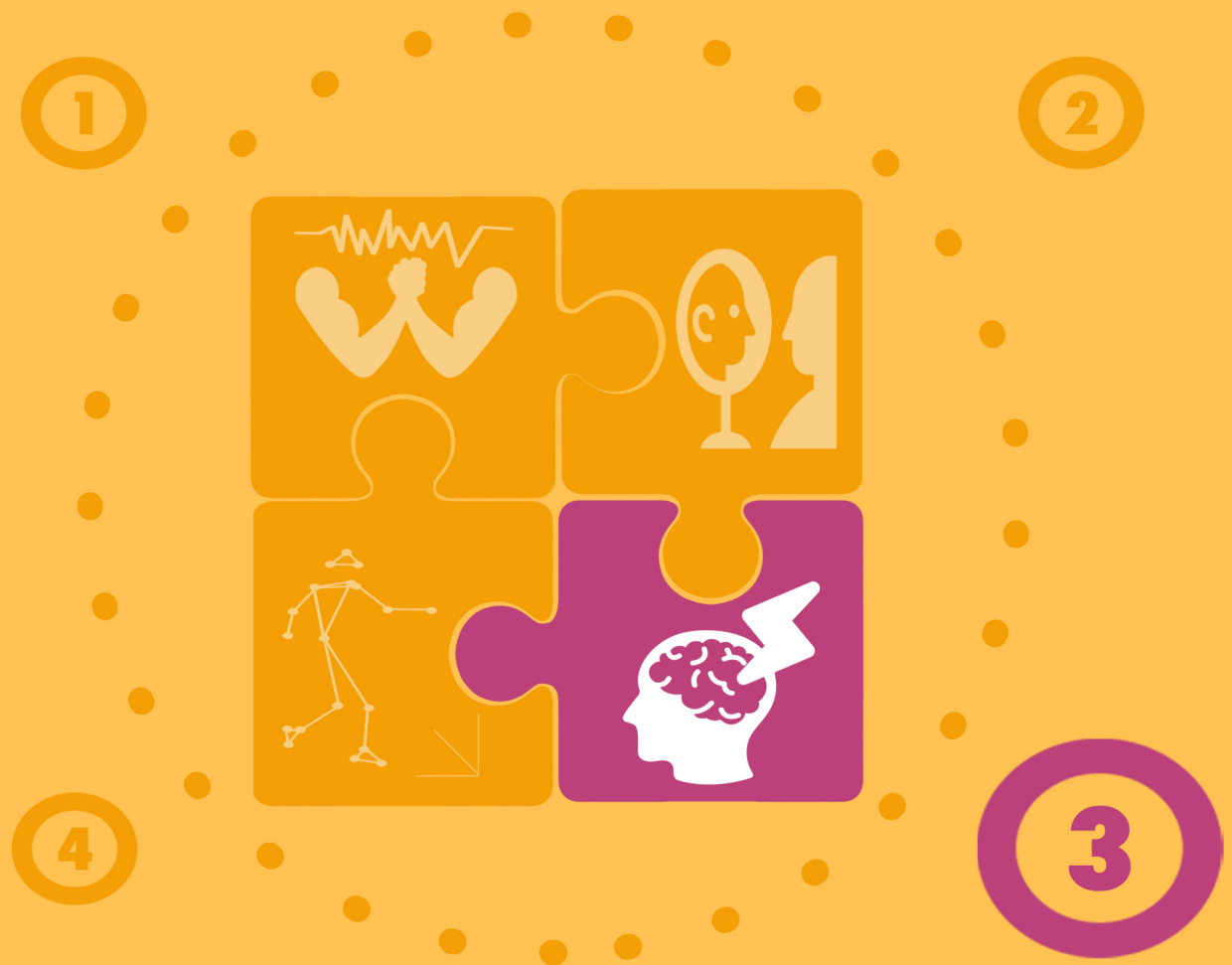
## FUTURE GUIDELINES

The results described above indicate that the effect of VF depends on the individual background of the subjects. Indeed, given the high inter-subject differences (specially linked to individual preferences or limitations during the execution of motor tasks), it is difficult to unequivocally predict the potential of VF in all possible scenarios. Thus, extending the database to cover matched groups with similar backgrounds in motor control would be very helpful to infer the meaning of these results.









### Study 3

# Interlimb Similarity in stroke patients

How is the ILS altered in patients with stroke? Can VF modulate the control structure?







# Abstract

*The lack of clinical reliable standards to measure motor impairment and the huge inter-subject variability found in stroke populations dramatically hinder the design of effective interventions. Several studies have described alterations in the number and composition of muscle synergies. However, little is known about how stroke affects activation coefficients or how these findings can be introduced into clinical practice to truly benefit patients. For this reason, and taking into account that stroke most frequently causes unilateral motor damage, we propose carrying out an integral characterization of the entire control structure (muscle synergies and activation coefficients) of patients with stroke and identifying deviations from healthy control structures that may serve as objective biomarkers of motor impairment. In this line, we propose applying the innovative concept of ILS to quantify motor impairment. Indeed, we have discovered significant differences between the ILS of healthy and impaired subjects. Thus, we have also conducted regression analyses with common clinical scales (FM and FIM) to determine whether the ILS can discriminate between motor impairment severity levels. Finally, in order to assess the power of VF as a potential rehabilitation tool, we have verified whether VF has the capacity to modulate the control structure of damaged brains in patients with stroke.*



# 17 SPECIFIC PROCEDURES (III)

## 17.1 EXPERIMENTAL SETUP

The experimental setup applied in this study is described in section 7. Experimental protocol (PART II. METHODS). In particular, the adaptation of the protocol for patients with stroke is detailed in 7.2. Protocol modifications for patients subsection.

## 17.2 DEFINING THE REFERENCE FRAMEWORK

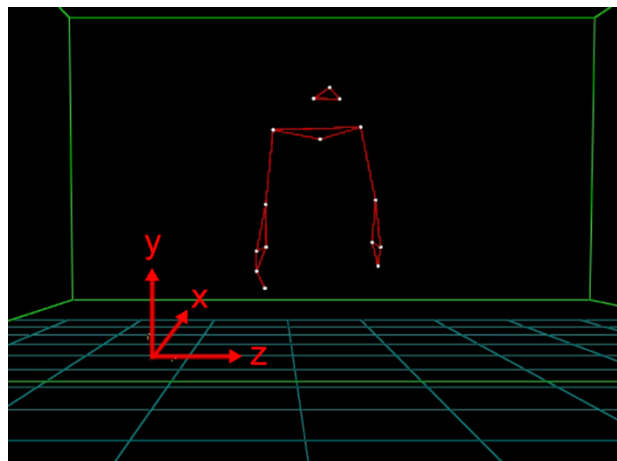


Figure 75 Location of the reference framework during the kinematics recordings

The reference framework used to record kinematics data was placed on the ground, aligned with the rear leg of the chair where patients sat down. The **x axis** was pointed at the back of the room, the **y axis** was set as the vertical axis pointing upwards



and the **z axis** was set as the horizontal axis pointing to the right side of the viewer (Figure 75).

**Table 30** defines, according to this reference framework, the rotation axis of each movement pair. We also defined the main displacement axis, as the axis along which the distal joint of the upper-limb (either the hand or the finger) described larger position shifts. Position changes in this axis were used to determine the onset and offset of each movement (see 17.3 **Quality of kinematic** ).

MOVEMENT PAIR	SHOULDER ABD / ADD	SHOULDER EXT/ INT ROTATION	ELBOW FLEXION / EXTENSION
<b>ROTATION AXIS</b>	X AXIS	Y AXIS	Z AXIS
<b>MAIN DISPLACEMENT AXIS</b>	Y AXIS	Z AXIS	Y AXIS

**Table 30** Definition of the rotation axis for each movement (first row) and the main displacement axis (second row). The main displacement axis represents the direction that holds the largest range of motion for each movement.

### 17.3 QUALITY OF KINEMATIC RECORDINGS

The quality of the kinematic recordings, varied from case to case. That is, in some cases, the system missed certain markers at certain time-points. Note that the recording system will only register the position of a marker, as long as at least 3 cameras out of the 6 cameras of the system detect such marker. Otherwise, the position of that marker at that time-point is not recorded.

Thus, we defined the quality of the kinematics recording ( $Q_k$ ) as the percent of time-points that were correctly detected by the system for the  $i$ -th marker:

$$Q_{K,i} = \frac{n}{L} \cdot 100 \quad (25)$$



Where,  $n$  is the number of positions that are correctly detected for the  $i$ -th marker and  $L$  is the total number of possible positions.

## 17.4 DETERMINING MOVEMENT ONSET AND OFFSET

### 17.4.1 Segmentation from position

We used the kinematics data (see **Chapter 9 Kinematic Data**) recorded during the movements performed by patients with stroke to determine the onset and offset of each repetition. To do so, we plotted the evolution of the position of the markers against time. Data series were smoothed using a 4th order low-pass Butterworth filter. We observed that movements were repeated every 2-3 seconds (depending on the patient), which is equivalent to a frequency of 0.33-0.5 Hz. Thus, the cutoff frequency of the filter was set to 1 Hz.

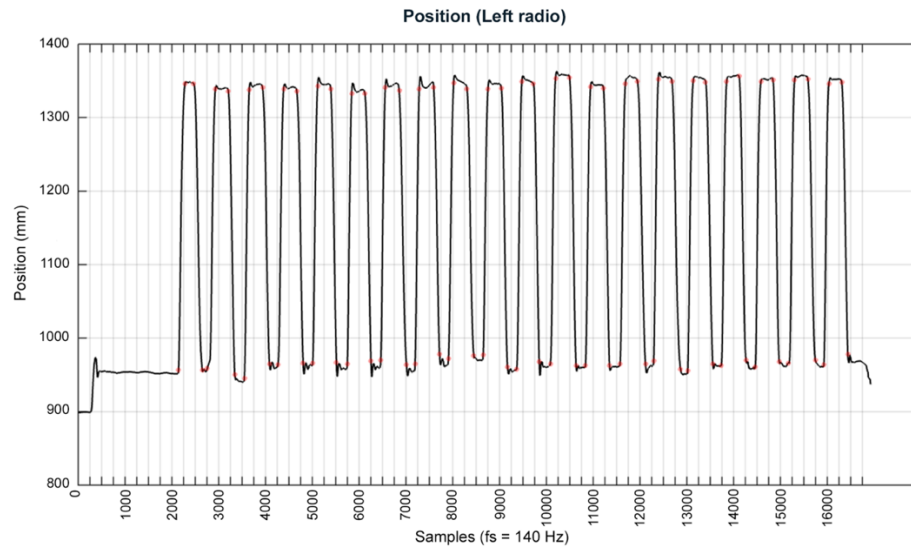
Positions were recorded in the 3-dimensional space and therefore, they were expressed as a 1 x 3 vectors ( $x,y,z$ ). However, for the sake of simplicity, we used only one axis to detect movement onsets and offsets: the main displacement axis (**Table 30**). Note that movements under analysis can be studied as planar movements. Thus, for every movement, there is an axis along which there is no movement and can be discarded. Then, from the remaining two axes, there is always one along which the range of motion is larger: the main displacement axis. Therefore, this is the most straightforward axis to determine movement onsets and offsets accurately.

As it has been said, the quality of the kinematics recordings varied from case to case, and in some cases some markers did not have enough points to accurately define movement onsets and offsets (**Table 32**). Thus, we could not define a single marker for each movement to complete this task. Instead, we analyzed each case individually and we chose the distal marker with a highest reconstruction to detect them.

For every movement, we used a plot like the one shown in **Figure 76** to identify the beginning and end of each repetition. Both, onsets and offsets were defined as



abrupt position changes in the plots. Thus, we manually identified those points by interactively selecting them over the plots (red points indicate the onsets and offsets defined for the given example).



**Figure 76 Evolution of the z position of left radio during left shoulder abduction and adduction.** This is an example of the plots used to determine movement onsets and offsets. Position is expressed in mm. Red dots indicate the time points that were considered indicative of the onset and offset of the 20 repetitions registered for each movement.



### 17.4.2 Segmentation from velocity

The analysis of velocity profiles to detect movement onset and offset was only used to complement the information provided by the position plots (see section 17.4.1 Segmentation from position), when these presented inconsistent or unclear curvatures. Theoretically, movement onset corresponds to the instant in which hand speed exceeds 0 m/s and movement offset to the instant in which hand speed turns back to 0 m/s. To calculate the 3D speed of the hand, we first smoothed the position time series of each axis using the moving average method (window size = 10 points). Then we calculated the 3 components of  $v$  as:

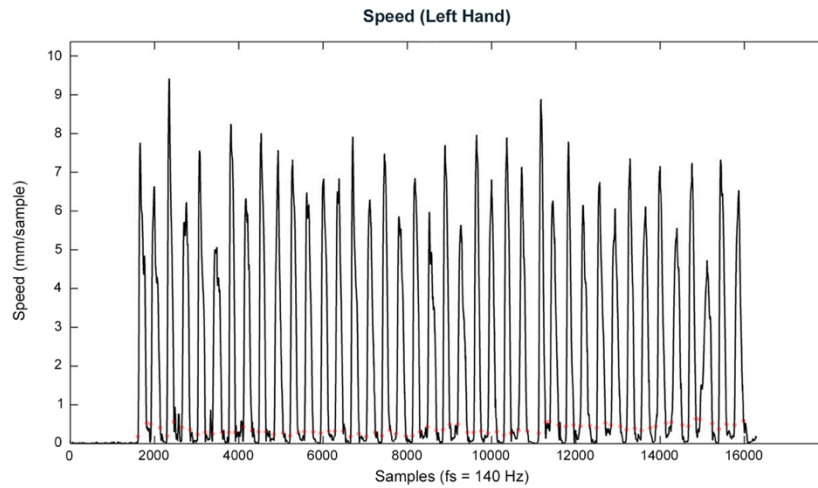
$$\begin{cases} v_x(t) = \dot{x}(t) \\ v_y(t) = \dot{y}(t) \\ v_z(t) = \dot{z}(t) \end{cases} \quad (26)$$

Finally, we got  $v$  as the norm of its 3 components:

$$v(t) = \sqrt{v_x(t)^2 + v_y(t)^2 + v_z(t)^2} \quad (27)$$

An example of the plots used to determine movement onsets and offsets is shown in Figure 77. Each plot illustrates the speed achieved by the moving hand during the 20 repetitions of each movement. Movement onset was identified when the hand started moving ( $v(t) > 0.2$  mm/sample) and movement offset when the hand stopped moving ( $v(t) < 0.2$  mm/sample). Due to the natural inability of the human body to stay motionless, the arm was considered to be still when  $v(t) < 0.2$  mm/sample. This threshold was checked with the video recordings showing not macroscopic movement when  $v(t) < 0.2$  mm/sample.





**Figure 77 3D speed of left hand during left shoulder abduction and adduction.** This is an example of the plots used to determine movement onsets and offsets. Speed is expressed in mm/sample. Red dots indicate the time points that were considered indicative of the onset and offset of the 20 repetitions registered for each movement.



## 17.5 ASSOCIATION ANALYSIS BETWEEN ILS AND CLINICAL MEASURES

We assessed the relationship between clinical measures of stroke and the ILS of patients. In particular, we analyzed the Fugl-Meyer (FM) score and the Motor-FIM score. Both the FM score and the FIM-motor scores were normalized to 1 (**Table 31**). The Motor-FIM refers to the normalized score attained in 13 items of the motor domain (See **Appendix C. Functional Independence Measure**).

	P1	P2	P3	P4	P5	P6
Fugl-Meyer score	0.8939	0.7121	0.8788	0.8939	0.6061	0.8788
Motor-FIM score	0.7686	0.9229	0.9557	1	0.9771	0.9786

**Table 31** Normalized Fugl-Meyer and FIM-motor scores of patients with stroke. Motor-FIM score is the score attained by patients in the motor domain of the FIM.

The association between variables was tested using linear regression analysis and Pearson's Correlation. Linear regression consists of finding the best-fitting straight line (regression line) through the data-points that predicts Y from X. In contrast, correlation does not fit a line through data-points. Instead, correlation quantifies the degree to which two variables are related, i.e., the correlation coefficient  $r$  estimates how much one variable tends to change when the other one does.

The relationship between variables was assessed separately for each movement. Also, we assessed the relationship between the clinical measures and the mean ILS of all movements for each subject. In both approaches, variables X and Y were assigned to the ILS and the clinical measures respectively. Because the potential diagnostic capacity of ILS should be assessed in physiological conditions, we used the ILS found in absence of VF ( $ILS_{nVF}$ ).



### 17.5.1 Linear regression

The linear regression model used in this study can be expressed as:

$$Y = b * X + c \quad (28)$$

Where Y is the criterion variable, and X is the predictor variable. In this specific case, the previous equation results in:

$$ILS_{nVF} = b * CM + c \quad (29)$$

Where  $ILS_{VF}$  is the ILS found with no VF and the CM is the clinical measure. To fit the linear data model in the model coefficients  $b$  and  $c$ , we used the least-squares fit. Goodness of fit was assessed through the coefficient of determination  $R^2$  that can be calculated as:

$$R^2 = 1 - \frac{SS_{resid}}{SS_{total}} \quad (30)$$

Where  $SS_{resid}$  is the residual sum of squares and  $SS_{total}$  is the total sum of squares. Given  $n$  data points and the fitted line  $y'$ , these are computed as:

$$SS_{resid} = \sum_{i=1}^n (Y - y')^2 \quad (31)$$



$$SS_{total} = (n - 1) * var(Y) \quad (32)$$

Note that for the ease of interpretation, the plots of the linear regression are rotated so that the Fugl-Meyer score is plotted in the horizontal axis and the ILS in the vertical axis.

### 17.5.2 Polynomial regression

In view of the spatial distribution of clinical measures in relation to the ILS of activation coefficients measured as 1 –ILD, we intuited a nonlinear relationship between the variables. Thus, we modeled this relationship using increasing grade polynomial regressions. We tested polynomials of  $d = 2 - 4$  degrees, and we selected the second grade polynomial as the best model to fit the data without overfitting it.

$$Y = a * X^2 + b * X + c \quad (33)$$

The goodness of fit of the polynomial regressions was teste using the Adjusted Coefficient of Determination ( $R^2_{adj}$ ). Using a higher degree polynomial usually results in a closer fit to data but at the expense of a more complex model, for which  $R^2$  cannot account. To solve this problem, the adjusted statistic includes a penalty for the degree  $d$  of the polynomial in the relation of the number of points  $n$  of the dataset:

$$R^2_{adj} = 1 - \frac{SS_{resid}}{SS_{total}} * \frac{n - 1}{n - d - 1} \quad (34)$$

### 17.5.3 Pearson's correlation

Pearson's correlation, is a type of linear correlation that quantifies the strength of a linear relationship between two variables. The advantage of using linear correlation is that we do not have to assume or fit a specific model to quantify the linear relationship between the two variables.



To compute the Pearson's correlation, we applied the *corrcoef* Matlab function, which returns the correlation coefficient  $r$ , and the p-value for testing the hypothesis that there is no relationship between the observed phenomena (null hypothesis). Significant association was considered when  $p < 0.05$ .

## 17.6 CROSS-RECONSTRUCTION

We investigated whether having the muscle synergies unaffected, the alteration of activation coefficients could lead to stroke-like EMG patterns. To do so, we synthetically cross-reconstructed the activation coefficients ( $H_x$ ) that would be needed to reproduce the original EMG patterns of the paretic arm from the unaffected synergies. Such hypothesis might be mathematically expressed as:

$$EMG_{paretic}(t) = W_{unaff} \cdot H_x(t) \quad t = 1 \dots 100 \quad (35)$$

Where,  $EMG_{paretic}$  is the EMG of the paretic muscles,  $W_{unaff}$  the muscle synergies of the unaffected arm and  $H_x$  is the synthetic activation coefficient that we want to cross-reconstruct. In order to eliminate, the inherent accuracy loss of the synergy extraction process  $EMG_{paretic}$  was approximated to:

$$EMG_{paretic} \cong V_{paretic}(t) = W_{paretic} \cdot H_{paretic}(t) \quad t = 1 \dots 100 \quad (36)$$

If we break down this matrix equation into individual equations, we get 8 groups of 100 linear equations (1 group per muscle  $m$ , and 100 equations per time points  $t_i$ ) of the form:



$$\begin{cases} V_{m,t_1} = W_{m,1} \cdot H_{x1,t_1} + W_{m,2} \cdot H_{x2,t_1} \\ \vdots \\ V_{m,t_{100}} = W_{m,1} \cdot H_{x1,t_{100}} + W_{m,2} \cdot H_{x2,t_{100}} \end{cases} \quad (37)$$

This formulation results into an over-determined linear system composed of 800 equations and 200 unknown variables (2 activation coefficients x 100 time points) that can be solved using optimization. The problem can be posed as a system of 8 equations (1 per muscle) to be solved for each time point  $t_i$ .

$$\begin{cases} \text{muscle 1: } W_{1,1} \cdot X1_{t_i} + W_{1,2} \cdot X2_{t_i} = V_{1,t_i} \\ \text{muscle 2: } W_{2,1} \cdot X1_{t_i} + W_{2,2} \cdot X2_{t_i} = V_{2,t_i} \\ \text{muscle 3: } W_{3,1} \cdot X1_{t_i} + W_{3,2} \cdot X2_{t_i} = V_{3,t_i} \\ \text{muscle 4: } W_{4,1} \cdot X1_{t_i} + W_{4,2} \cdot X2_{t_i} = V_{4,t_i} \\ \text{muscle 5: } W_{5,1} \cdot X1_{t_i} + W_{5,2} \cdot X2_{t_i} = V_{5,t_i} \\ \text{muscle 6: } W_{6,1} \cdot X1_{t_i} + W_{6,2} \cdot X2_{t_i} = V_{6,t_i} \\ \text{muscle 7: } W_{7,1} \cdot X1_{t_i} + W_{7,2} \cdot X2_{t_i} = V_{7,t_i} \\ \text{muscle 8: } W_{8,1} \cdot X1_{t_i} + W_{8,2} \cdot X2_{t_i} = V_{8,t_i} \end{cases} \quad (38)$$

Where  $H_x$  is built from the pair of (X1, X2) obtained in each solution:

$$H_x = \begin{bmatrix} X1(t_1) & X1(t_2) & \cdots & X1(t_{100}) \\ X2(t_1) & X2(t_2) & \cdots & X2(t_{100}) \end{bmatrix} \quad (39)$$

Because the activation coefficients are conceptually defined as nonnegative, this is nothing that a nonnegative least-squares constrained problem that can be expressed as:

$$\min_x \|C \cdot x - d\|_2^2, \quad x > 0 \quad (40)$$

The entire optimization process was performed separately for each subject and movement.



Finally, to assess whether the obtained synthetic activation coefficients  $H_x$  were physiologically relevant, we compared  $V_{\text{paretic}}$  with the cross-reconstructed patterns ( $W_{\text{unaff}} \cdot H_x$ ) using VAF. This VAF was termed as  $\text{VAF}_x$ .

## 17.7 STATISTICAL ANALYSES

### 17.7.1 *Interaction effects on ILS*

In order to detect interaction effects of factors being part of the experiment, we conducted N-way ANOVA tests. In particular, we identified 3 factors that could affect the outcome of the ILS measures: subjects, movement types and condition.

This defines a 3-way ANOVA with  $N = 2$  or  $6$  levels of each factor.

- Subjects (6 levels): {P1, P2, P3, P4, P5, P6}
- Movements (6 levels): {SAbd, SAdd, SERot, SIRot, EFlex, EExt}
- Condition (2 levels): {nVF, VF}

Therefore, every observation is identified by a combination of factor levels. The tests were performed using the *anovan* Matlab function with the ‘*interaction*’ model. This allows finding significant interactions between factors: subject \* movement, subject \* condition and movement \* condition. Statistical significance was considered for  $p < 0.05$ . That is, a  $p$  value below 0.05 for factor A suggests that at least one A-sample mean is significantly different from the other A-sample means; that is, there is a main effect due to factor A in the ILS value.



### 17.7.2 ILS: Healthy subjects vs Patients with Stroke

In order to detect statistical significance of the ILS comparisons between healthy subjects and patients with stroke, we applied the Wilcoxon rank-sum test. This test is also known as the Mann-Whitney U test and is a nonparametric test of the null hypothesis that two samples come from the same population. It is often referred as the nonparametric version of the  $t$ -test.

We used this test, instead of the Wilcoxon signed-rank test because in this case, the samples (healthy subjects vs patients with stroke) are not related, i.e., they do not belong to the same subject. Note that for instance, when we compare nVF and VF conditions, the values tested come from the same subject who is performing in different experimental conditions.

To detect significance differences in the ILS of the control structure between populations, we applied 6 different tests comparing the following variables of healthy subjects *versus* patients with stroke:

- ILS of muscle synergies (nVF)
- ILS of muscle synergies (VF)
- ILS of activation coefficients (nVF)
- ILS of activation coefficients (VF)
- ILS of activation coefficients measured as '1 – ILD' (nVF)
- ILS of activation coefficients measured as '1 – ILD' (VF)

Each dataset was comprised of the ILS measures of all the subjects composing each population. That is, it was represented as a vector of 72 values (6 subjects \* 6 movements \* 2 muscle synergies or activation coefficients). Statistical significance was considered for  $p < 0.05$ .



### 17.7.3 ILS: no VF vs VF

We compared the ILS between the right and left arm of each patient in absence and presence of VF. To determine statistical significance of the comparisons we applied the Wilcoxon signed-rank test. For this purpose, we separately performed 6 tests comparing one-to-one the ILS values of each patient:

1. ILS of W1: nVF vs VF
2. ILS of W2: nVF vs VF
3. Mean ILS of W1 and W2 ( $\langle W1, W2 \rangle$ ): nVF vs VF
4. ILS of H1: nVF vs VF
5. ILS of H2: nVF vs VF
6. Mean ILS of H1 and H2 ( $\langle H1, H2 \rangle$ ): nVF vs VF

Statistical significance was considered for  $p < 0.05$ .

### 17.7.4 ILS: Right-stroke vs left-stroke patients

In order to statistically compare the subpopulations of right and left stroke patients, we applied the Wilcoxon rank-sum test. Just in the previous subsection, we applied this test because the measures from the two populations are not related to each other, i.e., they belong to different subjects.

In this case, each population was comprised of 3 patients. Thus, the two datasets were balanced and did not need any extra correction. The Wilcoxon rank-sum tests were applied to test the following comparisons:

- ILS (nVF): right-stroke patients vs left-stroke patients (**Figure 120**)
- ILS (VF): right-stroke patients vs left-stroke patients (**Figure 120**)



- VF – induced ILS changes: right-stroke patients vs left-stroke patients (**Figure 121**)

The datasets used to test the statistical significance of VF-induced ILS changes were built by subtracting the ILS found in presence of VF and the ILS found in absence of VF for each subject and movement in each subpopulation. In all cases, the datasets were comprised of the ILS measures of all the subjects composing each population. That is, they were represented as a vector of 36 values (3 subjects \* 6 movements \* 2 muscle synergies or activation coefficients). Statistical significance was considered for  $p < 0.05$ .



# 18 RESULTS AND DISCUSSION (III)

## 18.1 QUALITY OF THE KINEMATIC RECORDINGS

**Table 32** summarizes the quality of the kinematics recordings acquired for each patient.

PATIENT	CONDITION	MOV.	SIDE	HEAD	R_TEM	L_TEM	GUIG	ELBOW	ULNA	RADIO	HAND	FINGER
P1	nVF	EFLX	L	100	100	100	100	100	68.61	100	71.31	100
			R	100	100	100	100	100	51.61	100	99.87	100
		SABD	L	100	100	100	100	100	100	100	100	100
			R	100	100	100	100	100	99.33	100	100	100
		SROT	L	100	100	100	100	100	13.45	100	20.00	100
			R	100	100	100	99.48	100	57.43	100	99.98	99.51
	VF	EFLX	L	100	100	100	100	100	65.72	99.05	92.57	100
			R	100	100	100	100	99.99	61.71	100	98.90	99.60
		SABD	L	100	100	100	100	100	100	100	100	100
			R	100	100	100	100	100	99.67	100	100	99.93
		SROT	L	99.59	100	100	99.82	100	91.01	100	99.99	100
			R	100	100	100	99.09	100	57.37	100	99.98	100
P2	nVF	EFLX	L	100	100	100	100	100	64.84	97.22	99.39	90.43
			R	100	100	100	100	69.96	67.62	82.60	71.50	97.35
		SABD	L	98.90	100	100	100	100	100	100	100	89.25
			R	100	100	100	100	86.65	100	100	100	100
		SROT	L	100	100	100	100	54.62	99.85	22.20	27.53	100
			R	100	100	100	100	46.69	83.66	100	99.56	100
	VF	EFLX	L	100	100	100	100	100	58.48	95.80	99.88	80.64
			R	100	100	100	100	40.71	59.46	93.07	78.28	99.92
		SABD	L	100	100	100	100	100	100	99.98	96.42	100
			R	100	100	100	100	95.76	99.98	100	100	100
		SROT	L	100	100	100	100	72.66	100	100	61.80	100
			R	100	100	100	100	80.09	92.70	100	100	100

**Table 32** Quality of the kinematics recordings expressed as percent of recorded positions. Conditions were no visual feedback (nVF) / visual feedback (VF); movements (MOV) were EFLX for elbow flexion/extension; SABD for shoulder abduction/adduction and SROT for shoulder internal/external rotation; and sides were left (L) and right (arms). Elbow, ulna, radio, hand and finger markers correspond to the side of the moving limb. Cells highlighted in yellow indicate a quality between 60% and 85%, and cells highlighted in red indicate a quality below 60%. The quality of right and left acromion markers is not indicated in the table as it was 100% in all cases.



PATIENT	CONDITION	MOVEMENT	SIDE	HEAD	R_TEM	L_TEM	GUIG	ELBOW	ULNA	RADIO	HAND	FINGER
P3	nVF	EFLX	L	100	100	100	100	100	73.84	76.32	90.46	99.99
			R	100	100	100	100	99.96	83.76	95.66	76.80	80.59
		SABD	L	100	100	100	100	100	99.99	95.09	100	100
			R	100	100	100	100	100	100	100	100	100
		SROT	L	100	100	100	100	100	87.32	79.99	99.86	99.22
			R	100	100	100	100	100	97.42	99.98	99.03	99.40
	VF	EFLX	L	100	100	100	100	100	68.16	71.55	96.05	99.91
			R	100	100	100	100	99.99	77.41	99.15	89.70	86.24
		SABD	L	100	100	100	100	100	99.97	75.34	100	100
			R	100	100	100	100	100	100	100	100	100
		SROT	L	99.07	99.85	99.36	99.99	100	89.10	71.73	99.54	99.55
			R	100	100	100	100	99.99	97.39	99.95	99.31	99.96
P4	nVF	EFLX	L	100	100	100	100	100	67.22	99.95	96.81	94.47
			R	100	100	100	99.37	99.96	54.24	81.27	91.33	88.11
		SABD	L	100	100	100	100	100	100	100	100	100
			R	100	100	100	100	100	99.98	100	100	99.96
		SROT	L	100	100	100	100	100	94.72	99.89	98.80	99.99
			R	100	99.97	99.78	99.35	100	93.56	100	99.90	99.93
	VF	EFLX	L	100	100	100	100	100	66.07	71.59	81.65	98.86
			R	100	100	100	99.99	99.99	59.91	98.72	74.16	97.59
		SABD	L	100	100	100	99.57	100	100	100	100	100
			R	100	100	100	100	100	100	100	100	95.41
		SROT	L	100	100	100	100	100	93.73	99.03	97.59	99.97
			R	100	100	100	100	100	91.79	100	99.46	100

Table 32 (cont 2/3) Quality of the kinematics recordings expressed as percent of recorded positions.



PATIENT	CONDITION	MOVEMENT	SIDE	HEAD	R_TEM	L_TEM	GUIG	ELBOW	ULNA	RADIO	HAND	FINGER
P5	nVF	EFLX	L	100	100	100	99.72	99.98	95.98	99.96	94.15	94.93
			R	100	100	100	100	100	99.36	99.99	84.26	99.98
		SABD	L	100	100	100	100	100	100	92.24	99.76	98.47
			R	100	100	100	100	100	100	100	97.81	100
		SROT	L	99.93	100	100	100	100	98.91	100	99.87	98.67
			R	99.94	100	100	100	69.53	99.52	99.99	90.49	100
	VF	EFLX	L	100	100	100	100	99.99	90.54	99.88	96.53	93.25
			R	100	100	100	100	93.32	99.48	96.84	76.27	97.74
		SABD	L	100	100	100	100	100	100	91.42	97.86	85.35
			R	100	100	100	100	100	100	96.68	70.46	98.83
		SROT	L	100	100	100	100	100	94.08	99.99	98.75	99.59
			R	100	100	100	100	99.05	99.91	100	85.27	99.89
P6	nVF	EFLX	L	100	100	100	100	100	89.46	99.99	95.68	98.03
			R	100	100	100	99.67	100	59.19	61.61	94.96	99.91
		SABD	L	100	100	100	100	100	100	100	100	100
			R	100	100	100	100	100	100	97.20	100	100
		SROT	L	100	100	100	100	100	99.06	100	99.89	100
			R	100	100	100	100	100	81.30	89.44	99.99	98.75
	VF	EFLX	L	100	100	100	100	100	60.40	94.54	94.53	99.28
			R	100	100	100	100	99.98	60.22	66.27	95.65	99.94
		SABD	L	100	100	100	100	100	100	99.94	100	100
			R	100	100	100	100	100	100	79.44	99.85	99.33
		SROT	L	100	100	100	100	100	98.83	99.95	99.84	100
			R	100	100	100	100	100	78.05	90.80	100	99.89

(cont 3/3) Quality of the kinematics recordings expressed as percent of recorded positions.



## 18.2 SELF - EVALUATION OF PATIENTS

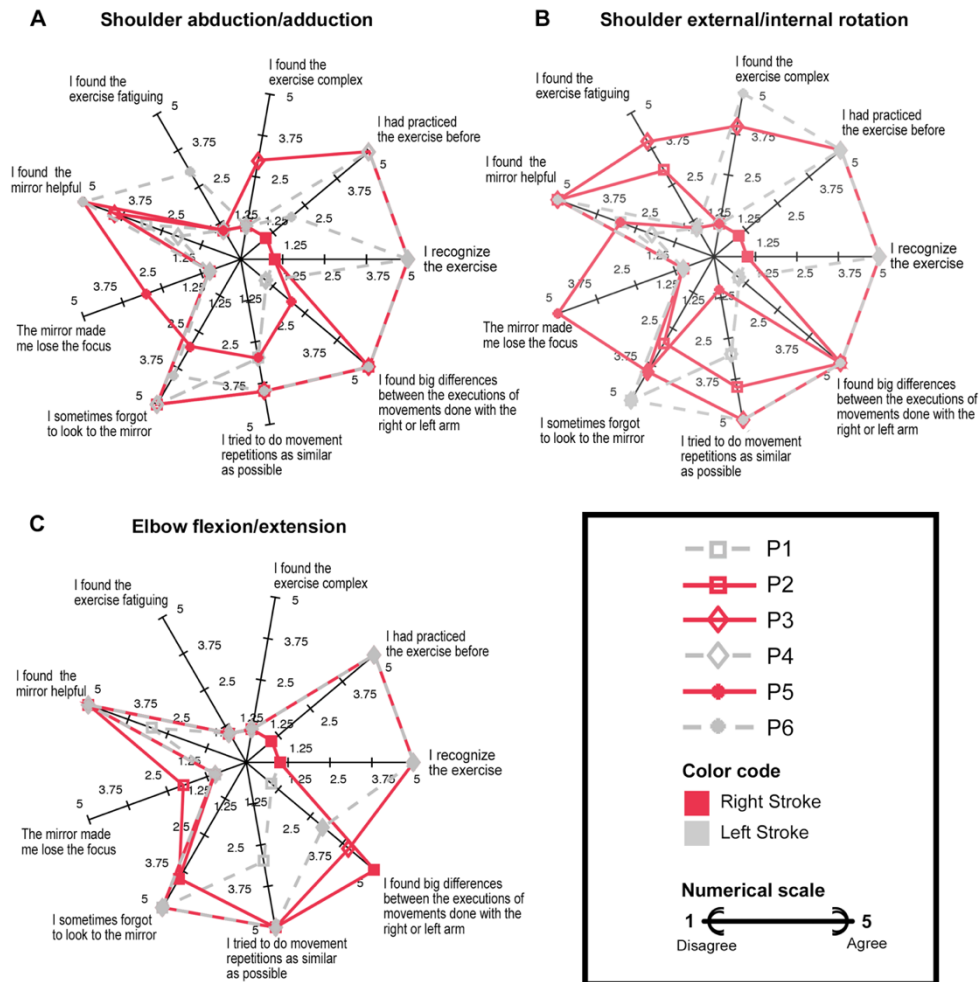
**Table 33** summarizes the answers given by patients after finishing the experimental slot of each movement. **Figure 78** represents graphically these answers. According to them, half of the patients did not recognize the exercises neither have practiced them before, while the other half did. Thus, potential motor learning effects should be considered during the analysis of data as a source of motor performance differences.

	P1			P2			P3			P4			P5			P6		
MOVEMENT	A	B	C	A	B	C	A	B	C	A	B	C	A	B	C	A	B	C
I recognize the exercise	1	1	1	1	1	1	5	5	5	5	5	5	1	1	1	5	5	5
I had practiced the exercises before*	1	1	1	1	1	1	5	5	5	5	5	5	1	1	1	2	5	5
I found the exercise complex	1	1	1	1	1	1	3	4	1	1	1	1	1	1	1	1	5	1
I found the exercise fatiguing	1	1	1	1	3	1	1	4	1	1	1	1	1	1	1	3	1	1
I found the mirror helpful	3	3	3	4	5	5	4	5	5	2	2	5	5	3	5	5	5	5
The mirror made me lose the focus*	1	1	1	1	1	2	1	1	1	1	1	1	3	5	1	1	1	1
I sometimes forgot to look to the mirror*	5	5	5	5	3	4	5	4	5	5	5	5	3	4	4	4	5	5
I tried to do movement repetitions as similar as possible*	3	3	3	4	4	5	4	5	5	3	3	5	3	1	5	4	5	5
I found big differences between the executions of movements done with the right or left arm*	1	1	1	5	5	5	5	5	4	1	1	3	2	5	5	5	5	3
DAMAGED HEMISPHERE	LEFT			RIGHT			RIGHT			LEFT			RIGHT			LEFT		
FUGL MEYER SCORE	59			47			58			59			40			58		

**Table 33** Answers given by patients in the auto-evaluation questionnaire delivered after the experiment. Questions marked with an asterisk (\*) were shared in questionnaires delivered to healthy subjects. Answers were given as numeric values ranging from 1 (I do not agree) to 5 (I fully agree). Movements refer to A: shoulder abduction/adduction, B: shoulder external/internal rotation and C: elbow flexion/extension.

Although the vast majority of the movements were not considered complex, two patients admitted to find difficulties performing shoulder rotations. Also, patients in general affirmed that the sessions were not fatiguing at all, so, we can discard potential interaction of muscle fatigue in the EMG signals.





**Figure 78** Radial representation of the questionnaires answered by patients after the experimental slot of each movement A – Shoulder abduction/adduction, B – Shoulder external/internal rotation and C – Elbow flexion/extension. The answers from patients with right stroke are represented with dashed red lines and from patients with left stroke with solid grey lines. Patients answered with a scale ranging from 1 to 5, with 1 meaning that they totally disagreed with the statements presented and 5 that they fully agreed.



The overall perception about VF was positive: most patients found the use of VF helpful and not disrupting. Certain patients even reported that after the experiment they realized that the use of VF was helpful to correct on-line the movements or that they may start using the mirror at home to practice their rehabilitation routines. Nevertheless, it has to be said that in general patients recognized not paying full attention on the movements or on the mirror. Indeed, many patients admitted not being able to concentrate at their full capacity on making movement repetitions as similar as possible. Of course, this is a circumstance to take into account, as it constitutes an independent factor that could introduce alterations into the ILS not related to pathological conditions.

The population was divided again when we interrogated about the interlimb performance differences. Half of the patients denied having found substantial differences between the right and left arms when performing the exercises, whereas the other half complained about the paretic arm being more difficult to control during the execution of the exercises. Interestingly, patients belonging to this group were left-strokes, whereas right-stroke patients belonged to the group not admitting differences. This preliminary analysis suggests that the lateral location of the neural lesion may play a determinant role in the motor outcome of patients.

In conclusion, because these inter-subject differences are directly related to motor control and the way VF can help learning or outperforming motor skills, it is very likely to find diverse inter-subject motor responses along the experiment. Therefore, as in the case of healthy subjects, these inter-subject particularities should be always kept in mind to ensure the adequate interpretation of the results.



## 18.3 CHARACTERIZING THE CONTROL STRUCTURE OF STROKE PATIENTS

This section is aimed at presenting the main characteristics of the control structure in patients with stroke, as well as to reveal some aspects of the synergy extraction process such as the VAF-threshold related decisions or the synergy matching process.

### 18.3.1 *Composition of the control structure and VAF*

In general, 2 muscle synergies (and the corresponding activation coefficients) were needed to achieve the VAF threshold of 90%. Only 12/144 exceptions were found (which represent the 8.33% of the entire dataset) that needed 3 muscle synergies to achieve such threshold (**Table 34**). However, in these cases, the average VAF was 88.21 +/- 1.29% and it was never below 85%. Thus, in order to simplify the comparison process of the control structures, we used the 2 element control structure for all patients.

It has to be highlighted that these exceptions were found in almost all subjects but only in elbow flexion and shoulder external rotation movements. 66.67% of the cases were found in absence of VF and 75% of the cases correspond to the unaffected arm. From these results one can expect a higher neuromuscular complexity in elbow flexion and shoulder external rotation movements that may explain why a larger number of muscle synergies is needed to control those movements. Similarly, some authors attribute to stroke a loss of motor complexity related to couplings of shoulder and elbow actions, and reduced ranges of joint motion<sup>118,119,124</sup>. Thus, it seems reasonable to find a larger number of muscle synergies to control the unaffected arm.



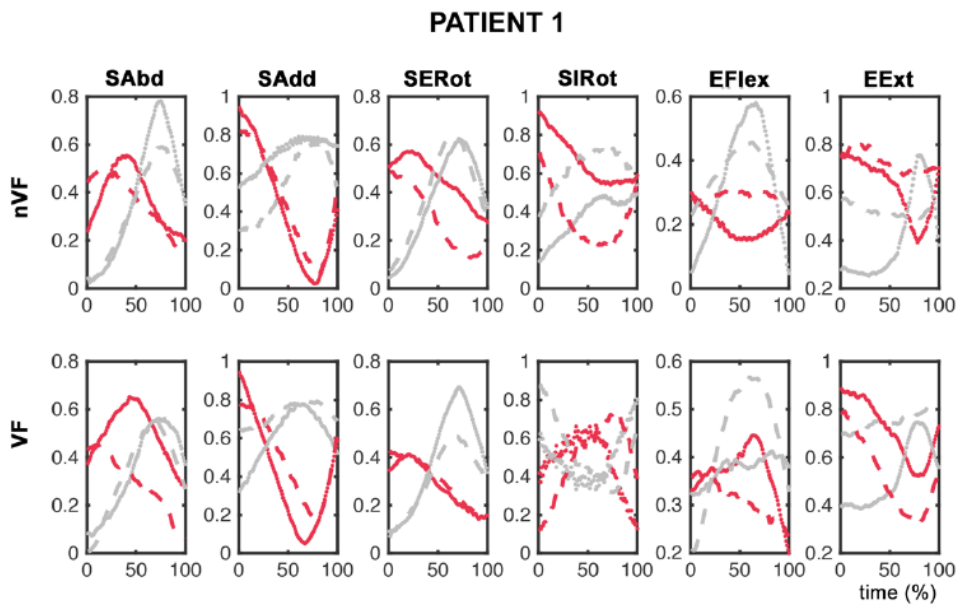
CONTROL STRUCTURES WITH VAF < 90%					
Patient	Condition	Movement	Arm	Paretic/Unaffected	VAF
P1	VF	EFlex	Left	Unaffected	0.882
P2	nVF	SERot	Left	Paretic	0.892
P2	nVF	EFlex	Left	Paretic	0.887
P2	VF	SERot	Right	Unaffected	0.89
P4	nVF	EFlex	Left	Unaffected	0.857
P4	VF	EFlex	Right	Paretic	0.884
P5	nVF	SERot	Right	Unaffected	0.884
P5	VF	SERot	Right	Unaffected	0.892
P6	nVF	SERot	Left	Unaffected	0.884
P6	nVF	EFlex	Left	Unaffected	0.854
P6	nVF	SERot	Left	Unaffected	0.887
P6	nVF	EFlex	Left	Unaffected	0.892

Table 34 VAF values of the control structures of 2 elements that did not exceed the threshold of 90%.



### 18.3.2 Synergy matching across conditions

We applied the algorithm described in the section 14.3 Within-Subject synergy matching across conditions located in the chapter **Specific Procedures (II)** from **Study 2** to match the synergies and activation coefficients across conditions (nVF vs VF). This is a process that is divided into two phases. The results of the first step are shown in the following set of 6 figures.



**Figure 79** Activation coefficients of PATIENT 1 after the first step of synergy matching. Rows 1 and 2 represent activation coefficients of movements performed in absence and presence of VF respectively. Red lines are H1 and grey lines are H2. Dotted lines correspond to left arm and dashed lines to right arm activation coefficients.



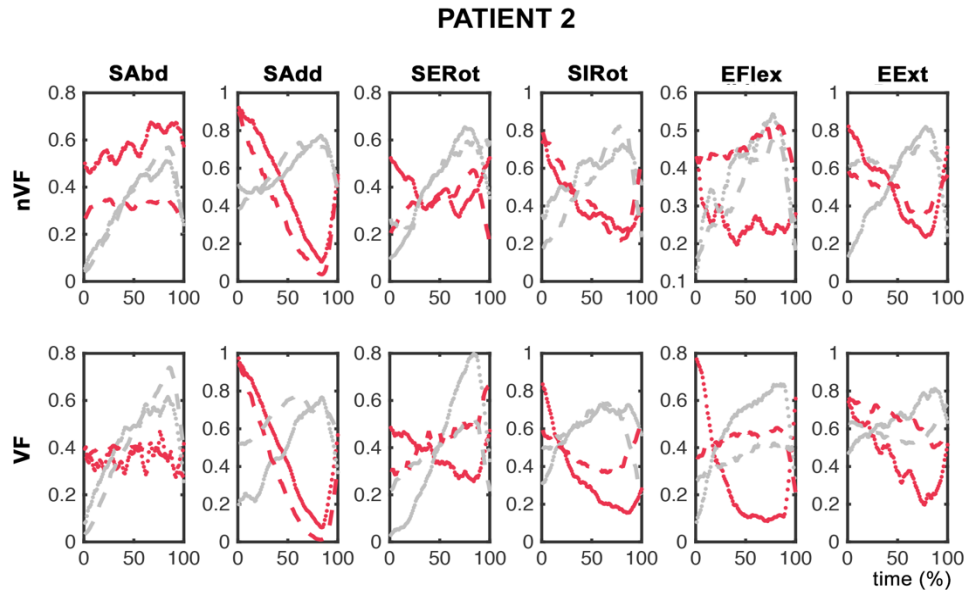


Figure 80 Activation coefficients of PATIENT 2 after the first step of synergy matching. See the legend of Figure 79 for a complete and detailed description of the figure.

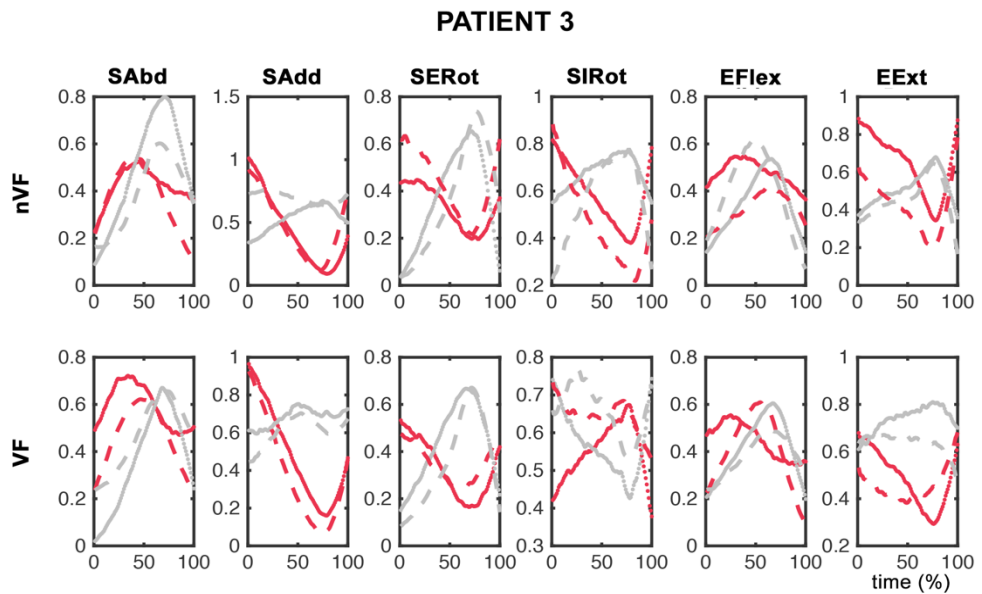


Figure 81 Activation coefficients of PATIENT 3 after the first step of synergy matching. See the legend of Figure 79 for a complete and detailed description of the figure.



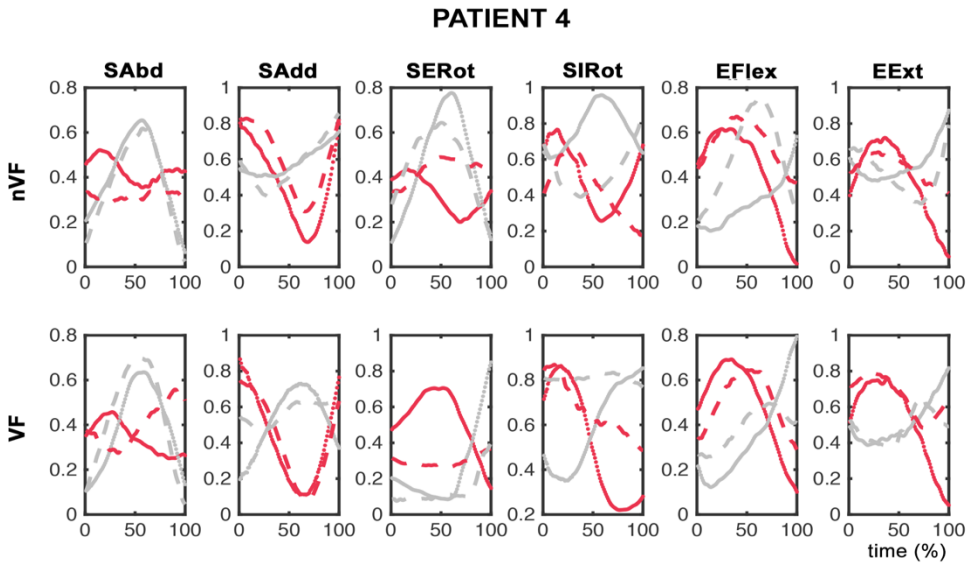


Figure 82 Activation coefficients of PATIENT 4 after the first step of synergy matching. See the legend of Figure 79 for a complete and detailed description of the figure.

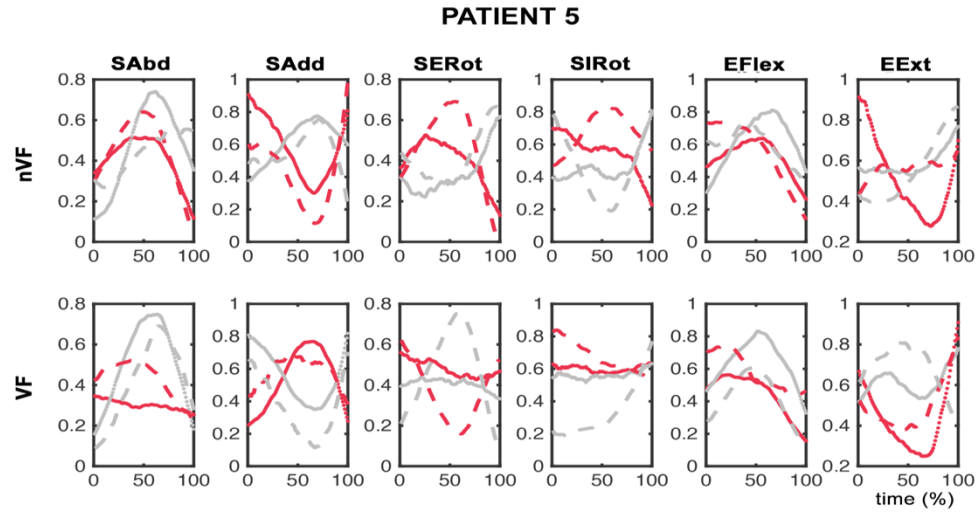
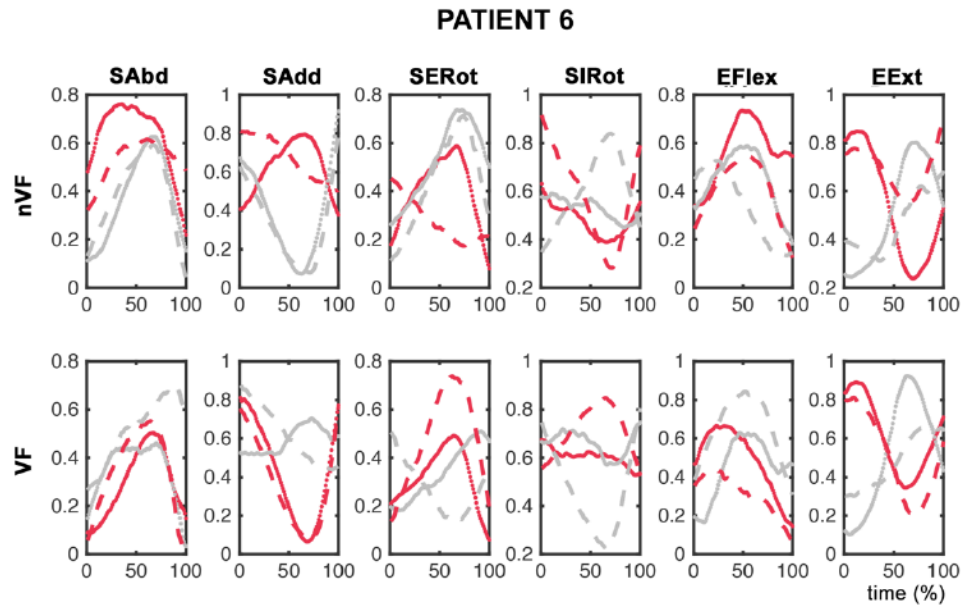


Figure 83 Activation coefficients of PATIENT 5 after the first step of synergy matching. See the legend of Figure 79 for a complete and detailed description of the figure.

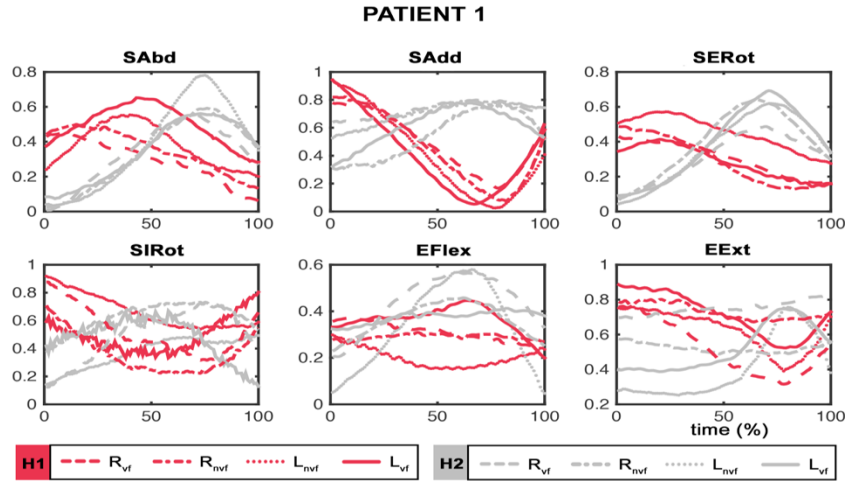




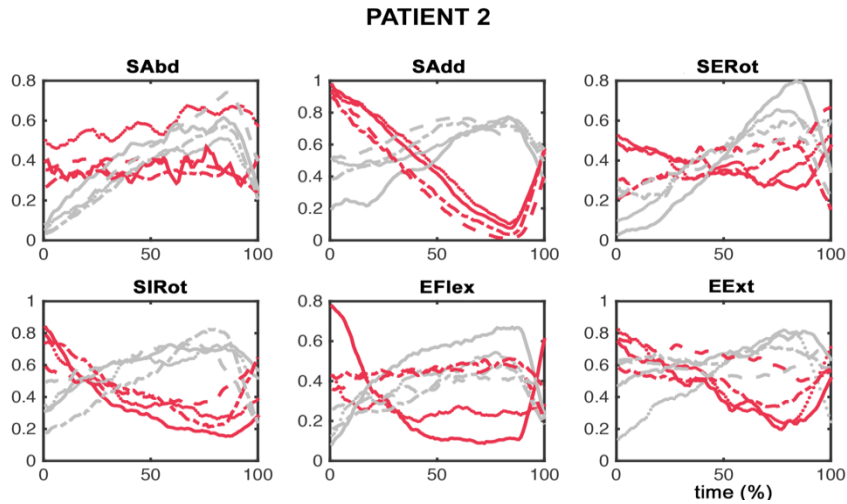
**Figure 84** Activation coefficients of PATIENT 6 after the first step of synergy matching. See the legend of **Figure 79** for a complete and detailed description of the figure.

As it happened in the synergy matching process of healthy subjects, some curves were not correctly matched across conditions (i.e. **Figure 79** – EFlex VF or **Figure 83** – EExt nVF). Thus, we applied the second step of the matching algorithm (see subsection **14.3 Within-Subject synergy matching** located in the section **Specific Procedures of the Study 2**).





**Figure 85** Activation coefficients of PATIENT 1 after the full process of synergy matching. Each plot displays the activation coefficients H1 (red lines) and H2 (grey lines) of each movement. R – Right arm, L – Left arm, nvf – movements performed in absence of visual feedback, vf – movements performed in presence of visual feedback.



**Figure 86** Activation coefficients of PATIENT 2 after the full process of synergy matching. See the legend of Figure 85 for a complete and detailed description of the figure.



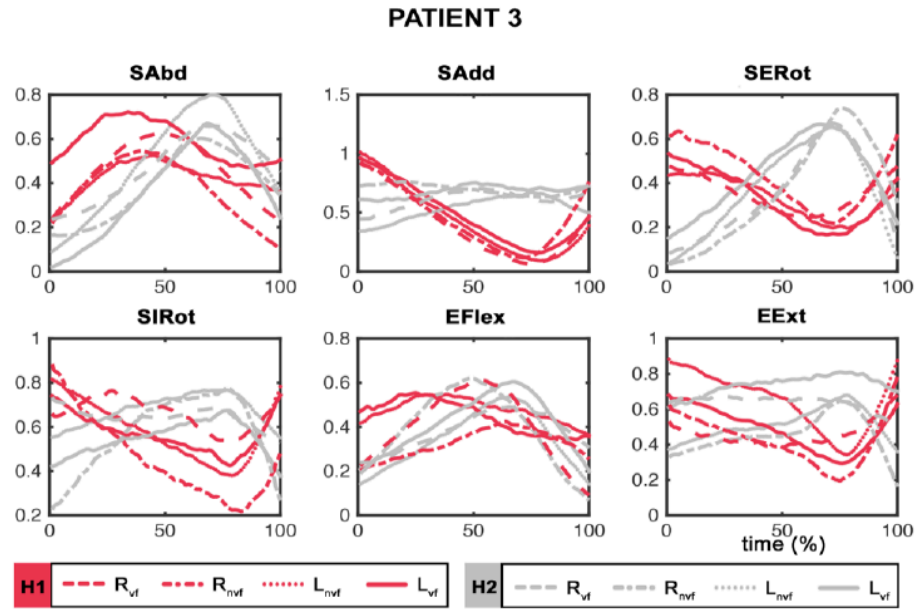


Figure 87 Activation coefficients of PATIENT 3 after the full process of synergy matching. See the legend of Figure 85 for a complete and detailed description of the figure.

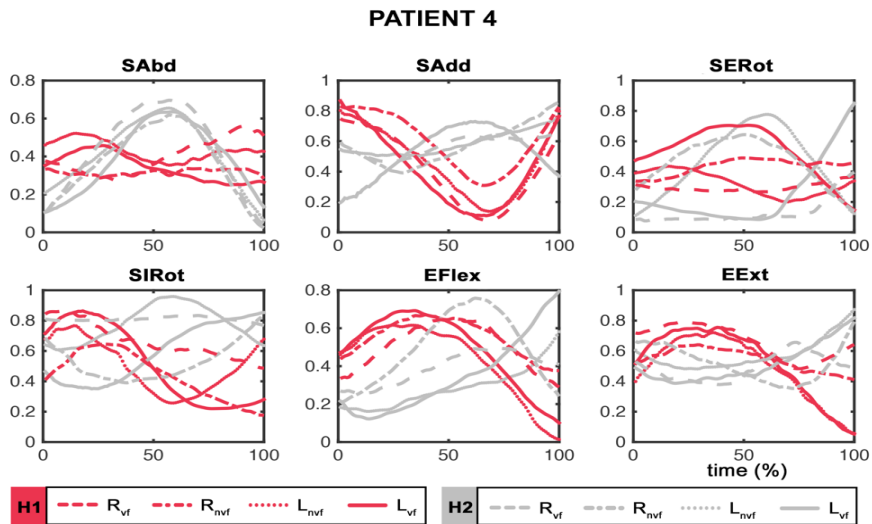


Figure 88 Activation coefficients of PATIENT 4 after the full process of synergy matching. See the legend of Figure 85 for a complete and detailed description of the figure.



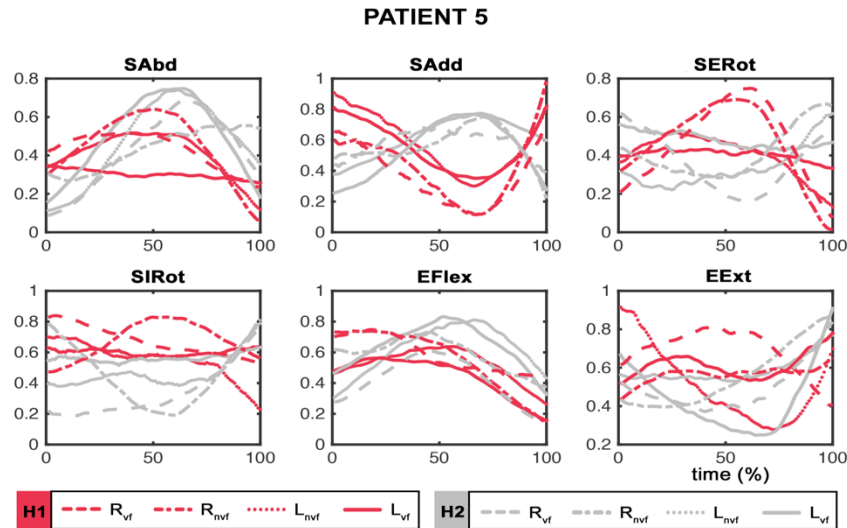


Figure 89 Activation coefficients of PATIENT 5 after the full process of synergy matching. See the legend of Figure 85 for a complete and detailed description of the figure.

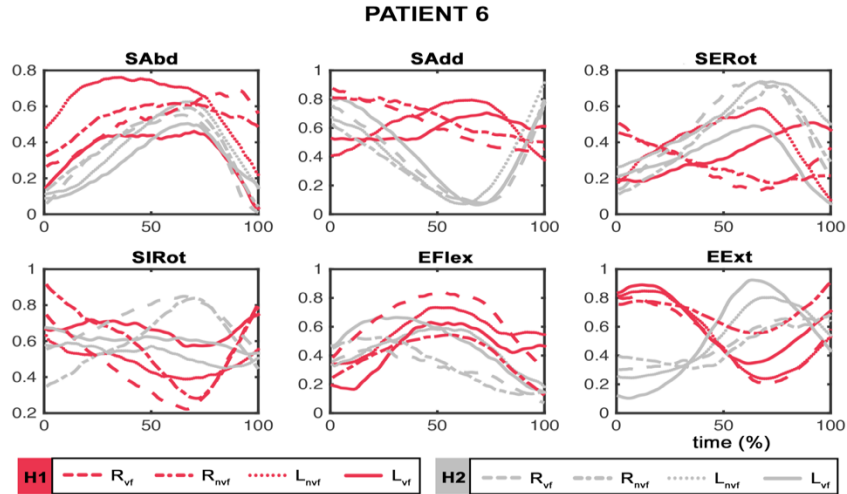
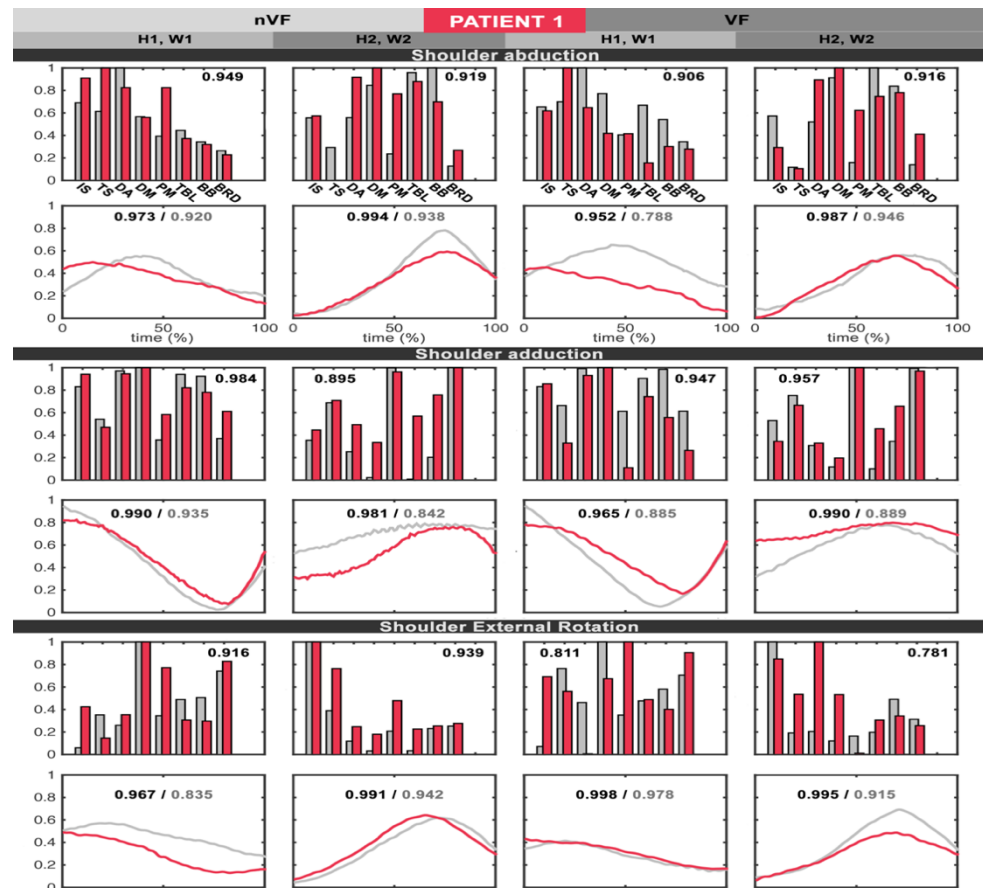


Figure 90 Activation coefficients of PATIENT 6 after the full process of synergy matching. See the legend of Figure 85 for a complete and detailed description of the figure.



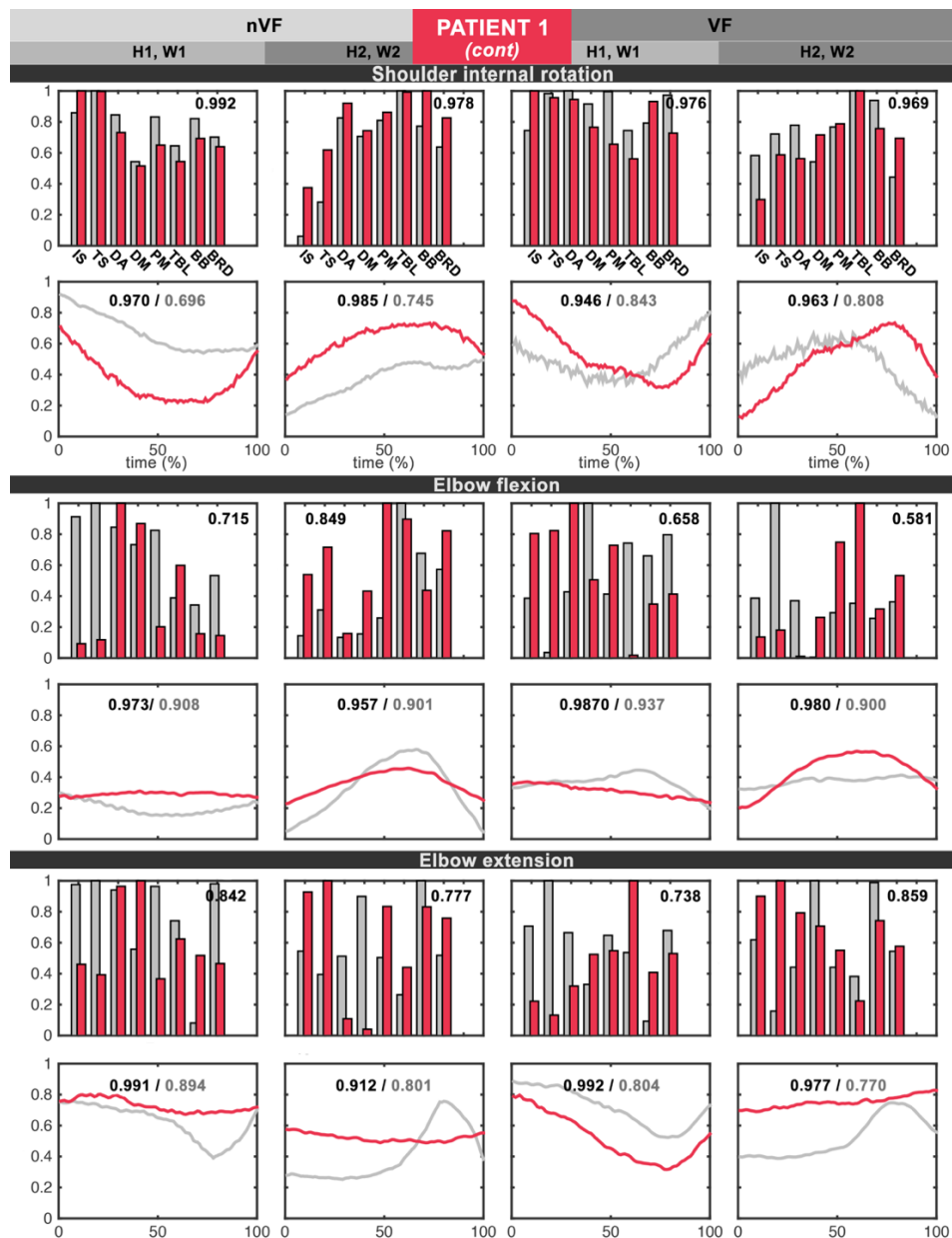
### 18.3.3 Graphical representation of the control structures

This section shows the graphical representation of the control structure of patients with stroke during the execution of movements under analysis in absence and presence of VF. Each plot includes the corresponding ILS measures, so the observer can qualitatively evaluate how these measures are reflected in the characteristics of the control structures.



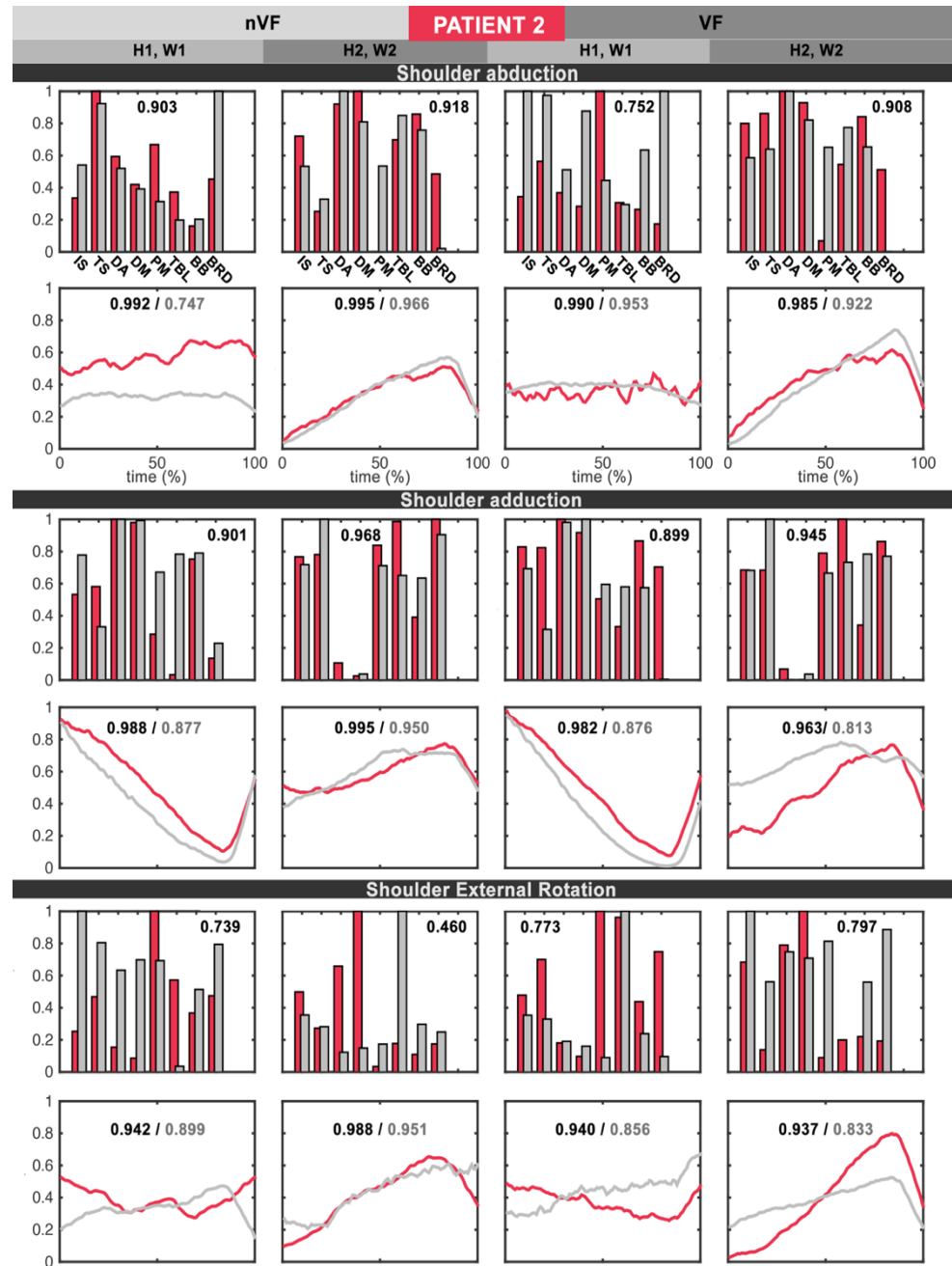
**Figure 91** Graphical representation of the control structure of PATIENT 1 and related ILS measures PART 1/2: shoulder abduction, shoulder adduction and shoulder external rotation. Bars are muscle synergies and curves are activation coefficients. Red elements belong to the control structure of the paretic arm and grey elements to the unaffected arm. The numbers indicated in each plot are scalar products for muscle synergies and **Cross-correlation coefficient / 1 - ILD** for activation coefficients.





**Figure 92** Graphical representation of the control structure of **PATIENT 1** and related ILS measures **PART 2/2**: shoulder internal rotation, elbow flexion and elbow extension. Bars are muscle synergies and curves are activation coefficients. Red elements belong to the control structure of the paretic arm and grey elements to the unaffected arm. The numbers indicated





**Figure 93** Graphical representation of the control structure of PATIENT 2 and related ILS measures  
**PART 1/2:** See the legend of Figure 91 for a complete and detailed description of the figure.



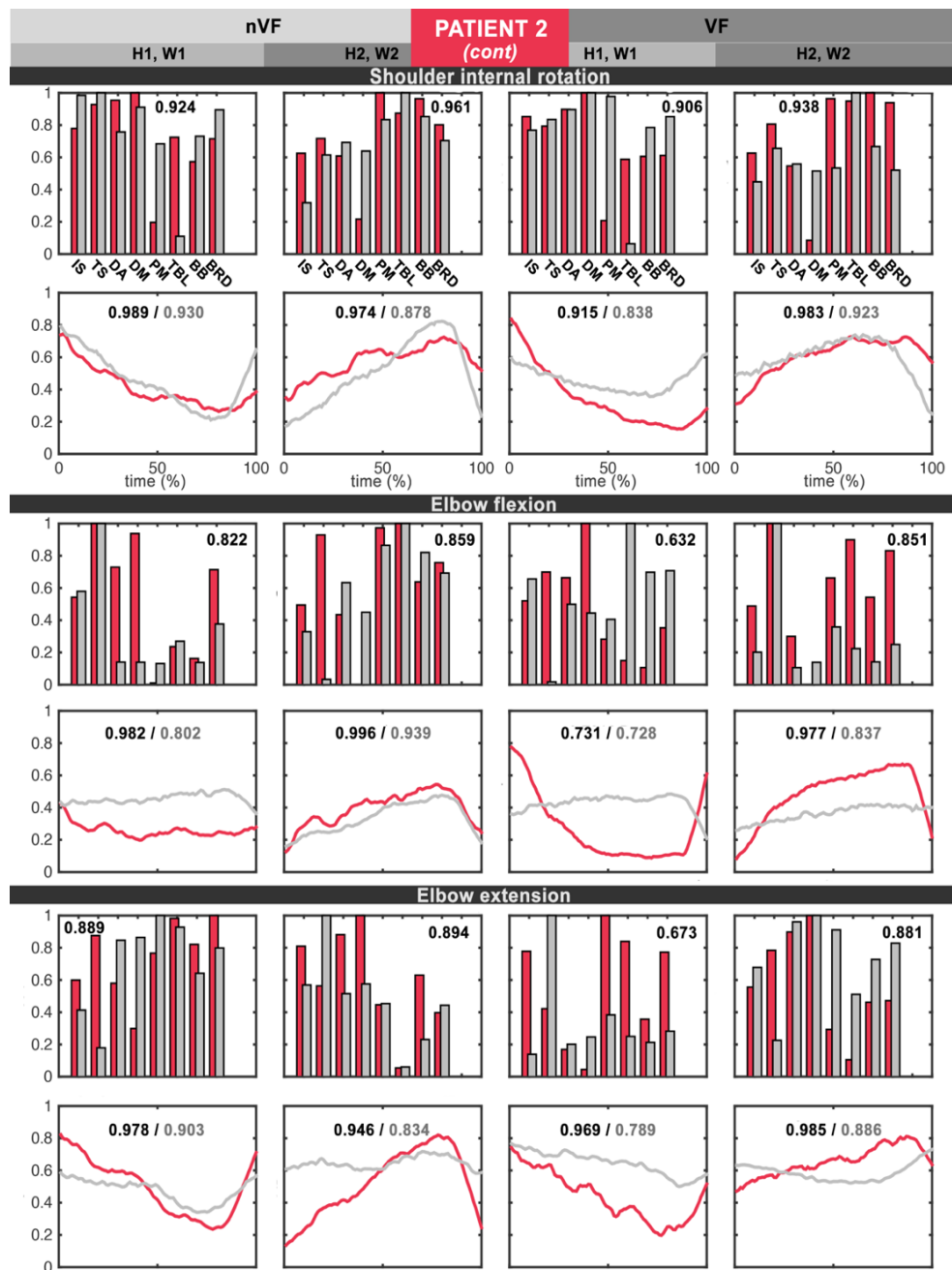


Figure 94 Graphical representation of the control structure of PATIENT 2 and related ILS measures PART 2/2: See the legend of Figure 92 for a complete and detailed description of the figure.



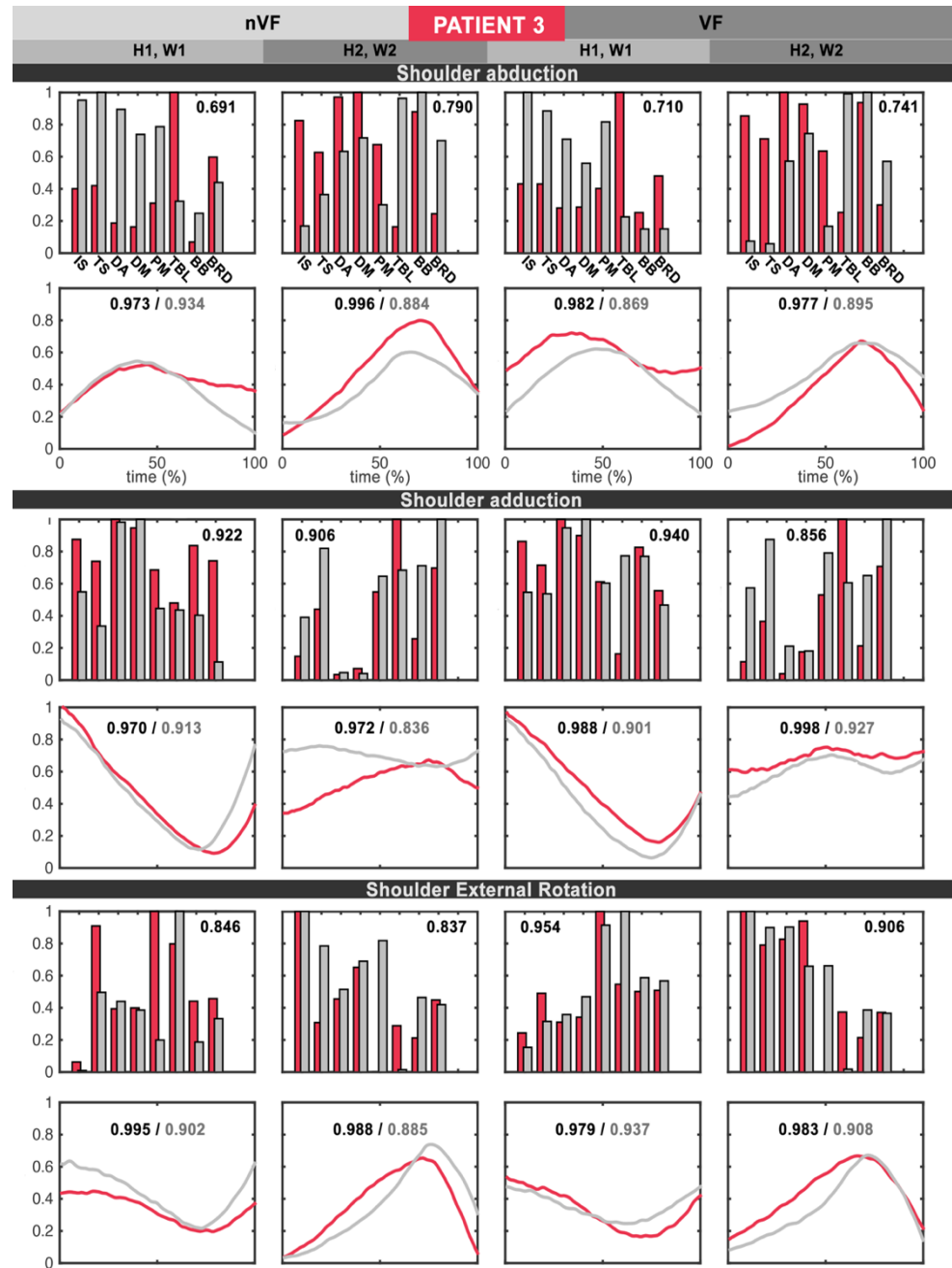


Figure 95 Graphical representation of the control structure of PATIENT 3 and related ILS measures  
 PART 1/2: See the legend of Figure 91 for a complete and detailed description of the figure.



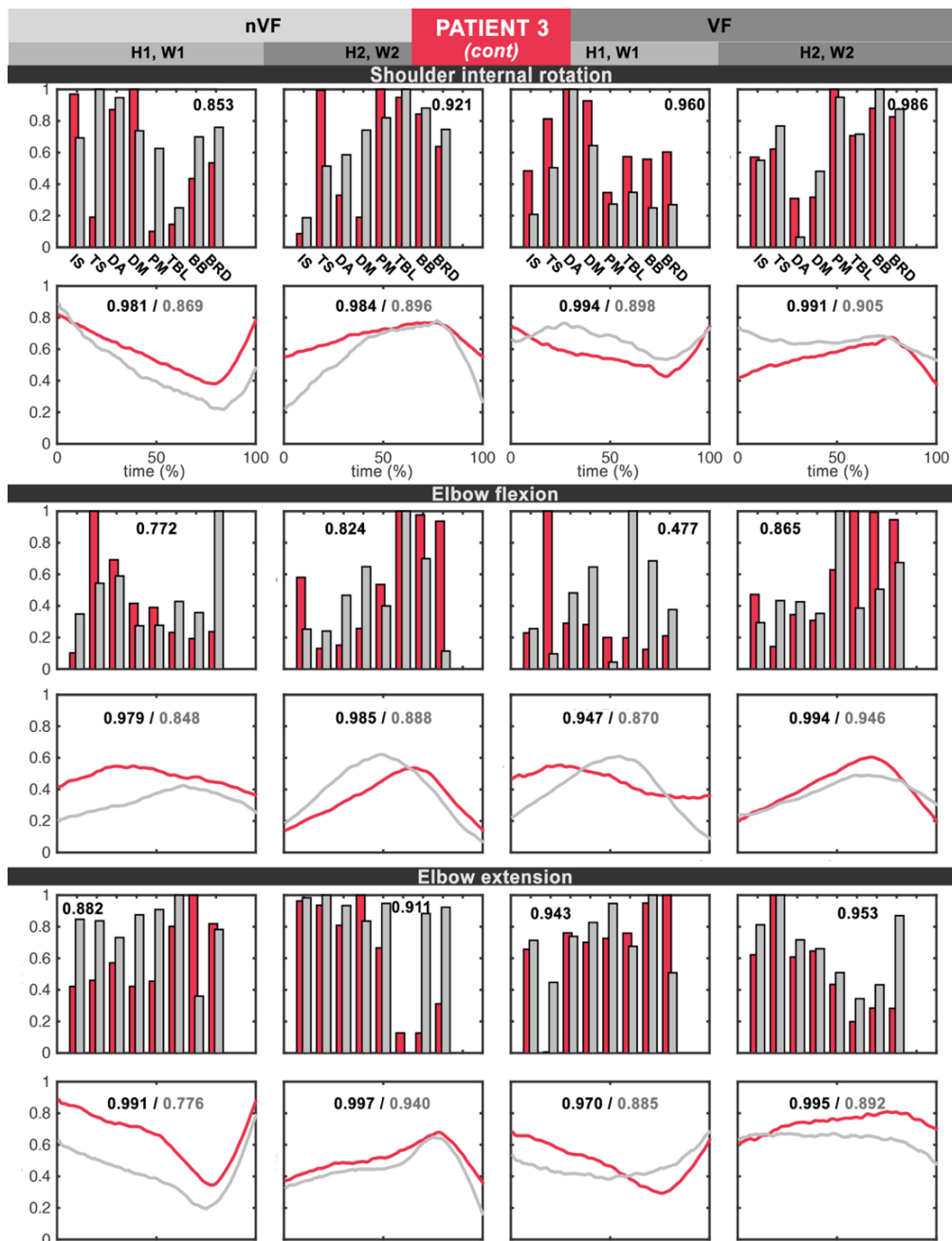


Figure 96 Graphical representation of the control structure of PATIENT 3 and related ILS measures PART 2/2: See the legend of Figure 92 for a complete and detailed description of the figure.



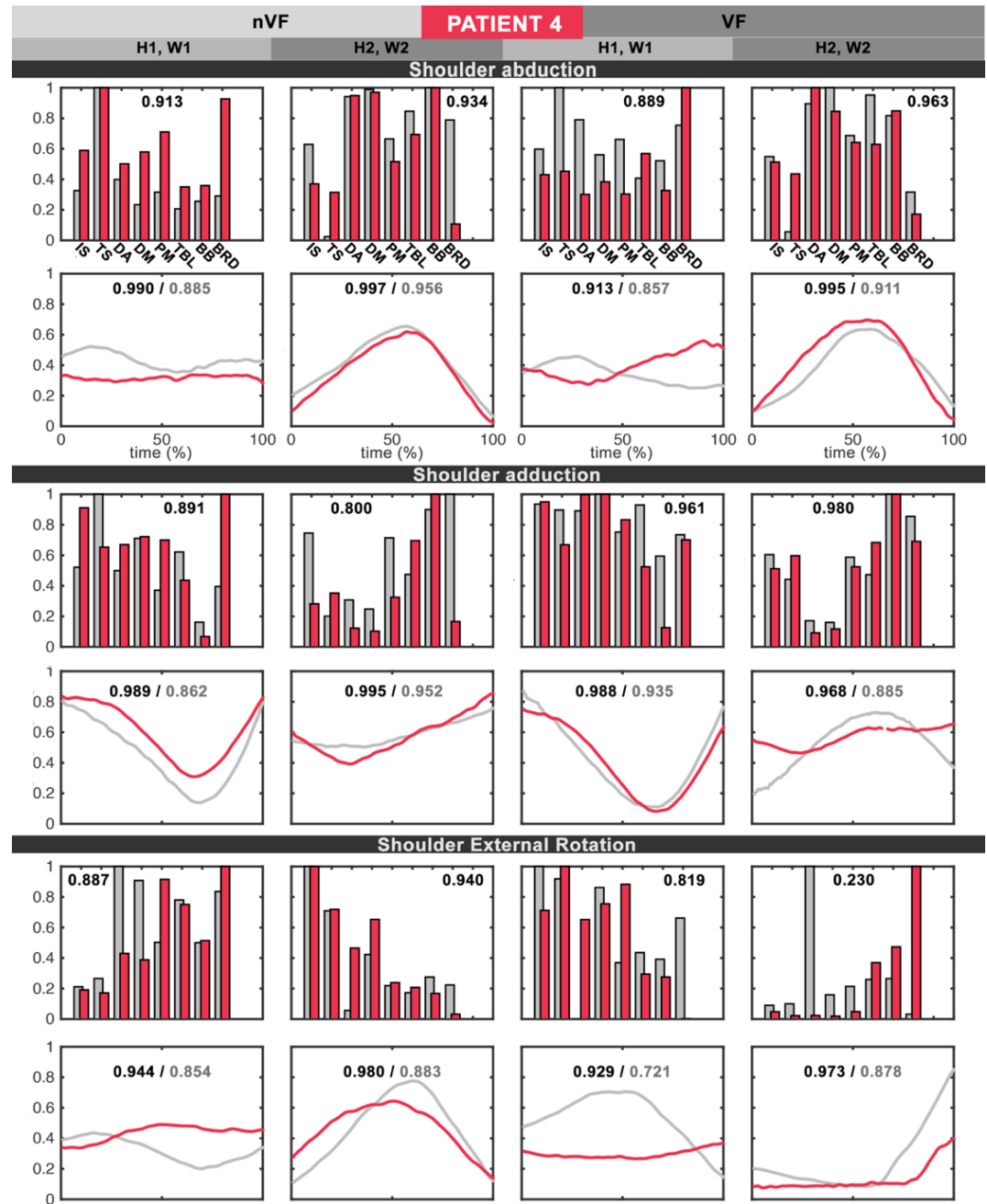


Figure 97 Graphical representation of the control structure of PATIENT 4 and related ILS measures  
 PART 1/2: See the legend of Figure 91 for a complete and detailed description of the figure.



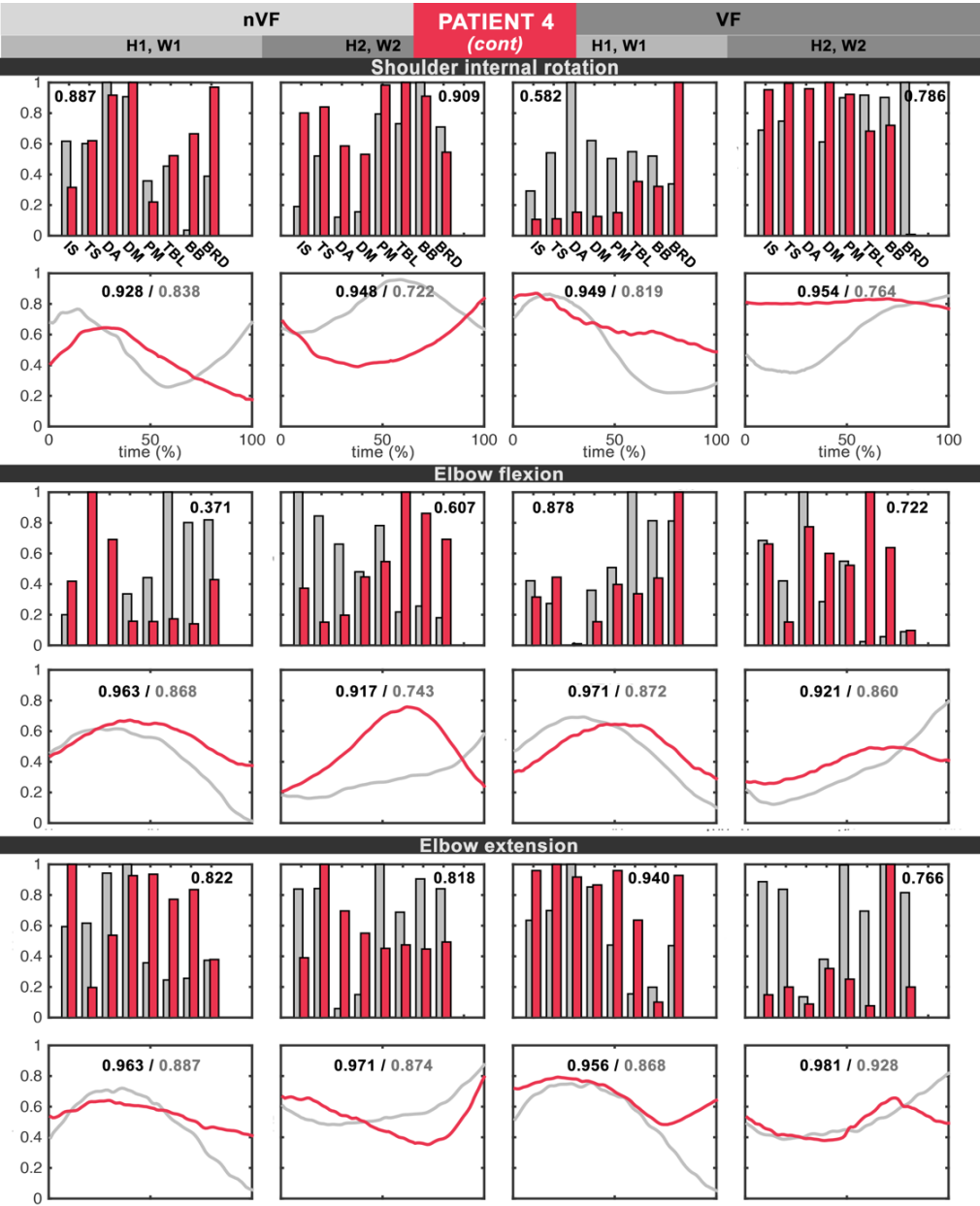


Figure 98 Graphical representation of the control structure of PATIENT 4 and related ILS measures  
PART 2/2: See the legend of Figure 92 for a complete and detailed description of the figure.



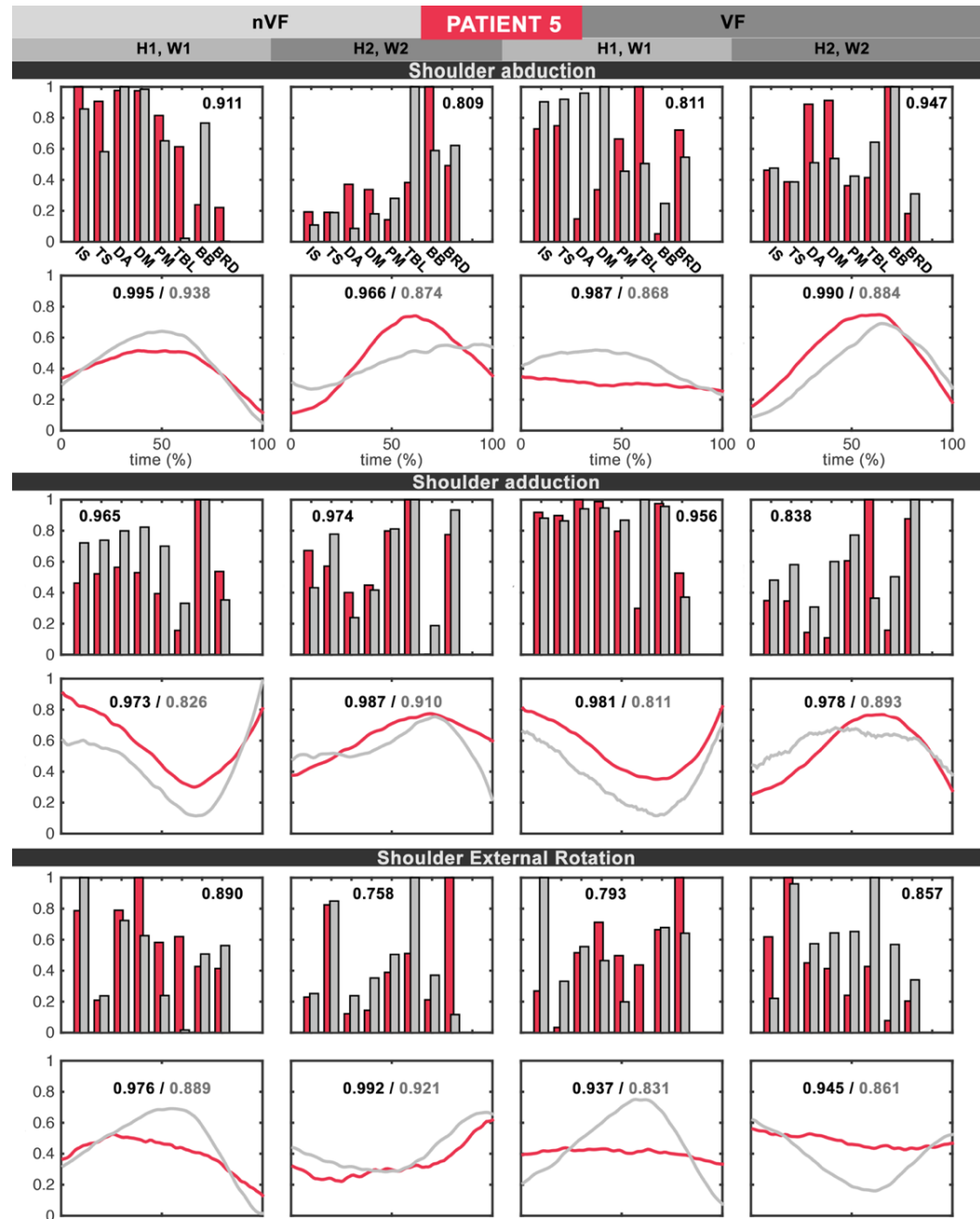


Figure 99 Graphical representation of the control structure of PATIENT 5 and related ILS measures  
PART 1/2: See the legend of Figure 91 for a complete and detailed description of the figure.



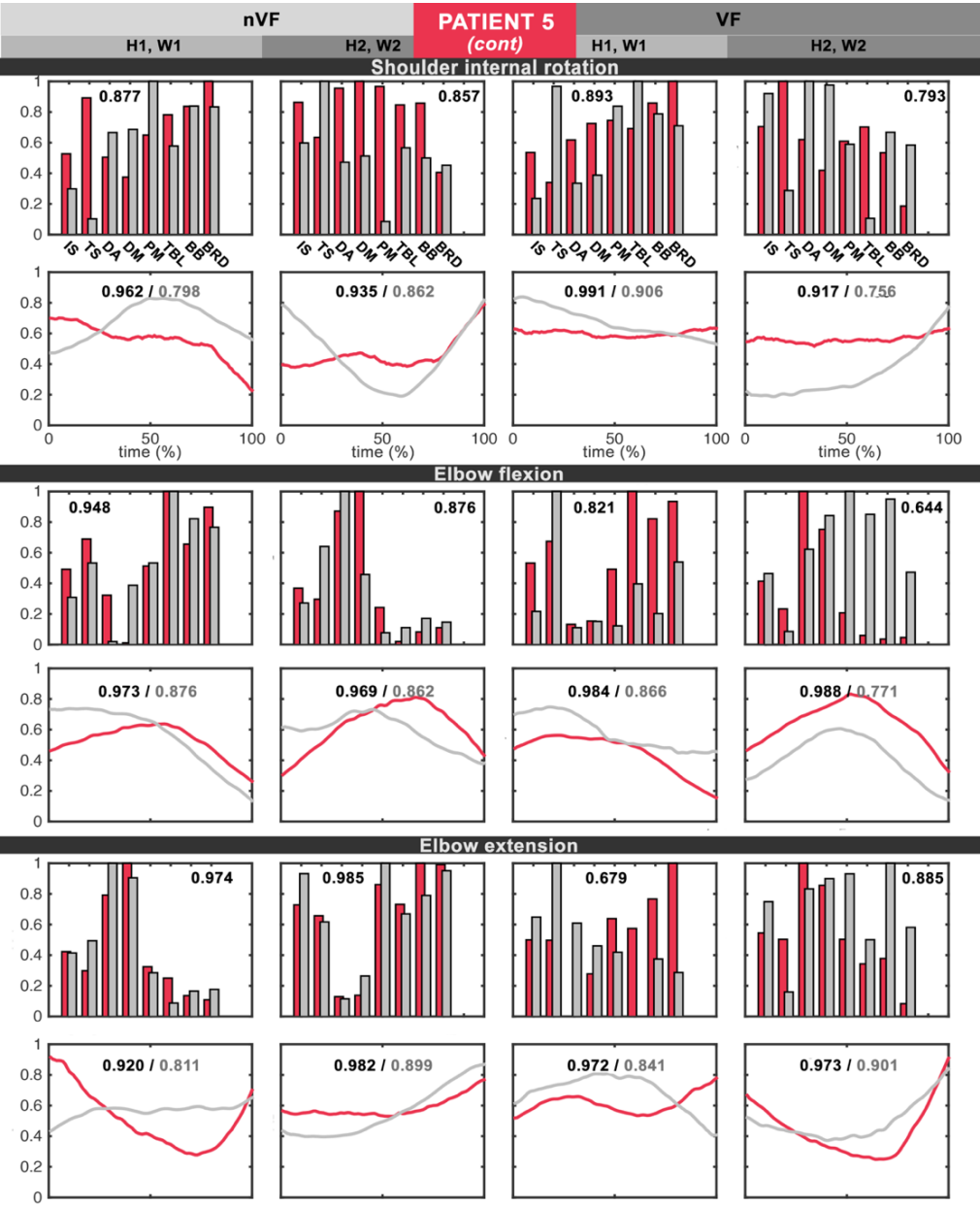


Figure 100 Graphical representation of the control structure of PATIENT 5 and related ILS measures  
PART 2/2: See the legend of Figure 92 for a complete and detailed description of the figure.



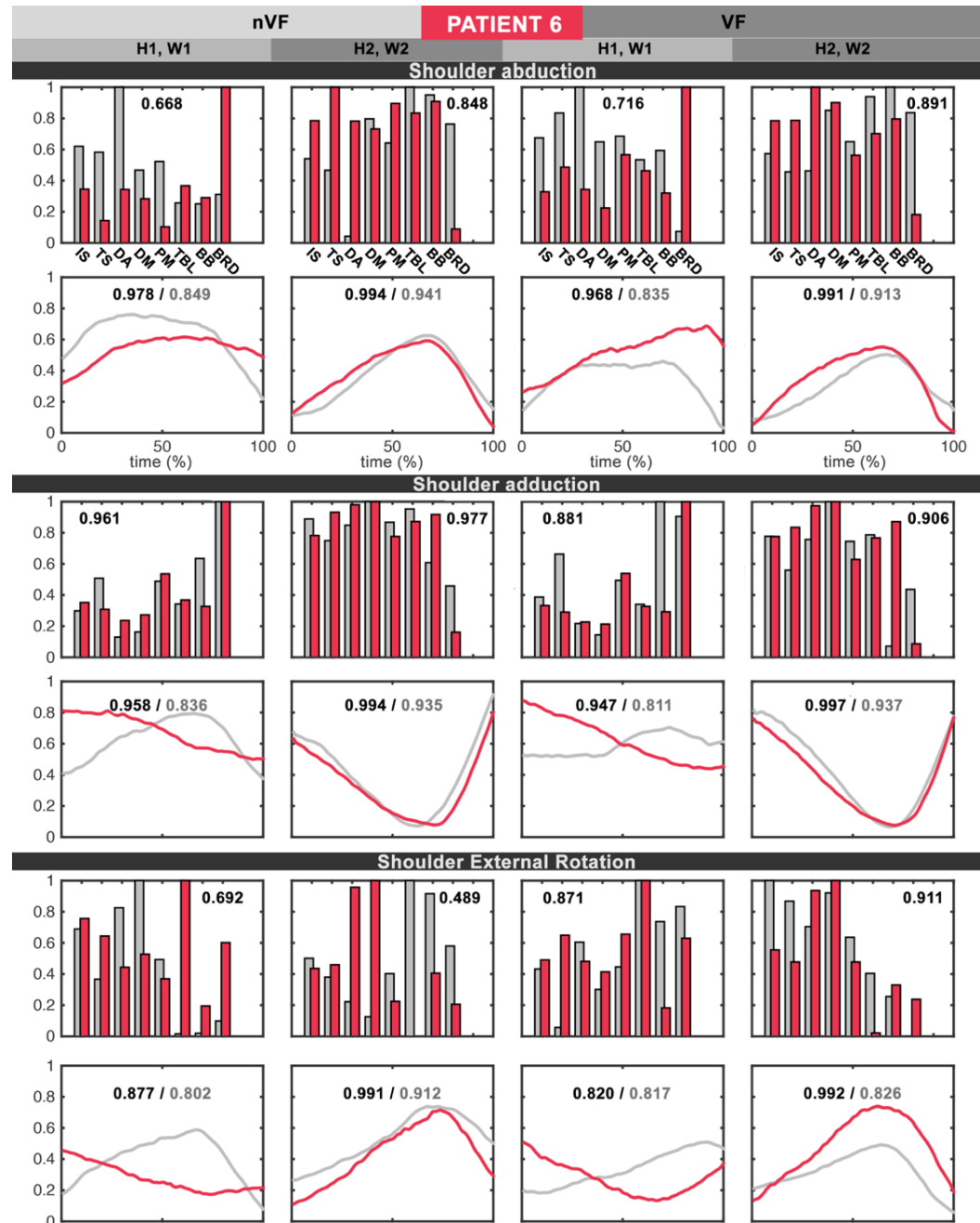


Figure 101 Graphical representation of the control structure of PATIENT 6 and related ILS measures PART 1/2: See the legend of Figure 91 for a complete and detailed description of the figure.



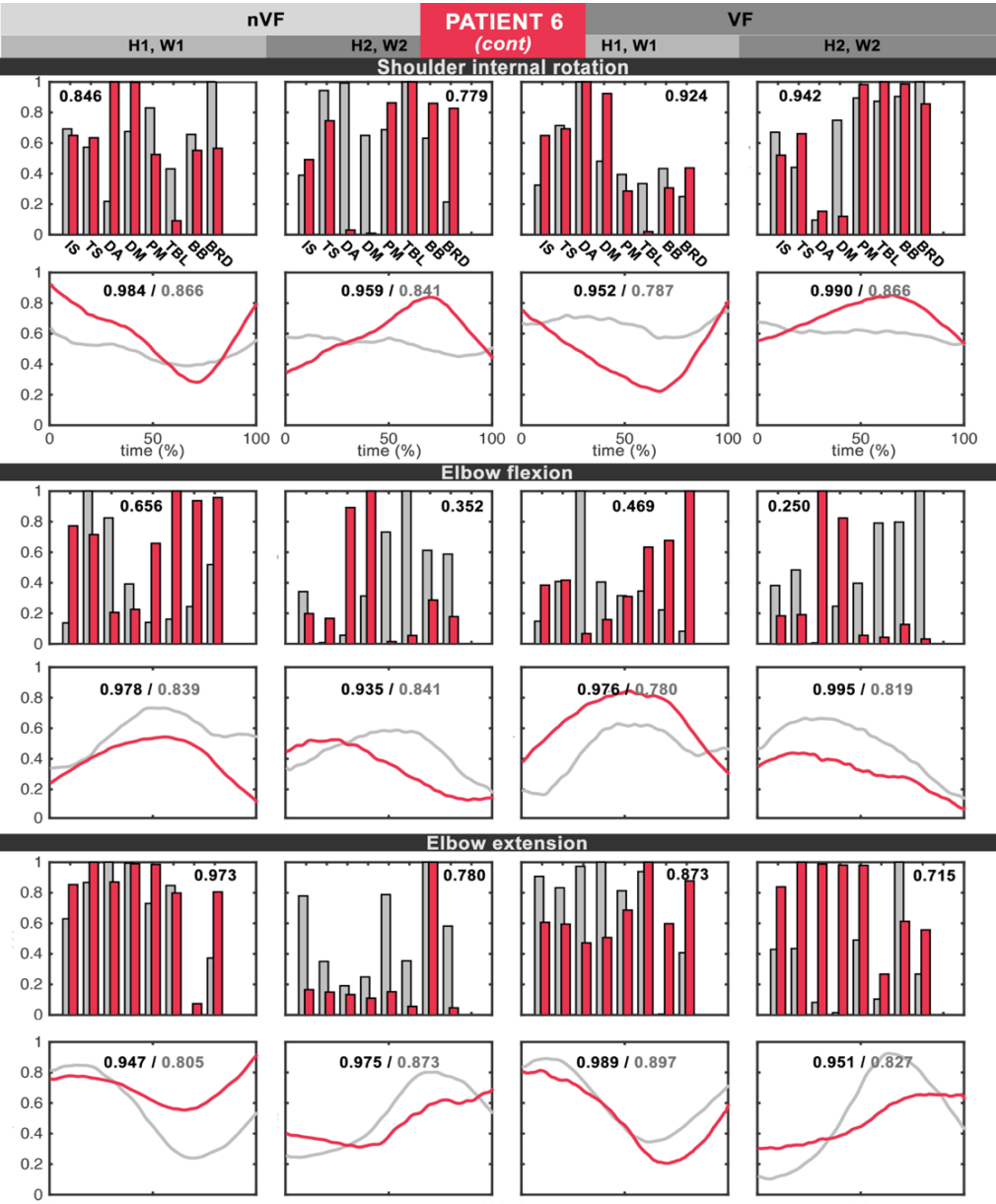


Figure 102 Graphical representation of the control structure of PATIENT 6 and related ILS measures  
PART 2/2: See the legend of Figure 92 for a complete and detailed description of the figure.



From these figures, we can qualitatively observe that the most severe patients (P2 and P4) tend to have less similar control structures in their paretic and unaffected arms, suggesting that the effect of stroke is reflected in the control structure of the paretic arm. At the level of muscle synergies, we observe a general trend on the paretic arm towards reduced muscle-weights compared to the weights of the unaffected arm. These differences in the magnitude of involvement of individual muscles within the synergies are very likely to be indicative of the characteristic weakness of the paretic arm.

On the other hand, the activation coefficients of the paretic arms, indicated in red, tend to be flatter and show a more undefined shape. See for instance Figure 92 in elbow flexion and extension, **Figure 100** in shoulder internal rotation or **Figure 101** in shoulder adduction and shoulder external rotation. It has to be noted that the activation coefficients of patient 2 show a kind of vibrations or high frequency noise that may be indicative of severe motor disability. According to the Henneman's principle, such vibrating patterns might be related to muscle weakness or insufficient frequency of excitation of the motor units<sup>230</sup>.

The last remark to do in these figures is about the utility of cross-correlation coefficients and the ILD as a measure to assess similarity between activation coefficients. From the comparison of the shapes of right and left activation coefficients, we can conclude that the cross-correlation coefficients tend to overestimate ILS. A clear example of this assertion can be found in Figure 100 during elbow extension in presence of VF. Right and left H1s resemble substantially less than right and left H2s. However, the cross-correlation coefficients are very similar in both cases (0.972 and 0.973 for H1 and H2 respectively). Paretic H1 describes a sort of convex curve first, followed by a concave curve, while unaffected H1 describes a sort of convex curve. In contrast, although paretic H2 is more pronounced, both right and left H2s describe concave curves. Such curves reveal the occurrence of diverse activation patterns that are not reflected by the cross-correlation coefficient. Instead, the ILD (in this case



expressed as  $1 - \text{ILD}$ ) reflects those differences, estimating the interlimb similarity between activation coefficients as 0.841 and 0.901 respectively.

Another good example is found in the shoulder adduction of Figure 91. Although the interlimb similarity of H1 (nVF) is higher than the interlimb similarity of H2 (VF), the cross-correlation coefficient is 0.990 in both cases while the ILD reflects such measures marking 0.935 and 0.889 respectively.

However, the ILD is not a perfect measure. In the case of the H1 of elbow flexion in absence and presence of VF in **Figure 92**, the H1s found in absence of VF are much less similar to each other than the H1s found in presence of VF, and still the ILS marks 0.894 and 0.804. This is because the ILD is biased by high differences in the amplitude of activation coefficients. In conclusion, when the amplitude changes are similar, ILD is a better estimator of shape similarity than the cross-correlation coefficients and vice-versa.



## 18.4 ILS IN PATIENTS WITH STROKE

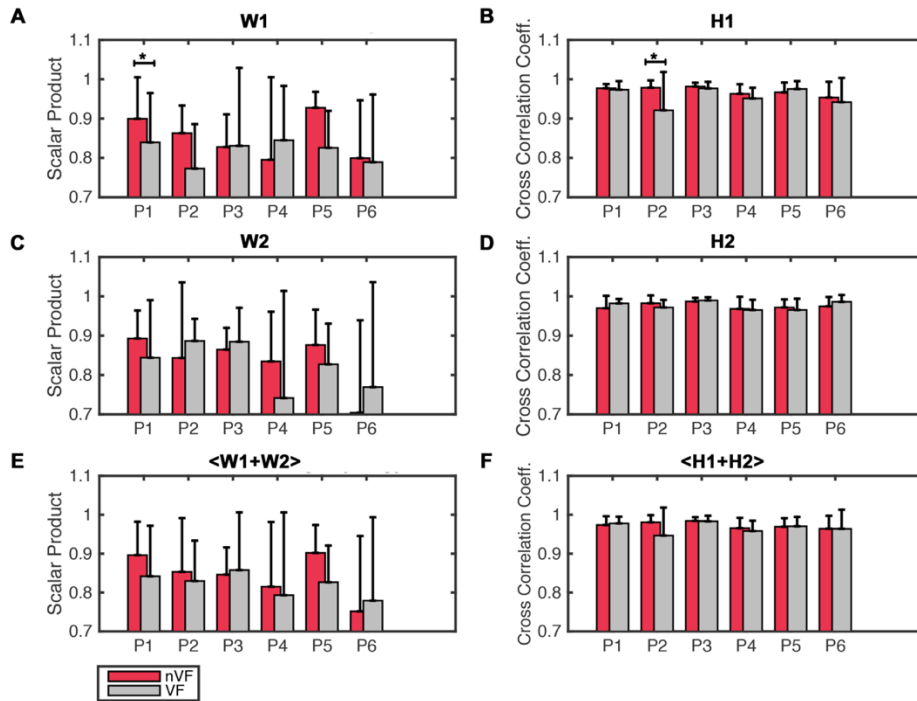
This section is aimed at studying the ILS of the control structure in patients with stroke in absence and presence of VF. In particular, we investigate whether the ILS of patients with stroke differs from the ILS of healthy subjects and whether VF has the ability to modify the ILS of muscle synergies and activation coefficients in patients with stroke.

### 18.4.1 Mean ILS: subject by subject

**Figure 103** shows the within-subject ILS of the control structure averaged across movements of each patient. In absolute terms, the ILS of the control structure is not dramatically low. In general, the ILS of muscle synergies ranges from 0.7 to 0.9 (**Figure 103E**), and the ILS of activation coefficients from 0.9 to 1 (**Figure 103F**). It has to be mentioned, though, that certain patients showed especially low ILS values in at least one of their muscle synergies. That was the case of P6 (**Figure 103C**), and P4 when using VF (**Figure 103A**).

Regarding VF, unlike in healthy subjects, the overall effect of VF in patients with stroke is to decrease the ILS of the control structure. **Figure 103E** shows that VF decreases the ILS of synergies in 4 out of 6 subjects. In the case of the activation coefficients (**Figure 103F**), the effect of VF is not dramatic. Only in patient 2, one can clearly observe that VF decreases his ILS; for the rest of the patients the effect of VF is less appreciable. However, P1 and P5 experience a slight increase in their ILS due to VF while P3, P4 and P6 experience slight decrease.





**Figure 103** Per subject ILS of A – Synergy 1, B – Activation coefficient 1, C – Synergy 2, D – Activation Coefficient 2, E – Average ILS of synergies 1 and 2, F – Average ILS of activation coefficients 1 and 2. Bars are mean ILS averaged across the 6 movements of each patient (P1-P6) +/- SD. Red bars represent the ILS found in absence of VF and grey bars represent the ILS found in presence of VF. \*  $p < 0.05$  for Wilcoxon Signed Rank test.

Wilcoxon signed rank tests determined that the effect of VF was only statistically significant in the case of the ILS of W1 in patient 1 (**Figure 103A**) and the ILS of H1 in patient 2 (**Figure 103B**). In both cases, VF decreases the ILS of these patients. **Table 35** shows the p-values of all patients resulting from the Wilcoxon signed rank tests.



P-VALUES OF WILCOXON SIGNED RANK TEST						
	P1	P2	P3	P4	P5	P6
W1	0.0313	0.1563	0.4375	0.6875	0.0938	0.6875
W2	0.5625	0.4375	0.5625	0.8438	0.5625	0.8438
<W1, W2>	0.0640	0.1514	0.2334	0.9697	0.9023	1
H1	0.8438	0.0313	0.5625	0.6875	0.5625	0.3125
H2	0.4375	0.4375	0.6875	1	0.8438	0.4375
<H1, H2>	0.7910	0.0522	0.9097	0.6221	0.8501	0.7910

**Table 35** p-values of Wilcoxon rank test comparing ILS in absence and presence of VF for each subject across the 6 movements. Significant results ( $p < 0.05$ ) are highlighted in orange. Wi, *ith* muscle synergy; Hi, *ith* activation coefficient (See Equation (4)); <X,Y>, mean value of X and Y.

Because we found that ILS depends on the movement analyzed (see subsection 18.4.2 Which factors affect the ILS of the control structure?), we hypothesized that the lack of statistical significance could be due to the fact that within the same subject the effect of VF may be different depending on the movement executed. Thus, we grouped the ILS of each patient in 2 groups: on the one hand, we grouped the ILS values of movements for which VF increased ILS and on the other hand, the ILS values of movements for which VF decreased ILS. Then, we repeated the Wilcoxon Signed Rank tests for each group separately (Table 36).

P-VALUES OF WILCOXON SIGNED RANK TEST IN GROUPED DATA							
GROUP		P1	P2	P3	P4	P5	P6
VF ↑ ILS	<W1, W2>	0.5000	0.5000	0.0625	0.1250	0.2500	0.0625
	<H1, H2>	0.2500	0.5000	0.1250	0.1250	0.0625	0.5000
VF ↓ ILS	<W1, W2>	0.0020	0.0020	0.3594	0.1563	0.0020	0.0586
	<H1, H2>	0.6074	0.0020	0.1563	0.0098	0.0254	0.2324

**Table 36** Grouped p-values of the Wilcoxon rank test comparing ILS in absence and presence of VF for each subject across the 6 movements. Data was grouped depending on whether VF increased (GROUP 1) or decreased (GROUP 2) ILS. Significant results ( $p < 0.05$ ) are highlighted in orange. Wi, *ith* muscle synergy; Hi, *ith* activation coefficient (See Equation (4)).

Results in Table 36 reveal two different scenarios. On the one hand, the ILS change in movements for which VF increases ILS is not statistically significant indicating that either the effect of VF is negligible, or there is another interfering factor that hinders achieving statistical significance. On the other hand, the ILS changes in



movements for which VF decreases ILS are very often statistically significant indicating that when the effect of VF is relevant, VF tends to significantly reduce the original similarity between the control structure of the paretic and the unaffected arm.

It is remarkable that the two patients showing a statistically significant decrease in the ILS of their muscle synergies and activation coefficients are patients whose brain damage is located in the right hemisphere. Interestingly, it has been suggested that the right hemisphere might play a role in the processing of the spatial information for both the left and right visual fields<sup>231,232</sup>. In particular, it seems that the right-hemisphere is crucial for sensory-feedback dependent closed-loop control of movements. In effect, patients were asked to use the VF to correct the paretic movements according to the position and trajectories described by the unaffected arm. Thus, the inability to use the visual information shown by these patients support the idea that the right hemisphere is specialized in sensory-mediated closed-loop mechanisms.

#### 18.4.2 *Which factors affect the ILS of the control structure?*

We carried out N-Way analysis of variance in order to detect possible interactions between factors (subjects, movements) and the effect of VF. In particular, we applied N-way ANOVA tests on 6 different datasets:

1. W1: ILS measures of W1s
2. W2: ILS measures of W2s
3. [W1, W2]: Concatenated ILS measures of W1 and W2 [ $ILS_{W1}$  ;  $ILS_{W2}$ ]
4. H1: ILS measures of H1s
5. H2: ILS measures of H2s
6. [H1, H2]: Concatenated ILS measures of H1 and H2 [ $ILS_{H1}$  ;  $ILS_{H2}$ ]



Results of the 6 N-way ANOVA tests may be found in tables **Table 37 -Table 39**. These results reveal a significant interaction ( $p < 0.05$ ) of movement types (*Movement*) in all cases except in the ILS of H1, for which no interaction factor was observed. However, this result can be disregarded as the concatenated case of activation coefficients ([H1, H2]) include the interaction of movement. In addition, in the concatenated case of synergies ([W1, W2]) we found a significant interaction of subjects and a significant mixed interaction of subjects and movements (*Subj x Movem*). These results bring to light the need to analyze the ILS measures separately for each movement and subject.

N-WAY ANOVA	DATASET: ILS OF W1				DATASET: ILS OF W2			
	Sum of Squares	d.f.	F	Prob > F	Sum of Squares	d.f.	F	Prob > F
Subject	0.0615	5	0.94	0.4698	0.1876	5	1.89	0.1323
Movement	0.4249	5	6.52	<b>0.0005</b>	0.5180	5	5.21	<b>0.0021</b>
Condition	0.0219	1	1.69	0.2058	0.0020	1	0.10	0.7539
Subj x Movem	0.3081	25	0.95	0.5547	0.5297	25	1.07	0.4368
Subj x Cond	0.0522	5	0.80	0.5596	0.0580	5	0.58	0.7120
Movem x Cond	0.0192	5	0.29	0.9112	0.0184	5	0.19	0.9654
Error	0.3258	25			0.4967	25		
Total	1.2137	71			1.8104	71		

**Table 37 Results of N-WAY ANOVA tests performed on ILS measures of synergies W1 and W2.** Significant p-values are highlighted in bold. d.f. degrees of freedom.



N-WAY ANOVA	DATASET: CONCATENATED ILS OF [W1, W2]				DATASET: CONCATENATED ILS OF [H1, H2]			
	Sum of Squares	d.f.	F	Prob > F	Sum of Squares	d.f.	F	Prob > F
Subject	0.1941	5	2.91	<b>0.0170</b>	0.0087	5	1.65	0.1534
Movement	0.8661	5	13	<b>0.0000</b>	0.0109	5	2.05	<b>0.0778</b>
Condition	0.0186	1	1.4	0.2401	0.0014	1	1.33	0.2520
Subj x Movem	0.5810	25	1.74	<b>0.0288</b>	0.0219	25	0.83	0.6989
Subj x Cond	0.0449	5	0.67	0.6446	0.0060	5	1.14	0.3461
Movem x Cond	0.0273	5	0.41	0.8413	0.0030	5	0.57	0.7262
Error	1.2925	97			0.1026	97		
Total	3.0246	143			0.1545	143		

Table 38 Results of N-WAY ANOVA tests performed on the concatenated ILS measures of synergies W1 and W2; and activation coefficients H1 and H2. Significant p-values are highlighted in bold. d.f. degrees of freedom.

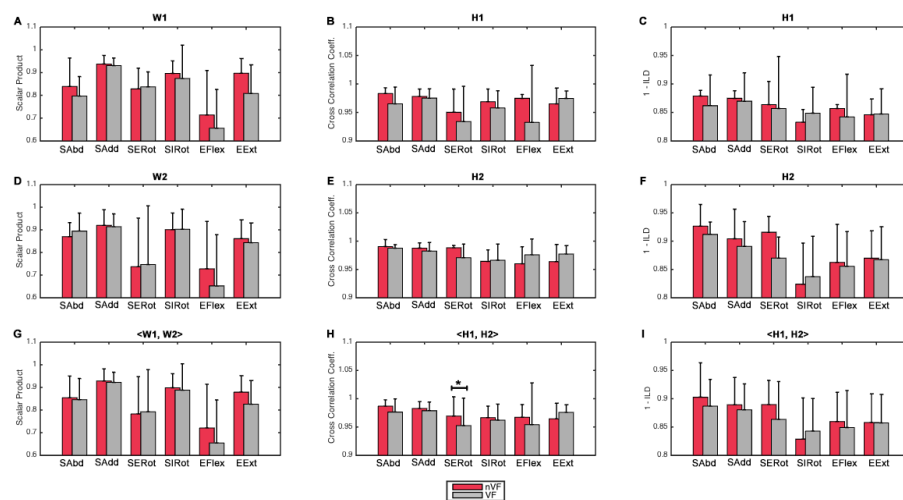
N-WAY ANOVA	DATASET: ILS OF H1				DATASET: ILS OF H2			
	Sum of Squares	d.f.	F	Prob > F	Sum of Squares	d.f.	F	Prob > F
Subject	0.0110	5	1.8	0.1491	0.0038	5	2.54	0.0543
Movement	0.0106	5	1.74	0.1632	0.0057	5	3.83	<b>0.0103</b>
Condition	0.0033	21	2.69	0.1132	0.000	1	0.06	0.8022
Subj x Movem	0.0471	25	1.54	0.1428	0.0133	25	1.8	0.0745
Subj x Cond	0.0078	5	1.28	0.3050	0.0013	5	0.89	0.5005
Movem x Cond	0.0045	5	0.73	0.6053	0.0023	5	1.56	0.2066
Error	0.0305	25			0.0074	25		
Total	0.1147	71			0.0338	71		

Table 39 Results of N-WAY ANOVA tests performed on ILS measures of activation coefficients H1 and H2. Significant p-values are highlighted in bold. d.f. degrees of freedom.



### 18.4.3 Mean ILS: movement by movement

Because we found significant interaction of subjects and movement-types with ILS values, the results described in this section are separately exposed for subjects and movements. First of all, we grouped the ILS measures of all patients for each movement and we calculated the mean ILS per movement separately for muscle synergies and activation coefficients (**Figure 104**).



**Figure 104 Mean ILS measures calculated for each movement.** ILS measures are expressed as scalar products for synergies (A, D, G), as cross-correlation coefficients for activation coefficients (B, E, H) and as  $1 - \text{ILD}$  for activation coefficients (C, F, I). Bars are mean ILS of all patients  $\pm$  SD. Red bars represent movements performed in absence of VF and grey bars represent movements performed in presence of VF. The ILS of the last row plots are calculated by averaging the ILSs of both G - synergies and H, I - activation coefficients. \*  $p < 0.05$  for Wilcoxon Signed Rank test.

At the level of muscle synergies, the effect of VF is negligible during the movements involving the shoulder. In contrast, during elbow flexion and extension, VF tends to decrease the ILS. On the other hand, at the level of activation coefficients the effect of VF is more evident, especially when the ILS is measured as  $1 - \text{ILD}$ . In this case, we observed a general trend to ILS reduction due to VF. In particular, VF decreased the ILS in all movements except in elbow extension (if the ILS was measured as cross-correlation coefficient, **Figure 104H**), and shoulder internal rotation and elbow



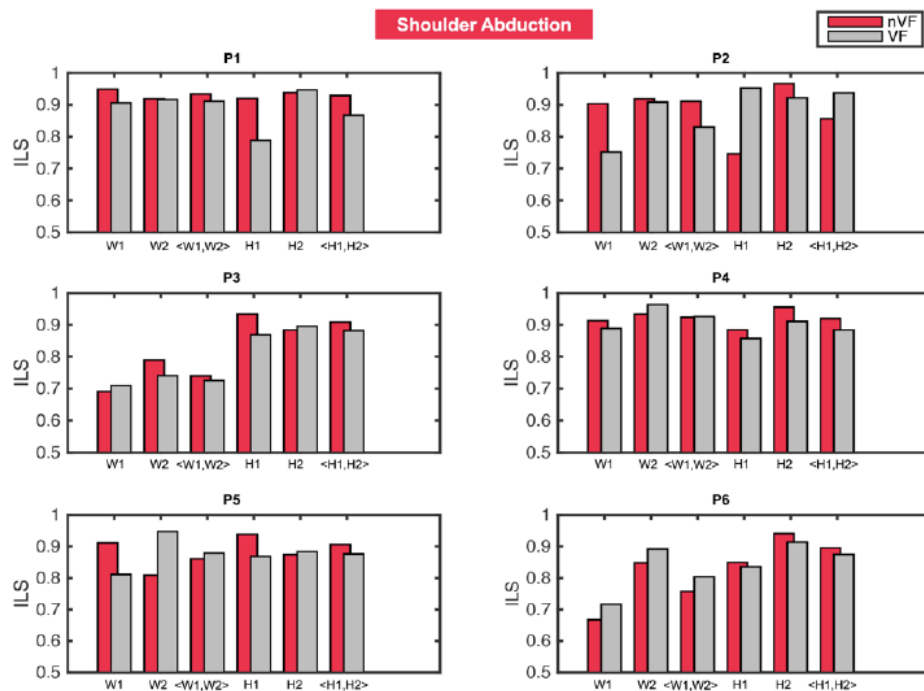
extension (if the ILS was measured as  $1 - \text{ILD}$ , **Figure 104I**). Wilcoxon-signed rank test only identified as significant the ILS decrease induced by VF in activation coefficients during shoulder external rotation.

The following set of figures analyzes the ILS of each movement at individual level. In this case, the ILS of activation coefficients is expressed as  $1 - \text{ILD}$  because, as we observed in **Figure 104**, the effect induced by VF on ILS can be better appreciated. This level of detail allows identifying inter-patient differences from the average trend of each movement. Indeed, the individual response of patients to VF is very variable even for the same movement:

- During shoulder abduction (**Figure 105**), the effect of VF is very small. However, P1 and P4 reduce their ILS of the activation coefficients due to VF, whereas P6 is able to increase his muscle synergies ILS with the aid of VF.
- During shoulder adduction (**Figure 106**), the effect of VF is also minimal. However, P2, P5 and P6 reduce the ILS of at least one component of the control structure, while P3 and P5 are able to increase their ILS.
- During shoulder external and internal rotation (**Figure 107** and **Figure 108**), the population is fairly divided. P3 and P6 are able to increase the ILS of at least one component with the aid of VF in both movements, whereas P4 and P5 decrease their ILS in both movements.
- During elbow flexion and extension (**Figure 109** and **Figure 110**), the general effect of VF is to decrease the ILS. However, P4 is again able to increase his ILS in both movements.



It is remarkable that P3 was able to increase the ILS of at least one component of the control structure in 4 movements, P4 in 3 movements and P6 in 3 movements, suggesting that some patients are more prone to benefit from the use of VF than others, at least in absence of previous training. Indeed, it is generally accepted that task- and performer-related factors influence the control mechanism, and therefore, the outcome of each movement<sup>233</sup>. Taken into account that our personal experiences induce changes in the motor cortex<sup>234,235</sup> and that we activate diverse lateralization patterns depending on task complexity<sup>236</sup>, it is reasonable to find substantial inter-subject and inter-movement differences in the ILS. In fact, in the questionnaires handed out after the experiments, patients describe fairly different experiences in front of the same experimental protocol.



**Figure 105 Within-subject ILS measures during SHOULDER ABDUCTION.** Bars are ILS measures (scalar product for synergies and  $1 - \text{ILD}$  for activation coefficients) of shoulder abduction for each patient (P1-P6). <W1,W2> and <H1,H2> represent the averaged ILS of the two synergies or activation coefficients respectively. Red bars represent movements performed in absence of VF and grey bars represent movements performed in presence of VF.



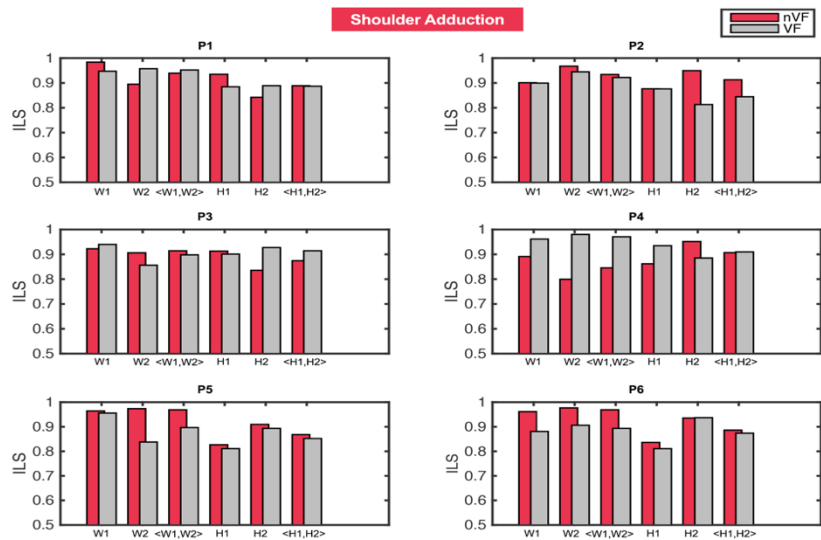


Figure 106 Within-subject ILS measures during SHOULDER ADDUCTION. See the legend of Figure 105 for a complete and detailed description of the figure.

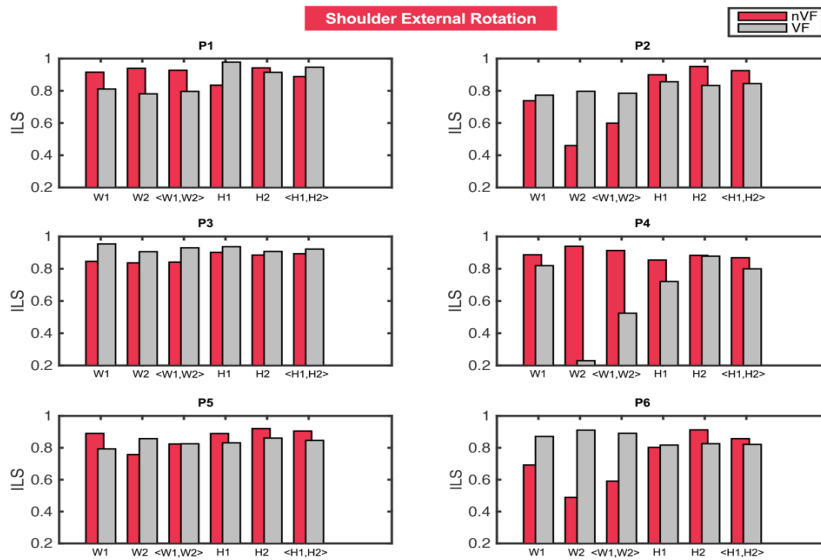
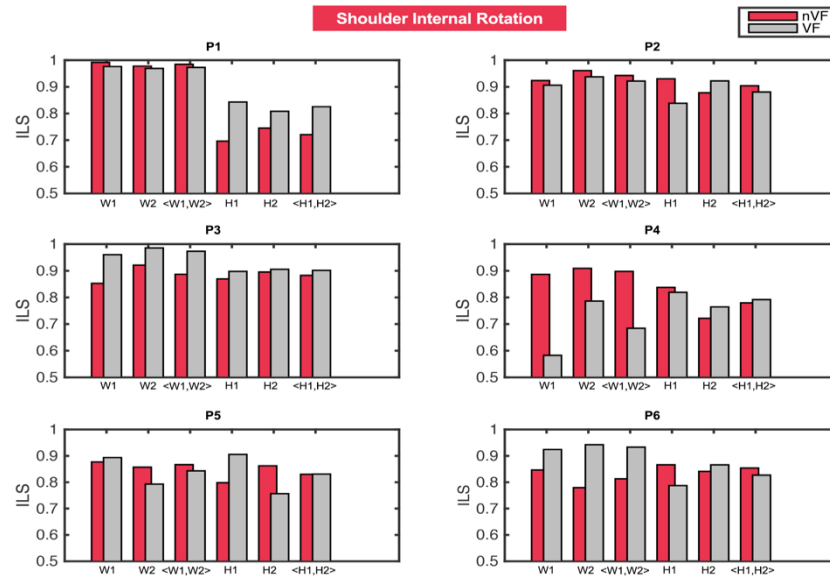
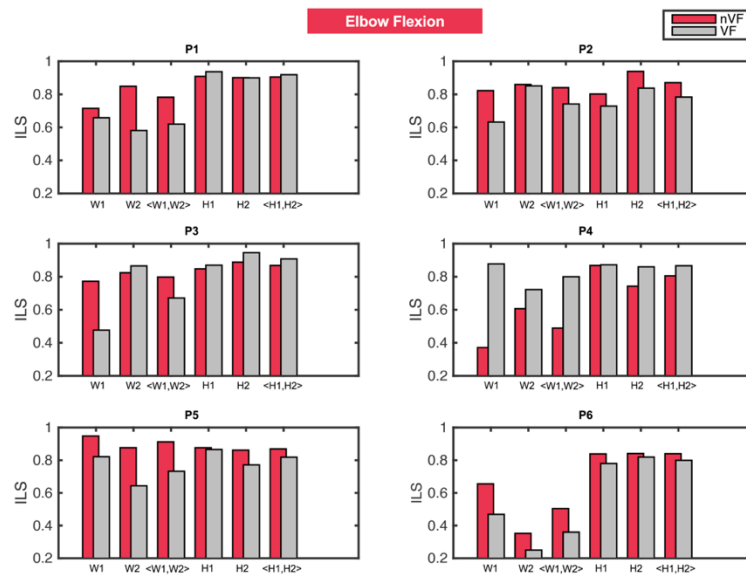


Figure 107 Within-subject ILS measures during SHOULDER EXTERNAL ROTATION. See the legend of Figure 105 for a complete and detailed description of the figure.



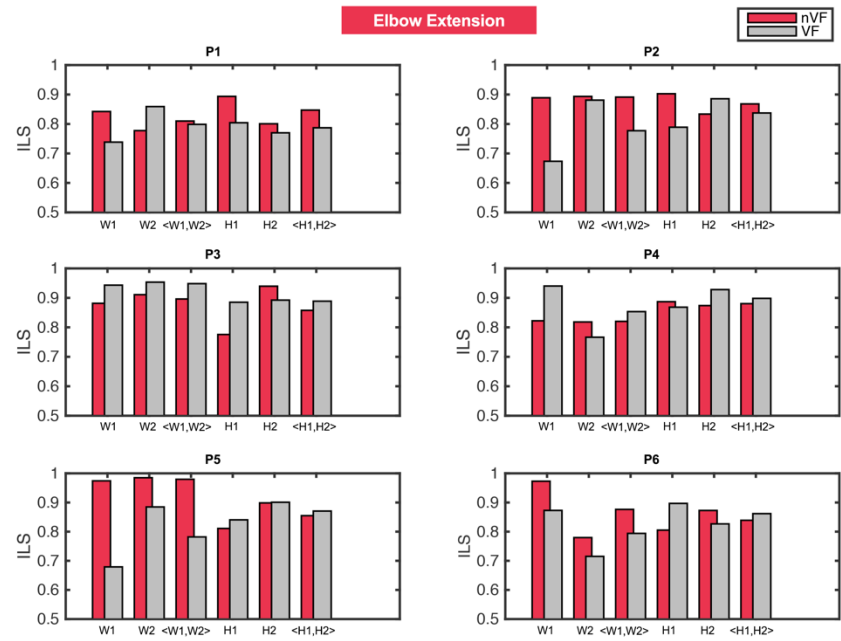


**Figure 108** Within-subject ILS measures during **SHOULDER INTERNAL ROTATION**. See the legend of **Figure 105** for a complete and detailed description of the figure.



**Figure 109** Within-subject ILS measures during **ELBOW FLEXION**. See the legend of **Figure 105** for a complete and detailed description of the figure.



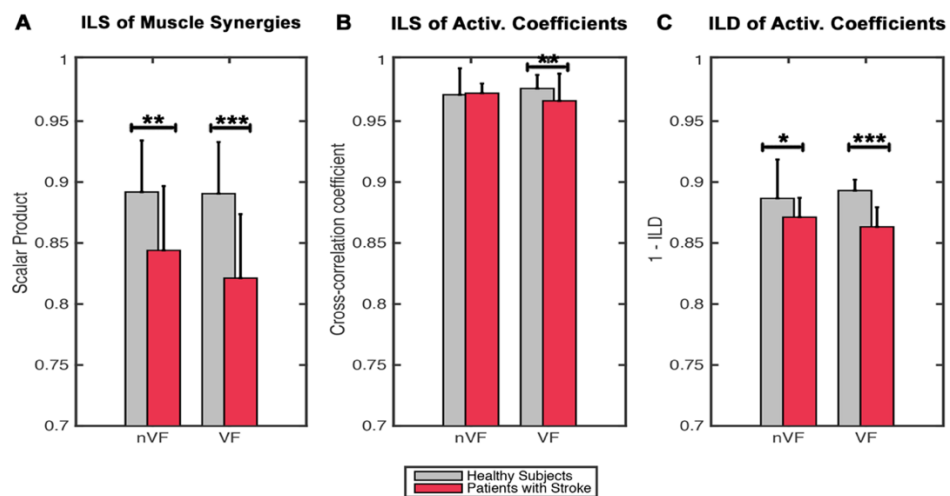


**Figure 110** Within-subject ILS measures during elbow extension. See the legend of **Figure 105** for a complete and detailed description of the figure.



## 18.5 MEAN ILS: STROKE PATIENTS VS HEALTHY SUBJECTS

As already highlighted in previous sections, the magnitude of the ILS found in patients with stroke was not dramatically low. In absence of VF, this was  $84.44 \pm 5.27$  % and  $97.29 \pm 0.8$  % for muscle synergies and activation coefficients respectively, and in presence of VF  $82.13 \pm 5.24$  % and  $96.66 \pm 2.23$  %. However, when comparing these values to the corresponding values from healthy subjects, we realized that the ILS of patients with stroke were generally lower. In healthy subjects the average ILSs found were  $89.19 \pm 4.22$  % and  $97.16 \pm 2.17$  % for muscle synergies and activation coefficients respectively in absence of VF; and  $89.05 \pm 4.23$  % and  $97.68 \pm 1.11$  % for muscle synergies and activation coefficients respectively in presence of VF (**Figure 111**).



**Figure 111 ILS of Patients with Stroke compared to ILS of Healthy Subjects.** A – ILS of muscle synergies measured as scalar products. B – ILS of activation coefficients measured as cross-correlation coefficients. C – 1-ILD of activation coefficients measures as 1 - ILD. Bars are mean measures of all subjects and movements per database  $\pm$  SD. Statistical significance was estimated using Wilcoxon rank-sum test: \*  $p < 0.05$ , \*\*  $p < 0.01$ , \*\*\*  $p < 0.001$ .

In the case of the ILS of activation coefficients measured as 1-ILD (equation ( 10 )), healthy subjects exhibited an ILS of  $88.66 \pm 3.19$  % and  $89.30 \pm 0.90$  %, and patients an ILS of  $87.13 \pm 1.58$  % and  $86.33 \pm 1.61$  % in absence and presence of VF respectively.



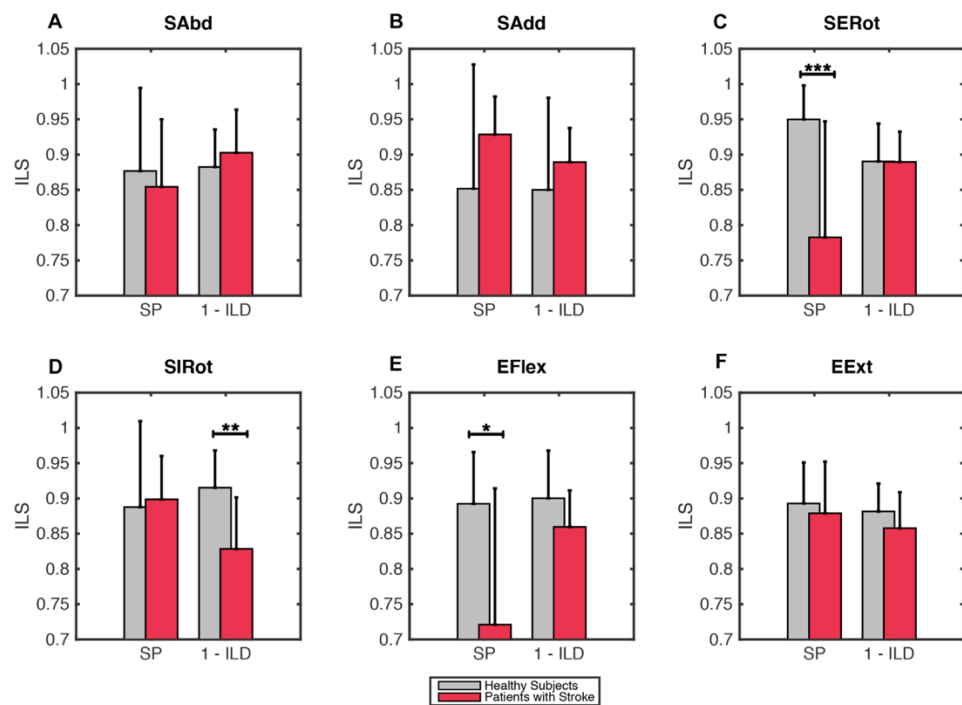
Indeed, when we compared both populations, significant differences arose. Patients with stroke exhibited a significantly lower ILS in muscle synergies both in absence ( $p < 0.01$ ) and presence of VF ( $p < 0.001$ ). These differences were up to the 5-7% of the ILS of healthy subjects. On the other hand, the differences found at the level of activation coefficients were better reflected by ILD measures. In this case, the ILS of activation coefficients of patients with stroke was also significantly lower both in absence ( $p < 0.05$ ) and presence of VF ( $p < 0.001$ ). In magnitude, these differences were up to 2-4% of the ILS of healthy subjects. When the ILS was measured with cross-correlation coefficients, differences between population were only found significant in presence of VF ( $p < 0.01$ ).

Taking everything together, from these results one can conclude that although the ILS of the control structure tends to be high in magnitude, stroke significantly decreases the ILS of the control structure, suggesting that ILS measures could constitute a potential marker of hemiparesis. On the other hand, these results also indicate that the ILD is more sensitive detecting abnormal ILS of activation coefficients than the cross-correlation coefficients in patients with stroke.



### 18.5.1 Inter-group ILS breakdown: movement by movement

Given the diagnostic potential of the ILS revealed in **Figure 111** and the inter-movement differences shown previously, we considered essential to translate movement effects to the frame of the comparisons of the ILS of patients and healthy subjects. Thus, in this section, we investigated the differences between the ILS of healthy subjects and patients for each movement in depth.



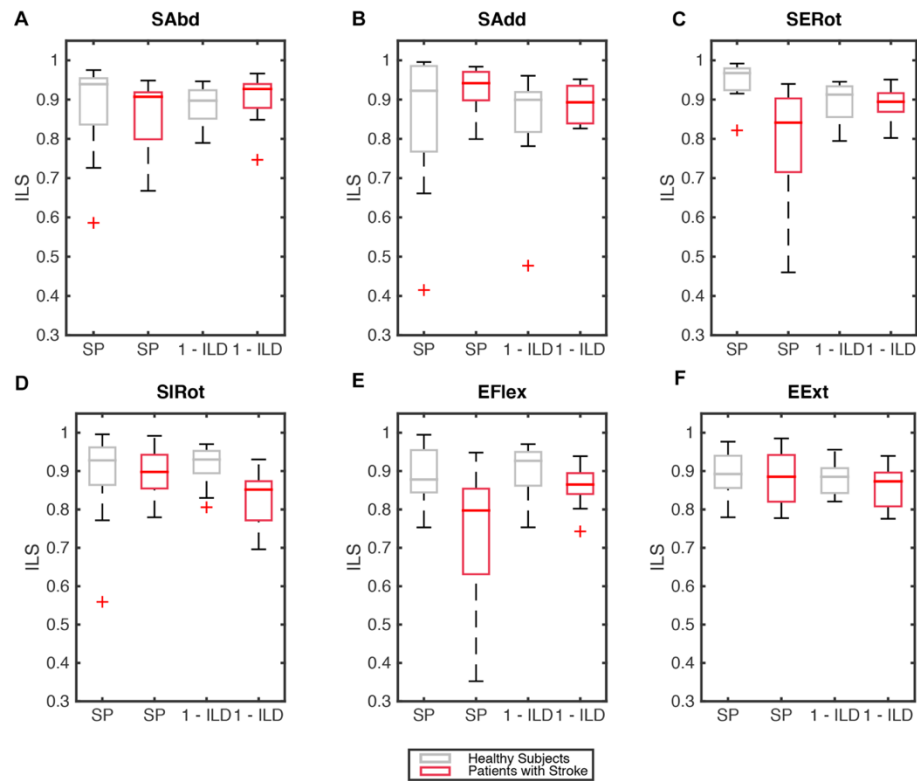
**Figure 112** ILS of patients with stroke compared to healthy subjects movement by movement. A – Shoulder abduction, B – Shoulder adduction, C – Shoulder external rotation, D – Shoulder internal rotation, E – Elbow flexion, F – Elbow extension. Bars are mean ILS of all subjects or patients  $\pm$  SD for each movement. ILS was measured as scalar products (SP) for muscle synergies and 1 – ILD for activation coefficients. Statistical significance was estimated using Wilcoxon rank-sum test: \*  $p < 0.05$ , \*\*  $p < 0.01$ , \*\*\*  $p < 0.001$ .



**Figure 112** shows the differences between the ILS of healthy subjects and patients for each movement. The ILS of activation coefficients was measured as  $1 - \text{ILD}$ , since in the previous section it stood out as the most relevant measure to reflect abnormal ILS of activation coefficients. The movement per movement analysis confirmed that the ILS is generally larger in healthy subjects than in patients with stroke. These differences are especially meaningful during shoulder rotations and elbow flexion-extension. Indeed, statistical tests confirmed significance in the ILS differences of muscle synergies during shoulder external rotation (**Figure 112C**) and elbow flexion (**Figure 112E**), and in the activation coefficients during shoulder internal rotation (**Figure 112D**).

Interestingly, although not statistically significant, during shoulder abduction and adduction, the differences between the ILS of patients seemed to be inverted. That is, during these movements, the ILS of patients was apparently higher. In a more detailed revision of the result, we observed that this trend inversion coincides with the movements with the most ILS variability in healthy subjects. Hence, in order to discard possible outlier effects, we analyzed the data distribution of the population using boxplots (**Figure 113**). Boxplots provide the descriptive statistics of the population (maximum, minimum, median, quartiles and outliers) and are helpful to shed light on this kind of cases.





**Figure 113** Boxplots of the ILS of patients with stroke compared to healthy subjects movement by movement. A – Shoulder abduction, B – Shoulder adduction, C – Shoulder external rotation, D – Shoulder internal rotation, E– Elbow flexion, F – Elbow extension. The internal horizontal line of the box is the median, the first and third quartiles are located below and above the median. The upper and lower whiskers represent the maximum and minimum of the population respectively. Outliers (red crosses) are 3 x interquartile range above or below the first and third quartile respectively.

In effect, the distribution of ILS medians of patients with stroke and healthy subjects confirmed that the exceptions described in the trend of the mean ILS differences between populations during shoulder abduction and adduction (**Figure 112A-B**) are the result of individual outliers that push the mean of the healthy population down. The boxplots reveal that the median ILS in healthy subjects is higher than in patients with stroke in all movements. Note that, the ILS distributions of both shoulder abduction (**Figure 113A**) and adduction (**Figure 113B**) of healthy subjects, contain an individual whose ILS is extremely low, causing a reduction in the mean ILS of healthy subjects that drops below the ILS of patients.



This variability in the ILS of healthy subjects may be due to many factors, such as different individual and motor skills, experience or attention<sup>237,238</sup>. Healthy subjects are endowed with a larger number of degrees of freedom in their upper-limb as well as wider ranges of motion that offer the possibility to create more complex motor patterns and trajectories. Regarding shoulder abduction and adduction, we believe that these ILS differences found in that particular individual (S4) might be caused simply because the movements that he described with both arms followed slightly different kinematics and not because real performance differences exist between his two arms. Unfortunately, we cannot validate such hypothesis as the database of healthy subjects lacks kinematics data.

In any case, from this study and once disregarded the contribution of S4 to the mean population of healthy subjects, we can conclude that stroke decreases the ILS of the control structure in the movements analyzed and thus, this might be a promising and simple measure to find abnormal motor patterns in patients with stroke.

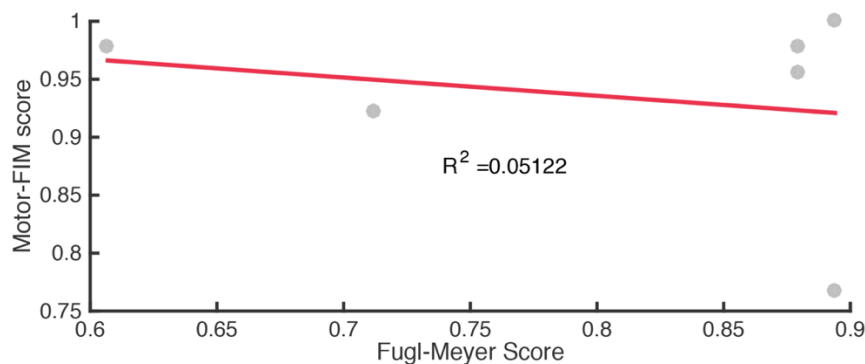


## 18.6 ILS AS A MARKER OF MOTOR IMPAIRMENT

Taken into account that the ILS of the control structure in patients with stroke is significantly lower than in healthy subjects (**Figure 111**), we hypothesized that the ILS may be indicative of the level of motor impairment. Thus, in this section we analyze the relationship between several clinical measures of stroke and the ILS of patients, in order to verify whether ILS can discriminate between motor impairment levels.

### 18.6.1 Association between Fugl-Meyer and Motor-FIM scores

The clinical measures selected to test the potential of ILS as a measure of motor impairment were the Fugl-Meyer score and the Motor-FIM score. The Motor-FIM score is the subscore of the FIM scale resulting from considering only the motor items (See **Appendix C - Functional Independence Measure**). Before anything else, we analyzed the correlation between the Fugl-Meyer score and the Motor-FIM score in order to figure out whether both measures provide similar information or not. The main reason for that preliminary analysis is not to duplicate results, since if both variables were correlated, analyzing their association with ILS would result redundant.



**Figure 114** Linear regression of the relationship between Fugl-Meyer score and Motor-FIM score.  $R^2$  is the r-square value that assesses the goodness of fit of the linear regression.



**Figure 114** shows the linear regression between Fugl-Meyer and Motor-FIM scores. At first sight, one can easily observe that Motor-FIM scores have a large dispersion in the upper-bound of the Fugl-Meyer scale, indicating a poor linear relationship between both variables. Indeed, the coefficient of determination of the linear regression is very low ( $R^2 = 0.051$ ) indicating that we cannot consider that both variables are linearly related.

These observations are clearly confirmed by the Pearson's correlation analysis, which returned a correlation coefficient as low as 0.226. In conclusion, from these results we can manifestly conclude that these variables are not correlated to each other. As a result, association analyses were conducted for Fugl-Meyer and Motor-FIM scores separately.

The data-point distribution shows that patients with high Fugl-Meyer scores might present various independence levels, as indicated by the FIM measures. This observation highlights a worrying limitation of the Fugl-Meyer score to assess the motor capabilities of patients with good motor recovery. It must be kept in mind that the Fugl-Meyer scale strictly measures motor impairment, and as such, it does not necessarily relate to functionality, as the present results demonstrate. The discovery of this “ceiling” effect is not totally new, neither it is the claim to develop a more sensitive scale to assess the functionality of patients that are at the top end of their rehabilitation<sup>22</sup>. That is the main reason why, it is usually recommended to combine the Fugl-Meyer score with an activity scale to increase the sensitivity of the evaluation in patients with mild motor impairment.



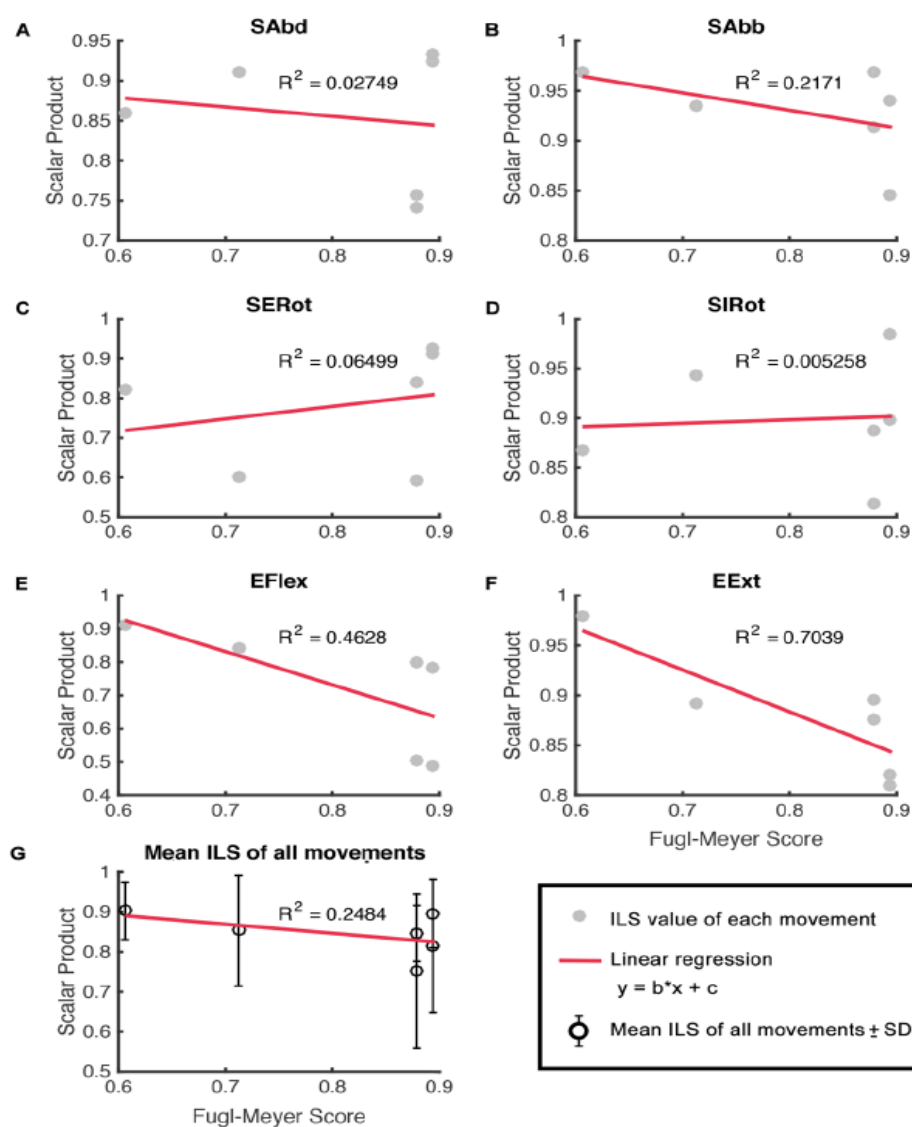
### 18.6.2 Association between ILS and Fugl-Meyer score

**Figure 115** and **Figure 116** plot the distribution of ILS measures of muscle synergies and activation coefficients as a function of Fugl-Meyer scores.

Before analyzing the results, it is important to note that the Fugl-Meyer score of patients in the present database is not homogeneously distributed along the full scale [0-1]. Instead, most of the patients (4/6) are located at the upper-bound of the scale, introducing a clear bias to the predictive capacity of the regression. In addition, the number of subjects is not large enough to cover the full range of clinical profiles or reliably detect outliers. Thus, this analysis is not intended to find an accurate estimator of motor performance. Instead, this analysis should serve as a preliminary approach to assess the potential of ILS to predict the motor impairment of patients with stroke.

From the analysis of **Figure 115**, we have to highlight the existing linear relationship between the Fugl-Meyer score and the ILS of muscle synergies recruited during the execution of elbow extension. According to our results, the  $R^2$  of this relationship is 0.7039, which indicates that the linear equation is able to predict 70.39% of the variance in the variable ILS during elbow extension. For the rest of the movements the linear relationship is rather weak, specially because patients with high motor performance (high FM scores) exhibit a wide range of ILS measures. In conclusion, these results suggest that the evaluation of the ILS during elbow extension may be a simple tool to assess motor performance and avoid the tedious application of the Fugl-Meyer scale.





**Figure 115** Linear regression of the relationship between Fugl-Meyer scores and ILS of muscle synergies. Dots are (A – F) ILS values of a subject for a given movement; (G) Mean ILS of all movements  $\pm$  SD for each subject.  $R^2$  is the r-square value that assesses the goodness of fit of the linear regression.



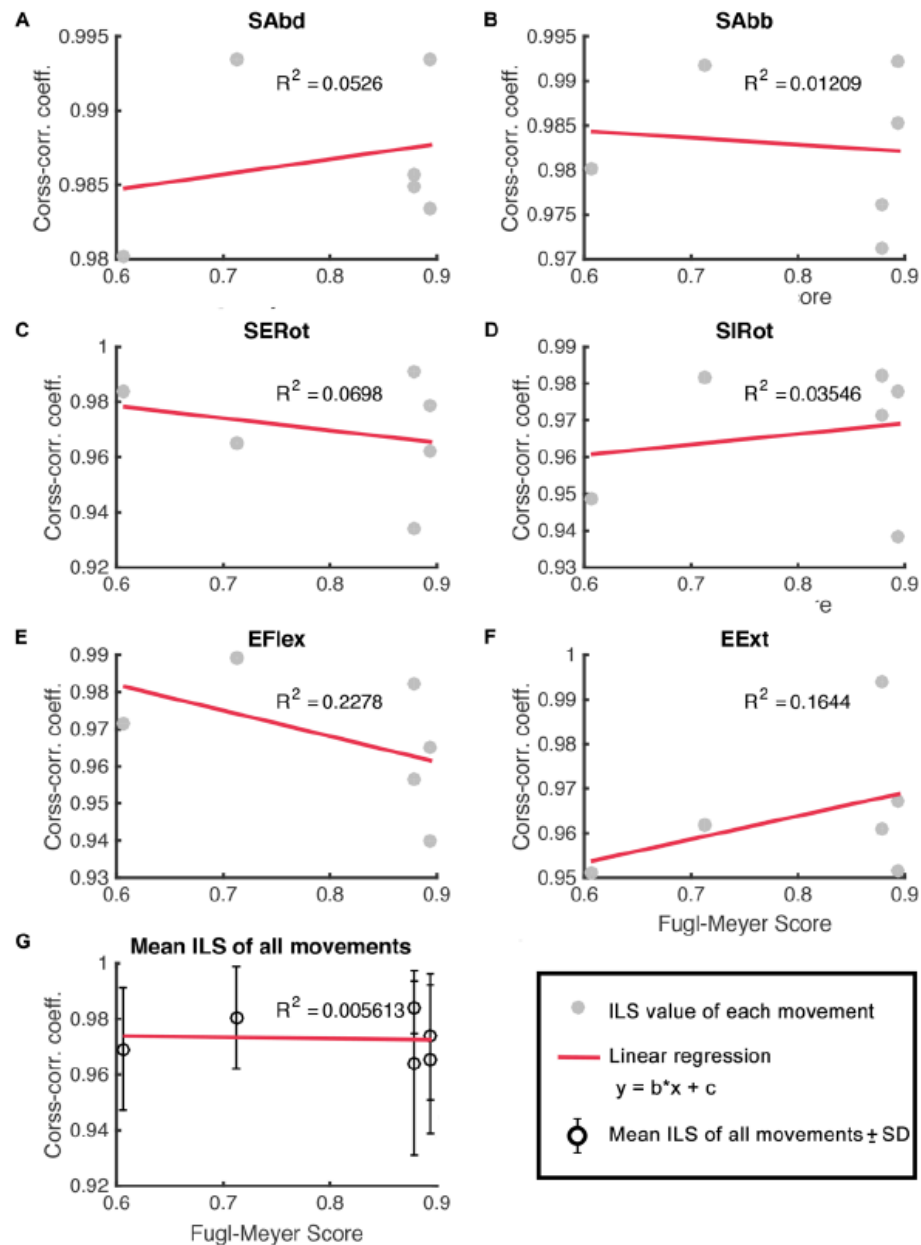


Figure 116 Linear regression of the relationship between Fugl-Meyer scores and ILS of activation coefficients. Dots are (A – F) ILS values of a subject for a given movement; (G) Mean ILS of all movements  $\pm$  SD for each subject.  $R^2$  is the r-square value that assesses the goodness of fit of the linear regression.



Finally, the analysis of **Figure 116** returned no notable linear relationships between Fugl-Meyer scores and the ILS of activation coefficients. We also observe in these plots likewise in muscle synergies (**Figure 101**), that the ILS measures of patients with high motor performance (high FM scores) are also very sparsely distributed for activation coefficients. In consequence, the Coefficients of determination of these linear regressions were below 25%, indicating that the analysis of the ILS of activation coefficients of at least these movements, are not direct indicators of motor performance in patients with stroke.

Taking everything together, it seems that generally speaking, ILS measures are especially useful to discriminate low motor performance cases, as patients with high motor performance show very variable ILS measures. However, during elbow extension the variance of ILS measures of muscle synergies at high motor performance levels is reduced, revealing this measure as a potential candidate to evaluate the motor performance of patients with stroke.

In order to estimate the strength of association between the Fugl-Meyer score and the ILS of each movement, we calculated the Pearson Correlation Coefficient  $r$  and its corresponding  $p$ -value (**Table 40**). As it was already revealed by the linear regression (**Figure 115F**), the Pearson's Correlation confirms a strong and significant correlation between the Fugl-Meyer score and the ILS of muscle synergies during elbow extension ( $r = -0.8390$ ,  $p < 0.05$ ). These results point out the control structure of the elbow flexion as a promising candidate to assess the motor outcome of patients with stroke.

For the rest of the movements, although the correlations are not statistically significant, one can observe that in general, the ILS of muscle synergies are more strongly correlated to the Fugl-Meyer score than the ILS of activation coefficients.



Notably, the ILS of the muscle synergies of the elbow flexion show a negative correlation of -0.6803, suggesting that the elbow function may play an important role to accurately diagnose the motor outcome of patients with stroke.

VARIABLE	ILS OF MUSCLE SYNERGIES		ILS OF ACTIVATION COEFFICIENTS	
	r	p-value	r	p-value
MOVEMENT				
Shoulder Abduction	-0.1658	0.7536	0.2293	0.662
Shoulder Adduction	-0.4659	0.3517	-0.11	0.8357
Shoulder External Rotation	-0.2549	0.6259	-0.2642	0.6129
Shoulder Internal Rotation	-0.0725	0.8914	0.1883	0.7209
Elbow Flexion	-0.6803	0.137	-0.4773	0.3384
Elbow Extension	<b>-0.8390</b>	<b>0.0368</b>	0.4054	0.4252
Mean of all movements	-0.4984	0.3144	-0.0749	0.8878

**Table 40** Pearson's Correlation between Fugl-Meyer score and ILS of muscle synergies (columns 2-3) or ILS of activation coefficients (columns 4-5). *r* is the Pearson's correlation coefficient and p-value is the associated statistic of the test. Statistical significance was considered for  $p < 0.05$ . Significant associations are highlighted in bold.

Strikingly, overall, the correlation coefficients between the Fugl-Meyer scores and the ILSs are negative, indicating that the higher the motor recovery, the lower the ILS. These results suggest that as motor recovery occurs, the paretic arm may develop new motor strategies that do not match with the original strategies existing prior to stroke that still remain in the unaffected arm. In effect, Cheung *et al.* reported the emergence of new synergies post-stroke as a possible response of the nervous system to adapt to brain injury<sup>122</sup>. Whether the emergence of new synergies is a process that responds to compensatory strategies or new adaptive neuroplastic changes requires further investigation.

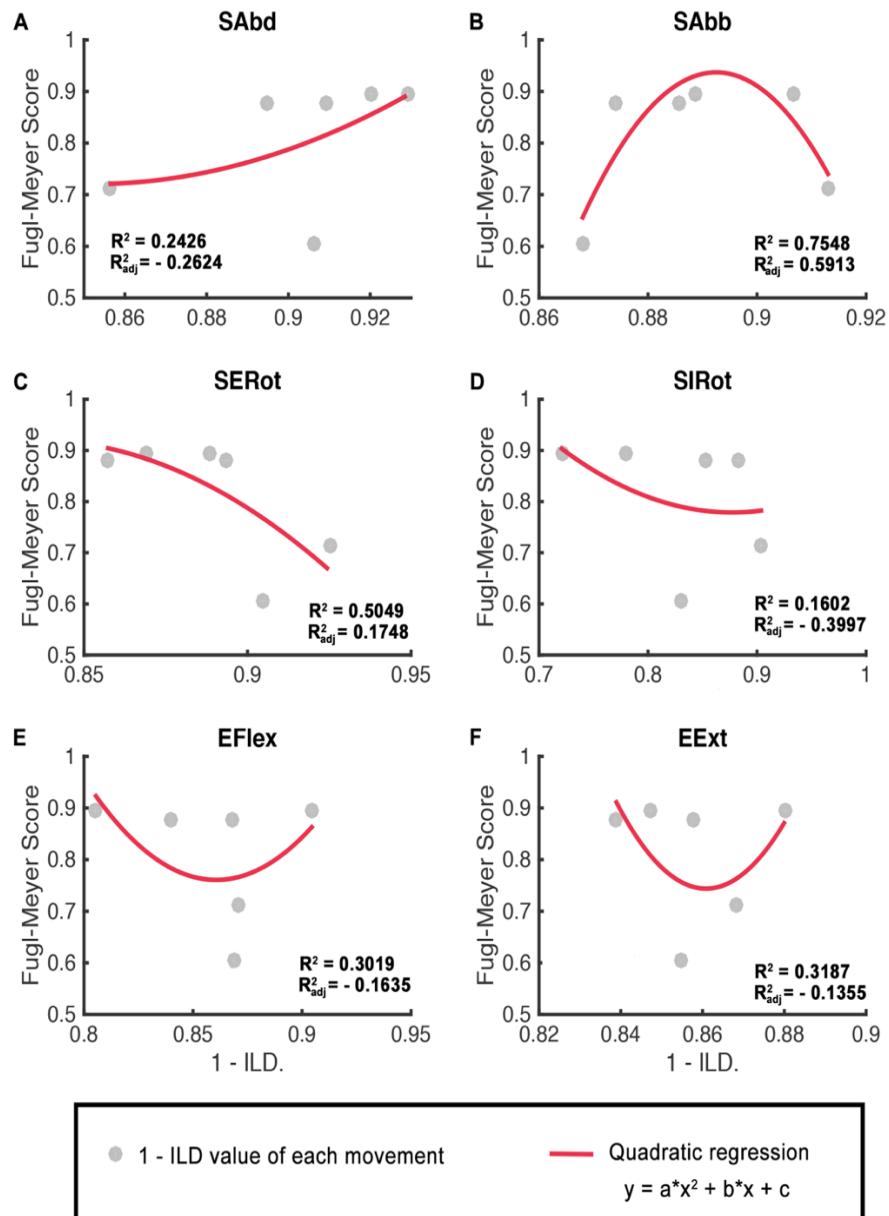
Finally, it has to be noted that the inexistence of linear association does not mean that these variables are not related, but only, that the tested variables are not linearly related. Instead, these variables could have nonlinear relationships, which correlation analysis or linear regression cannot detect. Indeed, when we plotted the Fugl-Meyer scores versus the ILS of activation coefficients expressed as  $1 - \text{ILD}$  we



visually identified nonlinear trends. Thus, we modeled the relationship between these variables using a second grade polynomial (**Figure 117**).

We observed a better fit of these data using a quadratic regression rather than a linear regression. Particularly interesting is the fit obtained in shoulder adduction (**Figure 117B**), which presents a Coefficient of Determination of 0.7548. According to this fit, the ILS of activation coefficients increases as the motor performance improves, up to a point from which, although the motor performance is stuck, the ILS continues increasing. This trend may point out the incapacity of the Fugl-Meyer score to adequately track the ongoing changes in the control structure that contribute to improve motor performance at the neuromuscular level. Indeed, it is widely accepted that the Fugl-Meyer score has limited capacity to assess the motor recovery of patients with mild motor impairment since the scale is characterized by a ceiling effect<sup>22</sup>.





**Figure 117 Quadratic regression of the relationship between Fugl-Meyer scores and ILS of activation coefficients using second grade equations.** Dots are (A – F) ILS values of each for a given movement. The goodness of fit is assessed via the Coefficient of determination ( $R^2$ ) and the adjusted Coefficient of Determination ( $R^2_{adj}$ ).

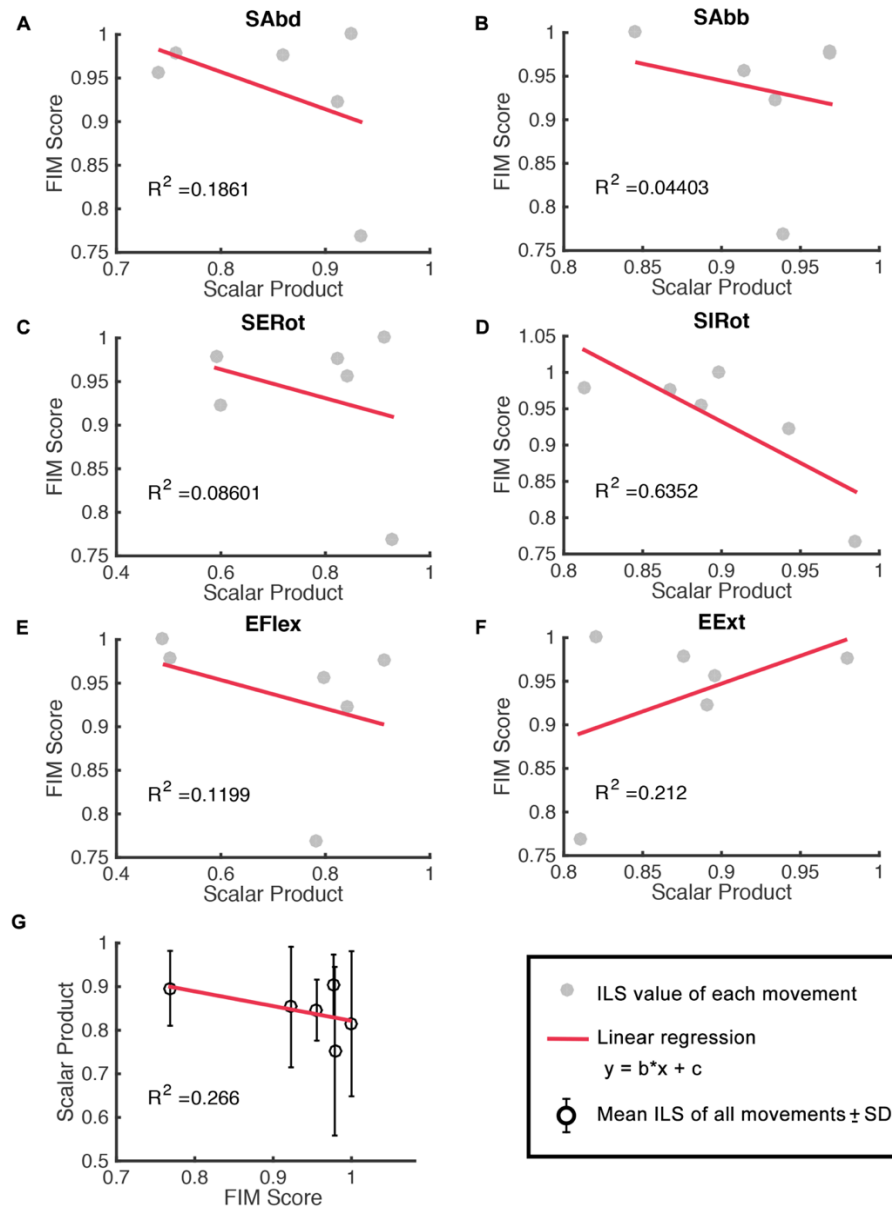


### 18.6.3 Association between ILS and Motor-FIM score

Linear regressions between Motor-FIM scores and ILS of muscles synergies presented an extremely poor linear relationship between both variables, with none of the determination coefficients exceeding 0.7 (**Figure 118**). As a result, a detailed analysis of the spatial distribution of the observations induced us to consider the patient with the lowest FIM (Motor-FIM = 0.77) as an outlier, since its location does not match the trend of the remaining observations. However, when we repeated the analysis discarding this potential outlier, the results of the linear regression did not improve for scalar products (data not shown).

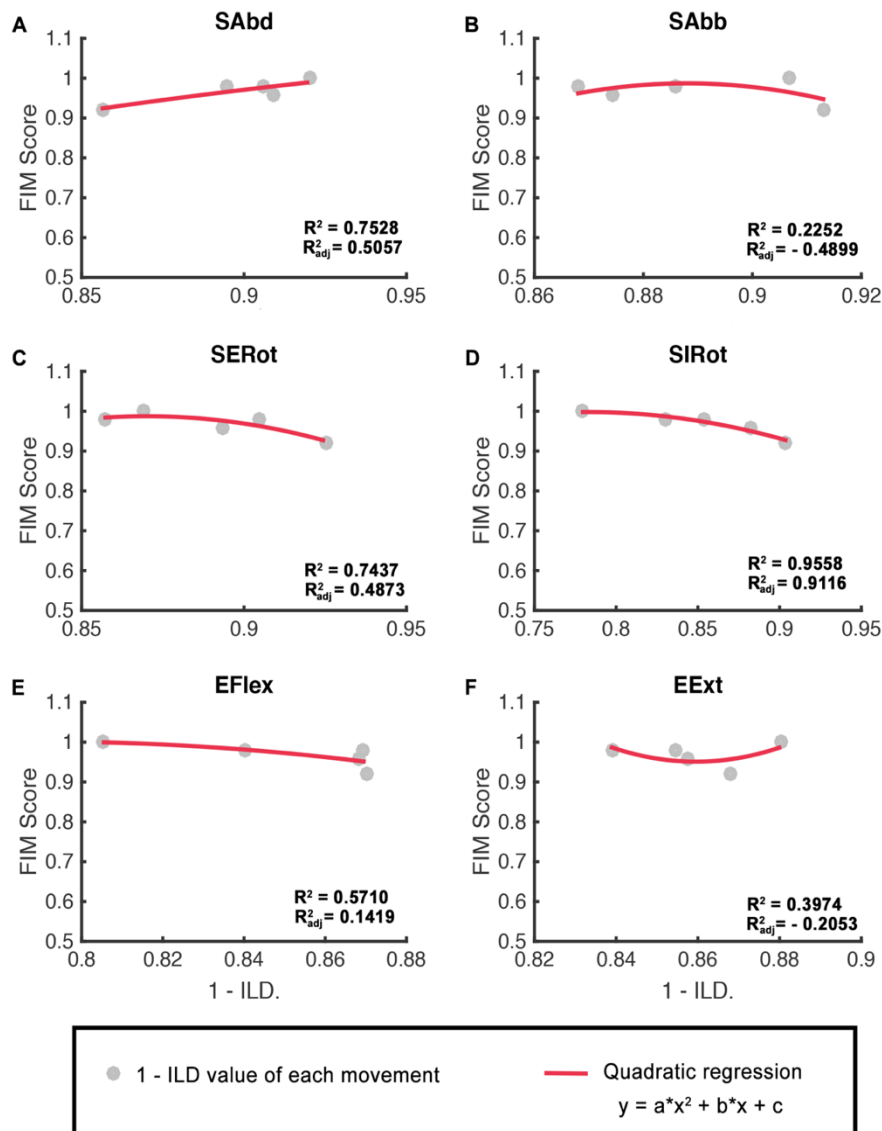
A totally different scenario was what we found after removing the aforementioned outlier in the case of the activation coefficients (**Figure 119**). In this case, the results of the association study improved substantially and revealed a powerful quadratic relationship between the shoulder rotations and the ILS of activation coefficients. Special attention merits the relationship between the ILS of the activation coefficients of shoulder internal rotation and Motor-FIM score (**Figure 119D**) which achieves a coefficient of determination of 0.9558 ( $R^2_{\text{adj}} = 0.9116$ ). According to this relationship, there is an inverse relationship between both markers. That is, it seems that as the functional motor improvement of patients increase, the ILS of activation coefficients during shoulder internal rotation reaches a maximum and even decreases slightly. Indeed, a similar decreasing trend can be intuited in the ILS of muscle synergies although the association strength is not so solid ( $R^2 = 0.6352$ , **Figure 118D**).





**Figure 118** Linear regression of the relationship between Motor-FIM scores and ILS of muscle synergies. Dots are (A - F) ILS values of a subject for a given movement; (G) Mean ILS of all movements  $\pm$  SD for each subject.  $R^2$  is the r-square value that assesses the goodness of fit of the linear regression.





**Figure 119 Quadratic regression of the relationship between Motor-FIM scores and ILS of activation coefficients using second grade equations after outlier removal.** Dots are (A – F) ILS values of each for a given movement. The goodness of fit is assessed via the Coefficient of determination ( $R^2$ ) and the adjusted Coefficient of Determination ( $R^2_{adj}$ ).



This model reinforces the hypothesis that during rehabilitation new compensatory or adaptive strategies emerge in the paretic arm that differ from the physiological motor function and adds a 2-phase perspective. That is, according to the regression, it is presumable that at the beginning of rehabilitation, the primary mechanism of the nervous system is to try to recover the original motor strategies, causing the ILS to increase. And then, it seems that due to brain damage, the ability to fully restore the original motor strategy is limited (this plateau possibly varies from subject to subject, depending on the lesion size and location). As a result, from that moment on, the motor recovery explores novel paths to improve motor performance causing the rehabilitation progression to undergo a phase during which the ILS decreases.

However, it is also possible that the reason why ILS decreases, is because the rehabilitation is not guided in a physiological way resulting in novel recovery patterns that accomplish the desired motor function but are different from the natural motor control. In other words, such ILS decrease might be a sign of maladaptive plasticity of the motor system that should be avoided during rehabilitation. In any case, further research is needed to understand why the ILS decreases when the functional independence is almost maximal.

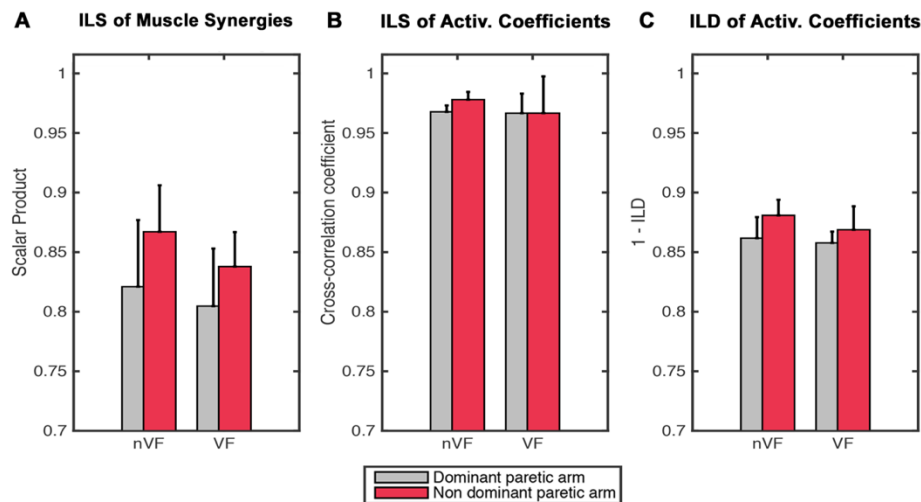
Interestingly, the correlation found between the Fugl-Meyer score and the activation coefficients of shoulder adduction (**Figure 117B**) also support this explanation. In any case, the present quadratic model can only be applicable to patients with high functional independence, as we lack information of patients with Motor-FIM scores located in the lower-bound of the scale.

Note that unlike in the case of the Fugl-Meyer score, we do not present the linear regressions for the ILS of the activation coefficients nor the relations of the Motor-FIM with the ILS expressed as cross-correlation coefficients. This is because the association between the ILS of activation coefficients expressed as  $1 - \text{ILD}$  and the Motor-FIM scores outstood the remaining relationships.



## 18.7 DOES THE DOMINANCE OF THE PARETIC ARM AFFECT ILS?

Many authors have reported a variety of differences between the dominant and non-dominant arm, specially focused on the motor performance (e.g.<sup>209,210,239,240</sup>). At the level of neuromuscular control, we have successfully demonstrated the existence of interlimb differences in healthy subjects in the control structure<sup>199</sup>. Indeed, in **Study 1 | ILS in healthy subjects** we elaborated on those differences. Brief, we show that the ILS of the activation coefficients of the right (dominant) arm is significantly higher than left arm inter-subject similarity. Also, ILS of left arm activation coefficients is more variable than right arm values. Therefore, in view of these facts we hypothesized that whether the paretic arm is the dominant (left-stroke) or nondominant (right-stroke) arm of the patient may affect his motor outcome.



**Figure 120 Comparison of the ILS based on the dominance of the paretic arm.** A – ILS of muscle synergies measured as scalar products. B – ILS of activation coefficients measured as cross-correlation coefficients. C – ILD of activation coefficients measures as 1 - ILD. Bars are mean measures of all subjects and movements per database  $\pm$  SD. Grey bars belong to patients whose paretic arm is the



dominant arm and red bars to patients whose paretic arm is the nondominant arm. Statistical significance was estimated using Wilcoxon rank-sum test: \*  $p < 0.05$ .

To test this hypothesis, we compared the ILS of patients whose paretic arm was the dominant arm against the ILS of patients whose paretic arm was the nondominant arm (**Figure 120**).

We discovered that the ILS of patients whose paretic arm was nondominant exhibited substantially higher ILS than patients whose paretic arm was dominant. This phenomenon was found in all the ILS measures examined, but it was especially remarkable when the ILS was measured with scalar products for muscle synergies, and as  $1 - \text{ILD}$  for activation coefficients.

Wilcoxon rank-sum tests determined that these differences were not statistically significant. However, we think that these results are due to insufficient dataset size. Note that to perform this analysis we were forced to reduce the size of the dataset to half-size, as the population of patients was divided into two smaller subsets of data (3 patients had their paretic arm dominant and 3 patients nondominant). Thus, in view of the magnitude of the mean-differences between the two populations we believe that if we were able to recruit a larger number of patients, the results of the statistical tests would have tested significant.

In any case, the first thing to highlight from these results is that when it comes to analyzing the ILS of patients with stroke, we should take into consideration the dominance of the paretic side. This implies that if we had to define a motor impairment marker from the ILS, we should take into account that the ILS measures vary depending on whether the affected side corresponds to the dominant or nondominant arm of the patient.

Apparently, the neuromuscular deficits caused by stroke in terms of ILS are more prominent when the dominant arm is affected: the ILS is dramatically reduced when the affected side is the dominant side in comparison to the nondominant side. In this case, taken into account that all patients were right-handed, when we refer to deficits



in the dominant side, these are characteristics of left strokes. Consistent to this observation, several authors reported that motor impairment differs depending on the hemisphere where brain damage is located<sup>241</sup>.

Neurophysiological evidence indicates that the left hemisphere controls bimanual movements and even fine motor tasks performed with either hand<sup>233</sup>. This supposition was early established in neuroscience. Already in 1908, Liepman described manual apraxia as the inability of patients with left-hemisphere damage to produce appropriate sequence of movements in both limbs despite adequate sensation and strength<sup>167</sup>. Our results corroborate these findings and show that when the damage caused by stroke is located in the left hemisphere, there is a general loss of manual coordination that decreases the ILS more than only if the right hemisphere was damaged. In fact, early studies in patients with intractable epilepsy that underwent callosotomy procedure report that these patients experienced difficulty producing voluntary movements with the left hand suggesting that such action requires input from the left hemisphere<sup>242</sup>. Today, it is well established, specially for right handers that specialized functions of the left hemisphere are required to control skilled movements in both hands<sup>243</sup>.

Taken everything together, it seems that the 'movement formulae' attributed by Liepman to the left-hemisphere<sup>233</sup> might be responsible for imposing a similar control strategy in both arms, i.e., in neuromuscular terms, a similar control structure. Such hypothesis is supported by the high ILS found in subjects with no neurological impairment together with the larger drop of ILS found in patients that have suffered a left-hemisphere stroke. Various lines of evidence convincingly support that after stroke, the neurons on the healthy hemisphere assist the damaged zones to compensate the loss of function in the affected hemisphere<sup>244–246</sup>. Thus, this finding



may suggest that the assistive potential of the left hemisphere in front of unilateral brain damage is larger than for the right-hemisphere.

Be that as it may, the reader should not forget that the sample size of the present study is not very large ( $N=6$ ), with the same amount of right and left strokes ( $N = 3$ ). Therefore, the results reported in this section should always be interpreted with the appropriate caution.

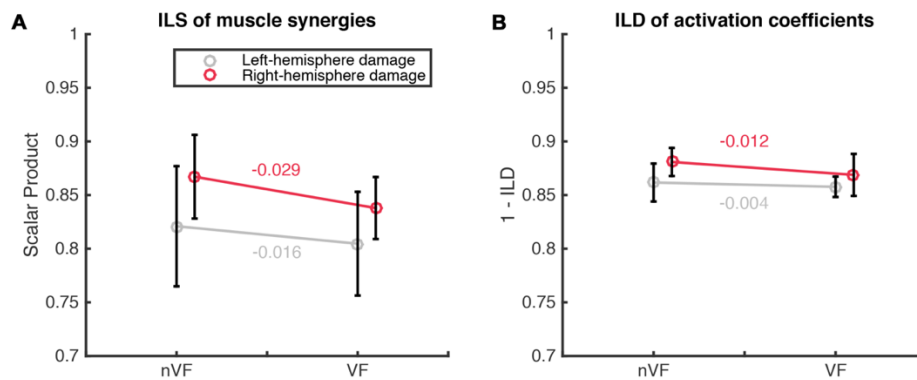
## 18.8 DOES THE EFFECTIVENESS OF VF DEPEND ON THE DAMAGED HEMISPHERE?

Along this study, we have cited numerous references to the asymmetric organization of motor control and we have provided evidence that such asymmetry is directly related with the manifestation of the control structure and the ILS. In particular, we have demonstrated that the effect of VF varies substantially, not only from movement to movement, but also, from patient to patient. Thus, in this subsection, we wonder whether the hemispheric location of the lesion affects the capacity of VF to modulate the ILS.

In order to answer this question, we quantified the ILS changes induced by VF separately in patients with left-hemisphere lesions and patients with right-hemisphere lesions (**Figure 121**). Results indicated that the ILS drop found in patients with right-hemisphere lesions is substantially larger than in patients with left-hemisphere damage. In particular, the ILS drop in muscle synergies was almost two times larger (**Figure 121A**), and the ILS drop in activation coefficient was 3 times larger (**Figure 121B**).



Wilcoxon rank sum tests determined that none of these differences was statistically significant. However, again, we believe that this lack of statistical significance is simply due to insufficient dataset size since the inter-group differences are considerable in magnitude, but not enough to overcome the large inter-subject variability. It is remarkable, that apart from clinical factors, such variability is also largely influenced by the individual attitude shown by patients in front of the experiment. We observed that during the experiment some patients had difficulty to maintain their level of attention and even momentarily deviated their sight from the mirror. Of course, although such behaviors are independent of the lesion side, they introduce a bias on the effect of VF that hinder the correct interpretation of data.



**Figure 121** VF-induced ILS changes depending on the damaged hemisphere in A – Muscle synergies and B – Activation coefficients. Grey symbols represent the population of patients with left-hemisphere damage and red symbols represent the population of patients with right-hemisphere damage. Data points are mean ILS of all patients  $\pm$  SD. The numerical values indicate the slope of the lines connecting the two data points in each series.

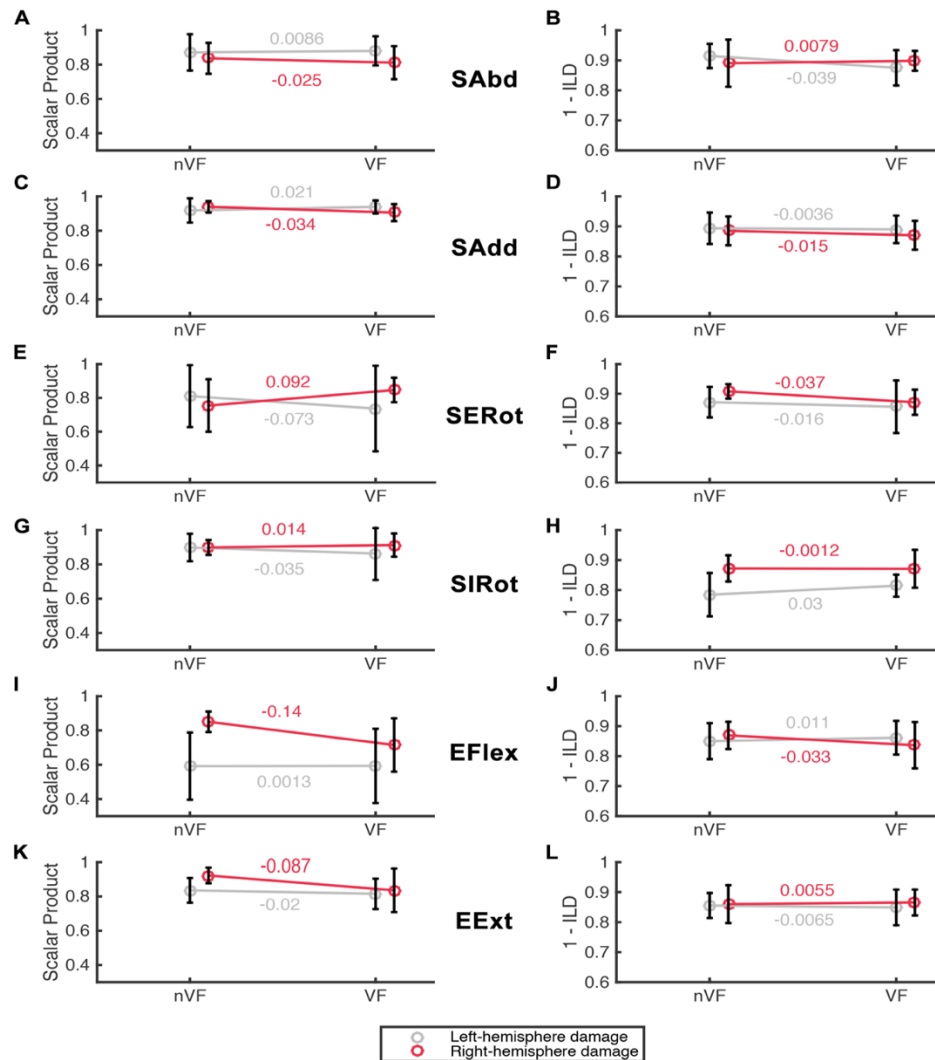


In any case, these results are in agreement with the premise that the right hemisphere plays a specialized role in sensory feedback mediated error correction mechanisms<sup>247</sup>. Right hemisphere is required to control movements when there are substantial visuo-spatial demands<sup>167</sup>. In fact, data from right-stroke patients show more difficulty to process on-line visual information for error correction<sup>241</sup>. Although it seems that in general terms, VF is not helpful to increase ILS in patients with stroke, it is evident that right-stroke patients have a much more reduced capacity to use VF to correct their movements. Thus, it is plausible that due to the side damaged by stroke these patients are not able to appropriately process and use the visual information provided by the mirror.

In effect, when we analyzed the VF-induced changes movement by movement (**Figure 122**), we discovered that right-stroke patients experience more difficulty to benefit from VF in almost all movements. In contrast, left-stroke patients showed moderated capacity to use VF to correct their movements during shoulder abduction (**Figure 122A**) and adduction (**Figure 122C**), shoulder internal rotation (**Figure 122H**) and elbow flexion (**Figure 122J**). Surprisingly, during certain movements such as shoulder rotations, right-stroke patients manifested potential to use VF (**Figure 122E,G**).

It is interesting to remark that only left-stroke patients were able to modulate their activation coefficients due to VF. Activation coefficients constitute the temporal control element of motion. Thus, their modulation is closely related to on-line closed-loop control mechanisms. The inability of right-stroke patients to modulate the activation coefficients due to VF supports the implication of the right-hemisphere in processing visual information and driving sensory-mediated error-correction mechanisms.





**Figure 122** VF-induced ILS changes depending on the damaged hemisphere by movement A,B – Shoulder abduction, C, D – Shoulder adduction, E, F – Shoulder external rotation, G, H – Shoulder internal rotation, I, J – Elbow flexion and K, L – elbow extension in muscle synergies and activation coefficients respectively. Grey symbols represent the population of patients with left-hemisphere damage and red symbols represent the population of patients with right-hemisphere damage. Data points are mean ILS of patients  $\pm$  SD. The numerical values indicate the slope of the lines connecting the two data points in each series.



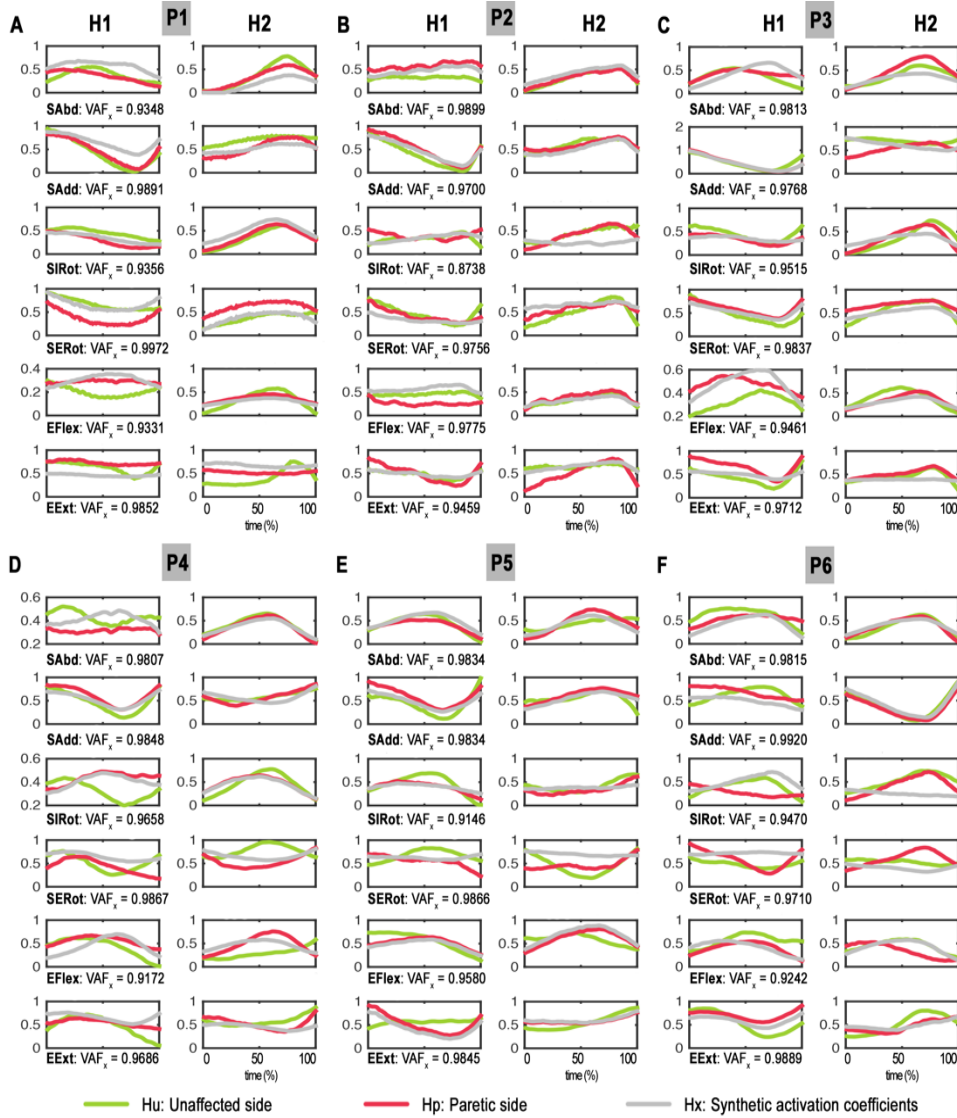
## 18.9 CROSS-RECONSTRUCTION OF THE CONTROL STRUCTURE

In order to better understand the effects of stroke in the control structure, we hypothesized that stroke could only alter the activation coefficients and still provoke the same deficient EMG patterns found in the paretic arm of patients with stroke without interfering with the muscle synergies. To test such hypothesis, we synthetically cross-reconstructed for each individual the activation coefficient  $H_x$  that would be needed to obtain the EMG patterns of the paretic arm, provided that the muscle synergies were not affected by stroke (i.e. we assumed that the paretic arm shared the muscle synergies of the unaffected arm. See Equation ( 35 )).

The mean cross-reconstruction accuracy achieved by the synthetic activation coefficients was very high ( $VA_{F_x} = 96.49 \pm 2.8\%$ ). That is, the muscle activity patterns obtained by linearly combining the unaffected muscle synergies and the synthetic activation coefficients was about 96.59% similar to the muscle activity patterns recorded in the paretic arm. Such finding indicates that the neuromuscular deficits induced by stroke can be caused by only affecting the activation coefficients and comes in agreement with *Cheung et al.* who reported that the muscle synergies of patients with moderate motor deficits were strikingly similar to the muscle synergies of healthy subjects<sup>122</sup>.

The synthetic activation coefficients were then compared to the original activation coefficients of the patients (paretic and unaffected arms). As expected, the synthetic activation coefficients were more similar to the paretic arm's activation coefficients than to the original unaffected arms. Such similarity between activation coefficients was quantified using 1 – ILD. The mean similarity with the unaffected activation coefficients was  $86.86 \pm 4.84\%$ , whereas with the paretic activation coefficients was  $88.23 \pm 5.99\%$ .





**Figure 123** Cross-reconstructed activation coefficients compared to the originals. A - F correspond to the activation coefficients of the 6 movements of patients P1 to P6 respectively.  $VAF_x$  measures the reconstruction accuracy compared to the original EMG patterns of the paretic arm.



The aforementioned comparisons can be visually inspected in **Figure 123**. As we can observe, in most patients the synthetic activation coefficient is very similar to the paretic activation coefficient (**Figure 123A**-EFlex, EExt; B-SAbd, SAdd, SERot; C – EFlex; D – SIRot, SERot, EFlex...).

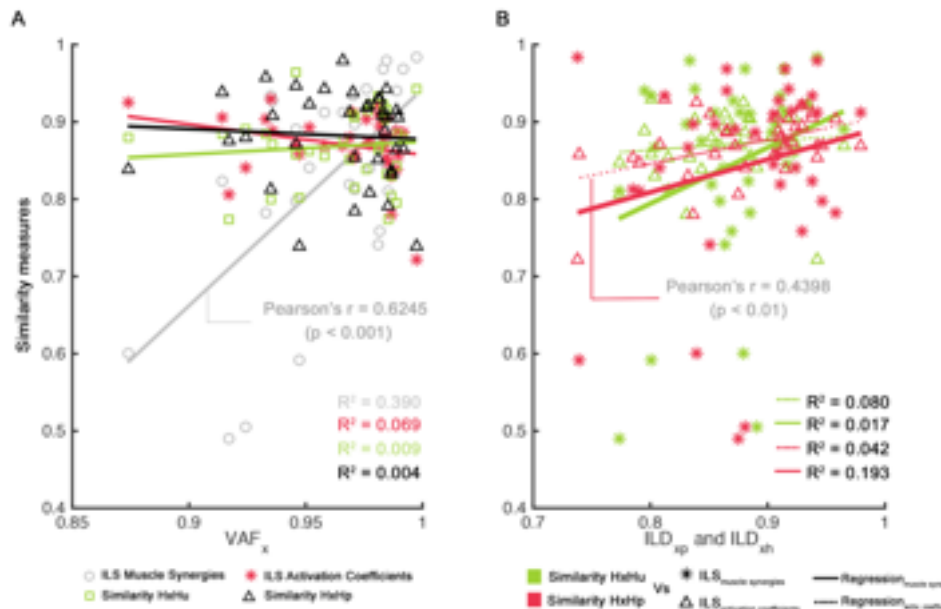
Nevertheless, in few cases, the synthetic activation coefficient is strikingly similar to the unaffected arm's (**Figure 123A**-SERot, F-SERot, SIRot), indicating that even if the activation coefficients were not affected, pathologic EMG patterns could arise. This may confirm that muscle synergies can be also affected by stroke even in moderate cases. Of course, the cases where the 3 activation coefficients are very similar to each other reflect control structures with high ILS between the paretic and unaffected arm.

In order to investigate the relationship between the similarity of the synthetic activation coefficients with the ILS of the original control structure, we ran several correlation and regression studies (**Figure 124**). We found a significant moderate positive correlation ( $r = 0.6245$ ,  $p < 0.001$ ) between the cross-reconstruction accuracy (VAFx) and the ILS of muscle synergies (**Figure 124A**). This indicates that the less the paretic muscle synergies differ from the unaffected muscle synergies, the higher the reconstruction with the synthetic activation coefficients is. This is totally logical as the VAFx measures the cross-reconstruction accuracy between (see section 17.6 **Cross-reconstruction**, Equations ( 35 ) and ( 36 )):

$$W_{unaff} \cdot H_x \leftrightarrow W_p \cdot H_p$$

The fact that the correlation is moderate indicates that there are other additional factors relevant to explain high VAF measures. Interestingly, we did not find a significant correlation between VAF and the similarity between  $H_x$  and  $H_p$ . This might be due to 2 factors. First, as we argued before, the similarity measures have limitations, and in this case, the ILD might not account for all possible similarity features. Second, it is plausible that alternative activation coefficients, different from the paretic activation coefficients lead to the same pathological neuromuscular activations such as in **Figure 123C**-EFlex, D- SAbd or SERot.





**Figure 124** Correlations and linear regressions with the synthetic activation coefficients. A –  $VAF_x$  vs similarity measures B – Similarity between synthetic and original activation coefficients vs ILS. ILS of muscle synergies and activation coefficients is measured with scalar products and  $1 - ILD$  respectively. Hx: synthetic activation coefficients, Hp: activation coefficients of the paretic side, Hu: activation coefficients of the unaffected side. Similarity between activation coefficients is measured as  $1 - ILD$ . Data points are mean measures of the two elements of the control structure (either W1 and W2 or H1 and H2) from each patient and movement.

On the other hand, we found a significant moderate positive correlation ( $r = 0.4398$ ,  $p < 0.01$ ) between the similarity of Hx and Hp, and the ILS of activation coefficients (**Figure 124B**). This indicates that the higher the ILS of activation coefficients (Hp vs Hu) is, the more similar is Hx to Hp. *A priori*, it seems that the lower the functional impairment is (high ILSs), the higher the probability that stroke affects only the activation coefficients, since the synthetic activation coefficient needed to reconstruct



---

the paretic neuromuscular activation in absence of muscle synergy damage increases its similarity to the paretic activation coefficient.

Interestingly, we did not find significant linear correlation between the similarity of Hx or Hp and the ILS of muscle synergies, which would support the previous hypothesis. Of course, the existence of nonlinear relationships might explain this fact. However, taken everything together, we can affirm that stroke can only affect activation coefficients and still lead to paretic motor behaviors, but we cannot categorically discard that stroke does not affect the muscle synergies in patients with moderate impairment.



# 19 CONCLUSIONS (III)

## 19.1 MAJOR FINDINGS

This study is aimed at studying the control structure of patients with stroke during the execution of various rehabilitative movements and the effect that stroke has on it. In particular, we investigate issues such as how different is the control structure of a patient compared to healthy subjects, whether patients can benefit from the use of VF to increase the ILS or how useful can be the ILS as a measure of motor impairment.

### THE CONTROL STRUCTURE OF PATIENTS WITH STROKE

- The control structure of patients with stroke is composed of 2 muscle synergies and activation coefficients, likewise in healthy subjects
- In some cases, 3-element control structures arose, specially during elbow flexion and shoulder external rotation in the unaffected arm.
- Weights from the muscle synergies in the paretic arm have generally less power than in the unaffected arm
- Paretic activation coefficients tend to be flatter and shaped with less defined trends



## INTER-PATIENT BACKGROUND DIFFERENCES

- Half of the patients recognized or had previously practiced the movements under analysis whereas the other half did not. This scenario leads to possible motor learning effects that may bias the results.
- Patients admitted having experienced difficulties during shoulder rotations
- Half of the patients (especially left-strokes) reported feeling more difficulties with their paretic arm than with the unaffected arm, whereas the other half reported no notable interlimb differences.
- These inter-patient differences constitute independent factors that undoubtedly condition the outcome of the motor performance studies, and should be taken into consideration when it comes to interpret the results. In many cases, though, the group size was too small so as to address them appropriately.

## ILS IN PATIENTS WITH STROKE

- Stroke significantly reduces the ILS compared to healthy subjects both at the level of muscle synergies and activation coefficients
- The ILS drop induced by stroke was generalizable to all movements, but only reached statistical significance during:
  - Shoulder external rotation
  - Shoulder internal rotation
  - Elbow flexion
- The ILS of patients with stroke is affected by movement-type and subject
- The ILD measure is a more useful measure of ILS than cross-correlation coefficients to detect abnormal motor patterns caused by stroke



## ILS AS A MAKER OF MOTOR IMPAIRMENT

- The Fugl-Meyer score and Motor-FIM score show low correlation, mainly due to a ceiling effect detected in the Fugl-Meyer score which is unable to discriminate between different independence levels when high performance levels are achieved.
- The FM-score is strongly correlated with:
  - The ILS of muscle synergies during elbow extension linearly
  - The ILS of activation coefficients during shoulder adduction quadratically
- The Motor-FIM score is strongly correlated with the ILS of activation coefficients during shoulder internal and external rotations quadratically
- Quadratic models suggest the existence of a two-phase recovery process

## THE EFFECT OF VF IN PATIENTS WITH STROKE

- Unlike in healthy subjects, in general, VF reduced the ILS in patients with stroke (especially in muscle synergies)
- Significant ILS drops were associated to right-stroke patients
- Certain patients were able to use the VF to increase the ILS of their control structure



## RIGHT VS LEFT STROKES

- The ILS of right strokes is substantially higher than in left strokes, suggesting a predominant role for the left hemisphere in bilateral motor control consistent with the literature
- Right stroke patients experience a larger ILS drop due to VF (up to 2- and 3-fold drop in muscle synergies and activation coefficients respectively), suggesting a role for the right hemisphere in sensory-feedback dependent closed loop control consistent with the literature
- Only left stroke patients are able to modulate the activation coefficients in presence of VF

\* Due to the high inter-subject variability and the reduced dataset size (the database of the patients was reduced to the half to perform these studies), results did not reach statistical significance.

## CROSS-RECONSTRUCTION

- The muscle activation patterns cross-reconstructed from the synthetic activation coefficients and the unaffected muscle synergies are about 96% similar to the pathological activation patterns, revealing that the motor deficits caused by stroke can be produced by only damaging the activation coefficients.
- The synthetic activation coefficients are more similar to the paretic activation coefficients than to the unaffected activation coefficients. Indeed, such similarity is significantly correlated to the ILS of activation coefficients.
- In certain cases, the synthetic activation coefficients differ from both the paretic and unaffected arm's, suggesting that stroke may also affect muscle synergies.



## 19.2 FINAL REMARKS

In this study we demonstrate that the motor impairment caused by stroke is clearly reflected at a neuromuscular level. We show, not only that the control structures present specific characteristics such as flatter activation coefficients or lower paretic muscle synergy weights, but also that stroke significantly reduces the ILS compared to the ILS found in healthy subjects. In particular, cross-correlation studies revealed that by only affecting the activation coefficients, stroke-like pathological activation patterns can be reproduced. However, from our study we cannot rule out that stroke can also affect muscle synergies.

To the best of our knowledge, this is the first time that the ILS is studied in patients with stroke, and what it is more interesting, the first time that it shows its potential to understand neural damage and assess motor impairment. Regarding the first application, i.e. the potential of ILS to understand neural damage, we have demonstrated that left-strokes are characterized by a more abrupt ILS drop than right-strokes, providing indirect support for those theories conjecturing that the left-hemisphere is involved in mastering the motor control of both sides. Similarly, we found that right-strokes experience more difficulty to increase their ILS using VF. Again, the ILS provides indirect evidence of the role of the right hemisphere in closed-loop control mechanisms.

On the other hand, regarding the second application, i.e., the potential of ILS to assess motor impairment, we discovered a high correlation between ILS and several clinical scales (Fugl Meyer score and Motor-FIM score) during the execution of certain movements. Of course, these are very promising results that set the fundamentals to develop the first neuromuscular scale of motor impairment.



In addition, this study provided evidence to presume a quadratic-shaped recovery process. According to the correlation models, it seems that the recovery process can be divided into two phases. During the first phase, our brain activates the mechanisms to recover the original motor strategies existing before the stroke. As a consequence, the ILS of patients increase. However, at a given point, this process reaches a limit, which is probably dependent on the lesion size and location, and from that moment on, the ILS starts to decrease. Such ILS drop, is attributed to the emergence of new adaptive or maybe, compensatory strategies necessary to continue the motor improvement.

Taken everything together, it is undeniable that the ILS is a measure with a huge potential in the clinical and neurorehabilitation fields that deserves to be explored in depth.

## FUTURE GUIDELINES

Further research is needed to validate the clinical potential of the ILS. In this regard, the present study should be reproduced with a larger database, first to overcome the huge existing inter-patient variability that is clearly affecting the statistical outcome of our results, and second to cover a wider range of motor impairment, since as we have already mentioned, the patients that constitute the database used in this study are affected by a mild to moderate motor impairment and do not include cases with low motor impairment scores.

On the other hand, it is essential that future research lines integrate brain imaging functional studies to unequivocally corroborate the functional role of brain hemispheres in motor control. Many of the hypotheses regarding motor control that settle the literature have been revealed in this study through the study of the ILS. However, the specific motor roles carried out by each brain hemisphere still needs solid direct brain confirmation.

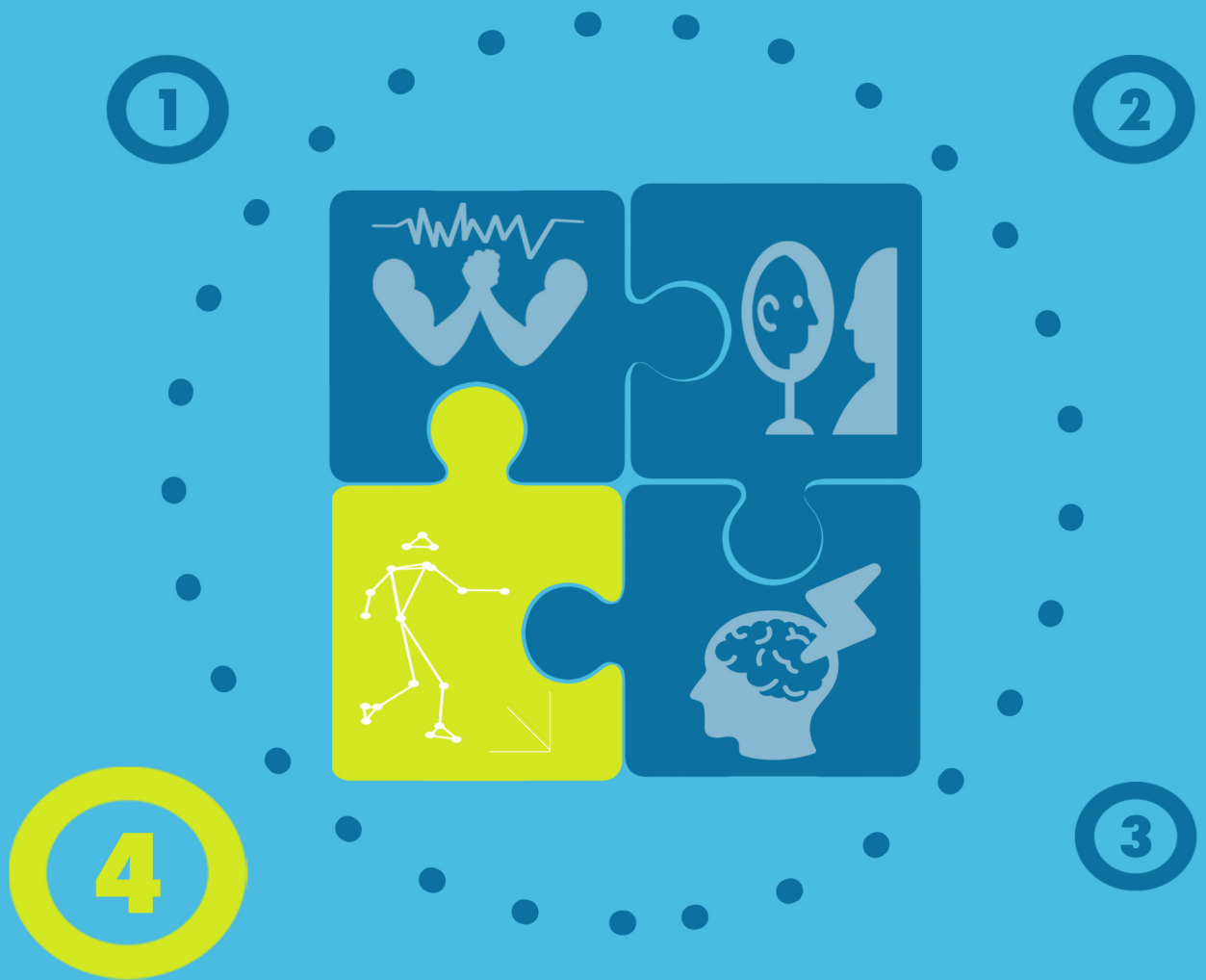












## Study 4

# Kinematic analysis of movements in stroke

*Are the alterations of the control structure  
reflected in movement kinematics?*







# Abstract

*The motor deficits induced by stroke are very apparently expressed at a kinematic level. In consequence, there is a wide variety of studies characterizing the kinematic behavior of stroke patients. However, the vast majority of these studies focus on goal-directed movements and ignore the individual kinematic baseline set by the unaffected arm. For this reason, we have applied the concept of ILS into upper-limb kinematics. Conceiving the experimental design multimodal adds incredible value to the thesis, since it allows connecting the neuromuscular function (the control structure) with the functional outcome (upper-limb kinematics). Therefore, in this study we characterize the motor performance of stroke patients by comparing widely-used kinematic indices between the paretic and the unaffected limb. Furthermore, we introduce a novel approach: the interlimb comparison of kinematic curves, that allow us assessing global kinematic patterns. Using these techniques, we have discovered significant ILS differences between impairment severity levels, which again have been tested through linear regressions with clinical impairment scales. Finally, to complete the study, we have studied whether the effect of VF discovered in the previous study is also reflected at a kinematic (functional) level.*



# 20 SPECIFIC PROCEDURES (IV)

## 20.1 KINEMATIC DATA ANALYSIS

The kinematic analysis developed here assumes that joint movement is pure rotation about a fixed joint axis and disregards joint translation. This assumption is valid for gross-motion activities as the ones under analysis<sup>94</sup>. In addition, for joints with two and 3 DOFs, the axes of rotation for abduction-adduction, external-internal rotation and flexion-extension, are usually assumed to be orthogonal to each other, coincide with the main anatomic axes and intersect at the joint center. As a consequence, by this assumption, the joint rotation planes lie in the anatomic planes and can be modeled as planar movements.

### 20.1.1 *Definition of planar motion*

Theoretically, a planar movement occurs when a plane figure moves in a single plane. To accommodate this motion to rigid bodies, we treat them as planes. That implies that during planar motion, all the points of a rigid body move parallel to some fixed plane. In other words, we consider that the segments of the upper-limb are plane.

	ROTATION AXIS	ROTATION PLANE
Shoulder abduction-adduction	Anteroposterior axis	Frontal plane
Shoulder internal-external rotation	Longitudinal axis	Transverse plane
Elbow flexion-extension	Lateromedial axis	Sagittal plane

Table 41 Definition of the movements under analysis as planar motion



General planar motion combines simultaneous rotational and translational motion. However, for the ease of simplification, we can consider that the movements under analysis are produced by pure rotational movements around the main joint (**Table 41**).

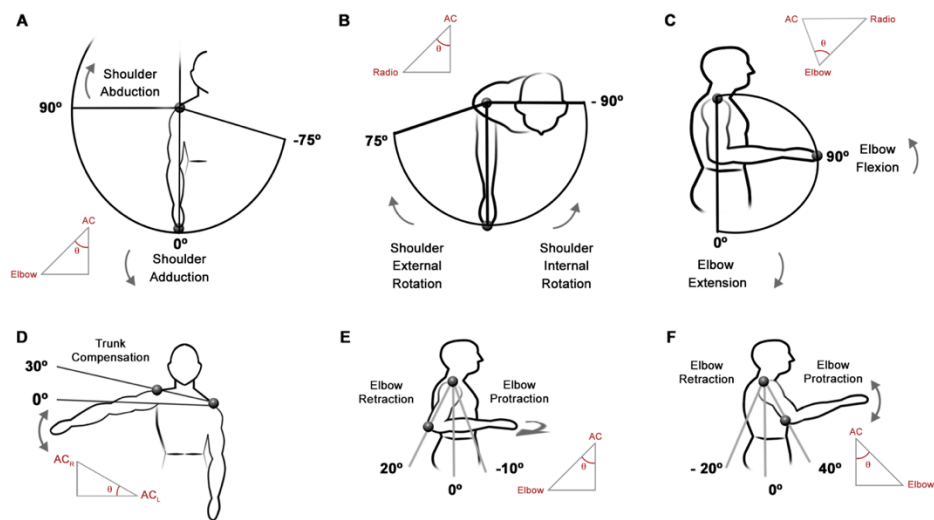
- *Shoulder abduction-adduction*: is produced when the upper-arm rotates about the anteroposterior axis due to the actuation of the glenohumera shoulder joint (See **Appendix D. Upper-Limb Joints And Muscle Function** for further information about the function of the upper-limb joints). The movement occurs within the frontal plane (**Figure 125A**).
- *Shoulder external-internal rotation*: is produced when the forearm rotates about the longitudinal axis of the body due to the actuation of the elbow or shoulder glenohumeral joint. Ideally, the upper-arm is fixed and attached to the trunk. The movement occurs within the transverse plane (**Figure 125B**).
- *Elbow flexion-extension*: is produced when the forearm rotates about the lateromedial axis due to the actuation of the elbow. Ideally, the upper-arm is fixed and attached to the trunk. The movement occurs within the sagittal plane (**Figure 125C**).



### 20.1.2 Definition of movement geometry

#### 20.1.2.1 Main angles

To study the kinematics of shoulder abduction-adduction, external-internal rotation and elbow flexion-extension we have defined the relative angles that describe the main rotations about the anatomical axes (**Figure 125A-C**). We have called these, the *main angles* of the movements.



**Figure 125 Description of main and compensatory angles of movements under analysis.** A – Main angle of shoulder abduction-adduction. B – Main angle of shoulder internal-external rotation. C – Main angle of elbow flexion-extension. D – Compensatory angle of shoulder abduction-adduction. E – Compensatory angle of shoulder internal-external rotation. F – Compensatory angle of elbow flexion-extension. Theta ( $\theta$ ) is the angle measured for the kinematic analysis of each movement pair. In red are indicated the markers used to calculate  $\theta$ .  $AC_R$  and  $AC_L$  are right and left acromion markers respectively.

#### Notation used to define kinematic angles:

- $P_{marker\_name}$ : position  $P$  in axis  $X$ ,  $Y$  or  $Z$  of the marker indicated in the subindex (See Figure 8 to consult available marker list)
- $\overline{M_1 M_2}$ : vector from the marker  $M_1$  to the marker  $M_2$
- $\|\overline{M_1 M_2}\|$ : norm of vector from marker  $M_1$  to marker  $M_2$



*Shoulder abduction-adduction* is defined by the angle  $\theta_{\text{SAbd-Add}}$  described between the upper-arm and the trunk (or the longitudinal axis), where the orientation of the trunk is defined as the axis orthogonal to the ground that passes through the acromion (**Figure 125A**).

$$\theta_{\text{SAbd-Add}} = \tan^{-1} \left( \frac{Z_{\text{elbow}} - Z_{\text{AC}}}{Y_{\text{AC}} - Y_{\text{elbow}}} \right) \quad (41)$$

*Shoulder internal-external rotation* is defined by the angle  $\theta_{\text{SErot-IRot}}$  described between the forearm and the anteroposterior axis, where the anteroposterior axis is defined as the axis parallel to the ground that passes through the acromion (**Figure 125B**).

$$\theta_{\text{SErot-IRot}} = \tan^{-1} \left( \frac{Z_{\text{radio}} - Z_{\text{AC}}}{X_{\text{AC}} - X_{\text{elbow}}} \right) \quad (42)$$

✋ P3 and P6 missed the radio marker, so we used the hand marker in its place.

*Elbow flexion-extension* is defined by the angle  $\theta_{\text{EFlex-Ext}}$  described between the upper-arm and the forearm. (**Figure 125C**).

$$\theta_{\text{EFlex-Ext}} = \cos^{-1} \left( \frac{\overline{\text{Elbow AC}} \cdot \overline{\text{Elbow Radio}}}{\|\overline{\text{Elbow AC}}\| \cdot \|\overline{\text{Elbow Radio}}\|} \right) \quad (43)$$

✋ P3 and P6 missed the radio, ulna and hand markers, so we used the finger marker in its place.



The 3 equations above define the main angles for the left arm. In order to ensure angular symmetry between the two sides and keep the sign of the angles consistent, the sign of the numerator must be inverted when computing the main angles of the right arm.

#### 20.1.2.2 Compensatory angles

In reality, geometrically ideal joints do not exist, even in healthy subjects. It has been widely described that patients with stroke tend to develop compensatory movements to overcome the limitations imposed by the disease. Thus, analyzing movement kinematics in subjects with motor impairments assuming geometrically ideal joints may be too simplistic and we probably ran the risk of overlooking kinematic details that may be relevant to determine the motor consequences of stroke.

In consequence, after exhaustive examination of the motion patterns of patients, we identified the major compensatory movements performed by patients during the experiment and we added them to the kinematic analysis (**Figure 125D-F**). To study these movements, we defined their corresponding *compensatory angles*.

During *shoulder abduction-adduction* patients tended to bench their trunk towards the opposite side of the moving limb. Such compensatory movement was defined by the angle described between the two acromions and the horizontal plane (**Figure 125D**).

$$\theta_{SAbd-Add}^{Comp} = \tan^{-1} \left( \frac{Y_{AC_L} - Y_{AC_R}}{Z_{AC_L} - Z_{AC_R}} \right) \quad (44)$$



During *shoulder external-internal rotation* patients tended to retract their elbow backwards. Such compensatory movement was defined by the angle described between the elbow and the longitudinal axis (**Figure 125E**).

$$\theta_{SERot-IRot}^{Comp} = \tan^{-1} \left( \frac{X_{elbow} - X_{AC}}{Y_{AC} - Y_{elbow}} \right) \quad (45)$$

During *elbow flexion-extension* patients tended to protract their elbow forwards. Such compensatory movement was defined by the angle described between the elbow and the longitudinal axis (**Figure 125F**).

$$\theta_{EFlex-Ext}^{Comp} = \tan^{-1} \left( \frac{X_{AC} - X_{elbow}}{Y_{AC} - Y_{elbow}} \right) \quad (46)$$

Again, in order to ensure angular symmetry between the two sides and keep the sign of the angles consistent, to compute the right compensatory angle during shoulder abduction-adduction the sign of the numerator must be inverted (Equation ( 44 )). The formulation of the other two angles remains invariable for both arms.

### 20.1.2.3 Angular evolution, velocity and acceleration

Angular kinematics (or rotational kinematics) concerns to the study of angle changes without consideration of the moving masses nor the forces that may have caused the motion. In this thesis, we have characterized the angular kinematics of each movement using a family of 4 curves:

1. Angular evolution of main angle
2. Angular evolution of compensatory angle
3. Angular velocity of main angle
4. Angular acceleration of main angle



*Angular evolution curves* describe the angular changes suffered by the main and compensatory angles along time. It is measured in degrees and normalized in time as we did with EMG signals (See section **8.3 EMG Preprocessing** ). That is, the length of the kinematic data corresponding to each movement repetition was normalized to 100 points. To this end we applied one-dimension interpolation via the Fast Fourier Transform method. This resamples the input signal to  $n$  equally spaced points ( $n = 100$ ). As a result, for each movement we had 20 kinematic curves per patient expressed as a percentage.

Once normalized, angular evolution curves were lowpass-filtered using a second order Butterworth filter in forward and reverse directions (zero-phase) with a cutoff frequency of 6Hz. Usually, the cutoff frequency to analyze upper-limb kinematics during voluntary movements is 5-6 Hz<sup>148,149,248,249</sup>. Finally, we averaged the 20 cycles to extract the mean angular evolution curve, from which angular velocity and angular acceleration curves were calculated.

*Angular velocity curves* describe the rate of change of angular displacement of the main angle. It is calculated as the first derivative of the mean angular evolution curve and measured in degrees per cycle percent (deg/%).

*Angular acceleration curves* describe the rate of change of angular velocity of the main angle. It is calculated as the second derivative of the mean angular evolution curve and measured in degrees per square cycle percent (deg/%<sup>2</sup>).



### 20.1.3 *Interlimb similarity measures of angular kinematics*

When we studied the angular evolutions of the main angle of each movement, we qualitatively observed substantial differences between the paretic arm and the unaffected arm of a subject. This kind of interlimb differences were also observed in the evolution of the angular velocity and the angular acceleration of the main angle. Therefore, we hypothesized that as it happened with the ILS of the control structure of patients with stroke, interlimb similarity of angular kinematics might also be an indicator of motor impairment. In other words, does the function of the paretic arm recover the kinematic behavior of the unaffected arm as long as it gets rehabilitated?

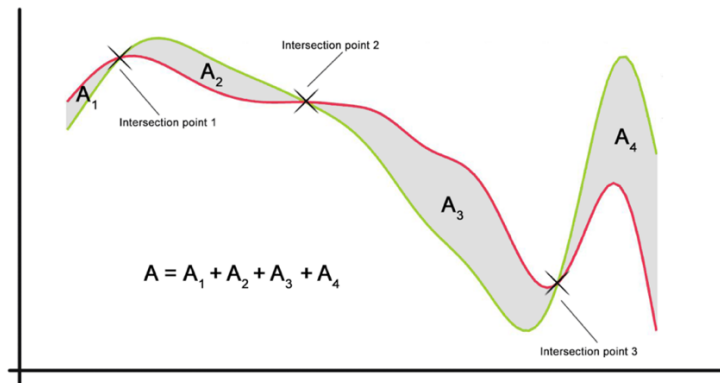
In order to shed light on such question, we quantified the within-subject interlimb similarity between the paretic and unaffected arm's kinematic curves. The metrics used to quantify the similarity between curves were termed *kinematic interlimb similarity* (ILS<sub>k</sub>) measures. The set of ILS<sub>k</sub> measures was composed of 3 different metrics usually employed to quantify the similarity between two curves. Thus, for each of the 3 curves (temporal evolution of the main angle, angular velocity and angular acceleration), we extracted a set of 3 ILS<sub>k</sub> measures:

1. *Area between curves (A)*:

*The area between the two curves* was approximated using the trapezoidal numerical integration. First we located the intersections between the two curves. If no intersecting points were detected, the area between the curves was calculated as the subtraction of the area between the upper curve minus the area of the lower curve. Otherwise, the area was calculated as the sum of the subareas  $A_i$  of each of the surfaces bounded by the curves along two consecutive intersection points (**Figure 126**).



$$A = \sum_{i=1}^n A_i \quad (47)$$



**Figure 126 Area between two curves that intersect.** The total area between the curves was calculated as the sum of all the subareas  $A_i$  located between the two curves and along subsequent intersection points. For the tails, the first subarea  $A_1$  was located in the interval between the starting point of the curve and the first intersection point, and the last subarea  $A_n$  was located in the interval between the last intersection point and the end of the curve. In the study, the green curve corresponds to the kinematic curve of the unaffected arm, and the red curve to the kinematic curve of the paretic arm.

2. *Cross-correlation coefficient (CC)*: (See subsection 8.4.2 **Interlimb similarity (ILS) measures** for further information).
3. *Hausdorff Distance (HD)*:

The Hausdorff Distance is a mathematical metric used to measure the distance between two sets of points of a metric space<sup>250</sup>. Basically, two sets are said to be close to each other if every point of either set is close to some point of the other set.



Given two nonempty sets  $X$  and  $Y$  of a compact metric space  $S$ , their HD is mathematically defined as:

$$HD(X, Y) = \left\{ \sup_{x \in X} \inf_{y \in Y} d(x, y), \sup_{y \in Y} \inf_{x \in X} d(x, y) \right\}, \quad (48)$$

where *sup* stands for *supremum* and *inf* for *infimum*. In this case, the points in the set  $X$  and  $Y$  formed the paretic and unaffected arm's kinematic curves.



#### 20.1.4 Kinematic Indices

Kinematic indices were extracted from the set of curves describing the angular kinematics of the movements: the evolution in time of main and compensatory angles, and the angular velocity and acceleration of the main angle. The set of kinematic indexes was designed to characterize the kinematic behavior of single-DOF movements based on major abnormalities described in the literature during reaching movements<sup>172,251</sup>. At all, the set of kinematic indices was composed of 11 indices:

- [I1] Movement time (s): time measured in seconds elapsed from the movement onset to the movement offset averaged across all repetitions.
- [I2] Mean instant variability (deg): angle variability expressed in degrees averaged across the 100 interpolated time-points. The angle variability was measured in each time-point as the standard deviation of all repetitions.
- [I3] Maximum main angle (deg): maximum angle expressed in degrees achieved during the main movement
- [I4] Maximum compensatory angle (deg): maximum angle expressed in degrees achieved during the associated compensatory movement
- [I5] Range of Motion (ROM) of the main angle (deg): difference expressed in degrees between the maximum and minimum angles achieved during the main movement. The ROM was calculated in the central 90% fraction of the cycle.
- [I6] Range of Motion (ROM) of the compensatory angle (deg): difference expressed in degrees between the maximum and minimum angles achieved during the associated compensatory movement. The ROM was calculated in the central 90%\* fraction of the cycle.
- [I7] Peak angular velocity (deg/cycle percent): maximum angular velocity achieved during the main movement in the central 90%\* fraction of the cycle.
- [I8] Mean angular velocity (deg/cycle percent): angular velocity achieved during the main movement averaged along the entire cycle.



- [19] Peak angular acceleration (*deg/cycle percent<sup>2</sup>*): maximum angular acceleration achieved during the main movement in the central 90%\* fraction of the cycle.
- [110] Number of peaks angular velocity (*units*): number of local maxima achieved by the angular velocity during the 90%\* fraction of the cycle. This is a way of measuring the level of segmentation of movements<sup>252</sup> \*\*\*.
- [111] Number of peaks angular acceleration (*units*): number of local maxima achieved by the angular acceleration during the 90%\* fraction of the cycle. This is an extended version of<sup>252</sup> to measure the level of segmentation of movements.

\* Because the movements under analysis are ballistic movements, we know that the maximum velocity is achieved approximately at the middle of the trajectory. Thus, in order to minimize errors due to numeric computation, experimental inaccuracies or kinematic marker shifts, we discarded the initial and last 5% of the cycles.

\*\* Kinematic features related with angular velocity were expressed as absolute values since the negative sign in this case only indicates the orientation of the movement (i.e. angle is decreasing like in shoulder adduction, shoulder internal rotation and elbow flexion).

\*\*\* Subjects with motor impairment caused by neurological lesions usually exhibit multiple peaks in the velocity profiles of their hands as a result of movement segmentation<sup>155</sup>. Therefore, quantifying the number of peaks is an indirect way of measuring movement segmentation.



## 20.2 LOGISTIC REGRESSION

In order to assess the predictive value of the kinematic indices, we ran a series of logistic regressions for each index using the algorithm described in <sup>253</sup>. The logistic regression (or logit model) is used to predict the probability that a binary response (also dependent or outcome variable) occurs, given one or more predictor variables. In this case, the response variable was defined as the level of motor impairment (0 = mild; 1 = moderate) according to the FM-UE scale, given the kinematic index (continuous variable) and the hemisphere affected by stroke (0 = left; 1 = right).

The logit model treats the log odds of the response as a linear combination of the predictor variables that can be either binary or continuous. In other words, in the simplest case (1 predictor) logistic regression applies the logit transformation to the response variable  $Y$ :

$$\text{logit}(Y) = \ln\left(\frac{\pi}{1 - \pi}\right) = A + Bx \quad (49)$$

where:

- $x$  is the predictor
- $\pi$  is the probability of  $Y$  happening
- $A$  is the  $Y$  intercept
- $B$  is the regression coefficient



Such equation can be extended to multiple predictors  $\{x_1, x_2, \dots\}$ :

$$\text{logit}(Y) = \ln\left(\frac{\pi}{1-\pi}\right) = A + B_1x_1 + B_2x_2 + \dots \quad (50)$$

The accuracy of the model predicting the response variable can be evaluated at different levels:

1. *Overall model evaluation*: a logistic model is considered to provide a better fit to the data if it improves the null model (also called intercept-only model). We considered that if the p-value of the likelihood ratio and the Wald test laid below the significance level ( $\alpha = 0.05$ ), the logistic model was more effective than the null model.
2. *Statistical tests of individual predictors*: we used the Wald chi-square statistic to determine whether the independent variables were significant predictors ( $p < 0.05$ ) of the response variable.
3. *Goodness-of-fit statistics*: these statistics evaluate the fit of the model against actual outcomes. We used the Hosmer-Lemeshow test to assess the fit. When  $p > 0.05$  the model is said to fit the data.



## 20.3 QUANTIFICATION OF VF-DRIVEN MOTOR IMPROVEMENT

In order to study the effect of VF in the performance of the upper-limb in patients with stroke, we compared the angular kinematics of the paretic limb in presence and absence of VF. Along this thesis we have proven that the behavior of the unaffected arm is a good reference to assess the motor impairment of stroke patients, both at a neuromuscular (see **Study 3**) and at a kinematic level (see **Study 4**). Furthermore, the use of ILS measures is a desirable strategy to avoid the inherent inter-subject differences of motor control and stroke effects that may hinder the adequate interpretation of the results. For these reasons, we have measured the effect of VF by comparing the ILS of angular kinematics in presence and absence of VF using the  $ILS_k$  measures described above.

In previous studies, we have reported a relationship between increased neuromuscular ILS and improved motor control (or reduced motor impairment). Indeed, in this study we show that this relationship is also extendible to the kinematic ILS. In light of these findings, we have considered that VF improves motor performance at a kinematic level if the  $ILS_k$  increases with respect to the  $ILS_k$  found in absence of VF. Thus, we have defined the VF-driven kinematic improvement as:

$$\Delta ILS_k(\%) = \frac{ILS_k(VF) - ILS_k(nVF)}{ILS_k(nVF)} \cdot 100 \quad (51)$$

We calculated the VF-driven kinematic improvement for each of the kinematic curves (temporal evolution of the main angle, angular velocity and angular acceleration) using the 3  $ILS_k$  measures defined above:  $ILS_k = \{A, CC, HD\}$ . However, for the ease of visualization (the kinematic improvement calculated through the 3  $ILS_k$  measures threw differently scaled magnitudes making the single-graphic visualization complicate) and because the CC was the only  $ILS_k$  measure exhibiting statistical significance in all the comparisons (due to lower inter-subject SD values), we only show the results for the CC.



## 20.4 STATISTICAL ANALYSES

We applied the Wilcoxon rank-sum test to compare values from moderate *versus* mild population (unbalanced groups). In contrast, we applied the Wilcoxon signed-rank test to compare values from paretic *versus* unaffected arm (balanced groups). In the same way, the Wilcoxon signed-rank test was used to evaluate the within-subject comparisons between the nVF and VF conditions. In all cases, statistical significance was considered in  $p < 0.05$ .



# 21 RESULTS AND DISCUSSION (IV)

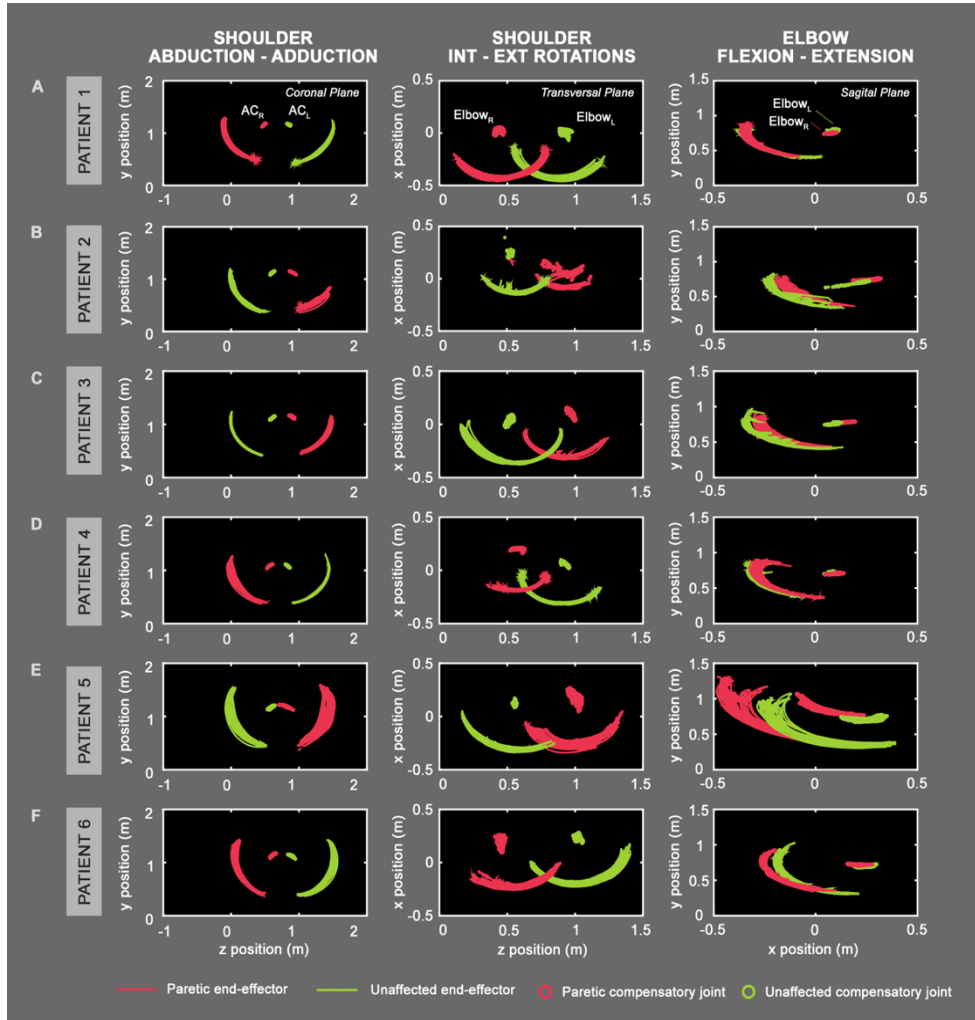
## 21.1 PLANAR TRAJECTORIES

**Figure 127** shows the trajectories described by the end-effector during movement execution. Also, the trajectories of acromions (during shoulder abduction-adduction) and elbows (during shoulder rotations and elbow flexion-extension) are indicated to reflect the magnitude of the compensatory movements in each patient. For the ease of comparison, each plot overlaps the trajectories of both the paretic (red) and unaffected arm in the same representation.

The figure unveils obvious interlimb differences in the trajectories, specially in most impaired subjects (P2, P5 - **Figure 127B,E**). The most easily detectable difference is related to the ROM of the end-effector: due to the loss of mobility, the paretic arm exhibit lower ROMs than the other arm. Probably, the most dramatic effect is observed in P2 (FM-UE = 47/66), whose paretic ROM is substantially inferior compared to the ROM of the unaffected arm in all 3 movement pairs (**Figure 127B**).

However, this effect is not exclusive of moderate subjects. It is interesting to observe that even subjects with high FM-UE scores have reduced ROMs, as it happens during the shoulder rotations of P4 (FM-UE = 59/66, **Figure 127D**) or elbow flexion-extension of P1 (FM-UE = 59/66, **Figure 127A**).





**Figure 127 Planar trajectories of the end-effectors of each patient (A-F).** The lines depict the trajectories described by the end-effector (finger\*) corresponding to the 20 repetitions performed by each patient's arm. Green graphics indicate the trajectory of the unaffected arm and red graphics of the paretic arm. Shoulder abduction-adduction is shown in the coronal plane, shoulder rotations in the transversal plane and elbow flexion-extension in the sagittal plane. The scatter plots show the compensatory movements exhibited by acromions (during shoulder abduction-adduction) and elbow (during shoulder rotations and elbow flexion-extension). \*Due to the loss of the left finger-marker during shoulder rotations of patient 2, we replaced both left and right finger-markers by the corresponding hand-markers.



The emergence of compensatory movements is also very apparent in these plots. This phenomenon is also more tangible in most impaired patients. For instance, note the huge lateral motion detected in the paretic elbow of P2 during shoulder rotations, which practically equals the ROM of the end-effector; or the dramatic protraction detected in the paretic elbow of P5 during elbow flexion-extension, which is as much as the half of the arch described by the end-effector. Generally, the surface occupied by the paretic joint is wider than the unaffected arm, denoting the existence of generalized compensatory motion. In all cases, the compensatory movements occur in the direction of the end-effector trajectory and therefore, contribute to increase the ROM. Thus, when evaluating the ROM of a movement, one should consider the contribution of the compensatory movement.

## 21.2 EVOLUTION OF ANGULAR KINEMATICS

This section describes the angular kinematics described by the paretic and unaffected limbs of patients with stroke from a qualitative view. The analysis includes the evolution of main and compensatory angles, and the angular velocity and acceleration of the main angles.

### 21.2.1 *Main angle evolution*

The following set of figures shows the temporal evolution of the main angles described in **Figure 125** during shoulder abduction-adduction (**Figure 128**), shoulder external-internal rotation (**Figure 129**) and elbow flexion-extension (**Figure 130**). At a first sight one can clearly observe the huge intra-subject kinematic variability existing even in the execution of simple movements (let's remind that all 3 movements have only 1 DOF). Note that this is an inherent characteristic of human movement that is present in the unaffected arm and apparently preserved after stroke, in the paretic arm as it has been demonstrated both at the level of control structure and kinematic performance.

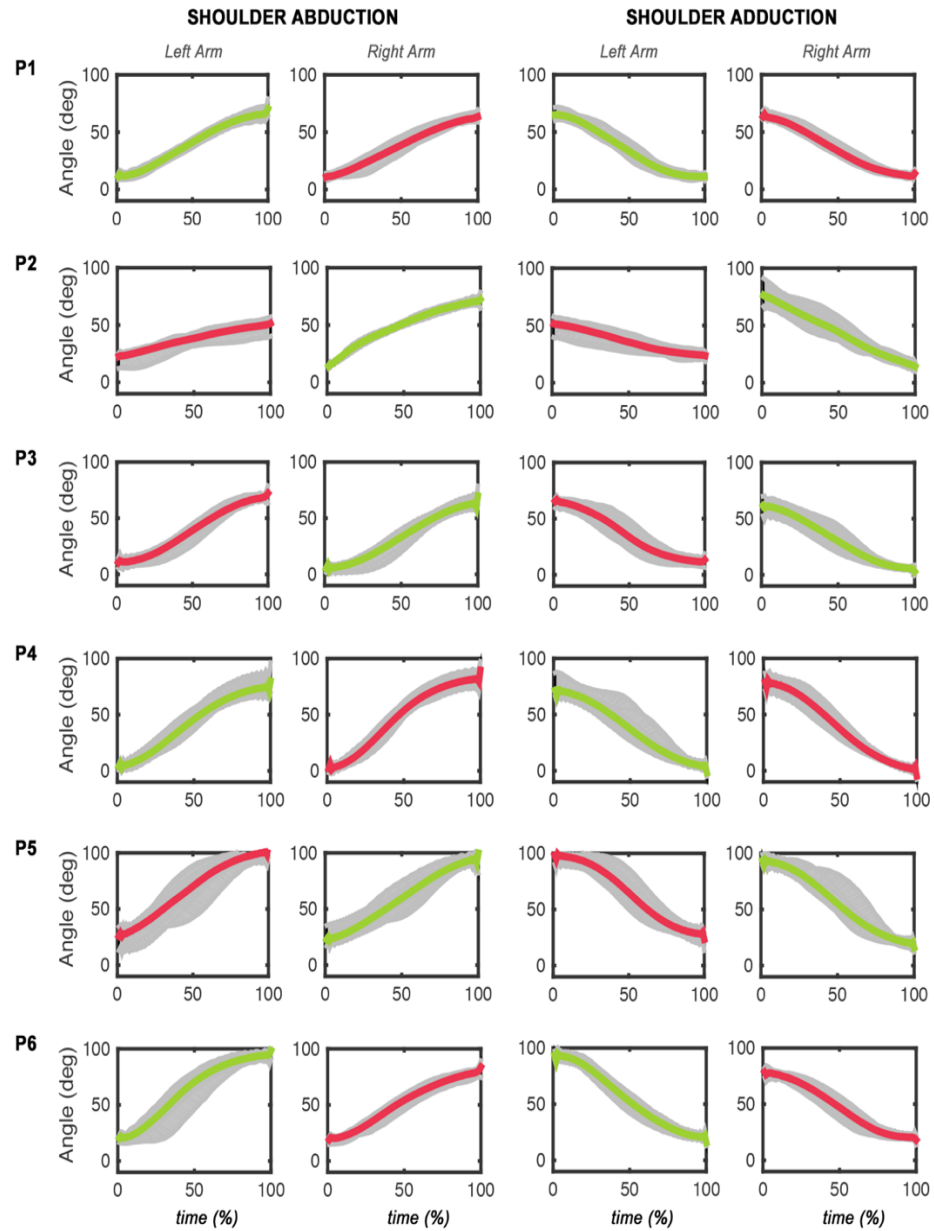


According to recent studies, the motor variability might be inversely related to task-relevance. In other words, higher motor variability is found during the phases that are not relevant to the final goal of the movement<sup>93</sup>. For instance, the distribution of the neuron activation in *Aplysia* is very similar when the animal is closing the grasper, but very variable in the remaining phases of feeding, or when the grasper fails to grasp the food as the neural activity is no longer functionally relevant for the task of feeding<sup>254</sup>. This phenomenon generalizes across species and multiple motor behaviors<sup>255–257</sup>.

Naturally, this inherent variability is enhanced between subjects. The curves shown in these figures vary substantially from subject to subject within the same movement. For instance, during shoulder external rotation the angular trajectory of the unaffected arm of P2 describes a quite flat linear progression, in P3 a steep (i.e. much faster) linear progression and in P4 the trajectory resembles a sigmoid (**Figure 129**).

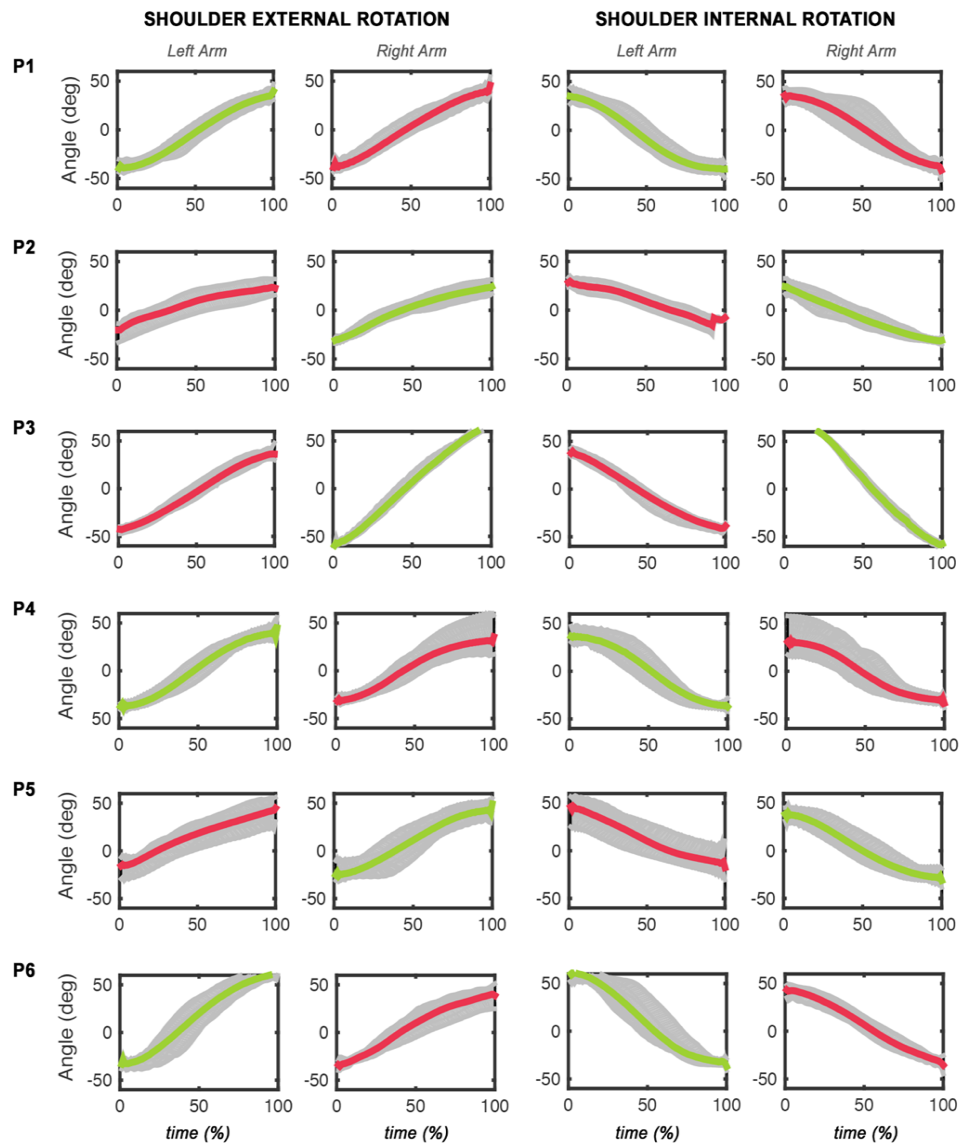
Needless to say, that the within-subject interlimb differences are also qualitatively very evident. For instance, the ROM of P2 and P6 during shoulder abduction-adduction (**Figure 128**) and external-internal rotation is larger in the unaffected arm (**Figure 129**). However, upon visual inspection it is difficult to identify a clear feature that differentiates the paretic arm from the unaffected arm and that generalizes across subjects. Note that for P3 and P4 the differences are visually inappreciable. These observations reflect the need to use quantitative indices to find meaningful interlimb kinematic differences.





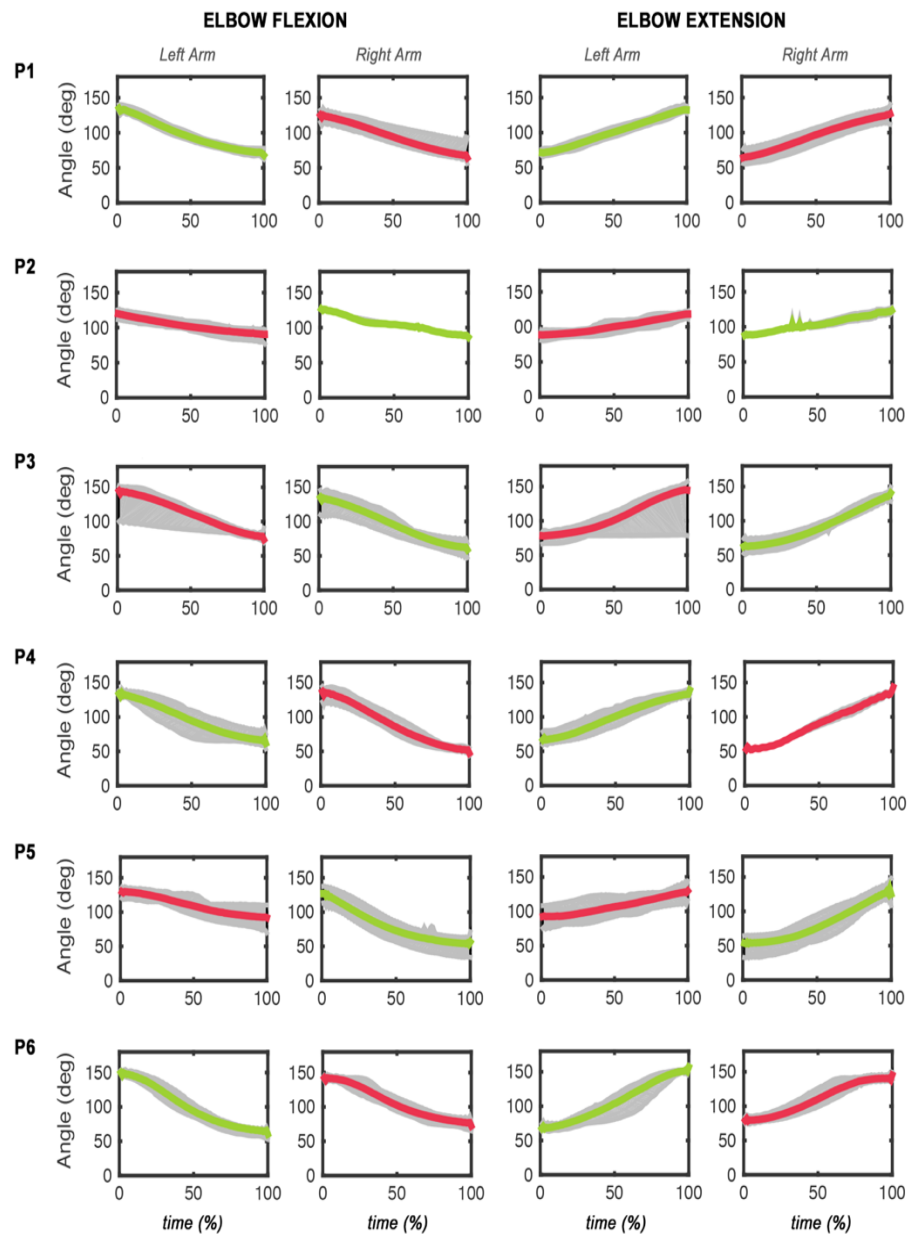
**Figure 128 Main angle evolution of shoulder ABDUCTION-ADDUCTION.** Each row depicts the angle evolutions of each of the 6 patients (P1-P6). Grey curves represent the angle evolution in one movement- repetition and colored thick curves represent the mean of all repetitions. Red curves correspond to the paretic arm and green curves to the unaffected arm.





**Figure 129 Main angle evolution of SHOULDER EXTERNAL-INTERNAL ROTATION.** Each row depicts the angle evolutions of each of the 6 patients (P1-P6). Grey curves represent the angle evolution in one movement- repetition and colored thick curves represent the mean of all repetitions. Red curves correspond to the paretic arm and green curves to the unaffected arm.





**Figure 130 Main angle evolution of ELBOW FLEXION-EXTENSION.** Each row depicts the angle evolutions of each of the 6 patients (P1-P6). Grey curves represent the angle evolution in one movement- repetition and colored thick curves represent the mean of all repetitions. Red curves correspond to the paretic arm and green curves to the unaffected arm.



### 21.2.2 *Compensatory angle evolution*

The following set of figures shows the temporal evolution of the major compensatory angles described in **Figure 125** during shoulder abduction-adduction (**Figure 131**), shoulder external-internal rotation (**Figure 132**) and elbow flexion-extension (**Figure 133**). We also studied other compensatory movements such as trunk compensation during shoulder internal-external rotation and elbow flexion-extension or lateral elbow aperture during shoulder internal-external rotation, but we did not find relevant development of those compensations during the execution of the main movements. Thus, we do not reflect the results here.

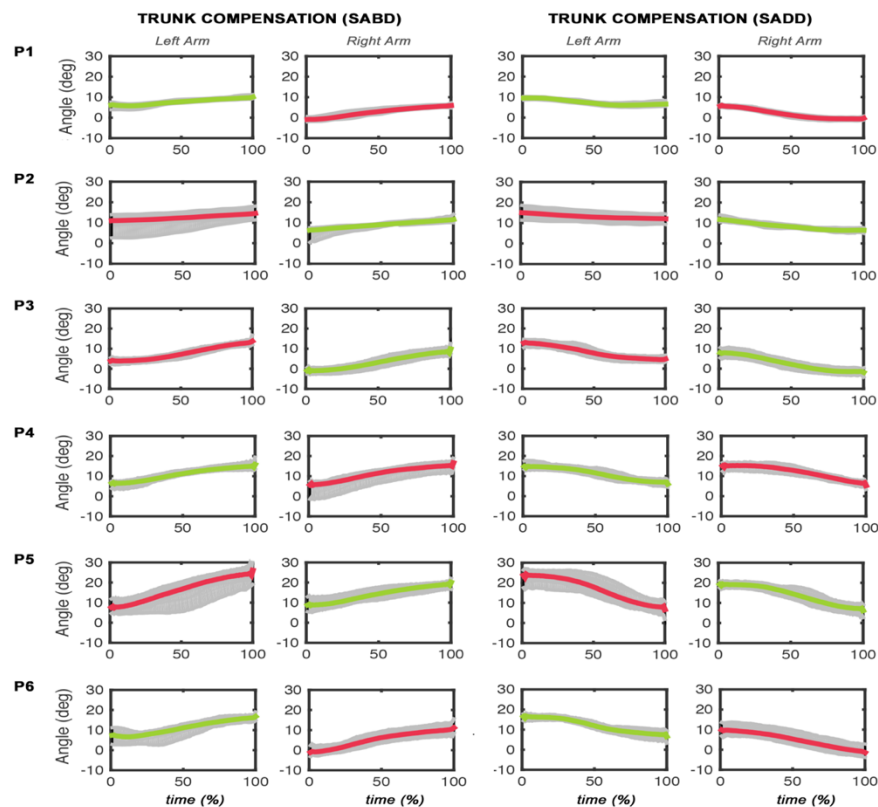
As it happened with the main angles, the evolution of the compensatory angles varies substantially from subject to subject. In this case, there is also a remarkable within-subject variability, which is especially noticeable in the paretic arm. This fact may indicate that patients do not have a fixed or preferred compensatory strategy to overcome the motor limitations imposed by stroke. Apparently, our motor system only needs few iterations of random searching to find suboptimal solutions of movement, which once found are reinforced by use-dependent neural plasticity<sup>258</sup>. Therefore, it is feasible that during the experiment patients entered an exploratory motor phase that would allow them, testing and after a given number of trials, selecting a proper compensatory motor strategy.

As expected, the magnitude of the compensatory movements is much notable in the paretic arm. They generally exhibit a deviation of  $\pm 20^\circ$  from the neutral position, but they can reach as much as  $30^\circ$  (P5, **Figure 131**) and even  $50^\circ$  (P5, **Figure 133**) of deviation. It is interesting to note, though, that some patients develop compensatory movements even when they execute the main movements with their unaffected arms,



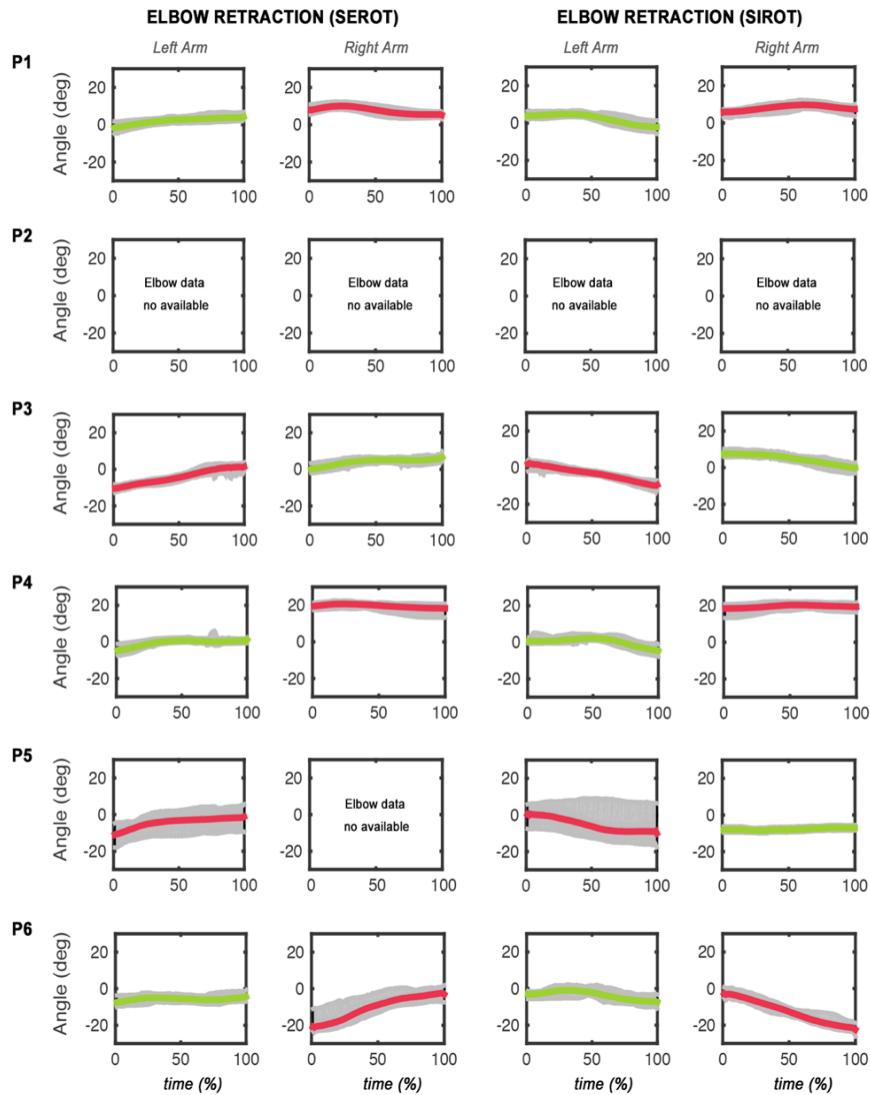
specially during shoulder abduction-adduction (for instance P3, P4 and P5 in **Figure 131**).

It also seems that the magnitude of the compensatory movements may be related with the severity of motor impairment. Indeed, as highlighted above, the maximal compensatory deviations are displayed by P5, who is the most impaired patient according to the FM-UE scale. In light of these observations, one may set out whether the emergence of compensatory movements respond to a transient motor strategy that may be attenuated as long as motor recovery progresses.



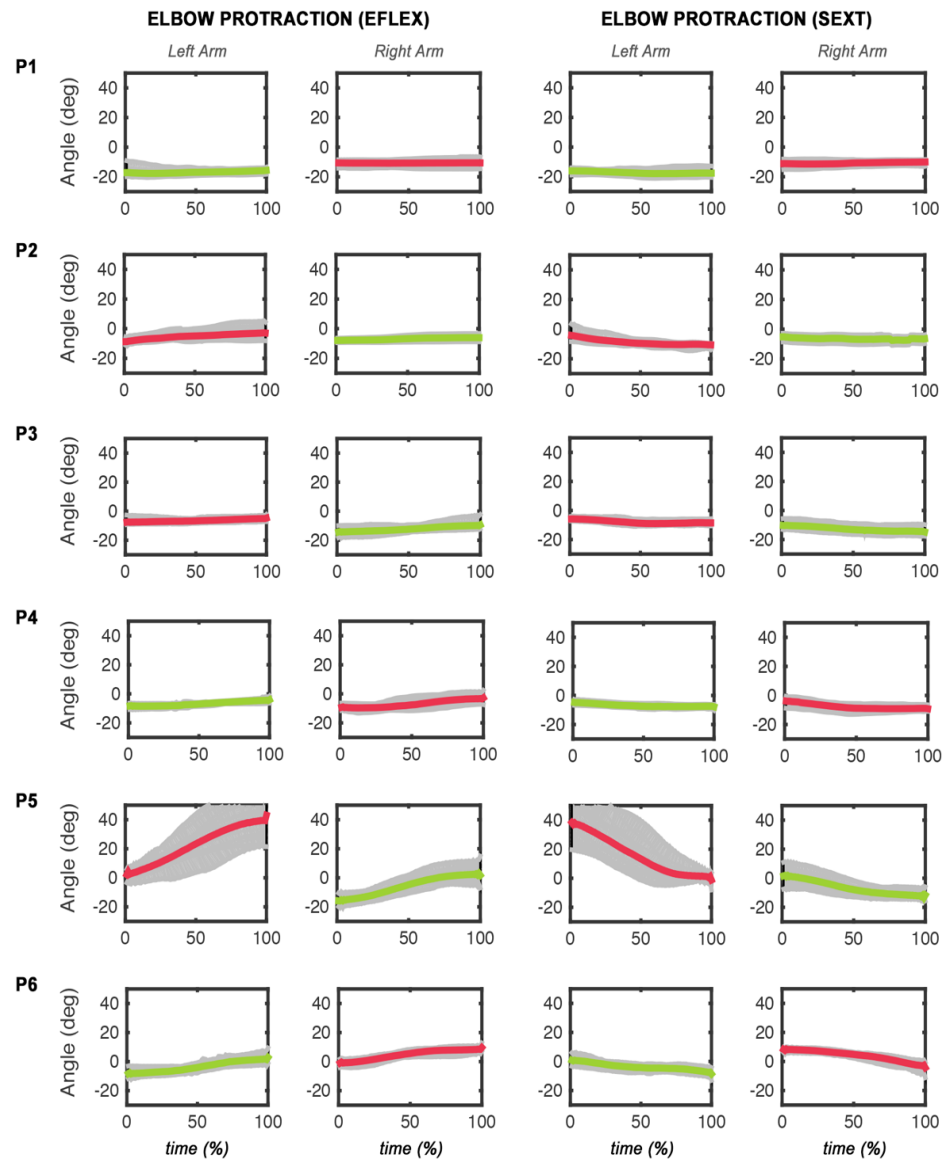
**Figure 131** Trunk compensation angle - compensatory angle evolution of shoulder ABDUCTION-ADDUCTION. Each row depicts the angle evolutions of each of the 6 patients (P1-P6). Grey curves represent the angle evolution in one movement- repetition and colored thick curves represent the mean of all repetitions. Red curves correspond to the paretic arm and green curves to the unaffected arm.





**Figure 132 Elbow retraction angle - compensatory angle evolution of SHOULDER EXTERNAL-INTERNAL ROTATION.** Each row depicts the angle evolutions of each of the 6 patients (P1-P6). Grey curves represent the angle evolution in one movement - repetition and colored thick curves represent the mean of all repetitions. Red curves correspond to the paretic arm and green curves to the unaffected arm.





**Figure 133 Elbow protraction angle - compensatory angle evolution of ELBOW FLEXION-EXTENSION.** Each row depicts the angle evolutions of each of the 6 patients (P1-P6). Grey curves represent the angle evolution in one movement- repetition and colored thick curves represent the mean of all repetitions. Red curves correspond to the paretic arm and green curves to the unaffected arm.



## 21.3 ANGULAR EVOLUTION, VELOCITY AND ACCELERATION

This section aims at comparing the angular kinematics exhibited by the paretic and the unaffected arm at subject level. The analyses focus on the angular kinematics of the main angles (i.e. the evolution of the main angle, the angular velocity and the angular acceleration) and on the evolution of the compensatory angle. The investigation is approached first from a qualitative and then from quantitative perspective.

### 21.3.1 *Qualitative interlimb comparisons*

The following set of figures show the angular kinematics of shoulder abduction-adduction (**Figure 134**), shoulder external-internal rotation (**Figure 135**) and elbow flexion-extension (**Figure 136**). These include the angular evolution of the main and compensatory angles, and the angular velocity and angular acceleration of the main angles.

Again, the differences between the paretic and unaffected arms are more evident specially in severely impaired patients (P2 and P5). This affirmation is generalizable to all four curves (main and compensatory angles, angular velocities and angular accelerations). As expected, the ROM of the paretic arm is reduced compared to the unaffected arm (See **Figure 134B,E** in P2 and P6 or **Figure 135B,E** in P3 and P6 for clear examples). The emergence of compensatory angles is also more apparent when the paretic arm is moving (See **Figure 134D,H** in P5; **Figure 135D,H** in P4 or **Figure 136D,H** in P5 for clear examples). As one can observe, this phenomenon seems to be strongly linked with severely impaired subjects.



In general unaffected arms seem to be faster than paretic arms during the entire execution of the movement (See **Figure 134B** in P2 and P6; **Figure 135B** in P3, P5 or **Figure 136B**, in P5, P6 for clear examples). That is, the unaffected arm does not only reach larger peak velocities; it moves faster from the beginning to the end of the movement, indicating that the paretic arm may also have compromised its accelerating capability. Consistently, higher velocities are usually associated to a better upper limb function within a given task<sup>155,251</sup>.

Human arm movements have symmetrical velocity profiles that depend on accuracy requirements of the task. Said another way, apparently the symmetry in the velocity profile is lost as the accuracy requirements of the task increase<sup>259</sup>. The velocity profiles of most patients here exhibit obvious symmetric signs in both arms, but patient 2, one of the most impaired subject, tended to loose such symmetry (**Figure 134**, **Figure 135**, **Figure 136**), suggesting that in severely impaired subjects the requirements to perform even simple tasks may be comparable to that of complex tasks in healthy or less impaired subjects.

The bell-shaped profiles exhibited by the angular velocities of the healthy arm demonstrate that the 3 movement pairs under analysis correspond to ballistic movements (i.e. biphasic movements reaching maximal velocity and acceleration). However, the bell shape is less evident in the paretic arm, especially in P2, one of the most severe patients. As a matter of fact, the velocity curves of preplanned goal-directed movements are bell-shaped in healthy subjects<sup>149</sup>, while stroke patients usually exhibit multiple peaks in their velocity profiles<sup>159,251</sup>. In this case, stroke also affects the velocity curves but in a slightly different manner: during single-joint movements the paretic arm loses the bell shape giving rise to a much flatter curve, but not to multiple peaks.

These phenomenon can be easily identified in certain movements, specially in most impaired subjects (**Figure 136B,F**, **Figure 135B,F** P2 and P5). The flatness of the velocity profile suggests that the motor impairment caused by stroke may hinder the



adequate acceleration of the arm. Indeed, stroke patients exhibit longer deceleration phases highlighting altered feed-forward and feedback control <sup>166</sup>.

The ability to develop ballistic movements is determined by high firing rates, high force production and very brief contraction times. Normally, this is achieved by a triphasic agonist/antagonist/agonist muscle activation <sup>160,260</sup>. Brief, the agonist muscle burst (starter) is followed by the antagonist muscle burst (braking force) which is finally followed by a burst in the agonist muscle (termination). Such incapacity to produce normal ballistic movements by stroke patients can be consistently attributed to a simultaneous influence of various well-described factors such as muscle weakness <sup>261</sup>, alterations in the motor acceleration mechanisms <sup>169</sup> or the abnormal coupling between the agonist and antagonist muscles <sup>262</sup>.



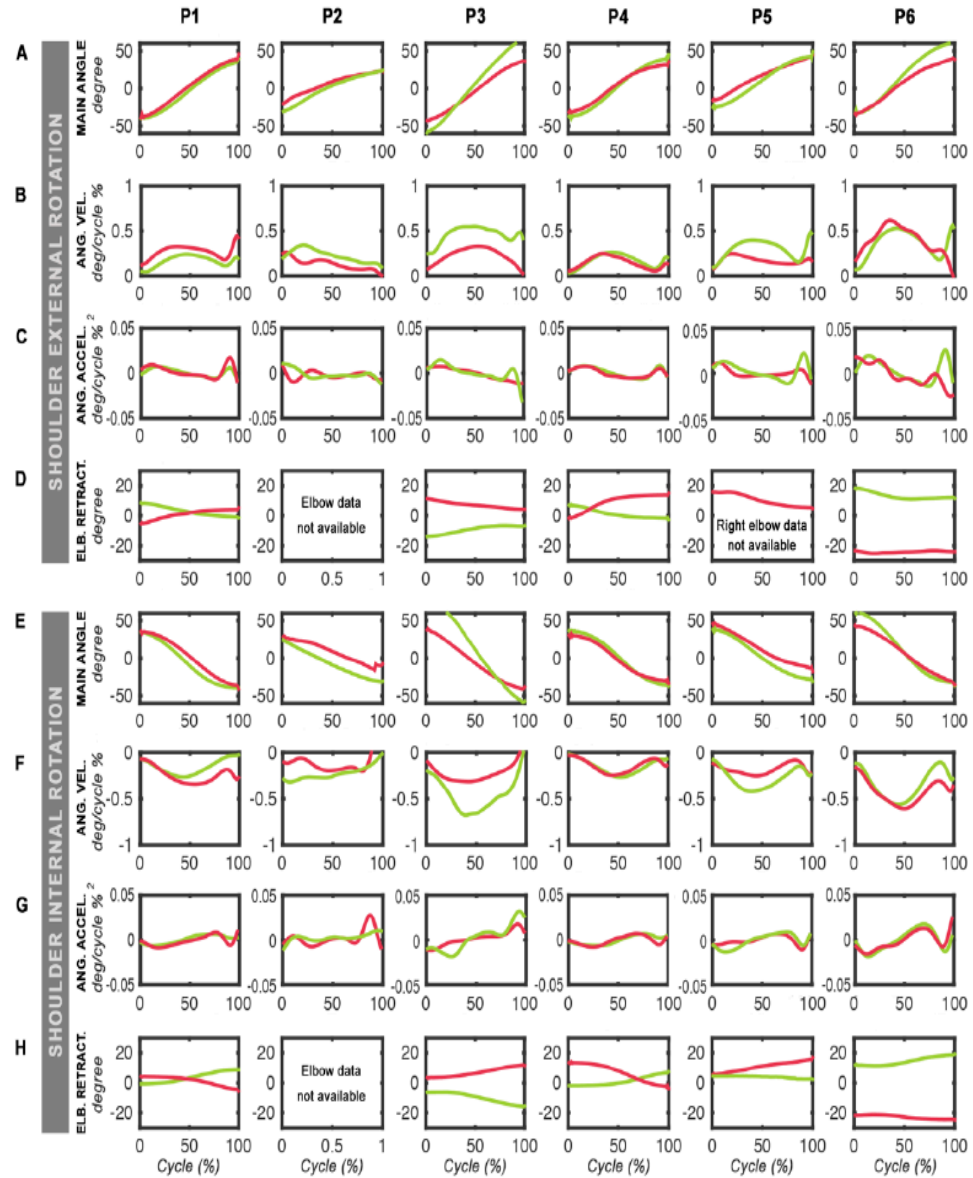


Figure 134 Paretic vs unaffected angular kinematic evolutions of (A-D) Shoulder abduction and (E-H) Shoulder adduction. A, E: main angle evolution; B, F: mean angular velocity; C, G: mean angular acceleration and D, H: trunk compensation angle of shoulder abduction and shoulder adduction respectively. Red curves correspond to the paretic arm and green curves to the unaffected arm.



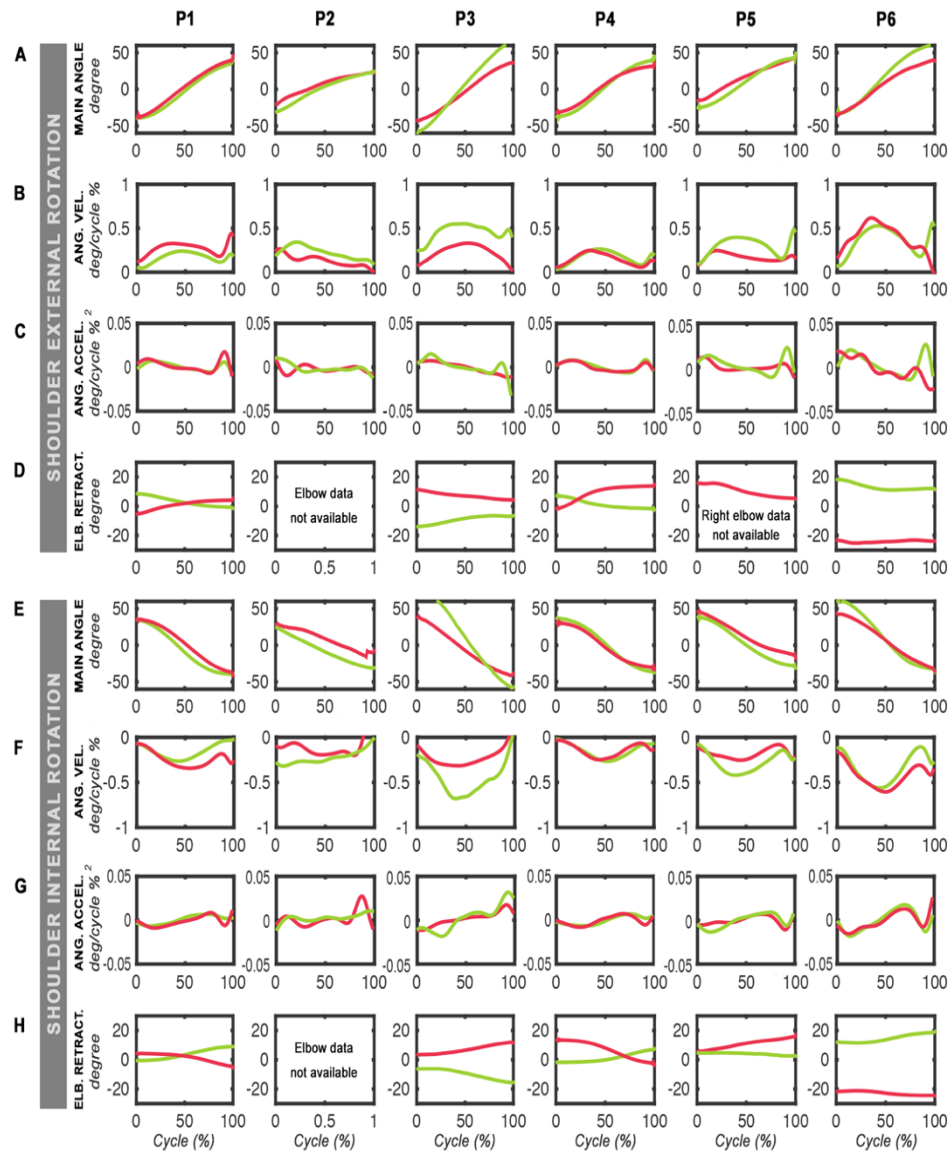
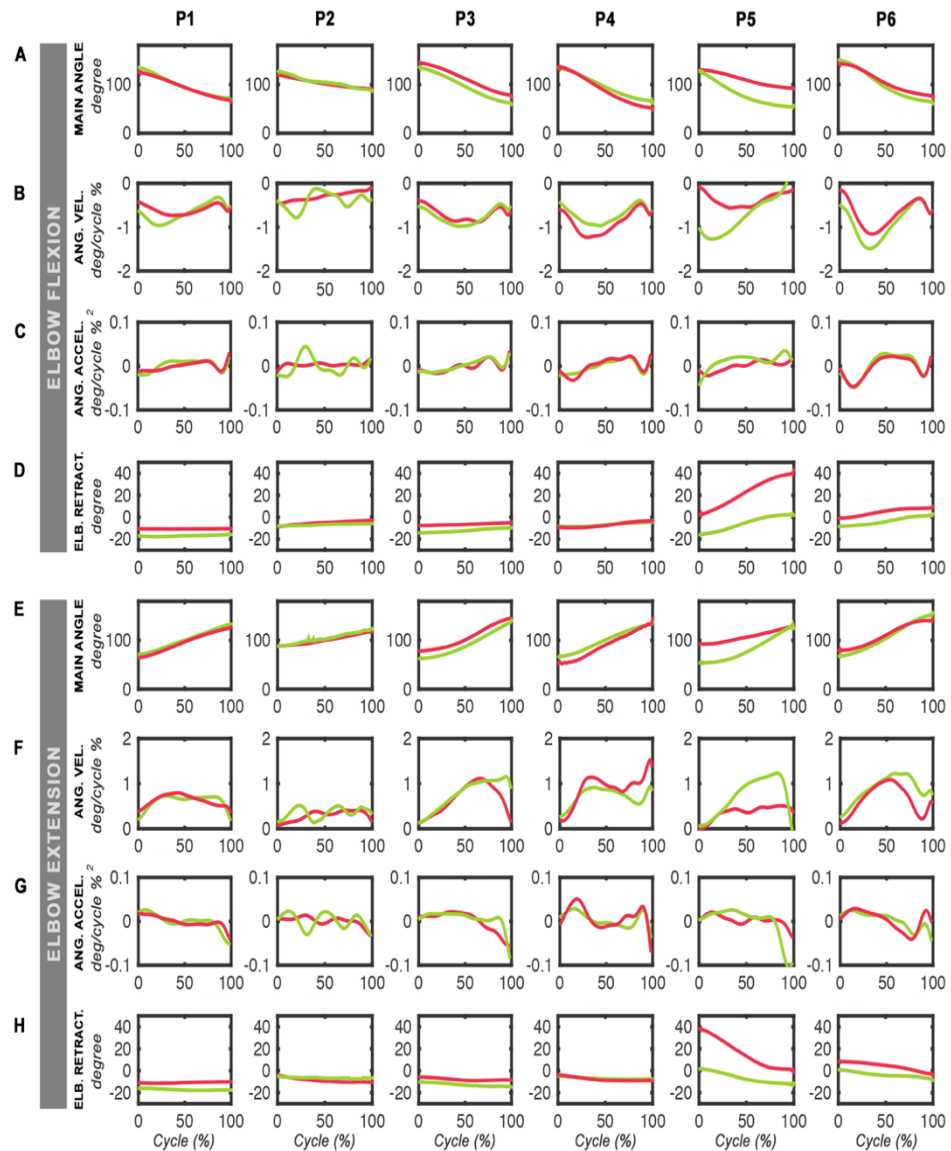


Figure 135 Paretic vs unaffected angular kinematic evolutions of (A-D) Shoulder external rotation and (E-H) Shoulder internal rotation. A, E: main angle evolution; B, F: mean angular velocity; C, G: mean angular acceleration and D, H: elbow retraction angle of shoulder external rotation and



shoulder internal rotation respectively. Red curves correspond to the paretic arm and green curves to the unaffected arm.



**Figure 136 Paretic vs unaffected angular kinematic evolutions of (A-D) Elbow flexion and (E-H) Elbow extension.** A, E: main angle evolution; B, F: mean angular velocity; C, G: mean angular acceleration and D, H: elbow protraction angle of elbow flexion and extension respectively. Red curves correspond to the paretic arm and green curves to the unaffected arm.



### 21.3.2 *Quantitative interlimb comparisons*

We employed 3 different measures in order to quantify the within-subject interlimb similarity of the kinematic curves between the paretic and the unaffected arm: the area between the curves, the cross-correlation coefficient and the Hausdorff distance (HD). The averages of these measures are shown in **Figure 136**. These measures were separately calculated for the mildly impaired population ( $FM \in [21-50]/66$ ) and the moderately impaired population ( $FM \in [51-66]/66$ ) according to their FM-UE scores.

#### 21.3.2.1 *Evolution of the main angle*

The first curve to analyze was the temporal evolution of the main angle defined for each movement (**Figure 136 - 1**). We found that during all movements, the differences between the angular evolution of paretic and unaffected limbs were larger in the mild population. All the 3 measures were absolutely consistent with this fact: the areas between the curves and the HF were greater, while the cross-correlation coefficient was smaller in the mildly impaired population. These results suggest that the restoration of the original spatial trajectories is a constitutive phase of the motor recovery process. Indeed, encouraging patients to take the trajectories described by their unaffected limbs as a reference to reproduce, could be a clever strategy to guide motor recovery according to physiological patterns and tailor the rehabilitation to the kinematic specificities of each patient.

#### 21.3.2.2 *Evolution of the angular velocity*

Next, we analyzed the angular velocity profiles developed by the patients as they executed each movement (**Figure 136 - 2**). Interestingly, the findings here were pretty much the same: the velocity patterns tended to be more similar between limbs in the



mildly impaired population. In fact, when we tested the statistical significance using the Wilcoxon rank-sum test, we found that differences between the two populations were very significant ( $p < 0.01$ ).

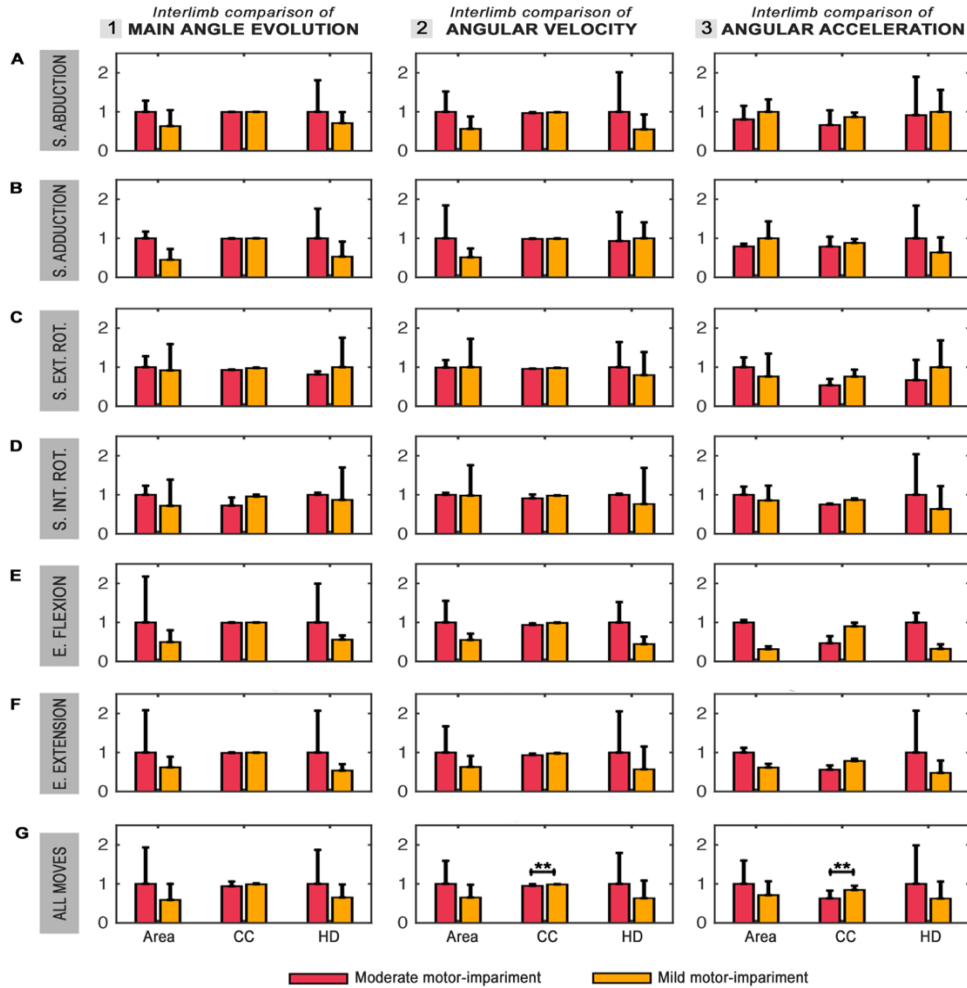
It has to be noted that in this case, the interlimb differences were less appreciable during shoulder rotations (**Figure 136 – C2,D2**). As opposed to the other movements, shoulder rotations imply exerting a constant anti-gravity force during the whole movement, as the height of the forearm remains invariable. Thus, for patients with stroke it might be easier to develop healthy-like velocity profiles under isodynamic conditions, rather than when they need to adapt the strength produced by the upper-limb to the trajectory, as it happens during shoulder abduction-adduction or elbow flexo-extension.

#### *21.3.2.3 Evolution of the angular acceleration*

The comparisons of the curves describing the evolution of the angular acceleration, also revealed that the angular acceleration profiles were much more similar between limbs in mildly impaired subjects than in moderately impaired subjects (**Figure 136 – 3**). In this case, though, the 3 measures were not as consistent as in the previous analyses, except the cross-correlation coefficients, which indicated that the similarity between the acceleration profiles was larger in all 6 movements for the mild population. Not only that, when we compared the means of all movements we found that (**Figure 136 – G3**) again, the differences were very significant between the two populations ( $p < 0.01$ ).

We find really appealing that while most of the clinical scales that are used to assess functionality and impairment focus on position-related items such as trajectories, ROM or end-effector reach, they ignore the characteristics that seem to be significant indicators of motor impairment degree such as velocity or acceleration profiles. In this sense, our results support that the cross-correlation coefficients of these profiles may constitute a good candidate to build new and more informative indices of motor impairment.





**Figure 137 Interlimb comparison of (1) main angle evolution, (2) angular velocity and (3) angular acceleration during (A) shoulder abduction, (B) shoulder adduction, (C) shoulder external rotation, (D) shoulder internal rotation, (E) elbow flexion and (F) elbow extension.** Bars are mean  $ILS_k$  measures of all subjects  $\pm$  SD for each movement, except in the panel (G) where the measures of all movements are averaged together. Red and orange bars differentiate patients with moderate ( $FM-UE \in [21,50]$ ) and mild ( $FM-UE \in [51,66]$ ) motor impairment respectively. Interlimb similarity measures used were: Area - normalized area between the curves; CC - cross-correlation coefficient and HD - normalized Hausdorff distance. Normalization was performed with respect to the maxima of each {paretic, unaffected} arm pair. Wilcoxon rank-sum test was applied to test the comparisons (\*\*  $p < 0.01$ ).



Taking everything together, these results should put the focus on the value of the interlimb similarity measures and on how powerful they can be, not only to assess motor impairment, but also to personalize the therapy and the understanding of each individual record. The reader should verify, that a similar conclusion was drawn in the previous studies dealing with the neuromuscular ILS. Therefore, it seems evident that ILS measures, both at the level of neuromuscular and kinematic level might be a right first approach to develop a physiological and quantitative index of motor impairment.

## 21.4 COMPARISON OF KINEMATIC INDICES

This section compares the set of kinematic indices extracted from the kinematic recordings across severity levels (mild vs moderate) and limbs (paretic vs unaffected).

### 21.4.1 *Paretic vs non paretic arm*

**Figure 138** compares the mean kinematic indices of the paretic limb (red bars) against the unaffected limb (green bars). **Figure 138A** provides an overview of the general trend of the population regardless the impairment grade of the patients. At this level of detail, we observe that (1) the compensatory angle described by the paretic limb is significantly greater than the compensatory angle found when the moving limb is unaffected (which, interestingly is not 0°, suggesting that the tendency to perform compensatory movements after stroke humbly spreads to the unaffected limb); and that (2) the mean angular velocity is significantly faster in the movements of the unaffected limb.

It has been repeatedly reported that during reaching motion, stroke patients exhibit slower, segmented and more variable movements restricted in ROM<sup>172,251</sup>. However, our results only show significant differences between the paretic and the unaffected arm in mean angular velocity and the amplitude of compensatory movements, revealing no significant differences in movement variability or segmentation. In consequence, it is possible that such kinematic characteristics only apply to goal-directed movements and not to single-DOF movements, as in the case.



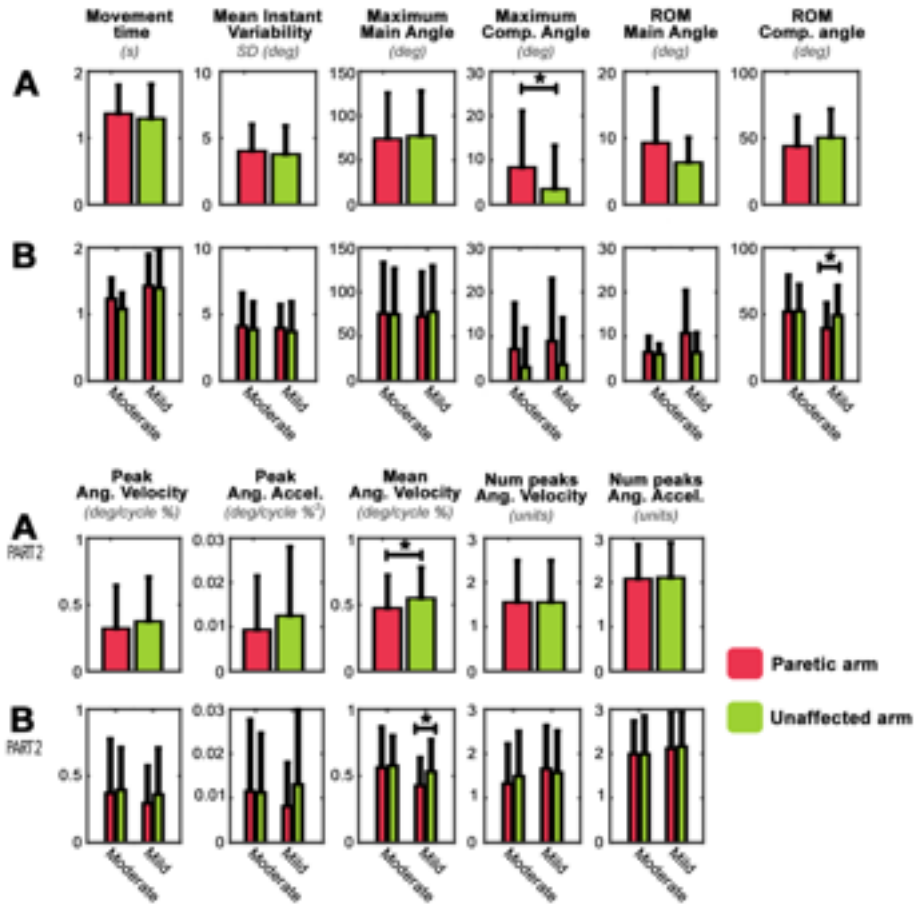


Figure 138 Interlimb comparison of kinematic indices. A – Kinematic indices averaged across all subjects and movements. B – Kinematic indices averaged across all movements and grouped according to the severity of motor impairment (Moderate: FM-UE  $\in$  [21,50]; Mild: FM-UE  $\in$  [51,66]). Bars are mean  $\pm$  SD. Statistical significance was assessed using Wilcoxon signed-rank test (\*  $p < 0.05$ ).

Another possibility is that the huge variability shown by the means mask meaningful differences in the database. Such variability is not only due to the kinematic diversity of the 3 movement-pairs under analysis, but also because the severity of the



population and therefore their motor outcome varies substantially from subject to subject. Thus, in order to limit such variability, we re-analyzed the results after grouping the population according to their grade of motor impairment (**Figure 138B**).

This new approach revealed obvious differences between the kinematic output of moderate and mild strokes. For instance, the paretic arms of mild patients were able to produce movements with larger ROMs, reflecting a clear improvement in mobility. The movements produced, though, were slower, both in terms of total movement time and mean angular velocity. On the one side, using a longer time is somehow logical, since the trajectory described by the arm is longer, as indicated by the ROM. On the other hand, this fact may also reflect a higher capacity to control and adapt the motion by mild subjects.

When we compared the performance of the unaffected arm between mild and moderate strokes we discovered very similar behaviors. This was something expected as in principle, stroke induces strictly hemiparetic effects. Nevertheless, we found that the time spent in movement production by the unaffected arm of mild strokes was longer than in moderate strokes although in this case the ROM was very similar. Also, the mean and peak velocity were slightly lower. Overall, it appears that mild strokes perform more slowly with their both arms, which again reinforces the hypothesis that slow motion may be indicative of a greater motor control capacity.

Regarding within-group interlimb differences, we found that the paretic arm of moderate patients performs slower movements (both in time and in velocity) and larger compensatory movements. In contrast, mild subjects seem to reduce the ROM of the compensatory angle and the angular velocity, as well as the peak acceleration.

It has to be highlighted, that deepening on the level of detail reduces sample size and causes difficulties to detect statistical significance among such a huge variability.

In order to investigate the potential variability sources affecting the global means displayed in **Figure 138**, we separately studied the kinematic indices for each of



the 6 movements under analysis, and their relationship with the motor impairment of patients using linear regressions (**Figure 139**).

#### 21.4.2 *Linear regressions: Fugl-Meyer score vs Kinematic indices*

Linear regressions were calculated according to the methods described in Study 3 (see section 17.5 Association analysis between ILS and clinical measures ). In this case, the criterion variable and the predictor variable were the kinematic index and the FM-UE score respectively (**Figure 139**). Although the amount of variability explained by linear correlations (quantified by  $R^2$ ) was not excessive, these plots allow studying general trends followed by the kinematic indices as motor impairment improves.

In general, we can observe that the improvement on the motor impairment of patients coincides with notable changes in their kinematic outcome. Quite a consistent behavior is found in the following kinematic indices across movements:

- *Movement time*: In all movements, the time used to execute the exercise tends to increase with motor improvement, reinforcing our previous hypothesis that greater execution times during relatively simple movements may be related to a greater motor control capacity (and greater ROM).
- *Movement instant variability*: the mean instant variability (mean SD of trajectories across the 20 repetitions) found between subjects did not follow any clear trend according to motor impairment.

Apparently, motor variability is a sign of our motor system exploring new movement patterns that produce useful motor output<sup>92,263–265</sup>. The fact that such variability does not decrease with motor recovery, may



indicate that during rehabilitation patients may enter a continuous exploratory phase that does not conclude until they relearn and fix optimal motor strategies. Another possibility is that according to optimality principles<sup>255,256,266</sup>, because this type of movements are not goal-directed, the margin for variability is higher given lower task-relevant constraints.

- *Maximum and ROM of main angle:* there is a clear improvement in the ROM of the main angles, specially during shoulder rotations (**Figure 139 C-D**) and elbow flexo-extension (**Figure 139 E-F**), indicating that motor improvement is strongly related to increased mobility.
- *Maximum and ROM of compensatory angle:* during all movements, either the maximum or the ROM of the compensatory angle is reduced with motor improvement. This behavior confirms that compensatory movements emerge to counteract motor limitations and suggests that the compensatory strategy is abandoned as the rehabilitation advances.
- *Peak angular velocity and acceleration:* these indices seem to be highly correlated. During shoulder abduction - adduction and elbow flexion, both peaks decrease while during shoulder rotations they increase. Note that in the first scenario, all 4 movements occurs in the vertical axis against gravity.

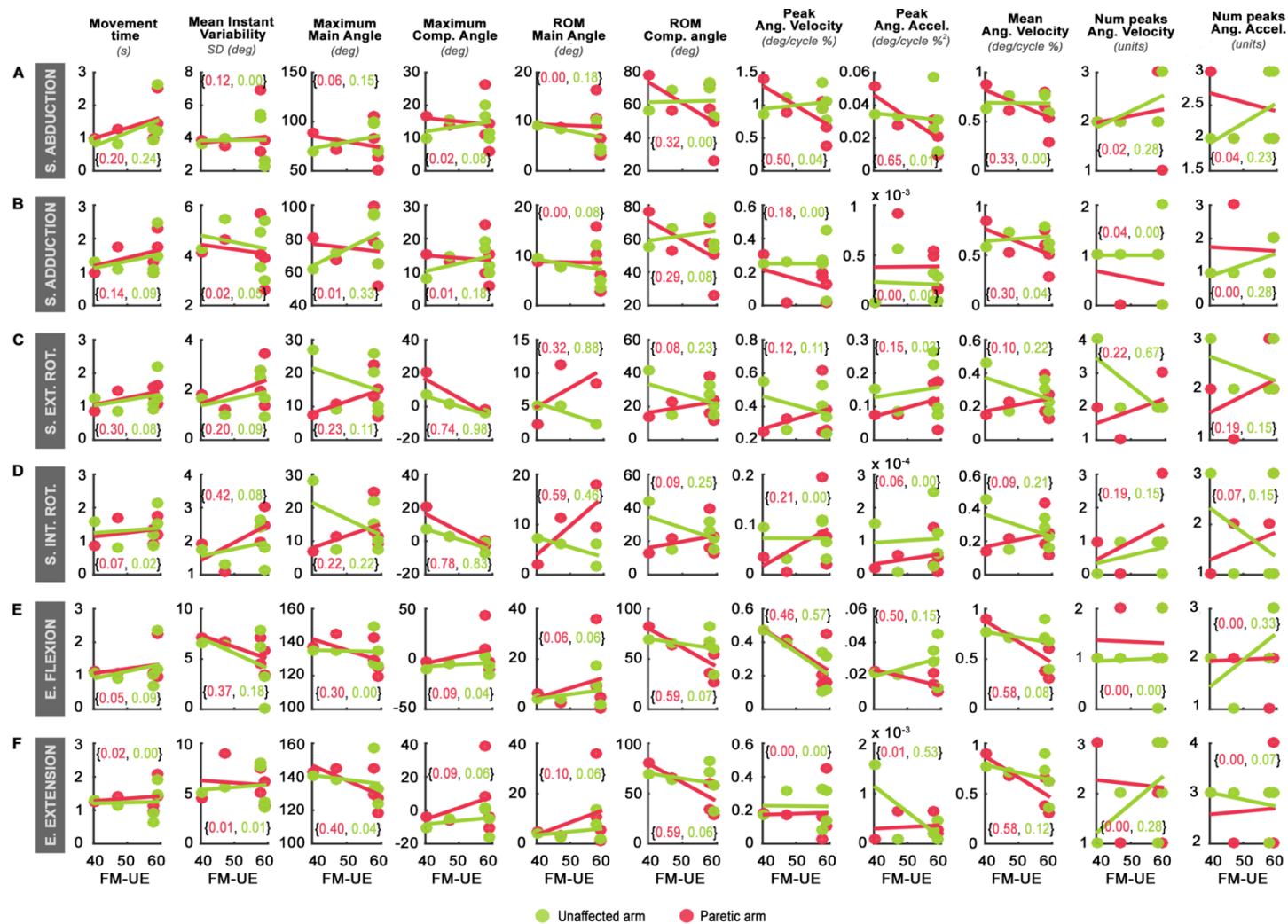
When patients executed these movements, we observed that the movements were not sustained in time. That is, when they had to lift their limb they tended to give it a high impulse to provide the limb with enough velocity to reach the end position. In contrast, during the opposite movement, they tended to let the limb drop, which probably made the limb move faster than it would have in absence of gravity (or if patients were able to strength-control the limb descent). Consistent with the studies about reaching or pointing<sup>164,165</sup>, these observations induce us to think that when the movement occurs in an axis different to gravity, increased velocity is a sign of motor recovery.



- *Mean angular velocity*: during the four anti-gravitational movements, the mean velocity decreases with motor improvement (**Figure 139** A-B,E-F). Taken everything together, it seems that patients regain strength during rehabilitation and recover the ability to precisely counteract the acceleration exerted by gravity in the limb. Indeed, during shoulder rotations in which the height of the limb remains constant, the mean velocity increases with motor improvement.

It is remarkable that, given that the movements analyzed in the study correspond to items of the Fug-Meyer scale, we expected higher correlation rates at least with the maximum and ROM of main and compensatory angles (see the pair of values between brackets in each plot of **Figure 139**). Again, as we observed with the neuromuscular state in Study 3, there is a high variability in the kinematic indices of patients with low motor-impairment, which in part, prevents the linear regression to be more accurate. These results make us wonder to what extent is the Fugl-Meyer scale appropriate to measure the motor impairment, specially when the impairment level is small. Following this line of thoughts, we wish to underline that the Fugl-Meyer scale does not consider relevant kinematic features such as velocity or acceleration profiles that have been proven to evolve together with motor impairment.





**Figure 139 Linear regressions: Kinematic indices vs Motor impairment level.** A - Shoulder abduction, B - Shoulder adduction, C - Shoulder External Rotation, D - Shoulder Internal Rotation, E - Elbow flexion, F - Elbow extension. Motor impairment level was measured with Fugl-Meyer - Upper Extremity (FM-UE) scores. The performance of the paretic arm is indicated by red data-points and the unaffected arm by green data-points. The pair of values between brackets indicate the R<sup>2</sup>-value of the linear regression for the paretic arm dataset (red text) and the unaffected arm dataset (green text).



## 21.5 KINEMATIC INDICES AS PREDICTORS: LOGISTIC REGRESSION

In order to extend the previous section and assess the predictive value of kinematic indices to determine the severity of the motor impairment, we used logistic regression. In particular, we fitted a logit-model to all possible pairs of predictors configured as {*ith* kinematic index, damaged hemisphere}. We found that the overall fit of all models determined by the likelihood ratio approached statistical significance ( $p \sim 0.08$ ) but none of the predictors was found significant ( $p > 0.05$ ) to predict the outcome {mild, moderate motor impairment}.

These results reinforce our hypothesis that kinematic indices alone are not sufficient to evaluate the motor state of patients. Although we have identified several solid indicators of kinematic evolution that correlated with motor improvement, these logistic regressions demonstrate that the predictive capacity of kinematic indices alone is rather weak. In consequence, in contrast to the clinical practice that basically focuses on functional aspects of patients with motor deficits whose evaluation is practically limited to a more or less accurate kinematic evaluation, we believe that a strong revision of traditional scales is needed to include physiological indices that reflect the neuromuscular state of the patients.

## 21.6 THE EFFECT OF VF IN ANGULAR KINEMATICS

This section is aimed at describing the effect that VF has on the motor performance of patients with stroke studied from a kinematic perspective. In particular, we focus on the ILS improvement driven by VF in the angular kinematics. Previously, we have proven that increased ILS is related to lower motor impairment both at the neuromuscular and kinematic level. Thus, demonstrating that VF is able to increase the kinematic ILS may shed light to the mechanisms underlying VF-driven recovery and lay the foundations to encourage the use VF during rehabilitation.



### 21.6.1 *ILS<sub>K</sub> measures across conditions (nVF and VF)*

**Figure 140** shows the ILS<sub>K</sub> measures that compare the 3 angular kinematic curves in mild and moderate populations. In general, we found that VF tended to increase the within-subject ILS between the angular kinematics of the paretic and unaffected arm. The ILS<sub>K</sub> measures are calculated for each movement separately (**Figure 140A-F**), and then averaged for all 3 movement pairs (**Figure 137G**). This last step is important because when we separate the population into moderate and mild groups, the sample-sizes are reduced (2 and 4 patients respectively) hindering the achievement of statistically significant results. In contrast, by averaging the data from all movements, we are able to present statistically significant comparisons.

#### 21.6.1.1 *VF on the evolution of the main angle*

Regarding the evolution of the main angle (**Figure 140-1**), we observed that VF tended to decrease both the area between the curves and the HD in both populations. The effect was especially remarkable in the moderately impaired population during shoulder abduction and shoulder rotations (**Figure 140-1A, C, D**) and in the mildly impaired population during elbow flexo-extension (**Figure 140-1E,F**). Conversely, the CC increased due to VF, consistently revealing an increase in the ILS<sub>K</sub>.

Indeed, we found that the ILS<sub>K</sub> increase induced by VF in the main angle evolution and measured by a decrease in HD was significant in the moderate population (**Figure 140-1G**). Note that although the HD means appear to be very close to each other, the Wilcoxon signed-rank test is a paired test that compares the ILS<sub>K</sub> values individually. That is, in this case, the test compared one by one the HD of a subject for a given movement performed in absence of VF (nVF) against its own VF value for that movement, along all movements and subjects and then, extrapolated the comparisons to the mean population.



### 21.6.1.2 VF on the evolution of the angular velocity

A similar scenario was found when we compared the evolution of the angular velocity. VF induced a substantial increase in the  $ILS_K$  of the angular velocity profiles of the moderate population, especially during shoulder rotations (**Figure 140-2C, D**). Conversely, no remarkable differences were found in the mild population induced by VF. Indeed, we found that overall, VF significantly increased the  $ILS_K$  in the angular velocity profiles of the moderate population (**Figure 140-2G**). Interestingly, while in absence of VF the  $ILS_K$  values between the moderate and mild populations were significantly different ( $p < 0.01$ ), VF suppressed such differences shifting the  $ILS_K$  of the moderate population within the range of the mild population. In other words, it seems that VF helps approaching the motor performance of moderately impaired patients to patterns similar to less impaired patients. Note that the difference of FM-UE score between these two populations is very high:  $43.5 \pm 4.95$  vs  $58.5 \pm 0.58$ , suggesting that VF may serve as a powerful catalyst to improve motor performance.

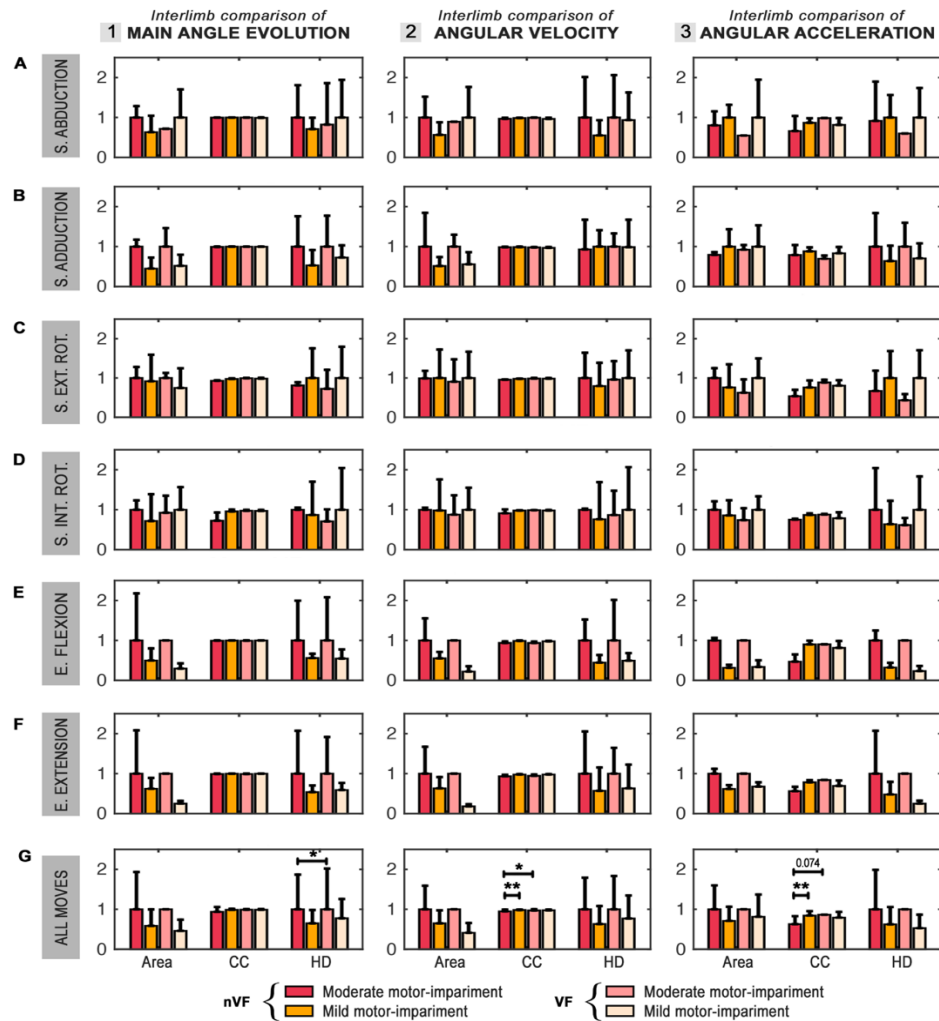
### 21.6.1.3 VF on the evolution of the angular acceleration

Finally, when we compared  $ILS_K$  of the evolution of the angular acceleration found in presence of VF with regard to the  $ILS_K$  found in absence of VF, we observed that again, the effect of VF in the moderate population was much more explicit, especially during shoulder abduction and lateral rotations (**Figure 140-3C, D, E**). For the mild population the differences induced by VF in the angular acceleration were not remarkable.

Overall, the  $ILS_K$  increase in angular acceleration induced by VF in the moderate population almost reached significance ( $p = 0.074$ ) (**Figure 140-3G**). In fact, as it happened with the angular velocity, while the differences between the moderate and mild populations in absence of VF were significant ( $p < 0.01$ ), the introduction of VF



increased the  $ILS_K$  levels of the moderate population close to the levels of the mild population, making the differences statistically insignificant.



**Figure 140**  $ILS_K$  measures of (1) main angle evolution, (2) angular velocity and (3) angular acceleration moderate in mild populations in absence (nVF) and presence (VF) of visual-feedback during (A) shoulder abduction, (B) shoulder adduction, (C) shoulder external rotation, (D) shoulder internal rotation, (E) elbow flexion and (F) elbow extension. Bars are mean  $ILS_K$  measures of all subjects  $\pm$  SD for each movement, except in the panel (G) where the measures of all movements are averaged together. Red and orange bars differentiate patients with moderate (FM-UE  $\in [21,50]$ ) and mild (FM-UE  $\in [51,66]$ ) motor impairment respectively.  $ILS_K$  measures were: Area - normalized area between the curves; CC - cross-correlation coefficient and HD - normalized Hausdorff distance. Normalization was performed with respect to the maxima of each {paretic, unaffected} arm pair. Wilcoxon rank-sum test was applied to compare populations (mild vs moderate) and Wilcoxon signed-rank test to compare conditions (nVF vs VF) (\*  $p < 0.05$ ; \*\*  $p < 0.01$ ).



Taking everything together, it seems that VF tends to increase the  $ILS_k$  in the 3 angular kinematic curves, reducing the differences of  $ILS_k$  values between the mild and moderate populations found in absence of VF. In general, the effect of VF is stronger in the moderate population, being especially prominent during shoulder abduction and lateral rotations.

The overall effect of VF during elbow flexo-extension is rather negligible. This is very likely to happen because during elbow flexo-extension, the mirror was placed in front of the patients, showing the coronal view and hiding the sagittal view. i.e., the plane where flexo-extension majorly occurred. This way, patients had only a partial view of their moving upper-limb i.e. they could see the elevation and descent of the end-effector, but not the position of the elbow or the orientation of the forearm. It seems that this information was not enough to interpret the spatial configuration the ongoing movement, nor to correct the movement online. In consequence, this induces us to think that in order to take full benefit of the potential of VF, a complete visualization of the movement is needed, at least in the plane where the main movement is happening.

### 21.6.2 VF-driven improvement of $ILS_k$

Next, we quantified the percentage of  $ILS_k$  change (increase or drop) induced by VF with regard to the basal  $ILS_k$  found in absence of VF (**Figure 141**). At a first view, we can immediately observe that the effect of VF is much more intensive in the moderate population than in the mild population.

In average, VF improved the  $ILS_k$  of the evolution of the main angle  $8.03 \pm 20.24\%$  in the moderate population, and  $0.20 \pm 1.89\%$  in the mild population (**Figure 141G1**).



Note that the huge SD of the moderate population is mainly due to the high inter-movement differences. For instance, the  $ILS_K$  improvement during shoulder internal rotation was  $40.68 \pm 43.21\%$  (**Figure 141D1**) while during shoulder adduction was only  $0.23 \pm 0.23\%$  (**Figure 141A1**). Indeed, during the experimental sessions certain patients reported that thanks to VF they realized that they tended to supinate their forearm during shoulder rotation, and that they were able to correct such deviation using the mirror.

In any case, VF increased the  $ILS_K$  of the moderate population in all movements except during elbow flexo-extension in which the contribution of VF was negligible (around  $\pm 0.1\%$ ). As we argued in the previous section, we believe that this is because the main view (the sagittal plane) was hidden to the patient due to the mirror frontal placement.

Regarding the angular velocity, VF improved the  $ILS_K$  of the moderate and mild populations in average  $2.60 \pm 5.00\%$  and  $-0.74 \pm 2.14\%$  respectively (**Figure 141G2**). Clearly, the effect of VF in the profile of the angular velocity is less pronounced than in the angular evolution. Nevertheless, in the moderate population, this is an improvement that must not be disregarded. Again, the contribution of VF was especially remarkable during shoulder rotations (**Figure 141-2C,D**), reaching a maximum improvement of as much as 17.49%.



Finally, we analyzed the effect of VF on the evolution of the angular acceleration and we discovered that the largest effect in regards to magnitude was found here. In average, the improvement of  $ILS_K$  induced by VF was  $28.39 \pm 40.37\%$  for the moderate population and  $-5.31 \pm 18.34\%$  for the mild population (**Figure 141G3**). Once again, shoulder rotations were the movement pair that most benefited from VF with an average improvement of  $74.85 \pm 65.58\%$  and  $16.89 \pm 1.18\%$  (external and internal rotations respectively, **Figure 141-3C,D**). In this case, though, elbow flexo-extension experimented a considerable  $ILS_K$  increase due to VF (  $51.43 \pm 0.00\%$  and  $31.81 \pm 0.00\%$  respectively<sup>1</sup>, **Figure 141-3E,F**).

Because patients had only the coronal view available to correct their motion, during elbow flexo-extension they could only track the vertical position of the end-effector. Obviously, this information may not be sufficient to correct the paretic joint configuration of shoulder and elbow according to the unaffected arm, but it may be useful to adapt the motion of the end-effector (i.e. velocity and acceleration). Indeed, we found that VF also contributed to increase the  $ILS_K$  of the angular velocity during elbow extension (**Figure 141-2F**), as opposed to its neutral effect on the evolution of the main angles (**Figure 141-1E,F**).

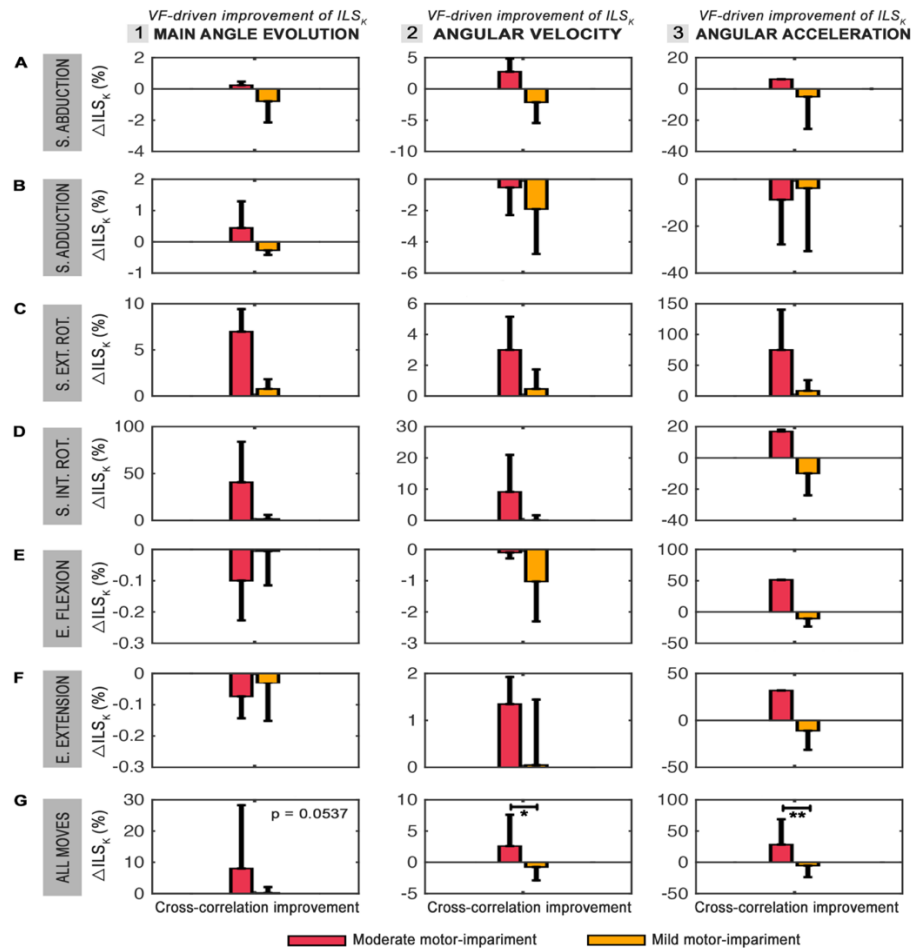
---

<sup>1</sup> SD is zero, because we missed the markers for one patients during elbow flexo-extension and as a result, the moderate group for this movement ended up having only one patient.





To sum up, VF tends to increase the  $ILS_K$  of all 3 angular curves in the moderate population. In terms of magnitude, though, the effect of VF stands out on the angular acceleration (**Figure 141G**). In contrast, the impact of VF in the mildly impaired population is rather negligible. In effect, the statistical tests indicate that the effect of VF is significantly larger in the moderate population compared to the mild population in improving the  $ILS_K$  of the evolution of the angular velocity ( $p < 0.05$ ) and the angular acceleration ( $p < 0.01$ ).



**Figure 141** VF-driven improvement of  $ILS_K$  measures of (1) main angle evolution, (2) angular velocity and (3) angular acceleration moderate in mild populations during (A) shoulder abduction, (B) shoulder adduction, (C) shoulder external rotation, (D) shoulder internal rotation, (E) elbow flexion and (F) elbow extension. Bars are mean  $\Delta ILS_K$  measures of all subjects  $\pm$  SD for each movement, except in the panel (G) where the improvement measures of all movements are averaged together. Wilcoxon rank-sum test was applied to compare populations (mild vs moderate) (\*  $p < 0.05$ ; \*\*  $p < 0.01$ ).



Taken everything together, it seems that VF might be especially helpful to improve the motor performance at the early stages of rehabilitation, when patients still have important kinematic deficits. Interestingly, the VF does not only correct the position deviations of the paretic arm, but it is also able to approach the angular velocity and acceleration profiles to physiological behavior (found in the unaffected arm).

It is plausible that when the differences between the performance of both arms are evident (moderately impaired patients), it is relatively easy for our motor control system to visually detect kinematic incongruences and correct them online. However, when interlimb differences are subtle, our kinematic awareness might not be enough to detect such tiny differences, reducing the effectiveness of VF. Thus, when the motor impairment is mild, alternative rehabilitation strategies might be sought to boost the final stages of motor recovery.

Finally, it has to be highlighted, that the effect of VF in the mild population is negligible rather than detrimental. In consequence, it is expected that using VF in the rehabilitation of mildly impaired patients does not hinder their recovery, but instead, has no effect on it.



# 22 CONCLUSIONS (IV)

## 22.1 MAJOR FINDINGS

This study is aimed at studying the kinematics of the paretic and unaffected arms of patients with stroke. The study brings into the focus the angular kinematics of the 6 movements under analysis. To this end, we have defined the main and compensatory angles observed during each movement pair.

From these data, we have directed the analysis following two different approaches. On the one hand, we have compared the curves of the angular kinematics (evolution of the main angle, angular velocity and angular acceleration) between the paretic and the unaffected arm. On the other hand, we have designed a set of 11 kinematic features to refine the comparisons that have also served as input data for a logit-model to predict the severity of the motor impairment.

Finally, we have studied the effect of VF on the ILS of the angular kinematics of patients. The study has been carried out separately for mildly and moderately impaired patients in order to investigate whether VF has differential effects depending on the motor impairment of the patient.



## QUALITATIVE INTERLIMB COMPARISONS OF ANGULAR KINEMATICS

- Obvious interlimb differences exist in the joint trajectories, especially in most impaired subjects. Most frequently:
  - Paretic arm exhibits visually smaller ROMs
  - Compensatory movements emerge when the paretic arm moves
  - The magnitude of the compensatory movements is related to impairment severity
- Kinematic measures are characterized by huge intra-subject and inter-subject variability
- During single-DOF movements, paretic arms perform slower than healthy arms:
  - The time to complete a movement is longer
  - Maximum velocity is lower
  - Velocity is lower during the entire trajectory
- In most impaired subjects, the velocity profiles of single-DOF movements:
  - Are less symmetric
  - Lose the bell shape, turning into flatter shaper
  - Do not present multiple peaks (as in goal-directed movements performed by stroke patients)
- Interlimb differences are more evident in severely impaired patients revealing a discriminatory capacity for kinematic measures.



## QUANTITATIVE INTERLIMB COMPARISONS OF ANGULAR KINEMATICS

- The ILS of kinematic curves is substantially higher in mildly impaired subjects than in moderately impaired subjects:
  - The ILS of main angular trajectories is higher in patients with mild impairment
  - The ILS of angular velocity profiles is significantly higher in patients with mild impairment
  - The ILS of angular acceleration profiles is significantly higher in patients with mild impairment

## KINEMATIC INDICES

- The interlimb comparisons of kinematic indices in patients with stroke (regardless severity) reveal that:
  - The compensatory angle is significantly larger in the paretic arm
  - The mean angular velocity is significantly slower in the paretic arm
- The comparisons of quantitative indices between severity groups reveal that mildly impaired patients exhibit:
  - Significantly larger ROM than moderately impaired patients
  - Significantly faster movements than moderately impaired patients
- Linear-regression models with respect to FM-UE score indicate that motor recovery (less severity) is correlated with:
  - Higher movement execution time (direct correlation)
  - Larger ROM (direct correlation)
  - Smaller compensatory movements (inverse correlation)
  - Higher peak angular velocity and accelerations during shoulder rotations (direct correlation)
  - No correlation was found with angular instant variability across repetitions
- Logit-models revealed low capacity of kinematic indices to discriminate between severity levels



## THE EFFECT OF VF ON KINEMATICS

- VF increases the ILS of angular kinematics, by shaping the profile of the paretic arm similar to the unaffected arm of each patient in. This effect is detected in all 3 kinematic curves:
  - Evolution of angular trajectories
  - Velocity profile
  - Acceleration profile
- The effect of VF is considerably larger in the moderate population in all 3 kinematic curves. However, the improvement induced by VF is only significant in the angular trajectories and velocity profiles (for the angular acceleration  $p = 0.07$ ).
- Thanks to VF, moderately impaired patients acquire ILS levels similar to the mild group
- In terms of magnitude, the effect of VF is most salient in the following order:
  - Angular acceleration (mean improvement =  $28.39 \pm 40.37\%$ )
  - Angular trajectories (mean improvement =  $8.03 \pm 20.24\%$ )
  - Angular velocity (mean improvement =  $2.60 \pm 5.00\%$ )
- The effect of VF is less apparent during elbow flexo-extension, probably because the mirror placement impeded the complete visualization of the moving limb.



## 22.2 FINAL REMARKS

In this last study, we demonstrate that the neuromuscular alterations reported in the previous studies have their counterpart at the kinematic level. We show that the alterations of the control structure provoked by stroke deviate the trajectory of the upper-limb joints and induce slower movements, reduced ROMs and the emergence of compensatory movements in the paretic arm. For this reason, the within-subject interlimb comparison of the kinematic features turns out to be an outstanding innovative strategy to detect and quantify motor impairment.

In this sense, our results indicate that the kinematic interlimb similarity ( $ILS_k$ ) is a good discriminant of motor severity levels. We have applied the concept  $ILS_k$  to compare (paretic vs unaffected arm) the new evolution of kinematic curves (global approach) and a set of 11 kinematic indices (local approach). The comparison of the kinematic curves is a global approach, as it considers the evolution of the kinematic characteristics of the movements along the full execution time. In contrast, the kinematic indices highlight punctual aspects of kinematics such as maximum velocity or acceleration. That is why we refer to them as a local approach. In any case, we have discovered that both approaches reveal significant differences between the two severity groups, highlighting the discriminatory potential of the kinematic study.

The local approach is the classical strategy found in literature, which has been widely used to characterize goal directed movements<sup>165,246,267</sup>. These studies, though, compare the kinematic performance of the paretic limb with the performance of healthy subjects, loosing any possibility to personalize the measures for every patient. Obviously, this is an important requirement when it comes to define new motor impairment measures, since it is increasingly accepted that every individual develops personalized motor strategies<sup>111,268,269</sup> subject to motor experience and training. Thus, comparing the kinematic indices between the paretic and unaffected arm is still a key innovative solution to personalize the assessment of patients based on classical indices.



Taken into account that the movements under analysis correspond to items of the Fugl-Meyer assessment scale, something that we did not expect was the low correlation found between the kinematic indices and the FM scores. This low correlation was mainly due to the high kinematic variability found among subjects that had similar FM-score, specially at the upper range of the scale. Therefore, these results confirm that the Fugl-Meyer scale might not capture subtle aspects characterizing the mild motor impairment, that scape to human eye. This may explain why the FM scale seems to present a saturation problem as previously suggested <sup>22</sup>. In this line and in view of the numerous limitations reported for the FM scale, we are forced to question whether the meaningfulness of our results may be compromised by the accuracy of the FM to detect motor-impairment or not.

The global approach extends the information given by kinematic indices covering the kinematic aspects of the entire movement execution. To the best of our knowledge, this is the first time that such a kind of approach is implemented. Our results indicate that motor recovery produces more similar kinematic profiles (angular trajectory, angular velocity and angular acceleration) between the two arms. Indeed, the  $ILS_K$  differences (measured with the cross-correlation coefficients) turned to be statistically significant between severity groups for the velocity and acceleration profiles. Thus, the interlimb cross-correlation of the kinematic curves outstands as a promising candidate to develop a new motor impairment index.

Interestingly, although interlimb differences in angular velocity and acceleration are significant discriminators of moderate and mild populations, the FM assessment scales (as other clinical measures such as the Barthel Index, modified Rankin Scale, Functional Independence Measure... ) do not consider this type of information. For this reason, this new approach opens the path to develop innovative metrics to



complement existing scales towards an integral evaluation of the motor capacity of the patient.

Variability is an inherent property of the motor system. Along this study, we have coped with huge variability both across subjects (inter-subject variability) and between repetitions (intra-subject variability). As a result, reaching statistical significance has become a difficult task in some cases due to insufficient sample-size issues. It is estimated that a size of 600 to 850 patients is needed to draw valid clinical conclusions about stroke<sup>125</sup>, which obviously is not attained in most studies including this one. Therefore, as we have argued along the study, it is likely that insufficient sample sizes have masked significant differences between groups. As a result, clear mean differences reported in our findings should thoughtfully considered relevant (even if they did not reach significance).

Along this line, it is believed, that subjects shape their own motor strategies according to their motor history and experience<sup>268,269</sup>. So, to what point makes sense to treat the group of stroke patients as a whole, instead of studying each case individually? In this sense, the interlimb comparison developed here are more meaningful to measure motor impairment than absolute comparisons of presumably highly heterogeneous groups.

Finding appropriate ways to deal with the inherent motor variability found in humans is critical in this kind of studies. Averaging the output of multiple repetitions is a widely used method to focus on the core features of a given motor behavior while avoiding intra-subject variability that probably arises from exploratory strategies and motor-system processing errors. Another good way to limit inherent intra-subject kinematic variability is the use of robotic devices that impose kinematic constraints on movement execution<sup>125,270,271</sup>. In addition, this kind of solutions provide anti-gravitational support to the upper-limb, reducing the interference that the effect gravity may introduce in the results. This last aspect seems to be a key feature as indicated by the differences observed in the velocity and acceleration patterns of



shoulder rotations, compared to the remaining movements that occurred in the direction of gravity.

Finally, we evaluated the impact of VF in the kinematic output of patients. Following the same strategy of comparing the paretic and unaffected angular kinematics, we found that VF contributes to increase the  $ILS_K$  by molding the paretic curves to the shape of unaffected arm's curves. VF showed capacity to modulate the 3 kinematic curves: angular trajectory, angular velocity and angular acceleration.

The effect of VF was much more prominent in the moderate population suggesting that VF may be a powerful tool to boost the efficacy of rehabilitation in early-intermediate stages. We found that VF contributed to increase the  $ILS_K$  of moderately impaired patients to the levels found in the mild group, which supports the hypothesis that motor recovery goes through a series of sequential well-defined motor stages<sup>35</sup>. Taken everything together, it seems that VF contributes to accelerate the progression to the next recovery stage.









## **PART IV**

# **Concluding Remarks**







The efforts to understand motor impairment and recovery have exponentially increased in the last few decades; however, the outcome of stroke motor rehabilitation remains pretty much the same. In consequence, the urgent need to improve stroke rehabilitation and find new objective measures of motor impairment is indisputable. This thesis has been conceived with the objective of developing a new quantitative metric of motor impairment and exploring new strategies to enhance motor recovery. To this end, we have conducted a detailed neuromuscular and kinematic analysis of the motor behavior of healthy subjects and stroke patients.

In particular, we have worked on the hypothesis that the interlimb differences between the paretic and the healthy arm may constitute a powerful tool to objectively assess the motor impairment of patients in a highly personalized manner. On the other hand, we have investigated the usefulness of visual feedback (VF) as a tool to boost motor recovery, based on the fact that VF is able to modulate neural plasticity and improve motor performance<sup>85,86</sup>.

In rough outlines, the major findings are as follows:

1. Healthy subjects share task-specific control structures between their two arms.



2. VF is able to modulate the control structure in healthy subjects by approaching the motor strategy of the nondominant arm to the dominant arm's.
3. Stroke affects the control structure of the paretic arm of patients, both at the level of muscle synergies and activation coefficients.
4. The interlimb similarity (ILS) of patients with stroke is significantly lower than in healthy subjects.
5. The ILS has sound power to detect and classify motor impairment grades.
6. The ILS of the control structure offers the neuromuscular perspective that lack existing assessment scales.
7. The kinematic ILS can discriminate between severity levels.
8. VF is able to significantly increase the ILS of patients with stroke, specially at a kinematic level.

## ILS, A NEW METRIC TO MEASURE IMPAIRMENT

It has been recently suggested that subjects may have their own motor programs that differ from the rest of the individuals. The existence of individual motor styles is naturally found in a wide range of animals <sup>272–275</sup> and in humans <sup>111,268,269</sup>. In consequence, focusing in averaged motor solutions is not an optimal approach since individual subjects develop their own motor solutions to solve neuromotor problems <sup>93</sup>. In addition, the way that individuals react to stroke and motor recovery is highly variable across subjects, even if the overall traits of the stroke are comparable <sup>276,277</sup>. As a result, trying to develop global standards to measure motor deficits and boost motor recovery may not be an adequate approach.

In this scenario, the concept of interlimb similarity (ILS) offers interesting advantages over traditional metrics. First, it is a quantitative metric that does not



depend on the subjective appreciation of therapists. Second, the ILS is fully personalized as it refers to the individual physiological state (preserved in the unaffected limb) of each patient, getting rid of unnecessary (and often wrong) global assumptions about motor performance and recovery. And third, the ILS of the control structure reflects the neuromuscular state of each patient, unlike traditional scales that are purely based on visual observation. This last attribute is absolutely essential to delve into the understanding of the physiological processes underlying motor recovery.

Interestingly, we have proven that the ILS of patients with stroke significantly differs from healthy subjects, both at the level of muscle synergies and activation coefficients and has potential to discriminate between motor impairment levels. Furthermore, the ILS provides means to identify which muscles present altered motor behaviors due to stroke, which allows purposely guiding rehabilitation. As a result, the ILS arises as a very promising tool to assess motor impairment and overcome current limitations of traditional scales.

Not only that, given the characteristics of the ILS, its potential goes beyond being a powerful motor impairment level to become a reliable reference to guide rehabilitation according to the patient's own physiological features. In this thesis we have demonstrated that using the control structure of one limb, we can reliably cross-reconstruct the muscle activity of the opposite limb with an accuracy over 90% in healthy subjects. Thus, we propose taking the control structure of the unaffected arm as a reference to purposely guide the rehabilitation of the paretic arm. This is undoubtedly an important advance in the field of rehabilitation, not only because the approach can be personalized to every patient (note that we have shown that not all subjects follow the same motor strategy to perform a given movement) but also because it provides insights about the natural neuromuscular state of the patient prior to stroke.



## VF AS A REHABILITATION TOOL

VF has been proven to be an effective method to improve motor performance<sup>79</sup>. However, the exact mechanisms by which VF modulates the motor control remain unclear, and naturally this understating is essential to effectively exploit VF-based rehabilitation. In this thesis, we have demonstrated that VF is able to induce changes both at a kinematic level and also at a neuromuscular level. Interestingly, the scope of VF changes with the pathological condition.

In healthy subjects, VF is able to modulate the control structure and increase the ILS. In particular, we show that VF induces intermanual transfer (IMT) of motor programs from the dominant side to the nondominant side. In contrast, in patients with stroke, VF is able to increase the kinematic ILS but loses its ability to modulate the control structure. Therefore, it is possible that the injured motor system requires a longer time lag before kinematic changes are fixed in the neuromuscular system.

Humans acquire and refine new motor patterns through exploration since early childhood stages<sup>278</sup>. This process requires only a few iterations of random searching to find locally optimal solutions that once found, are fixed by use-dependent neural plasticity<sup>258</sup>. Therefore, kinematic changes induced by VF might be the transient result of a successful exploratory phase that could be later fixed at a neuromuscular level if adequately reinforced over the time through training. In this scenario, it is very likely that the neural damage caused by stroke alters this mechanism, hindering the motor learning process.

Guiding motor learning over rehabilitation is critical to avoid the emergence of unwanted symptoms including compensatory movements<sup>172,279</sup>, delayed-onset involuntary abnormal movements<sup>280,281</sup> and ipsilateral motor projections<sup>194,282,283</sup>. All these symptoms have their origin in maladaptive neural changes and require to be recognized during rehabilitation to suppress their manifestation through proper



rehabilitative interventions<sup>282,284,285</sup>. Therefore, tools with the ability to modulate the control structure, like VF, are absolutely essential to this purpose.

Apparently, not all subjects can benefit equally from VF. Here again, inter-subject variability plays an important role. On the baseline, certain healthy subjects recognized that the use of VF made them lose the focus. Interestingly, these were the only subjects for whom the effect of VF was neutral or even deleterious. It is important to highlight that subjects were not taught to use VF (each subject entered the experimental session once). Therefore, it is plausible that subjects may be trained to learn how to use VF to enhance their rehabilitation. Indeed, none of the studied stroke patients (who were used to watch themselves into mirrors) recognized such a distraction problem due to VF. In any case, the need to conduct a longitudinal study is essential to test this hypothesis.

Precisely, it is important to test the durability of VF-driven effects. Studies in this field demonstrate that after learning optimal movement patterns, subjects tend to revert to habitual patterns, even if they are suboptimal<sup>286–288</sup>. This finding supports the need for a thorough long-term study that would confirm whether the beneficial changes induced by VF remain once VF is removed.

Finally, it has to be highlighted the importance of placing the mirror adequately. From what we have observed along this thesis, it seems that placing the mirror in front of the plane that holds the movement is critical in order to get most from the benefits of VF to place the mirror in front of the plane that holds the movement. E.g. During shoulder abduction in the coronal plane, during elbow flexion in the sagittal plane.

Be it as it may, this thesis demonstrates that VF is able to modulate the motor control structure and thus, supports VF as a promising tool to boost stroke rehabilitation. Nevertheless, further research is needed to confirm whether use-



dependent plasticity is able to turn the kinematic changes induced by VF into stable neuromuscular changes. Similarly, it is still to tune up how to train patients to effectively use VF.

## FUTURE WORK

This thesis offers a series of relevant and innovative advances in the fields of stroke assessment and neurorehabilitation. Overall, it lays the foundation of a new framework based on the original concept of interlimb similarity that opens the path to understand motor recovery and explore a wide variety of neurorehabilitation techniques in a physiological manner. Naturally, the results found along this thesis have raised a number of new questions that need to be answered in order to strengthen the framework and enhance its utility.

On the one hand, given the huge inter-subject and intra-subject variability inherent to the human motor system, which is even accentuated by the motor damage exerted by stroke, it seems that if we want to delve into the pathophysiology of stroke and its neurorehabilitation we need to include more patients in the study. The present thesis has been elaborated on 6 healthy subjects and 6 stroke patients. This number has proven to be enough to reliably investigate a wide variety of issues concerning the entire population. However the detailed analysis of aspects that require splitting the population into smaller groups such as the effect of the lesion size or location, the laterality of the affected hemisphere or the dominance of the paretic arm may require increasing such number.

Indeed, we have reported along the thesis that the lack of statistical significance found in certain sections was caused by insufficient sample size facing huge variability. More specifically, when comparing severity levels, the population was divided into two groups of 2 and 4 patients. Although mean differences between groups were considerable, comparing 2 versus 4 patients seems to be too few as to reach statistical significance. Hence, it is very likely that those results can be statistically confirmed just



by increasing the sample size. In other words, the bunch of initial results reported here are robust, but a larger database would confer further soundness.

On the other hand, the severity grade represented in this study is biased towards the upper bound of the impairment scale. Our database lacks severely impaired patients (the most severe patient exhibited a FM score of 40/66). The reason for that is that the severe patients that accomplished the inclusion criteria and were willing to enroll the study in the Guttmann Institute did not have enough residual motion to complete all the tasks in the experimental session. In consequence, we cannot ensure that the conclusions drawn in this pilot study can be extended to the most severe patients.

In consequence, in the close future we plan to enlarge the current database recruiting new patients that cover the widest possible range in the impairment scale. If needed, we contemplate the possibility of further modifying the experimental protocol to adapt it to a broader range of impairment. This is an indispensable tweak, if we want to define a complete metric to assess motor impairment. In fact, we are considering including additional goal-directed exercises to be able to evaluate the importance of task-relevant constraints in the control structure.

Finally, this thesis provides a detailed overview of the neuromuscular state of patients studied in a given time frame of the motor recovery process. This kind of experimental design has proven very useful to set the fundamentals of the innovative ILS concept presented here. However, it does not offer the possibility to study the effect of training and rehabilitation. To this end, we propose conducting a longitudinal study that allows us assessing the evolution of the ILS of the control structure and its kinematic counterpart throughout the process of motor recovery.









## **PART V**

# **Bibliography**







1. US National library of Medicine. MedlinePlus. Available at: <https://www.nlm.nih.gov/medlineplus/stroke.html>. (Accessed: 1st August 2014)
2. Federación Española del Ictus, C. *Dossier de comunicación*. (2014).
3. US National Library of Medicine. MedlinePlus - Stroke. Available at: <https://www.nlm.nih.gov/medlineplus/ency/article/000726.htm>. (Accessed: 1st August 2014)
4. Nichols, M., Townsend, N., Scarborough, P. & Rayner, M. European Cardiovascular Disease Statistics 2012. (2012). Available at: <http://www.escardio.org/The-ESC/Initiatives/EuroHeart/2012-European-Cardiovascular-Disease-Statistics>. (Accessed: 1st August 2014)
5. Stroke Association. Stroke Statistics. Available at: [http://www.stroke.org.uk/sites/default/files/Stroke\\_statistics.pdf](http://www.stroke.org.uk/sites/default/files/Stroke_statistics.pdf). (Accessed: 1st August 2014)
6. Federación Española de Ictus. El ictus. Available at: <http://www.ictusfederacion.es/el-ictus/>. (Accessed: 1st August 2014)
7. Townsend, N. *et al. Coronary heart disease statistics (2012)*. (2012).
8. Intercollegiate Stroke Working Party. National clinical guideline for stroke, 4th edition. Available at: <https://www.rcplondon.ac.uk/sites/default/files/national-clinical-guidelines-for-stroke-fourth-edition.pdf>. (Accessed: 1st September 2014)
9. Biller, J. *et al. Stroke in Children and Young Adults (Second Edition)*. (W.B. Saunders, 2009). doi:<http://dx.doi.org/10.1016/B978-0-7506-7418-8.00018-5>
10. Royal College of Physicians. National Sentinel Stroke Clinical Audit 2010 Round 7. (2011). Available at: [https://www.rcplondon.ac.uk/sites/default/files/documents/national\\_sentinel\\_stroke\\_clinical\\_audit\\_round\\_7\\_-\\_supplementary\\_report\\_on\\_therapy\\_intensity\\_march\\_2012.pdf](https://www.rcplondon.ac.uk/sites/default/files/documents/national_sentinel_stroke_clinical_audit_round_7_-_supplementary_report_on_therapy_intensity_march_2012.pdf). (Accessed: 1st August 2014)
11. Royal College of Physicians. Royal College of Physicians. National Sentinel Stroke Clinical Audit 2010. Available at: [https://www.rcplondon.ac.uk/sites/default/files/national-sentinel-stroke-audit-2010-public-report-and-appendices\\_0.pdf](https://www.rcplondon.ac.uk/sites/default/files/national-sentinel-stroke-audit-2010-public-report-and-appendices_0.pdf). (Accessed: 5th August 2014)
12. Adamson, J., Beswick, A. & Ebrahim, S. Is stroke the most common cause of disability? *J. Stroke Cerebrovasc. Dis.* 13, 171–7



## PART V. BIBLIOGRAPHY

---

13. Department of Health National Audit Office. Progress in improving stroke care London: The Stationary Office. (2010). Available at: <http://www.nao.org.uk/wp-content/uploads/2010/02/0910291.pdf>. (Accessed: 7th July 2014)
14. Nakayama, H., Jørgensen, H. S., Raaschou, H. O. & Olsen, T. S. Recovery of upper extremity function in stroke patients: the Copenhagen Stroke Study. *Arch. Phys. Med. Rehabil.* 75, 394–8 (1994).
15. National Stroke Association. National Stroke Association. Available at: <http://www.stroke.org/we-can-help/survivors/stroke-recovery/first-steps-recovery/preventing-another-stroke>. (Accessed: 22nd June 2016)
16. Price, C. I., Curless, R. H. & Rodgers, H. Can stroke patients use visual analogue scales? *Stroke.* 30, 1357–61 (1999).
17. Balasch i Bernat, M. *et al.* Determining cut-off points in functional assessment scales in stroke. *NeuroRehabilitation* 37, 165–172 (2015).
18. Brott, T. *et al.* Measurements of acute cerebral infarction: a clinical examination scale. *Stroke.* 20, 864–70 (1989).
19. Levine, S. *et al.* Stroke Scales: An Update. *Natl. Stroke Assoc.* 16, 1–7 (2006).
20. Sanford, J., Moreland, J., Swanson, L. R., Stratford, P. W. & Gowland, C. Reliability of the Fugl-Meyer assessment for testing motor performance in patients following stroke. *Phys. Ther.* 73, 447–54 (1993).
21. Rehabilitation Institute of Chicago. Rehabilitation Measures Database. Available at: <http://www.rehabmeasures.org/lists/rehabmeasures/disppform.aspx?ID=908>. (Accessed: 15th August 2014)
22. Gladstone, D. J., Danells, C. J. & Black, S. E. The Fugl-Meyer Assessment of Motor Recovery after Stroke: A Critical Review of Its Measurement Properties. *Neurorehabil. Neural Repair* 16, 232–240 (2002).
23. Wang, C.-H., Hsieh, C.-L., Dai, M.-H., Chen, C.-H. & Lai, Y.-F. Inter-rater reliability and validity of the stroke rehabilitation assessment of movement (stream) instrument. *J. Rehabil. Med.* 34, 20–4 (2002).
24. Lamontagne, A., Malouin, F. & Richards, C. L. Locomotor-specific measure of spasticity of plantarflexor muscles after stroke. *Arch. Phys. Med. Rehabil.* 82, 1696–704 (2001).
25. Dobkin, B. H., Firestine, A., West, M., Saremi, K. & Woods, R. Ankle dorsiflexion as an fMRI paradigm to assay motor control for walking during rehabilitation. *Neuroimage* 23, 370–81 (2004).
26. Nadeau, S., Arsenault, A. B., Gravel, D. & Bourbonnais, D. Analysis of the clinical factors determining natural and maximal gait speeds in adults with a stroke. *Am. J. Phys. Med. Rehabil.* 78, 123–30 (1999).
27. Kollen, B., van de Port, I., Lindeman, E., Twisk, J. & Kwakkel, G. Predicting improvement in gait after stroke: a longitudinal prospective study. *Stroke.* 36, 2676–80 (2005).
28. Gor-García-Fogeda, M. D. *et al.* Scales to Assess Gross Motor Function in Stroke



- Patients: A Systematic Review. *Arch. Phys. Med. Rehabil.* 95, 1174–1183 (2014).
29. Duncan, P. W., Jorgensen, H. S. & Wade, D. T. Outcome Measures in Acute Stroke Trials: A Systematic Review and Some Recommendations to Improve Practice. *Stroke* 31, 1429–1438 (2000).
  30. Balu, S. Differences in psychometric properties, cut-off scores, and outcomes between the Barthel Index and Modified Rankin Scale in pharmacotherapy-based stroke trials: systematic literature review. *Curr. Med. Res. Opin.* 25, 1329–41 (2009).
  31. Inouye, M., Hashimoto, H., Mio, T. & Sumino, K. Influence of admission functional status on functional change after stroke rehabilitation. *Am. J. Phys. Med. Rehabil.* 80, 121–5, 146 (2001).
  32. Hacke, W. *et al.* Intravenous thrombolysis with recombinant tissue plasminogen activator for acute hemispheric stroke. The European Cooperative Acute Stroke Study (ECASS). *JAMA* 274, 1017–25 (1995).
  33. Hacke, W. *et al.* Randomised double-blind placebo-controlled trial of thrombolytic therapy with intravenous alteplase in acute ischaemic stroke (ECASS II). Second European-Australasian Acute Stroke Study Investigators. *Lancet (London, England)* 352, 1245–51 (1998).
  34. Furlan, A. *et al.* Intra-arterial prourokinase for acute ischemic stroke. The PROACT II study: a randomized controlled trial. Prolyse in Acute Cerebral Thromboembolism. *JAMA* 282, 2003–11 (1999).
  35. Brunnström, S. *Movement therapy in hemiplegia*. (Medical Dept., Harper & Row, 1970).
  36. Fugl-Meyer, A. R., Jääskö, L., Leyman, I., Olsson, S. & Steglind, S. The post-stroke hemiplegic patient. 1. a method for evaluation of physical performance. *Scand. J. Rehabil. Med.* 7, 13–31 (1975).
  37. Knox, V. & Evans, A. L. Evaluation of the functional effects of a course of Bobath therapy in children with cerebral palsy: a preliminary study. *Dev. Med. Child Neurol.* 44, 447–60 (2002).
  38. Woollacott, M. H. & Shumway-Cook, A. Changes in posture control across the life span--a systems approach. *Phys. Ther.* 70, 799–807 (1990).
  39. Kleim, J. A. & Jones, T. A. Principles of experience-dependent neural plasticity: implications for rehabilitation after brain damage. *J. Speech. Lang. Hear. Res.* 51, S225-39 (2008).
  40. Boyd, L. & Winstein, C. Explicit information interferes with implicit motor learning of both continuous and discrete movement tasks after stroke. *J. Neurol. Phys. Ther.* 30, 46-57-9 (2006).



## PART V. BIBLIOGRAPHY

---

41. Lennon, S. & Ashburn, A. The Bobath concept in stroke rehabilitation: a focus group study of the experienced physiotherapists' perspective. *Disabil. Rehabil.* 22, 665–74 (2000).
42. Levin, M. F., Kleim, J. A. & Wolf, S. L. What do motor 'recovery' and 'compensation' mean in patients following stroke? *Neurorehabil. Neural Repair* 23, 313–9 (2009).
43. Graham, J. V., Eustace, C., Brock, K., Swain, E. & Irwin-Carruthers, S. The Bobath concept in contemporary clinical practice. *Top. Stroke Rehabil.* 16, 57–68
44. Kollen, B. J. *et al.* The effectiveness of the Bobath concept in stroke rehabilitation: what is the evidence? *Stroke.* 40, e89-97 (2009).
45. Paci, M. Physiotherapy based on the Bobath concept for adults with post-stroke hemiplegia: a review of effectiveness studies. *J. Rehabil. Med.* 35, 2–7 (2003).
46. Cramer, S. C. The EXCITE trial: a major step forward for restorative therapies in stroke. *Stroke.* 38, 2204–5 (2007).
47. Levy, C. E., Nichols, D. S., Schmalbrock, P. M., Keller, P. & Chakeres, D. W. Functional MRI evidence of cortical reorganization in upper-limb stroke hemiplegia treated with constraint-induced movement therapy. *Am. J. Phys. Med. Rehabil.* 80, 4–12 (2001).
48. Swinnen, S. P. Intermanual coordination: from behavioural principles to neural-network interactions. *Nat. Rev. Neurosci.* 3, 348–59 (2002).
49. van Delden, A. (Lex) E. Q., Peper, C. (Lieke) E., Kwakkel, G. & Beek, P. J. A Systematic Review of Bilateral Upper Limb Training Devices for Poststroke Rehabilitation. *Stroke Res. Treat.* 2012, 1–17 (2012).
50. Stinear, C. M., Barber, P. A., Coxon, J. P., Fleming, M. K. & Byblow, W. D. Priming the motor system enhances the effects of upper limb therapy in chronic stroke. *Brain* 131, 1381–90 (2008).
51. van Delden, A. E. Q., Peper, C. E., Beek, P. J. & Kwakkel, G. Unilateral versus bilateral upper limb exercise therapy after stroke: a systematic review. *J. Rehabil. Med.* 44, 106–17 (2012).
52. Langhorne, P., Coupar, F. & Pollock, A. Motor recovery after stroke: a systematic review. *Lancet. Neurol.* 8, 741–54 (2009).
53. Coupar, F. *et al.* Simultaneous bilateral training for improving arm function after stroke ( Review ) Simultaneous bilateral training for improving arm function after stroke. *Heal. (San Fr.* (2010). doi:10.1002/14651858.CD006432.pub2.Copyright
54. Stewart, K. C., Cauraugh, J. H. & Summers, J. J. Bilateral movement training and stroke rehabilitation: a systematic review and meta-analysis. *J. Neurol. Sci.* 244, 89–95 (2006).
55. Cauraugh, J. H., Lodha, N., Naik, S. K. & Summers, J. J. Bilateral movement training and stroke motor recovery progress: a structured review and meta-analysis. *Hum. Mov. Sci.* 29, 853–70 (2010).
56. Whittall, J. *et al.* Bilateral and unilateral arm training improve motor function through differing neuroplastic mechanisms: a single-blinded randomized controlled trial.



- Neurorehabil. Neural Repair* 25, 118–29 (2011).
57. Maciejasz, P., Eschweiler, J., Gerlach-Hahn, K., Jansen-Troy, A. & Leonhardt, S. A survey on robotic devices for upper limb rehabilitation. *J. Neuroeng. Rehabil.* 11, 3 (2014).
  58. Hamid, S. & Hayek, R. Role of electrical stimulation for rehabilitation and regeneration after spinal cord injury: an overview. *Eur. Spine J.* 17, 1256–1269 (2008).
  59. Takano, Y. *et al.* Increasing muscle strength and mass of thigh in elderly people with the hybrid-training method of electrical stimulation and volitional contraction. *Tohoku J. Exp. Med.* 221, 77–85 (2010).
  60. Mehrholz, J., Platz, T., Kugler, J. & Pohl, M. Electromechanical and robot-assisted arm training for improving arm function and activities of daily living after stroke. *Cochrane database Syst. Rev.* CD006876 (2008). doi:10.1002/14651858.CD006876.pub2
  61. Kwakkel, G., Kollen, B. J. & Krebs, H. I. Effects of robot-assisted therapy on upper limb recovery after stroke: a systematic review. *Neurorehabil. Neural Repair* 22, 111–21 (2008).
  62. Waldner, A., Tomelleri, C. & Hesse, S. Transfer of scientific concepts to clinical practice: recent robot-assisted training studies. *Funct. Neurol.* 24, 173–7
  63. Reinthal, A. *et al.* ENGAGE: Guided Activity-Based Gaming in Neurorehabilitation after Stroke: A Pilot Study. *Stroke Res. Treat.* 2012, 784232 (2012).
  64. Ertelt, D. *et al.* Action observation has a positive impact on rehabilitation of motor deficits after stroke. *Neuroimage* 36 Suppl 2, T164-73 (2007).
  65. Laver, K. E., George, S., Thomas, S., Deutsch, J. E. & Crotty, M. Virtual reality for stroke rehabilitation. *Cochrane database Syst. Rev.* CD008349 (2011). doi:10.1002/14651858.CD008349.pub2
  66. Feng, W. W., Bowden, M. G. & Kautz, S. Review of transcranial direct current stimulation in poststroke recovery. *Top. Stroke Rehabil.* 20, 68–77
  67. Dimyan, M. a & Cohen, L. G. Neuroplasticity in the context of motor rehabilitation after stroke. *Nat. Rev. Neurol.* 7, 76–85 (2011).
  68. Chrysikou, E. G. & Hamilton, R. H. Noninvasive brain stimulation in the treatment of aphasia: exploring interhemispheric relationships and their implications for neurorehabilitation. *Restor. Neurol. Neurosci.* 29, 375–94 (2011).
  69. Woodford, H. & Price, C. EMG biofeedback for the recovery of motor function after stroke. *Cochrane database Syst. Rev.* CD004585 (2007). doi:10.1002/14651858.CD004585.pub2



## PART V. BIBLIOGRAPHY

---

70. Rayegani, S. M. *et al.* Effect of neurofeedback and electromyographic-biofeedback therapy on improving hand function in stroke patients. *Top. Stroke Rehabil.* 21, 137–51 (2014).
71. Shadmehr, R., Smith, M. a & Krakauer, J. W. Error correction, sensory prediction, and adaptation in motor control. *Annu. Rev. Neurosci.* 33, 89–108 (2010).
72. Robinson, D. in *Basic Mechanisms of Ocular Motility and Their Clinical Implications* (eds. Bachyrita, P. & Lennerstrand, G.) 337–374 (Pergamon Press, 1975).
73. Pasalar, S., Roitman, A. V, Durfee, W. K. & Ebner, T. J. Force field effects on cerebellar Purkinje cell discharge with implications for internal models. *Nat. Neurosci.* 9, 1404–11 (2006).
74. Milner, T. E. A model for the generation of movements requiring endpoint precision. *Neuroscience* 49, 487–96 (1992).
75. Woodworth, R. Accuracy of voluntary movement. *Psychol. Rev. Monogr. Suppl.* 3, i-114 (1899).
76. Crossman, E. R. & Goodeve, P. J. Feedback control of hand-movement and Fitts' Law. *Q. J. Exp. Psychol. A.* 35, 251–78 (1983).
77. Vallbo, A. B. & Wessberg, J. Organization of motor output in slow finger movements in man. *J. Physiol.* 469, 673–91 (1993).
78. Ikegami, T., Hirashima, M., Osu, R. & Nozaki, D. Intermittent Visual Feedback Can Boost Motor Learning of Rhythmic Movements: Evidence for Error Feedback Beyond Cycles. *J. Neurosci.* 32, 653–657 (2012).
79. Thieme, H., Mehrholz, J., Pohl, M., Behrens, J. & Dohle, C. Mirror therapy for improving motor function after stroke. *Stroke* 44, 2013–2015 (2013).
80. Yavuzer, G. *et al.* Mirror therapy improves hand function in subacute stroke: a randomized controlled trial. *Arch. Phys. Med. Rehabil.* 89, 393–8 (2008).
81. Dohle, C. *et al.* Mirror Therapy Promotes Recovery From Severe Hemiparesis: A Randomized Controlled Trial. *Neurorehabil. Neural Repair* 23, 209–217 (2008).
82. Yang, Y.-R. *et al.* Effects of interactive visual feedback training on post-stroke pusher syndrome: a pilot randomized controlled study. *Clin. Rehabil.* 29, 987–993 (2015).
83. Saunders, J. A. Visual Feedback Control of Hand Movements. *J. Neurosci.* 24, 3223–3234 (2004).
84. Seidler, R. D., Kwak, Y., Fling, B. W. & Bernard, J. A. Neurocognitive mechanisms of error-based motor learning. *Adv. Exp. Med. Biol.* 782, 39–60 (2013).
85. Bartur, G. *et al.* Electrophysiological manifestations of mirror visual feedback during manual movement. *Brain Res.* 1606, 113–124 (2015).
86. Nojima, I. *et al.* Human motor plasticity induced by mirror visual feedback. *J. Neurosci.* 32, 1293–300 (2012).
87. Bütefisch, C. M. *et al.* Mechanisms of use-dependent plasticity in the human motor cortex. *Proc. Natl. Acad. Sci. U. S. A.* 97, 3661–5 (2000).
88. Garry, M. I., Loftus, a. & Summers, J. J. Mirror, mirror on the wall: Viewing a



- mirror reflection of unilateral hand movements facilitates ipsilateral M1 excitability. *Exp. Brain Res.* 163, 118–122 (2005).
89. Warraich, Z. & Kleim, J. a. Neural plasticity: the biological substrate for neurorehabilitation. *PM R* 2, S208-19 (2010).
  90. Jang, S. H. Motor function-related maladaptive plasticity in stroke: A review. *NeuroRehabilitation* 32, 311–6 (2013).
  91. Bernshtein, N. A. *The co-ordination and regulation of movements*. (Pergamon Press, 1967).
  92. Wu, H. G., Miyamoto, Y. R., Castro, L. N. G., Ölveczky, B. P. & Smith, M. A. Temporal structure of motor variability is dynamically regulated and predicts motor learning ability. *Nat. Neurosci.* 17, 312–321 (2014).
  93. Ting, L. H. *et al.* Neuromechanical principles underlying movement modularity and their implications for rehabilitation. *Neuron* 86, 38–54 (2015).
  94. Zatsiorsky, V. M. *Kinematics of Human Motion*. (Human Kinetics, 1998).
  95. Latash, M. L. The bliss (not the problem) of motor abundance (not redundancy). *Exp. Brain Res.* 217, 1–5 (2012).
  96. Latash, M. L. & Anson, J. G. Synergies in health and disease: relations to adaptive changes in motor coordination. *Phys. Ther.* 86, 1151–60 (2006).
  97. Torres-Oviedo, G., Macpherson, J. M. & Ting, L. H. Muscle synergy organization is robust across a variety of postural perturbations. *J. Neurophysiol.* 96, 1530–46 (2006).
  98. Olshausen, B. A. & Field, D. J. Sparse coding of sensory inputs. *Curr. Opin. Neurobiol.* 14, 481–7 (2004).
  99. De Groote, F., Jonkers, I. & Duysens, J. Task constraints and minimization of muscle effort result in a small number of muscle synergies during gait. *Front. Comput. Neurosci.* 8, 115 (2014).
  100. McKay, J. L. & Ting, L. H. Optimization of muscle activity for task-level goals predicts complex changes in limb forces across biomechanical contexts. *PLoS Comput. Biol.* 8, e1002465 (2012).
  101. Steele, K. M., Tresch, M. C. & Perreault, E. J. The number and choice of muscles impact the results of muscle synergy analyses. *Front. Comput. Neurosci.* 7, 105 (2013).
  102. Tresch, M. C., Saltiel, P. & Bizzi, E. The construction of movement by the spinal cord. *Nat. Neurosci.* 2, 162–167 (1999).
  103. Cheung, V. C. K. Central and Sensory Contributions to the Activation and Organization of Muscle Synergies during Natural Motor Behaviors. *J. Neurosci.* 25,



## PART V. BIBLIOGRAPHY

---

- 6419–6434 (2005).
104. d’Avella, A. & Bizzi, E. Shared and specific muscle synergies in natural motor behaviors. *Proc. Natl. Acad. Sci. U. S. A.* 102, 3076–3081 (2005).
  105. d’Avella, A., Fernandez, L., Portone, A. & Lacquaniti, F. Modulation of phasic and tonic muscle synergies with reaching direction and speed. *J. Neurophysiol.* 100, 1433–54 (2008).
  106. Ting, L. H. & Macpherson, J. M. A limited set of muscle synergies for force control during a postural task. *J. Neurophysiol.* 93, 609–13 (2005).
  107. McKay, J. L. & Ting, L. H. Functional muscle synergies constrain force production during postural tasks. *J. Biomech.* 41, 299–306 (2008).
  108. Overduin, S. A., d’Avella, A., Roh, J. & Bizzi, E. Modulation of Muscle Synergy Recruitment in Primate Grasping. *J. Neurosci.* 28, 880–892 (2008).
  109. d’Avella, A., Saltiel, P. & Bizzi, E. Combinations of muscle synergies in the construction of a natural motor behavior. *Nat. Neurosci.* 6, 300–308 (2003).
  110. Torres-Oviedo, G. & Ting, L. H. Muscle synergies characterizing human postural responses. *J. Neurophysiol.* 98, 2144–56 (2007).
  111. Torres-Oviedo, G. & Ting, L. H. Subject-specific muscle synergies in human balance control are consistent across different biomechanical contexts. *J. Neurophysiol.* 103, 3084–98 (2010).
  112. d’Avella, A., Portone, A., Fernandez, L. & Lacquaniti, F. Control of Fast-Reaching Movements by Muscle Synergy Combinations. *J. Neurosci.* 26, 7791–7810 (2006).
  113. Krishnamoorthy, V., Scholz, J. P. & Latash, M. L. The use of flexible arm muscle synergies to perform an isometric stabilization task. *Clin. Neurophysiol.* 118, 525–537 (2007).
  114. Wakeling, J. M. & Horn, T. Neuromechanics of muscle synergies during cycling. *J. Neurophysiol.* 101, 843–54 (2009).
  115. Chvatal, S. a & Ting, L. H. Common muscle synergies for balance and walking. *Front. Comput. Neurosci.* 7, 48 (2013).
  116. Hug, F., Turpin, N. A., Couturier, A. & Dorel, S. Consistency of muscle synergies during pedaling across different mechanical constraints. *J. Neurophysiol.* 106, 91–103 (2011).
  117. Twitchell, T. E. The restoration of motor function following hemiplegia in man. *Brain* 74, 443–80 (1951).
  118. Beer, R. F., Given, J. D. & Dewald, J. P. Task-dependent weakness at the elbow in patients with hemiparesis. *Arch. Phys. Med. Rehabil.* 80, 766–72 (1999).
  119. Dewald, J. P. A., Pope, P. S., Given, J. D., Buchanan, T. S. & Rymer, W. Z. Abnormal muscle coactivation patterns during isometric torque generation at the elbow and shoulder in hemiparetic subjects. *Brain* 118, 495–510 (1995).
  120. Cheung, V. C. K. *et al.* Stability of muscle synergies for voluntary actions after cortical stroke in humans. *Proc. Natl. Acad. Sci. U. S. A.* 106, 19563–8 (2009).



121. Trumbower, R. D., Ravichandran, V. J., Krutky, M. A. & Perreault, E. J. Contributions of altered stretch reflex coordination to arm impairments following stroke. *J. Neurophysiol.* 104, 3612–24 (2010).
122. Cheung, V. C. K. *et al.* Muscle synergy patterns as physiological markers of motor cortical damage. *Proc. Natl. Acad. Sci. U. S. A.* 109, 14652–6 (2012).
123. Roh, J., Rymer, W. Z., Perreault, E. J., Yoo, S. B. & Beer, R. F. Alterations in upper limb muscle synergy structure in chronic stroke survivors. *J. Neurophysiol.* 109, 768–81 (2013).
124. Clark, D. J., Ting, L. H., Zajac, F. E., Neptune, R. R. & Kautz, S. a. Merging of healthy motor modules predicts reduced locomotor performance and muscle coordination complexity post-stroke. *J. Neurophysiol.* 103, 844–857 (2010).
125. Krebs, H. I. *et al.* Robotic Measurement of Arm Movements After Stroke Establishes Biomarkers of Motor Recovery. *Stroke* 45, 200–204 (2014).
126. The National Institute of Neurological Disorders and Stroke rt-PA Stroke Study Group. Tissue plasminogen activator for acute ischemic stroke. *N. Engl. J. Med.* 333, 1581–7 (1995).
127. Hacke, W. *et al.* Thrombolysis with alteplase 3 to 4.5 hours after acute ischemic stroke. *N. Engl. J. Med.* 359, 1317–29 (2008).
128. Hoyer, E. H. & Celnik, P. a. Understanding and enhancing motor recovery after stroke using transcranial magnetic stimulation. *Restor. Neurol. Neurosci.* 29, 395–409 (2011).
129. Safavynia, S. a. & Ting, L. H. Task-level feedback can explain temporal recruitment of spatially fixed muscle synergies throughout postural perturbations. *J. Neurophysiol.* 107, 159–177 (2012).
130. Dipietro, L. *et al.* Changing Motor Synergies in Chronic Stroke. *J. Neurophysiol.* 98, 757–768 (2007).
131. Ellis, M. D., Holubar, B. G., Acosta, A. M., Beer, R. F. & Dewald, J. P. A. Modifiability of abnormal isometric elbow and shoulder joint torque coupling after stroke. *Muscle Nerve* 32, 170–8 (2005).
132. Schaechter, J. D. Motor rehabilitation and brain plasticity after hemiparetic stroke. *Prog. Neurobiol.* 73, 61–72 (2004).
133. Turton, A., Wroe, S., Trepte, N., Fraser, C. & Lemon, R. N. Contralateral and ipsilateral EMG responses to transcranial magnetic stimulation during recovery of arm and hand function after stroke. *Electroencephalogr. Clin. Neurophysiol.* 101, 316–28 (1996).



134. Traversa, R., Cicinelli, P., Pasqualetti, P., Filippi, M. & Rossini, P. M. Follow-up of interhemispheric differences of motor evoked potentials from the 'affected' and 'unaffected' hemispheres in human stroke. *Brain Res.* 803, 1–8 (1998).
135. Calautti, C., Leroy, F., Guincestre, J. Y., Marié, R. M. & Baron, J. C. Sequential activation brain mapping after subcortical stroke: changes in hemispheric balance and recovery. *Neuroreport* 12, 3883–6 (2001).
136. Calautti, C., Leroy, F., Guincestre, J. Y. & Baron, J. C. Dynamics of motor network overactivation after striatocapsular stroke: a longitudinal PET study using a fixed-performance paradigm. *Stroke.* 32, 2534–42 (2001).
137. Fujii, Y. & Nakada, T. Cortical reorganization in patients with subcortical hemiparesis: neural mechanisms of functional recovery and prognostic implication. *J. Neurosurg.* 98, 64–73 (2003).
138. Feydy, A. *et al.* Longitudinal study of motor recovery after stroke: recruitment and focusing of brain activation. *Stroke.* 33, 1610–7 (2002).
139. Carey, J. R. *et al.* Analysis of fMRI and finger tracking training in subjects with chronic stroke. *Brain* 125, 773–88 (2002).
140. Liepert, J., Graef, S., Uhde, I., Leidner, O. & Weiller, C. Training-induced changes of motor cortex representations in stroke patients. *Acta Neurol. Scand.* 101, 321–6 (2000).
141. van der Lee, J. H. *et al.* Forced use of the upper extremity in chronic stroke patients: results from a single-blind randomized clinical trial. *Stroke.* 30, 2369–75 (1999).
142. Mudie, M. H. & Matyas, T. A. Upper Extremity Retraining Following Stroke: Effects of Bilateral Practice. *Neurorehabil. Neural Repair* 10, 167–184 (1996).
143. Platz, T., Bock, S. & Prass, K. Reduced skilfulness of arm motor behaviour among motor stroke patients with good clinical recovery: does it indicate reduced automaticity? Can it be improved by unilateral or bilateral training? A kinematic motion analysis study. *Neuropsychologia* 39, 687–98 (2001).
144. Kinzel, G. L., Hall, A. S. & Hillberry, B. M. Measurement of the total motion between two body segments-I. Analytical development. *J. Biomech.* 5, 93–105 (1972).
145. American Academy of Orthopaedic Surgeons. *Joint Motion: Method of Measuring and Recording.* (The Academy, 1965).
146. Magermans, D. J., Chadwick, E. K. J., Veeger, H. E. J. & van der Helm, F. C. T. Requirements for upper extremity motions during activities of daily living. *Clin. Biomech. (Bristol, Avon)* 20, 591–9 (2005).
147. van Andel, C. J., Wolterbeek, N., Doorenbosch, C. A. M., Veeger, D. H. E. J. & Harlaar, J. Complete 3D kinematics of upper extremity functional tasks. *Gait Posture* 27, 120–7 (2008).
148. Murgia, A., Kyberd, P. & Barnhill, T. The use of kinematic and parametric information to highlight lack of movement and compensation in the upper extremities during activities of daily living. *Gait Posture* 31, 300–306 (2010).
149. Alt Murphy, M., Willén, C. & Sunnerhagen, K. S. Kinematic variables quantifying



- upper-extremity performance after stroke during reaching and drinking from a glass. *Neurorehabil. Neural Repair* 25, 71–80 (2011).
150. Alt Murphy, M., Willén, C. & Sunnerhagen, K. S. Responsiveness of upper extremity kinematic measures and clinical improvement during the first three months after stroke. *Neurorehabil. Neural Repair* 27, 844–53
  151. Kim, K. *et al.* Kinematic analysis of upper extremity movement during drinking in hemiplegic subjects. *Clin. Biomech. (Bristol, Avon)* 29, 248–56 (2014).
  152. Butler, E. E., Ladd, A. L., Lamont, L. E. & Rose, J. Temporal-spatial parameters of the upper limb during a Reach & Grasp Cycle for children. *Gait Posture* 32, 301–6 (2010).
  153. Fitts, P. M. The information capacity of the human motor system in controlling the amplitude of movement. *J. Exp. Psychol.* 47, 381–91 (1954).
  154. Cacho, E. W. A., de Oliveira, R., Ortolan, R. L., Varoto, R. & Cliquet, A. Upper limb assessment in tetraplegia: clinical, functional and kinematic correlations. *Int. J. Rehabil. Res.* 34, 65–72 (2011).
  155. De Los Reyes-Guzmán, A. *et al.* Quantitative assessment based on kinematic measures of functional impairments during upper extremity movements: A review. *Clin. Biomech.* 29, 719–727 (2014).
  156. van der Heide, J. C., Fock, J. M., Otten, B., Stremmelaar, E. & Hadders-Algra, M. Kinematic characteristics of reaching movements in preterm children with cerebral palsy. *Pediatr. Res.* 57, 883–9 (2005).
  157. Osu, R. *et al.* Quantifying the quality of hand movement in stroke patients through three-dimensional curvature. *J. Neuroeng. Rehabil.* 8, 62 (2011).
  158. Zariffa, J. *et al.* Relationship between clinical assessments of function and measurements from an upper-limb robotic rehabilitation device in cervical spinal cord injury. *IEEE Trans. Neural Syst. Rehabil. Eng.* 20, 341–50 (2012).
  159. Trombly, C. A. & Wu, C. Y. Effect of rehabilitation tasks on organization of movement after stroke. *Am. J. Occup. Ther.* 53, 333–44 (1999).
  160. Lee, J. B. *et al.* Coactivation of the flexor muscles as a synergist with the extensors during ballistic finger extension movement in trained kendo and karate athletes. *Int. J. Sports Med.* 20, 7–11 (1999).
  161. Dennard, M. Abnormal Muscle Coactivation Patterns During Isometric Torque Generation at the Elbow and Shoulder in Hemiparetic Subjects. *J. Neurol. Phys. Ther.* 21, 94–95 (1997).
  162. Radomski, M. V & Latham, C. A. T. *Occupational Therapy for Physical Dysfunction.*



## PART V. BIBLIOGRAPHY

---

- (Lippincott Williams & Wilkins, 2008).
163. Gowland, C., DeBruin, H., Basmajian, J. V, Plews, N. & Burcea, I. Agonist and antagonist activity during voluntary upper-limb movement in patients with stroke. *Phys. Ther.* 72, 624–33 (1992).
  164. Trombly, C. A. Deficits of reaching in subjects with left hemiparesis: a pilot study. *Am. J. Occup. Ther.* 46, 887–97 (1992).
  165. Levin, M. F. Interjoint coordination during pointing movements is disrupted in spastic hemiparesis. *Brain* 119 ( Pt 1, 281–93 (1996).
  166. Shumway-Cook, A. & Woollacott, M. H. *Motor Control: Translating Research Into Clinical Practice*. (Lippincott Williams & Wilkins, 2007).
  167. Fisk, J. D. & Goodale, M. A. The effects of unilateral brain damage on visually guided reaching: hemispheric differences in the nature of the deficit. *Exp. Brain Res.* 72, 425–435 (1988).
  168. Honeycutt, C. F. & Perreault, E. J. Planning of Ballistic Movement following Stroke: Insights from the Startle Reflex. *PLoS One* 7, (2012).
  169. Thielman, G. T., Dean, C. M. & Gentile, A. M. Rehabilitation of reaching after stroke: task-related training versus progressive resistive exercise. *Arch. Phys. Med. Rehabil.* 85, 1613–8 (2004).
  170. Cirstea, M. C., Mitnitski, A. B., Feldman, A. G. & Levin, M. F. Interjoint coordination dynamics during reaching in stroke. *Exp. brain Res.* 151, 289–300 (2003).
  171. Levin, M. F., Liebermann, D. G., Parmet, Y. & Berman, S. Compensatory Versus Noncompensatory Shoulder Movements Used for Reaching in Stroke. *Neurorehabil. Neural Repair* 1–12 (2015). doi:10.1177/1545968315613863
  172. Cirstea, M. C. Compensatory strategies for reaching in stroke. *Brain* 123, 940–953 (2000).
  173. Thielman, G., Kaminski, T. & Gentile, A. M. Rehabilitation of reaching after stroke: comparing 2 training protocols utilizing trunk restraint. *Neurorehabil. Neural Repair* 22, 697–705
  174. Bobath, B. *Adult Hemiplegia: Evaluation and Treatment*. (Butterworth–Heinemann, 1990).
  175. Michaelsen, S. M. & Levin, M. F. Short-term effects of practice with trunk restraint on reaching movements in patients with chronic stroke: a controlled trial. *Stroke.* 35, 1914–9 (2004).
  176. Caimmi, M. *et al.* Using kinematic analysis to evaluate constraint-induced movement therapy in chronic stroke patients. *Neurorehabil. Neural Repair* 22, 31–9
  177. Lum, P. S., Burgar, C. G., Shor, P. C., Majmundar, M. & Van der Loos, M. Robot-assisted movement training compared with conventional therapy techniques for the rehabilitation of upper-limb motor function after stroke. *Arch. Phys. Med. Rehabil.* 83, 952–9 (2002).
  178. Cheung, V. C. K. *et al.* Muscle synergy patterns as physiological markers of motor cortical damage. *Proc. Natl. Acad. Sci. U. S. A.* 109, 14652–6 (2012).



179. Oldfield, R. C. The assessment and analysis of handedness: the Edinburgh inventory. *Neuropsychologia* 9, 97–113 (1971).
180. Perotto, A. *Anatomical Guide for the Electromyographer, The Limbs and Trunk*. (Springfield, 2005).
181. Lee, D. D. & Seung, H. S. in *Advances in Neural Information Processing Systems* (MIT Press, 2001).
182. Lin, C.-J. Projected gradient methods for nonnegative matrix factorization. *Neural Comput.* 19, 2756–79 (2007).
183. Costa, U. 3D motion analysis of daily living, implications in neurorehabilitation. in *Gait and Posture* (2010).
184. Rab, G., Petuskey, K. & Bagley, A. A method for determination of upper extremity kinematics. *Gait Posture* 15, 113–119 (2002).
185. Milner-Brown, H. S., Stein, R. B. & Yemm, R. The orderly recruitment of human motor units during voluntary isometric contractions. *J. Physiol.* 230, 359–70 (1973).
186. Yao, W., Fuglevand, A. J., Enoka, R. M., Fuglevand, A. J. & Enoka, R. M. Motor-Unit Synchronization Increases EMG Amplitude and Decreases Force Steadiness of Simulated Contractions. 441–452 (2000).
187. Suzuki, H., Conwit, R. a, Stashuk, D., Santarsiero, L. & Metter, E. J. Relationships between surface-detected EMG signals and motor unit activation. *Med. Sci. Sports Exerc.* 34, 1509–1517 (2002).
188. Stewart, D., Behrens, C., Roth, J. & Wistuba, I. Exponential decay nonlinear regression analysis of patient survival curves: preliminary assessment in non-small cell lung cancer. *Lung Cancer* 71, 217–223 (2011).
189. Ettema, G. J. C. & Meijer, K. Muscle contraction history : modified Hill versus an exponential decay model. 500, 491–500 (2000).
190. Bigland-Ritchie, B., Jones, D. A. & Woods, J. J. Excitation frequency and muscle fatigue: electrical responses during human voluntary and stimulated contractions. *Exp. Neurol.* 64, 414–27 (1979).
191. Basmajian, J. V & De Luca, C. J. *Muscles Alive: Their Functions Revealed by Electromyography*. (Williams and Wilkins, 1985).
192. Colebatch, J. G. & Gandevia, S. C. The distribution of muscular weakness in upper motor neuron lesions affecting the arm. *Brain* 112 ( Pt 3, 749–63 (1989).
193. Fujiwara, T., Sonoda, S., Okajima, Y. & Chino, N. The relationships between trunk function and the findings of transcranial magnetic stimulation among patients with stroke. *J. Rehabil. Med.* 33, 249–55 (2001).



## PART V. BIBLIOGRAPHY

---

194. Werhahn, K. J., Conforto, A. B., Kadom, N., Hallett, M. & Cohen, L. G. Contribution of the ipsilateral motor cortex to recovery after chronic stroke. *Ann. Neurol.* 54, 464–72 (2003).
195. Konrad, P. *The ABC of EMG: A practical introduction to kinesiological electromyography*. (Noraxon Inc., 2005).
196. Fallentin, N., Jørgensen, K. & Simonsen, E. B. Motor unit recruitment during prolonged isometric contractions. *Eur. J. Appl. Physiol. Occup. Physiol.* 67, 335–41 (1993).
197. Maton, B. & Gamet, D. The fatigability of two agonistic muscles in human isometric voluntary submaximal contraction: an EMG study. II. Motor unit firing rate and recruitment. *Eur. J. Appl. Physiol. Occup. Physiol.* 58, 369–74 (1989).
198. Duchêne, J. & Goubel, F. EMG spectral shift as an indicator of fatigability in an heterogeneous muscle group. *Eur. J. Appl. Physiol. Occup. Physiol.* 61, 81–7 (1990).
199. Urra, O., Casals, A. & Jané, R. Synergy analysis as a tool to design and assess an effective stroke rehabilitation. *Conf. Proc. ... Annu. Int. Conf. IEEE Eng. Med. Biol. Soc. IEEE Eng. Med. Biol. Soc. Annu. Conf.* 2014, 3550–3 (2014).
200. Wright, Z. A., Rymer, W. Z. & Slutzky, M. W. Reducing Abnormal Muscle Coactivation After Stroke Using a Myoelectric-Computer Interface: A Pilot Study. *Neurorehabil. Neural Repair* 28, 443–451 (2013).
201. Urra, O., Casals, A. & Jané, R. in *IFMBE Proceedings* 1795–1798 (Springer International Publishing, 2014). doi:10.1007/978-3-319-00846-2\_443
202. Vollestad, N. K. in *The Thorax* (ed. Roussos, C.) 235–253 (Marcel Dekker, 1995).
203. Franz, E. a, Rowse, A. & Ballantine, B. Does handedness determine which hand leads in a bimanual task? *J. Mot. Behav.* 34, 402–412 (2002).
204. Latash, M. L., Scholz, J. P. & Schöner, G. Motor control strategies revealed in the structure of motor variability. *Exerc. Sport Sci. Rev.* 30, 26–31 (2002).
205. Kargo, W. J. & Nitz, D. A. Early skill learning is expressed through selection and tuning of cortically represented muscle synergies. *J. Neurosci.* 23, 11255–69 (2003).
206. Nazarpour, K., Barnard, a. & Jackson, a. Flexible Cortical Control of Task-Specific Muscle Synergies. *J. Neurosci.* 32, 12349–12360 (2012).
207. Ranganathan, R., Wieser, J., Mosier, K. M., Mussa-Ivaldi, F. A. & Scheidt, R. A. Learning redundant motor tasks with and without overlapping dimensions: facilitation and interference effects. *J. Neurosci.* 34, 8289–99 (2014).
208. Tseng, Y., Scholz, J. P. & Galloway, J. C. The organization of intralimb and interlimb synergies in response to different joint dynamics. *Exp. brain Res.* 193, 239–54 (2009).
209. Bagesteiro, L. B. & Sainburg, R. L. Handedness: dominant arm advantages in control of limb dynamics. *J. Neurophysiol.* 88, 2408–21 (2002).
210. Wang, J. & Sainburg, R. L. The dominant and nondominant arms are specialized for stabilizing different features of task performance. *Exp. brain Res.* 178, 565–70 (2007).
211. Zhou, P. *et al.* Decoding a new neural machine interface for control of artificial limbs.



- J. Neurophysiol.* 98, 2974–82 (2007).
212. Gallina, A. & Botter, A. Spatial localization of electromyographic amplitude distributions associated to the activation of dorsal forearm muscles. *Front. Physiol.* 4, 367 (2013).
  213. Howlett, O. A., Lannin, N. A., Ada, L. & McKinstry, C. *Functional Electrical Stimulation Improves Activity After Stroke: A Systematic Review With Meta-Analysis. Archives of Physical Medicine and Rehabilitation* 96, (Elsevier Ltd, 2015).
  214. Vafadar, A. K., Côté, J. N. & Archambault, P. S. Effectiveness of functional electrical stimulation in improving clinical outcomes in the upper arm following stroke: a systematic review and meta-analysis. *Biomed Res. Int.* 2015, 729768 (2015).
  215. Davoodi, R. & Andrews, B. J. Computer simulation of FES standing up in paraplegia: a self-adaptive fuzzy controller with reinforcement learning. *IEEE Trans. Rehabil. Eng.* 6, 151–61 (1998).
  216. Riener, R. & Fuhr, T. Patient-driven control of FES-supported standing up: a simulation study. *IEEE Trans. Rehabil. Eng.* 6, 113–24 (1998).
  217. Lemay, M. A. & Crago, P. E. A dynamic model for simulating movements of the elbow, forearm, an wrist. *J. Biomech.* 29, 1319–30 (1996).
  218. Davoodi, R., Brown, I. E. & Loeb, G. E. Advanced modeling environment for developing and testing FES control systems. *Med. Eng. Phys.* 25, 3–9 (2003).
  219. Roh, J., Cheung, V. C. K. & Bizzi, E. Modules in the brain stem and spinal cord underlying motor behaviors. *J. Neurophysiol.* 106, 1363–1378 (2011).
  220. Waters-Metenier, S., Husain, M., Wiestler, T. & Diedrichsen, J. Bihemispheric Transcranial Direct Current Stimulation Enhances Effector-Independent Representations of Motor Synergy and Sequence Learning. *J. Neurosci.* 34, 1037–1050 (2014).
  221. Pereira, E. A. H., Raja, K. & Gangavalli, R. Effect of training on interlimb transfer of dexterity skills in healthy adults. *Am. J. Phys. Med. Rehabil.* 90, 25–34 (2011).
  222. Yoo, I. *et al.* Effect of specialized task training of each hemisphere on interlimb transfer in individuals with hemiparesis. *NeuroRehabilitation* 32, 609–15 (2013).
  223. Sainburg, R. L. & Kalakanis, D. Differences in control of limb dynamics during dominant and nondominant arm reaching. *J. Neurophysiol.* 83, 2661–2675 (2000).
  224. Sainburg, R. Evidence for a dynamic-dominance hypothesis of handedness. *Exp. Brain Res.* 142, 241–258 (2002).
  225. Chiang, J., Wang, Z. J. & McKeown, M. J. Study of stroke condition and hand dominance using a hidden Markov, multivariate autoregressive (HMM-mAR) network



- framework. *Conf. Proc. IEEE Eng. Med. Biol. Soc.* 2008, 189–92 (2008).
226. Hinder, M. R., Carroll, T. J. & Summers, J. J. Inter-limb transfer of ballistic motor skill following non-dominant limb training in young and older adults. *Exp. Brain Res.* 227, 19–29 (2013).
227. Hinder, M. R., Schmidt, M. W., Garry, M. I., Carroll, T. J. & Summers, J. J. Absence of cross-limb transfer of performance gains following ballistic motor practice in older adults. *J Appl Physiol* 110, 166–175 (2011).
228. UT Southwestern Medical Center, D. of N. and N. The Internet Stroke Center. Available at: <http://www.strokecenter.org/patients/about-stroke/stroke-statistics/>. (Accessed: 16th June 2016)
229. Urrea, O., Casals, A. & Jane, R. The impact of visual feedback on the motor control of the upper-limb. in *2015 37th Annual International Conference of the IEEE Engineering in Medicine and Biology Society (EMBC)* 3945–3948 (IEEE, 2015). doi:10.1109/EMBC.2015.7319257
230. Henneman, E., Somjen, G. & Carpenter, D. O. Functional Significance of Cell Size in Spinal Motoneurons. *J. Neurophysiol.* 28, 560–580 (1965).
231. Corbetta, M., Miezin, F. M., Shulman, G. L. & Petersen, S. E. A PET study of visuospatial attention. *J. Neurosci.* 13, 1202–26 (1993).
232. Mesulam, M. M. Spatial attention and neglect: parietal, frontal and cingulate contributions to the mental representation and attentional targeting of salient extrapersonal events. *Philos. Trans. R. Soc. Lond. B. Biol. Sci.* 354, 1325–1346 (1999).
233. Serrien, D. J., Ivry, R. B. & Swinnen, S. P. Dynamics of hemispheric specialization and integration in the context of motor control. *Nat. Rev. Neurosci.* 7, 160–6 (2006).
234. Karni, a *et al.* The acquisition of skilled motor performance: fast and slow experience-driven changes in primary motor cortex. *Proc. Natl. Acad. Sci. U. S. A.* 95, 861–868 (1998).
235. Doyon, J. *et al.* Experience-dependent changes in cerebellar contributions to motor sequence learning. *Proc. Natl. Acad. Sci. U. S. A.* 99, 1017–1022 (2002).
236. Haaland, K. Y., Elsinger, C. L., Mayer, A. R., Durgerian, S. & Rao, S. M. Motor sequence complexity and performing hand produce differential patterns of hemispheric lateralization. *J. Cogn. Neurosci.* 16, 621–636 (2004).
237. Menegaldo, L. L. & Oliveira, L. F. An EMG-driven model to evaluate quadriceps strengthening after an isokinetic training. *Procedia IUTAM* 2, 131–141 (2011).
238. Norton, J. A. & Gorassini, M. A. Changes in cortically related intermuscular coherence accompanying improvements in locomotor skills in incomplete spinal cord injury. *J. Neurophysiol.* 95, 2580–2589 (2006).
239. Kovalski, J. E., Heitman, R. J., Gurchiek, L. R. & Trundle, T. L. Reliability and effects of arm dominance on upper extremity isokinetic force, work, and power using the closed chain rider system. *J. Athl. Train.* 34, 358–61 (1999).
240. Ghosh, B., Swami, P., Gandhi, T., Santhosh, J. & Anand, S. Interhemispheric interaction and cause of hindrance during handedness activity: An electro-



- physiological evidence. *2009 Int. Multimedia, Signal Process. Commun. Technol.* 193–196 (2009). doi:10.1109/MSPCT.2009.5164208
241. Winstein, C. J. & Pohl, R. S. Effects of unilateral brain damage on the control of goal-directed hand movements. *Exp Brain Res* 105, 163–174 (1995).
  242. Sperry, R. W. Brain research: some head-splitting implications. *The voice* 15, 11–16 (1966).
  243. Knecht, S. *et al.* Handedness and hemispheric language dominance in healthy humans. *Brain* 123 Pt 12, 2512–2518 (2000).
  244. Mitchell, E. J., Dewar, D. & Maxwell, D. J. Is Remodelling of Corticospinal Tract Terminations Originating in the Intact Hemisphere Associated with Recovery following Transient Ischaemic Stroke in the Rat? *PLoS One* 11, e0152176 (2016).
  245. Buma, F. E. *et al.* Brain activation is related to smoothness of upper limb movements after stroke. *Exp Brain Res* In press, (2015).
  246. Mohapatra, S. *et al.* Role of contralesional hemisphere in paretic arm reaching in patients with severe arm paresis due to stroke: A preliminary report. *Neurosci. Lett.* 617, 52–58 (2016).
  247. Bagesteiro, L. B. & Sainburg, R. L. Nondominant arm advantages in load compensation during rapid elbow joint movements. *J. Neurophysiol.* 90, 1503–13 (2003).
  248. Chang, J. J., Wu, T. I., Wu, W. L. & Su, F. C. Kinematical measure for spastic reaching in children with cerebral palsy. *Clin. Biomech.* 20, 381–388 (2005).
  249. Chen, H., Lin, K., Liang, R., Wu, C. & Chen, C. Kinematic measures of Arm-trunk movements during unilateral and bilateral reaching predict clinically important change in perceived arm use in daily activities after intensive stroke rehabilitation. *J. Neuroeng. Rehabil.* 12, 84 (2015).
  250. Henrikson, J. Completeness and total boundedness of the Hausdorff metric. *MIT Undergrad. J. Math.* 1, 69–79 (1999).
  251. Kamper, D. G., McKenna-Cole, A. N., Kahn, L. E. & Reinkensmeyer, D. J. Alterations in reaching after stroke and their relation to movement direction and impairment severity. *Arch. Phys. Med. Rehabil.* 83, 702–707 (2002).
  252. Archambault, P., Pigeon, P., Feldman, A. G. & Levin, M. F. Recruitment and sequencing of different degrees of freedom during pointing movements involving the trunk in healthy and hemiparetic subjects. *Exp. Brain Res.* 126, 55–67 (1999).
  253. Peng, C. C.-Y. J., Lee, K. L. K. & Ingersoll, G. M. An Introduction to Logistic Regression Analysis and Reporting. *J. Educ. Res.* 96, 3–14 (2002).



## PART V. BIBLIOGRAPHY

---

- 254. Cullins, M. J., Shaw, K. M., Gill, J. P. & Chiel, H. J. Motor neuronal activity varies least among individuals when it matters most for behavior. *J. Neurophysiol.* 113, 981–1000 (2015).
- 255. Valero-Cuevas, F. J., Venkadesan, M. & Todorov, E. Structured variability of muscle activations supports the minimal intervention principle of motor control. *J. Neurophysiol.* 102, 59–68 (2009).
- 256. Scholz, J. P. & Schöner, G. The uncontrolled manifold concept: identifying control variables for a functional task. *Exp. brain Res.* 126, 289–306 (1999).
- 257. Beer, R. D., Chiel, H. J. & Gallagher, J. C. Evolution and analysis of model CPGs for walking: II. General principles and individual variability. *J. Comput. Neurosci.* 7, 119–47
- 258. Tsianos, G. a, Goodner, J. & Loeb, G. E. Useful properties of spinal circuits for learning and performing planar reaches. *J. Neural Eng.* 11, 56006 (2014).
- 259. Burdet, E. & Milner, T. E. Quantization of human motions and learning of accurate movements. *Biol. Cybern.* 78, 307–318 (1998).
- 260. Zehr, E. P. & Sale, D. G. Ballistic movement: muscle activation and neuromuscular adaptation. *Can. J. Appl. Physiol. = Rev. Can. Physiol. Appl.* 19, 363–78 (1994).
- 261. Bourbonnais, D. & Vanden Noven, S. Weakness in patients with hemiparesis. *Am. J. Occup. Ther.* 43, 313–9 (1989).
- 262. el-Abd, M. A., Ibrahim, I. K. & Dietz, V. Impaired activation pattern in antagonistic elbow muscles of patients with spastic hemiparesis: contribution to movement disorder. *Electromyogr. Clin. Neurophysiol.* 33, 247–55 (1993).
- 263. Herzfeld, D. J. & Shadmehr, R. Motor variability is not noise, but grist for the learning mill. *Nat. Neurosci.* 17, 149–50 (2014).
- 264. Huang, V. S., Shadmehr, R. & Diedrichsen, J. Active learning: learning a motor skill without a coach. *J. Neurophysiol.* 100, 879–87 (2008).
- 265. Loeb, G. E. Optimal isn't good enough. *Biol. Cybern.* 106, 757–65 (2012).
- 266. Todorov, E. & Jordan, M. I. Optimal feedback control as a theory of motor coordination. *Nat. Neurosci.* 5, 1226–35 (2002).
- 267. Ellis, M. D., Sukal, T., DeMott, T. & Dewald, J. P. A. Augmenting Clinical Evaluation of Hemiparetic Arm Movement With a Laboratory-Based Quantitative Measurement of Kinematics as a Function of Limb Loading. *Neurorehabil. Neural Repair* 22, 321–329 (2007).
- 268. Welch, T. D. J. & Ting, L. H. A feedback model reproduces muscle activity during human postural responses to support-surface translations. *J. Neurophysiol.* 99, 1032–8 (2008).
- 269. Furuya, S. & Altenmüller, E. Flexibility of movement organization in piano performance. *Front. Hum. Neurosci.* 7, 173 (2013).
- 270. Kan, P., Huq, R., Hoey, J., Goetschalckx, R. & Mihailidis, A. The development of an adaptive upper-limb stroke rehabilitation robotic system. *J. Neuroeng. Rehabil.* 8, 33 (2011).



271. Brokaw, E. B., Nichols, D., Holley, R. J. & Lum, P. S. Robotic therapy provides a stimulus for upper limb motor recovery after stroke that is complementary to and distinct from conventional therapy. *Neurorehabil. Neural Repair* 28, 367–76 (2014).
272. Calabrese, R. L., Norris, B. J., Wenning, A. & Wright, T. M. Coping with variability in small neuronal networks. *Integr. Comp. Biol.* 51, 845–55 (2011).
273. Golowasch, J., Goldman, M. S., Abbott, L. F. & Marder, E. Failure of averaging in the construction of a conductance-based neuron model. *J. Neurophysiol.* 87, 1129–31 (2002).
274. Marder, E. & Goaillard, J.-M. Variability, compensation and homeostasis in neuron and network function. *Nat. Rev. Neurosci.* 7, 563–74 (2006).
275. Prinz, A. A., Bucher, D. & Marder, E. Similar network activity from disparate circuit parameters. *Nat. Neurosci.* 7, 1345–52 (2004).
276. Muir, K. W. Heterogeneity of stroke pathophysiology and neuroprotective clinical trial design. *Stroke* 33, 1545–1550 (2002).
277. Kent, T. A., Soukup, V. M. & Fabian, R. H. Heterogeneity affecting outcome from acute stroke therapy: making reperfusion worse. *Stroke*. 32, 2318–27 (2001).
278. Yang, J. F. *et al.* Infant stepping: a window to the behaviour of the human pattern generator for walking. *Can. J. Physiol. Pharmacol.* 82, 662–74
279. Michaelsen, S. M. *et al.* Effect of Trunk Restraint on the Recovery of Reaching Movements in Hemiparetic Patients. (2010).
280. Lehericy, S. *et al.* Clinical characteristics and topography of lesions in movement disorders due to thalamic lesions. *Neurology* 57, 1055–66 (2001).
281. Ghika, J. & Bogousslavsky, J. in *Stroke syndromes* (eds. Bogousslavsky, J. & Caplan, L. R.) 162–181 (Cambridge University Press). doi:10.1017/CBO9780511586521.013
282. Calautti, C. & Baron, J.-C. Functional neuroimaging studies of motor recovery after stroke in adults: a review. *Stroke*. 34, 1553–66 (2003).
283. Jang, S. H. A review of the ipsilateral motor pathway as a recovery mechanism in patients with stroke. *NeuroRehabilitation* 24, 315–20 (2009).
284. Engineer, N. D. *et al.* Reversing pathological neural activity using targeted plasticity - Supplementary Information. *Nature* 470, 101–4 (2011).
285. Fregni, F. *et al.* A sham-controlled trial of a 5-day course of repetitive transcranial magnetic stimulation of the unaffected hemisphere in stroke patients. *Stroke* 37, 2115–2122 (2006).
286. de Rugy, A., Loeb, G. E. & Carroll, T. J. Muscle coordination is habitual rather than



- optimal. *J. Neurosci.* 32, 7384–91 (2012).
287. Ganesh, G., Haruno, M., Kawato, M. & Burdet, E. Motor memory and local minimization of error and effort, not global optimization, determine motor behavior. *J. Neurophysiol.* 104, 382–90 (2010).
288. Snaterse, M., Ton, R., Kuo, A. D. & Donelan, J. M. Distinct fast and slow processes contribute to the selection of preferred step frequency during human walking. *J. Appl. Physiol.* 110, 1682–90 (2011).
289. Mateo, S. *et al.* Upper limb kinematics after cervical spinal cord injury: a review. *J. Neuroeng. Rehabil.* 12, 9 (2015).
290. Berry, M. W., Browne, M., Langville, A. N., Pauca, V. P. & Plemmons, R. J. Algorithms and applications for approximate nonnegative matrix factorization. *Comput. Stat. Data Anal.* 52, 155–173 (2007).





## **PART VI**

# **Derived publications**







This section enumerates the publications that have been derived from the present thesis. The list of publications is sorted chronologically according to the publication date.

- [1] Urra O, Casals A and Jané R. “Decoding the Spatial Characteristics of Arm Movements from EMG signals”. Presented in the 6<sup>th</sup> IBEC Symposium (Barcelona, 2013). [\[Conference Proceedings\]](#)
- [2] Urra O, Casals A and Jané R. “Evaluating Spatial Characteristics of Upper-Limb Movements from EMG Signals”. XIII Mediterranean Conference on Medical and Biological Engineering and Computing 2013 IFMBE Proceedings Volume 41, 2014, pp 1795-98. [\[Book Chapter\]](#)
- [3] Lambrecht S, Urra O, Grosu S, Pérez S. “Emerging rehabilitation in cerebral palsy” *Biosystems & Biorobotics* Springer Berlin Heidelberg Volume 4, 2014, pp 23-49. [\[Book Chapter\]](#)
- [4] Urra O, Casals A and Jané R. “Synergy Analysis as a Tool to Design and Assess an Effective Stroke Rehabilitation”. Presented in the 35th Annual International Conference of the IEEE Engineering in Medicine and Biology Society (EMBC 2014, Chicago), pp 3550-53. [\[Conference Proceedings\]](#)  
**PMID: 25570757**
- [5] Urra O, Casals A and Jané R. “Synergies as a Tool to Design and Assess an Effective Stroke Rehabilitation”. Presented in the 7<sup>th</sup> IBEC Symposium (Barcelona, 2014). [\[Conference Proceedings\]](#)



- [6] Urrea O, Casals A and Jané R. "Study of synergy patterns during the execution of stroke rehabilitation exercises" in the Annual Congress of the Spanish Society of Biomedical Engineering (CASEIB 2014), pp 1-4. [\[Conference Proceedings\]](#)



*Awarded with the prize Jose María Ferrero Corral to the best PhD student contributions*

- [7] Urrea O, Casals A and Jané R. "The impact of visual feedback on the motor control of the upper-limb " in the Conf Proc IEEE Eng Med Bio Soc (EMBC 2015, Milan), pp 3945-48. [\[Conference Proceedings\]](#)

**PMID: 26737157**

- [8] Urrea O, Casals A and Jané R. "Visual feedback facilitates Intermanual transfer of the motor control of the dominant arm towards the nondominant arm" in the Annual Congress of the Spanish Society of Biomedical Engineering (CASEIB 2015), pp 503-6. [\[Conference Proceedings\]](#)

- [9] Urrea O, Casals A and Jané R. "Interlimb differences of human upper-limb motor control during natural motor behaviors" Eur J of App Physiol (Pending submission) [\[Journal Article\]](#)

- [10] Urrea O, Casals A and Jané R. "The interlimb similarity of the control structure of stroke patients as a neuromuscular marker of motor impairment". Presented in the 9<sup>th</sup> IBEC Symposium (Barcelona, 2016) [\[Conference Proceedings\]](#)



*Awarded with the prize to the best Flash Presentation*

- [11] Urrea O, Casals A and Jané R. "Nobel approach to improve stroke diagnosis and neurorehabilitation based in the interlimb similarity of muscle synergies" J Neuroeng & Rehab (Pending submission) [\[Journal Article\]](#)













## **PART VII**

# **Appendices**







## A. EDINBURGH HANDEDNESS INVENTORY

*Please indicate your preferences in the use of hands in the following activities by putting + in the appropriate column. Where the preference is so strong that you would never try to use the other hand unless absolutely forced to, put ++. If in any case you are really indifferent put + in both columns.*

*Some of the activities require both hands. In these cases, the part of the task, or object, for which hand preference is wanted is indicated in brackets. Please try to answer all the questions, and only leave a blank if you have no experience at all of the object or task.*

EDINBURGH HANDEDNESS INVENTORY	LEFT	RIGHT
1. Writing		
2. Drawing		
3. Throwing		
4. Scissors		
5. Toothbrush		
6. Knife (without fork)		
7. Spoon		
8. Broom (upper hand)		
9. Striking Match (match)		
10. Opening box (lid)		
i. Which foot do you prefer to kick with?		
ii. Which eye do you use when using only one?		

Table 42 Items of the Edinburgh Handedness Inventory



## B. FUGL – MEYER SCALE

FMA-UE PROTOCOL

Rehabilitation Medicine, University of Gothenburg

**FUGL-MEYER ASSESSMENT**  
**UPPER EXTREMITY (FMA-UE)**  
**Assessment of sensorimotor function**

ID:  
 Date:  
 Examiner:

*Fugl-Meyer AR, Jaasko L, Leyman I, Olsson S, Steglind S: The post-stroke hemiplegic patient. A method for evaluation of physical performance. Scand J Rehabil Med 1975, 7:13-31.*

<b>A. UPPER EXTREMITY, sitting position</b>				
<b>I. Reflex activity</b>		<b>none</b>	<b>can be elicited</b>	
Flexors: biceps and finger flexors (at least one)		0	2	
Extensors: triceps		0	2	
Subtotal I (max 4)				
<b>II. Volitional movement within synergies, without gravitational help</b>		<b>none</b>	<b>partial</b>	<b>full</b>
<b>Flexor synergy:</b> Hand from contralateral knee to ipsilateral ear. From extensor synergy (shoulder adduction/ internal rotation, elbow extension, forearm pronation) to flexor synergy (shoulder abduction/ external rotation, elbow flexion, forearm supination). <b>Extensor synergy:</b> Hand from ipsilateral ear to the contralateral knee	Shoulder retraction	0	1	2
	elevation	0	1	2
	abduction (90°)	0	1	2
	external rotation	0	1	2
	Elbow flexion	0	1	2
	Forearm supination	0	1	2
	Shoulder adduction/internal rotation	0	1	2
	Elbow extension	0	1	2
Forearm pronation	0	1	2	
Subtotal II (max 18)				
<b>III. Volitional movement mixing synergies, without compensation</b>		<b>none</b>	<b>partial</b>	<b>full</b>
Hand to lumbar spine hand on lap	cannot perform or hand in front of ant-sup iliac spine hand behind ant-sup iliac spine (without compensation) hand to lumbar spine (without compensation)	0	1	2
Shoulder flexion 0°- 90° elbow at 0°	immediate abduction or elbow flexion abduction or elbow flexion during movement	0	1	2
pronation-supination 0°	flexion 90°, no shoulder abduction or elbow flexion			2
Pronation-supination elbow at 90°	no pronation/supination, starting position impossible	0	1	2
shoulder at 0°	limited pronation/supination, maintains starting position full pronation/supination, maintains starting position			2
Subtotal III (max 6)				
<b>IV. Volitional movement with little or no synergy</b>		<b>none</b>	<b>partial</b>	<b>full</b>
Shoulder abduction 0 - 90° elbow at 0° forearm pronated	immediate supination or elbow flexion supination or elbow flexion during movement abduction 90°, maintains extension and pronation	0	1	2
Shoulder flexion 90° - 180° elbow at 0°	immediate abduction or elbow flexion abduction or elbow flexion during movement	0	1	2
pronation-supination 0°	flexion 180°, no shoulder abduction or elbow flexion			2
Pronation/supination elbow at 0°	no pronation/supination, starting position impossible	0	1	2
shoulder at 30°- 90° flexion	limited pronation/supination, maintains start position full pronation/supination, maintains starting position			2
Subtotal IV (max 6)				
<b>V. Normal reflex activity</b> assessed only if full score of 6 points is achieved in part IV; compare with the unaffected side		<b>0 (IV), hyper</b>	<b>lively</b>	<b>normal</b>
biceps, triceps, finger flexors	2 of 3 reflexes markedly hyperactive or 0 points in part IV 1 reflex markedly hyperactive or at least 2 reflexes lively maximum of 1 reflex lively, none hyperactive	0	1	2
Subtotal V (max 2)				
<b>Total A (max 36)</b>				



## C. FUNCTIONAL INDEPENDENCE MEASURE

	ADMISSION	DISCHARGE	FOLLOW-UP
<b>Self-Care</b>			
A. Eating			
B. Grooming			
C. Bathing			
D. Dressing – Upper Body			
E. Dressing – Lowe Body			
F. Toileting			
<b>Sphincter Control</b>			
G. Bladder Management			
H. Bowel Management			
<b>Transfers</b>			
I. Bed, Chair, Wheelchairs			
J. Toilet			
K. Tub, Shower			
<b>Locomotion</b>			
L. Walk/Wheelchair			
M. Stairs			
<i>Motor subtotal score</i>			
<b>Communication</b>			
N. Comprehension			
O. Expression			
<b>Social Cognition</b>			
P. Social Interaction			
Q. Problem Solving			
R. Memory			
<i>Cognitive subtotal score</i>			
<b>TOTAL FIM SCORE</b>			

Table 43 Items of the Functional Independence Measure



## D. UPPER-LIMB JOINTS AND MUSCLE FUNCTION

JOINT	MUSCLES	FUNCTION	NERVE
SHOULDER SCAPULO - THORACIC	Serratus Anterior	Protraction & upward rotation	Long thoracic
	Trapezius superior	Elevation	Accessory spinal
	Trapezius middle part	Retraction	
	Trapezius inferior	Downward rotation	
	Pectoralis minor	Depression & anterior tipping	Medial
SHOULDER GLENO- HUMERAL	Deltoid anterior	Flexion	Axillary
	Deltoid medius	Abduction	
	Deltoid posterior	Extension	
	Pectoralis major upper part	Flexion/Adduction/Medial rotation	Lateral pectoral
	Pectoralis major middle + lower parts	Flexion/Adduction/Medial rotation	Medial pectoral
	Lattissimus dorsi	Extension/Adduction/Medial rotation	Thoracodorsal
	Teres major	Extension/Adduction/Medial rotation	Subscapularis
	Subscapularis	Medial rotation	
	Supraspinatus	Abduction	
	Infraspinatus	Lateral Rotation	
	Teres minor	Lateral rotation	Axillary
ELBOW	Biceps brachii	Flexion	Musculo- cutaneous
	Brachialis	Flexion	
	Brachioradialis	Flexion	
	Triceps brachii	Extension	Radial
WRIST	Extensor carpi + radialis longus	Extension	Radial
	Extensor carpi ulnaris	Extension	
	Flexor carpi radials	Flexion	Median
	Flexor carpi ulnaris	Flexion	Ulnar

Table 44 Upper limb joints, muscle function and nerves. Adapted from <sup>289</sup>



## E. CUSTOM GUI FOR UPPER-LIMB MOTOR ANALYSIS

In order to automate the analyses performed and facilitate the replicability of the results, we developed a package of Matlab functions that allowed us to carry out the complete study of the control structure of the upper-limb. The package usability was enhanced by bundling the collection of functions into a Graphic User Interface (GUI) (**Figure 142**). The was inspired by the GUI developed by the CSIC for lower limb function

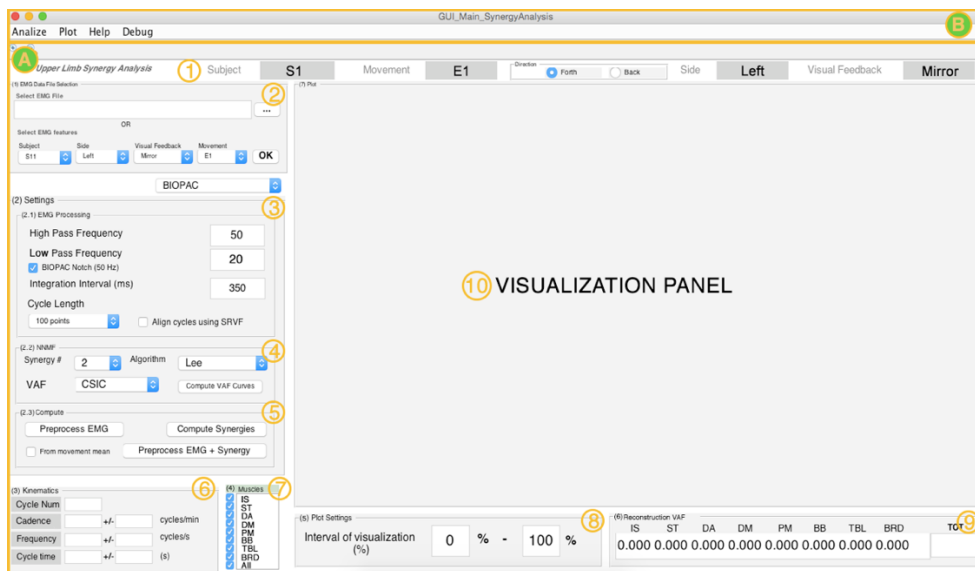


Figure 142 Custom designed Graphic User Interface to analyze the control structure of the upper-limb.

The GUI is separated into 2 main areas, the graphical interaction dashboard **Figure 142A** and the menu bar **Figure 142B**. In order to perform a complete analysis, first we need to setup the analysis parameters in the graphical dashboard. Next, the menu bar provides series of post-analysis functions.



## A – GRAPHICAL DASHBOARD

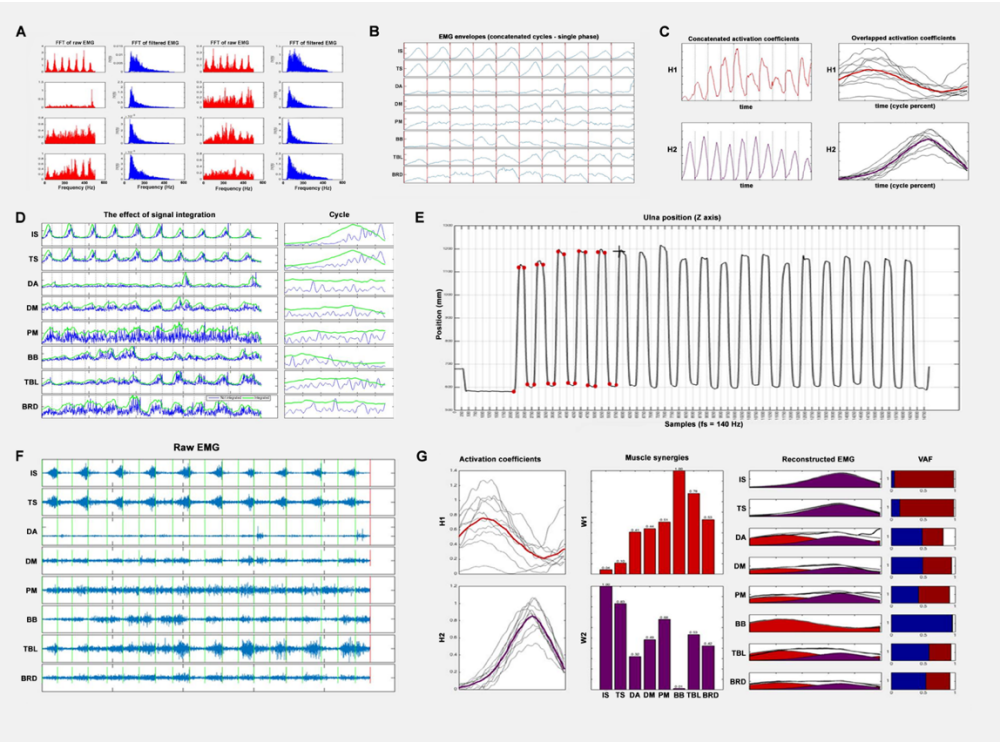
The graphical dashboard is divided into numerated panels to sequentially guide the user through the analysis process.

1. **Selection viewer** | Displays the experimental details of the file that is been analyzed (subject ID, movement-type, movement direction, arm side, visual feedback condition). If no file is selected, the text-boxes in this panel are empty.
2. **Load EMGs** | Allows the user to manually select the folder where the EMG recordings are stored.
3. **Preprocessing Settings** | Allows the user setting up the EMG preprocessing parameters (filter cutoffs, built-in filters, integration interval, time normalization length, cycle alignment function). In this step it is important to indicate the acquisition system used, so that the software can adequately manipulate the recording files.
4. **Nonnegative Matrix Factorization settings** | Allows the user selecting the number of modules to extract, the algorithm used to apply NMF (Lee<sup>181</sup>, Lee & Lin<sup>182</sup>, Alternating Least Squares, Multiplicative rules or Gradient descent<sup>290</sup>) and the VAF type calculated.
5. **Compute** | These buttons allow separating preprocessing stage and muscle synergy extraction stage or either linking both stages one after the other.
6. **Kinematic summary** | This panel summarizes basic kinematic features such as the number of repetitions, average repetition frequency, time cycle...
7. **Muscle selection panel** | This panels allows selecting which muscles to include in the analysis
8. **Plot interval** | This panel allows delimiting the cycle-percentage to display in the visualization panel (10)
9. **Reconstruction VAF** | This panel displays the reconstruction VAF for each analyzed muscle and the overall reconstruction VAF (TOT)
10. **Visualization panel** | This panel displays the plots selected in the tab Plot of the Menu Bar (**Figure 142B**)



B – MENU BAR

The menu bar is composed of 4 tabs that group a variety of functions:



**Figure 143** Some of the plots available in the visualization panel. A – FFT of the signals before and after filtering. B – EMG envelopes. C - Activation coefficients. D – The effect of signal integration. E – Event segmentation through kinematic data. F – Raw EMG. G – Summary of the control structure.

1. **Analyze** | Provides a series of functions to



- 1.1. **Detect events from kinematics:** opens a new GUI to manually determine movement onset and offset from upper-joints position or velocity evolution (**Figure 143E**).
- 1.2. **Exclude cycles:** allows user to exclude certain cycles (or movements repetitions) from the analysis
- 1.3. **VAF analysis:** creates VAF curves to determine the optimal number of muscle synergies needed to explain the underlying modular structure
- 1.4. **Activations:** provides ILS measures between selected activation coefficients
- 1.5. **Compare synergies:** provides ILS measures between selected muscle synergies
  
2. **Plot |** Provides a series of visualization capabilities to supervise, assess and interpret the synergy extraction process. Plots are displayed in the visualization panel (**Figure 142-A10**)
  - 2.1. **Raw EMG:** plots raw EMG signals after event-segmentation (**Figure 143F**).
  - 2.2. **Filtered EMG:** plots the filtered EMG.
  - 2.3. **FFT:** plots the Fast Fourier Transform (FFT) before and after filtering (**Figure 143A**).
  - 2.4. **Integration effect:** plots the effect of signal integration set in panel (3) (**Figure 143D**).
  - 2.5. **Raw-filt-envelopes:** plots raw EMG, filtered EMG and envelopes in a single plot.
  - 2.6. **Cycles:** plots the EMG cycles after time normalization.
  - 2.7. **Envelopes:** plots final envelopes that are input for synergy extraction (**Figure 143B**).
  - 2.8. **Activation:** plots activation coefficients (**Figure 143C**).
  - 2.9. **Reconstructed EMG signals:** plots the entire control structure and associated VAF plots (**Figure 143G**).
  - 2.10. **VAF curves:** plots VAF curves



- 2.11. **Repetition vs mean CS:** plots the control structure extracted from averaging EMG repetitions *versus* the control structure extracted from individual EMG repetitions and then averaging resulting control structures.
- 3. **Help** | Redirects to a basic user manual to use the GUI
- 4. **Debug** | Activates debugging mode for developer purpose